Control of systems with actuator nonlinearities

Stuart Crawshaw
Trinity College

Control Group

Department of Engineering
University of Cambridge

A dissertation submitted for
the degree of Doctor of Philosophy

May 26, 2000

Abstract

The problem of controlling linear systems subject to actuator nonlinearities is considered in three parts: modelling of the combined system for control, analysing the stability and performance properties of nonlinear systems, and implementation of controllers which (wholly or partially) compensate for actuator nonlinearities.

We start with the analysis problem. A simple $\mathcal{H}_\infty$-norm based stability criterion for sector $[0, 1]$ nonlinearities is given, which additionally provides an $\mathcal{L}_2$ performance bound if the nonlinearity is an ideal deadzone. We then derive a novel method for analysing the local stability properties of systems with ideal deadzone nonlinearities, and generalise this result to a class of deadzone-like nonlinearities. This method is shown to be simple to calculate, and to highlight the important open-loop properties affecting the results.

The question of modelling nonlinear actuators is then considered, with particular emphasis on magnitude and/or rate limitations. We propose to model only the linear region of the actuator's behaviour, and to condition ("precompensate") the controller output so as to remain within this region of linear operation by, for example, saturating the control signal. The main advantages of such a scheme are that the nonlinear perturbation is measurable (since it is implemented within the controller) and that complex actuator behaviours outside the linear regime need not be modelled.

Finally, we consider applying anti-windup control schemes to systems with nonlinear actuators and "precompensation" as described above. For stable plants with magnitude and/or rate limitations we show that it is always possible to globally stabilise the system, and for the common case of a magnitude limitation we give a synthesis method which guarantees $\mathcal{L}_2$ performance. For unstable plants we show that global stability cannot be achieved, and discuss synthesis to improve local stability.

Acknowledgements

My very grateful thanks go to my supervisor, Dr Glenn Vinnicombe, for his support and encouragement during my research. Thanks also to the staff and students of the control group, particularly my comtemporaries Paresh, Alex, Richard and Camille.

I cannot mention individually the many hundreds of others who have made my time in Cambridge so enjoyable, but my best wishes go to all of you, wherever you may now be.

I am grateful for financial support from the UK Engineering & Physical Sciences Research Council, Cambridge University Engineering Department, and Trinity College, Cambridge.

As required by University Statute, I hereby declare that this dissertation is not substantially the same as any that I have submitted for a degree at any other University, is the result of my own work, and includes nothing which is the outcome of work done in collaboration.

Stuart Crawshaw
Trinity College, Cambridge
May 26, 2000

Contents

List of Figures

Chapter 1

Introduction and summary

This thesis is concerned with the problems of modelling, analysing and controlling systems comprising a linear time-invariant “plant” driven by a nonlinear “actuator”. Many real systems may be assumed to be of this form, even though there may be no discernible “actuators” in the system, and even in many cases if the “plant” is nonlinear, provided that it is linear around some nominal operating point.

For example, a spacecraft can be assumed to comprise a mass (the “plant”) driven by an impulsive force (the “actuator”). In this case it is clear that the actuator is nonlinear: the rocket motor cannot supply an infinitely large impulse. It is equally clear that the plant is linear: it follows Newton’s laws of motion ... or does it?

If we try to model the system with perfect fidelity, then we must accept that Newton’s laws break down for speeds comparable to the speed of light. So, the plant is not really linear! However, we can clearly ignore this nonlinearity, since the rocket motor probably has insufficient fuel to reach such a high velocity, and hence for this spacecraft our assumption of plant linearity and actuator nonlinearity is justified.

In general, the assumption of plant linearity is justified provided that the plant behaves linearly within the limitations imposed by the actuator nonlinearity.

We approach the topic in three distinct sections, which respectively consider **nonlinear stability analysis**, **nonlinear actuators** and **anti-windup control**.

Nonlinear stability analysis

The first part of the thesis (Chapter 3) is concerned with methods for determining the stability (or otherwise) of systems comprising the feedback interconnection of a linear, time-invariant transfer function and a nonlinear operator.

We consider both *global* and *local* results, ie results which hold for all signals in some space (eg $v \in \mathcal{L}_2$) or only for some subset of that space (eg $v \in \mathcal{L}_2$ such that $\|v\|_2 < \varepsilon$) respectively.

It is worth taking a moment to consider exactly what is meant by a “local” result:

Consider a linear, time invariant transfer function $G \in \mathcal{H}_\infty$. It is well known that for any $v \in \mathcal{L}_2$ and $w = Gv$

$$\|w\|_2 \leq \|G\|_\infty \|v\|_2$$

This is a typical example of a global result[1]: it holds for all $v \in \mathcal{L}_2$. We say that $\|G\|_\infty$ is the *gain* of the operator G.

Now consider a nonlinear function (actually an ideal deadzone function) defined by

$$w(t) = \begin{cases} v(t) - 1 & \text{if } v(t) > 1 \\ 0 & \text{if } |v(t)| \leq 1 \\ v(t) + 1 & \text{if } v(t) < -1 \end{cases}$$

For this function it is quite easy to see that $\|w\|_2 \leq \|v\|_2$ for any $v \in \mathcal{L}_2$; it is also clear that $\|w\|_2 = 0$ if $\|v\|_\infty \leq 1$. In fact, there is a simple relationship which connects these two results

$$\|w\|_2 \leq \begin{cases} 0 & \text{if } \|v\|_\infty \leq 1 \\ \left(1 - \frac{1}{\|v\|_\infty}\right) \|v\|_2 & \text{if } \|v\|_\infty > 1 \end{cases}$$

This, then, is a local result: if v is in some restricted set (for example, if $\|v\|_\infty < \varepsilon$) then the "gain" of the operator (to use the term loosely) may be bounded (by zero if $\varepsilon \leq 1$ and by $1 - \frac{1}{\varepsilon}$ otherwise)

The same concept can be extremely useful if the operator does not satisfy a global gain bound: consider a nonlinear function defined by

$$w(t) = \left\{v(t)\right\}^2$$

This function does not have a finite gain: for any $\gamma > 0$ there exists $v \in \mathcal{L}_2$ such that $\|w\|_2 > \gamma \|v\|_2$; however, the following local relationship *does* hold for all $v \in \mathcal{L}_2$ with bounded magnitude

$$\|w\|_2 \leq \|v\|_\infty \|v\|_2$$

These two simple examples were dependent on the magnitude ($\mathcal{L}_\infty$-norm) of the input signal v; the local stability results we derive in Chapter 3 will relate the energy content ($\mathcal{L}_2$-norm) of the external input z and output w of a nonlinear system, and will take the following form:

$$\|w\|_2 < \mathcal{F}(\varepsilon) \|z\|_2 \quad \text{if } \|z\|_2 < \varepsilon$$

where we give methods for (conservatively) estimating the nonlinear "gain" $\mathcal{F}(\varepsilon)$ for values of ε in some range (which may be finite or infinite, depending on whether the nonlinear system is stable.)

Our motivation is that bounding the energy content is a good way to model isolated disturbances (such as wind gusts affecting an aircraft), although of course it is less good for modelling persistent disturbances (such as noisy measurements.)

[1]With the assumption of causality, all such results will also hold on truncated time intervals $[0, T]$, ie

$$\|\Pi_T w\|_2 \leq \|G\|_\infty \|\Pi_T v\|_2$$

where Π_T denotes the truncation operator (which we define on page 13)

Nonlinear actuators

The second part of the thesis (Chapter 4) is concerned with the modelling and control of systems with nonlinear actuators.

As stated earlier, we assume that the system comprises a linear plant and a nonlinear actuator. We then assume that the actuator has two distinct regimes of operation: a linear time-invariant behaviour for input signals in a nominal range, and a nonlinear behaviour for other signals. This may be considered a vast over-simplification, but it is a common assumption (and much more realistic than assuming, for example, perfect ideal saturation)

We then introduce the concept of modifying the control signal so that the actuator remains in its nominal range of operation. This concept is not new — it is common practice to saturate the control signal before applying it to the system (indeed, a Digital-to-Analogue Converter does this implicitly!) — but the approach does not appear to have been discussed widely in the anti-windup literature.

For a number of common actuator nonlinearities (including magnitude and/or rate limitations) we provide a method of achieving this modification in a manner which is robust to errors in estimating the parameters of the actuator nonlinearity.

Anti-windup control

The final part of the thesis (Chapter 5) is concerned with designing control systems which (wholly or partially) compensate for actuator nonlinearities.

We assume that the system can be represented by linear time-invariant dynamics with an input-additive nonlinear perturbation, and furthermore assume that a linear, time-invariant controller for the nominal dynamics is provided *a priori*.

We then show how to parametrise families of linear, time-invariant anti-windup compensators which recover the nominal linear behaviour if the nonlinearities are inactive for all time.

Anti-windup compensator synthesis for a simple magnitude limitation (saturation) is discussed in some detail; we state under what conditions the closed-loop system may be stabilised, and give a synthesis method for this case which guarantees $\mathcal{L}_2$ performance (in a certain sense.)

In the case when the closed-loop system may not be stabilised, we discuss how to synthesise an anti-windup controller to optimise local stability (in a certain sense.)

We then briefly discuss anti-windup synthesis for other actuator nonlinearities.

1.1 Outline of the thesis

Chapter 2: Preliminaries

In Section 2.1 we briefly outline some essential standard information about spaces of constants, signals, linear operators and nonlinear operators. Then in Section 2.2 we discuss in some detail the properties of saturation and deadzone functions. Finally, in Section 2.3 we present a method for determining approximate solutions to mixed $\mathcal{H}_2$-$\mathcal{H}_\infty$ problems.

Chapter 3: Stability analysis of nonlinear systems

In Section 3.1 we motivate and formulate our stability analysis problem, followed in Section 3.2 by a discussion of a generalisation of the $\mathcal{H}_\infty$ norm which will play a large part in the local stability analysis. Then, in Section 3.3 we collect a number of known results relating to *global* stability analysis. In this section we also give a simple $\mathcal{H}_\infty$-norm-based stability criterion for $[0, 1]$ sector-bounded nonlinearities, which is related to the well-known Circle criterion.

In Section 3.4 we present a novel method for determining the *local* stability properties of a simple system comprising a linear, time-invariant transfer function and a nonlinear feedback. The method is derived initially for the ideal unity deadzone nonlinearity, and then generalised to a large class of deadzone-like nonlinearities. This analysis is illustrated by a number of examples.

Chapter 4: Systems with nonlinear actuators

In Section 4.1 we discuss how to model nonlinear actuators and introduce the idea of a precompensator to ensure that the actuator remains in its nominal linear regime, then in Section 4.2 we discuss sets of signals which do not violate specified magnitude or rate constraints.

In Section 4.3 we then consider models and precompensators for some common actuator nonlinearities, including magnitude and/or rate limitations. Having determined the appropriate precompensator for each case we then show how the resulting interconnection is suitable for anti-windup compensation.

Chapter 5: Anti-windup control

In Section 5.1 we discuss the concept of anti-windup compensation, and formulate the problem of synthesising a compensator to guarantee stability in both a global and a local sense. Section 5.2 then proposes a tractable parametrisation of all (useful) anti-windup compensators, based on coprime factors and derived from the unified framework of Kothare *et al* [KCMN94].

Finally, in Section 5.3 we combine many results from the preceeding chapters to give a complete overview of the anti-windup control problem for each of the actuator nonlinearities discussed in Chapter 4.

The question of synthesis in the case of an input magnitude limitation (saturation) is discussed in some detail, and a method is proposed which guarantees both global stability and $\mathcal{L}_2$ performance (in a certain sense) for stable nominal plants. For unstable nominal plants we discuss how to optimise local stability, in the sense of Section 3.4.

Synthesis for other limitations is briefly discussed, and it is shown that a (suboptimal, in some sense) scheme exists which guarantees global stability in each case, provided that the nominal plant is stable.

Chapter 6: Conclusions

The main contributions of the thesis are summarised, and some suggestions for future work are made.

Appendix A: Design example

To illustrate the methods presented in the body of the thesis we give a design example which demonstrates the synthesis and analysis of an anti-windup compensator for a simple unstable plant.

1.2 List of symbols and definitions

General symbols & definitions (used throughout)

$\mathbb{R}$, $\mathbb{C}$	The real and complex numbers respectively
$\mathrm{Diag}\{a_1, a_2, \cdots, a_n\}$	The diagonal composition of $a_1, a_2, \cdots, a_n$
$\mathcal{L}_p$ and $\mathcal{L}_{pe}$	Spaces of Lebesgue integrable signals, and their extensions
$\mathcal{C}$	The space of continuous signals
$\mathcal{D}_+$	The space of right-differentiable signals
$\mathcal{R}_p$	The space of proper real-rational transfer functions
$\left[\begin{array}{c\|c} A & B \\ \hline C & D \end{array}\right]$	State-space representation of a member of $\mathcal{R}_p$
$\mathcal{RH}_\infty$	The stable subspace of $\mathcal{R}_p$
$\mathcal{RH}_2$	The strictly proper subspace of $\mathcal{RH}_\infty$
Π_T	Equation 2.1 on page 13
Coprime factorisations	Definition 2.1 on page 17
$\mathcal{Q}$	Equation 2.5 on page 17
Saturation functions	Definitions 2.2 & 2.3 on pages 21 & 24
Sat_a & $\mathbf{Sat}_A$	Equations 2.8 & 2.15 on pages 22 & 24
Dzn_a & $\mathbf{Dzn}_A$	Equations 2.9 & 2.16 on pages 22 & 24
Sgn & **Sgn**	Equations 2.11 & 2.17 on pages 23 & 24
$\boldsymbol{\Delta}_\psi$	Definition 2.4 on page 27
Well-posedness	Definition 3.3 on page 52
Stability	Definition 3.4 on page 52
Local stability	Definition 3.5 on page 53

Symbols & definitions specific to Chapter 3 (Stability analysis)

Many of the following symbols are defined twice: once for the specific case of the deadzone nonlinearity (in Section 3.4.1), and then later in a more general way (in Section 3.4.2) In these cases, the equation number and page reference for the general definition are given first, with the deadzone-specific case given in parentheses.

μ	Equation 3.12 on page 51
ρ	Equation 3.13 on page 51
$\mathrm{Sq}_{\boldsymbol{M}}$, $\mathrm{Sq}_{[\mathrm{upper}]}$ & $\mathrm{Sq}_{[\mathrm{lower}]}$	Equations 3.1, 3.2 & 3.3 on pages 42, 43 & 43
$\Gamma_{[F,G]}$, $\Gamma_{[\mathrm{upper}]}$ & $\Gamma_{[\mathrm{lower}]}$	Definition 3.1 on page 44
$\gamma_{[F,G]}$, $\gamma_{[\mathrm{upper}]}$ & $\gamma_{[\mathrm{lower}]}$	Definition 3.2 on page 47
$\lambda^0_{[F,G]}$, $\lambda^0_{[\mathrm{upper}]}$ & $\lambda^0_{[\mathrm{lower}]}$	Equations 3.34 (3.19), 3.40 & 3.40 on pages 70 (57), 71 & 71
$\lambda^1_{[F,G]}$, $\lambda^1_{[\mathrm{upper}]}$ & $\lambda^1_{[\mathrm{lower}]}$	Equations 3.35 (3.20), 3.41 & 3.41 on pages 70 (57), 71 & 71
$\lambda^{\mathrm{opt}}_{[F,G]}$	Equation 3.50 (3.31) on page 81 (67)
$\boldsymbol{\Lambda}_{[\boldsymbol{F},\boldsymbol{G}]}$, $\boldsymbol{\Lambda}_{[\mathrm{upper}]}$ & $\boldsymbol{\Lambda}_{[\mathrm{lower}]}$	Equations 3.36 (3.21), 3.42 & 3.42 on pages 71 (58), 71 & 71
$Z_{[F,G]}$, $Z_{[\mathrm{upper}]}$ & $Z_{[\mathrm{lower}]}$	Equations 3.37 (3.22), 3.43 & 3.43 on pages 71 (62), 71 & 71
$Z^0_{[F,G]}$, $Z^0_{[\mathrm{upper}]}$ & $Z^0_{[\mathrm{lower}]}$	Equations 3.38 (3.24), 3.44 & 3.44 on pages 71 (63), 71 & 71
$Z^{\mathrm{opt}}_{[F,G]}$, $Z^{\mathrm{opt}}_{[\mathrm{upper}]}$ & $Z^{\mathrm{opt}}_{[\mathrm{lower}]}$	Equations 3.39 (3.23), 3.45 & 3.45 on pages 71 (62), 71 & 71

Symbols & definitions specific to Chapter 4 (Systems with nonlinear actuators)

$P_{\mathrm{lin}}(s)$	LTI dynamics of plant
$P_{\mathrm{act}}(s)$	Nominal dynamics of limited-authority actuator
$\boldsymbol{\mathcal{U}}_{\mathrm{act}}$	Output constraint space for limited-authority actuator
$\boldsymbol{\mathcal{U}}_{\mathrm{nom}}$	Nominal input space for limited-authority actuator
$\hat{\boldsymbol{\mathcal{U}}}_{\mathrm{nom}}$	Estimated subset of $\boldsymbol{\mathcal{U}}_{\mathrm{nom}}$
Precompensator admissability	Definition 4.1 on page 99
$\mathfrak{M}_a$ & $\boldsymbol{\mathfrak{M}}_A$	Equations 4.3 & 4.4 on page 100
$\mathfrak{R}_b$ & $\boldsymbol{\mathfrak{R}}_B$	Equations 4.5 & 4.6 on page 100
$\mathfrak{M}^1_{a,c}$ & $\boldsymbol{\mathfrak{M}^1}_{A,C}$	Equations 4.7 & 4.8 on page 101
$\mathfrak{R}^1_{b,c}$ & $\boldsymbol{\mathfrak{R}^1}_{B,C}$	Equations 4.9 & 4.10 on page 103

Symbols & definitions specific to Chapter 5 (Anti-windup compensators)

Anti-windup stabilisation problem	Problem 5.1 on page 131
Local anti-windup stabilisation problem	Problem 5.2 on page 131

Chapter 2

Preliminaries

2.1 Spaces of constants, signals and operators

2.1.1 Scalars, vectors and matrices

Let $\mathbb{R}$ and $\mathbb{C}$ denote the real and complex numbers respectively. Intervals of real numbers (possibly including the point at infinity) are denoted in the usual way[1] as $[a, b]$, $[a, b)$, $(a, b]$ and (a, b). The interval $[0, \infty)$, ie the non-negative reals, is denoted $\mathbb{R}_+$.

$v \in \mathbb{R}$ (or $v \in \mathbb{C}$) is then a *constant scalar*, $\boldsymbol{v} \in \mathbb{R}^m$ (or $\boldsymbol{v} \in \mathbb{C}^m$) a *constant vector*, and $A \in \mathbb{R}^{m\times n}$ (or $A \in \mathbb{C}^{m\times n}$) a *constant matrix*. We will often omit the dimension if it is essentially arbitary, or clear from context, and unless otherwise noted we shall observe the convention of **bold**face for vectors and capital letters for matrices. We identify the individual elements of $\boldsymbol{v}$ and A as:

$$\boldsymbol{v} = \begin{bmatrix} v_1 \\ v_2 \\ \vdots \\ v_m \end{bmatrix} \qquad A = \begin{bmatrix} A_{11} & A_{12} & \cdots & A_{1n} \\ A_{21} & A_{22} & \cdots & A_{2n} \\ \vdots & \vdots & \ddots & \vdots \\ A_{m1} & A_{m2} & \cdots & A_{mn} \end{bmatrix}$$

and will use the notation $A = \mathrm{Diag}\{A_1, A_2, \cdots, A_n\}$ to mean

$$A = \begin{bmatrix} A_1 & 0 & \cdots & 0 \\ 0 & A_2 & \cdots & 0 \\ \vdots & \vdots & \ddots & \vdots \\ 0 & 0 & \cdots & A_n \end{bmatrix}$$

Note that we will occasionally write $A = \mathrm{Diag}\{A_i\}$ as shorthand.

The *trace* of a square matrix is defined as

$$\mathrm{Trace}(A) = A_{11} + A_{22} + A_{33} + \cdots + A_{nn}$$

and is equal to the sum of the eigenvalues[2] of A.

[1] Some authors insist that $a \leq b$ for the interval to be defined; we do not take this view, but simply assume that if $a > b$ then the interval is empty.

[2] A scalar λ is an eigenvalue of H if there exists some $\boldsymbol{v}$ such that $H\boldsymbol{v} = \lambda\boldsymbol{v}$.

We measure the size of scalars, vectors and matrices in the usual way as

$$|v| := \sqrt{v^* v}$$
$$\|\boldsymbol{v}\| := \sqrt{\boldsymbol{v}^* \boldsymbol{v}}$$
$$\|A\| := \sqrt{\lambda_{\max}(A^* A)}$$

where A^* denotes the complex conjugate transpose of A (note that for real A this is identical to the transpose A^T) and $\lambda_{\max}(A^* A)$ denotes the largest eigenvalue of $A^* A$.

2.1.2 Signals and signal spaces

The basic signal spaces considered in this thesis are the $\mathcal{L}_p$ spaces ($1 \leq p \leq \infty$), which are Banach spaces[3] of equivalence classes[4] of Lebesgue measurable[5] signals defined on positive time.

For $1 \leq p < \infty$, the elements of $\mathcal{L}_p$ are those signals for which the pth power of the absolute instantaneous value of the signal is Lebesgue integrable and finite. The norm on $\mathcal{L}_p$ is then defined as

$$\|\boldsymbol{v}\|_p := \left(\int_0^\infty \|\boldsymbol{v}(t)\|^p \, dt \right)^{\frac{1}{p}}$$

The elements of $\mathcal{L}_\infty$ are those signals which are essentially bounded. The norm on $\mathcal{L}_\infty$ is then defined as

$$\|\boldsymbol{v}\|_\infty := \operatorname*{ess\,sup}_{t \in [0,\infty)} \|\boldsymbol{v}(t)\|$$

We also use the so-called extended spaces $\mathcal{L}_{pe}$ ($1 \leq p \leq \infty$), for which we require the *truncation operator* Π defined for $T \geq 0$ as

$$(\Pi_T \boldsymbol{v})(t) := \begin{cases} \boldsymbol{v}(t) & \text{for } t \in [0, T] \\ 0 & \text{otherwise} \end{cases} \tag{2.1}$$

which allows us to define $\mathcal{L}_{pe}$ ($1 \leq p \leq \infty$) as

$$\mathcal{L}_{pe} := \left\{ \boldsymbol{v} : \Pi_T \boldsymbol{v} \in \mathcal{L}_p \text{ for all finite } T \geq 0 \right\} \tag{2.2}$$

[3]A Banach space is a *complete* normed vector space, ie one where every Cauchy sequence converges; a Cauchy sequence $\boldsymbol{v}_1, \boldsymbol{v}_2, \ldots$ is one where, for any $\varepsilon > 0$, there exists some integer N such that $\|\boldsymbol{v}_n - \boldsymbol{v}_m\| < \varepsilon$ for all $n, m \geq N$.

[4]Two signals $\boldsymbol{v}_1, \boldsymbol{v}_2$ are said to be *equivalent* if they are equal almost everywhere.

[5]A signal $\boldsymbol{v}(t)$ is Lebesgue measurable if all of its scalar components are Lebesgue measurable; a scalar signal $v_i(t)$ is Lebesgue measurable if its inverse maps any Borel subset of $\mathbb{R}$ to another Borel subset of $\mathbb{R}$; a Borel set is one which is generated by any countable number of unions and/or intersections of intervals.

Note that the norm on $\mathcal{L}_p$ (for any $1 \leq p \leq \infty$) is a true norm on the equivalence classes, but only a semi-norm on the signals which make up those equivalence classes. For example, the nonzero signal

$$v(t) = \begin{cases} 2 & \text{when } t = 2 \\ 0 & \text{otherwise} \end{cases}$$

has $\mathcal{L}_p$-norm of zero (for any $1 \leq p \leq \infty$), since it is in fact equivalent to the signal $\tilde{v}(t) = 0 \quad \forall T \geq 0$.

Certain useful properties of the $\mathcal{L}_p$ and $\mathcal{L}_{pe}$ spaces are collected in the following proposition (these are all standard analysis results; see eg Weir [Wei73]):

Proposition 2.1

- $\mathcal{L}_p \subset \mathcal{L}_{pe}$ *for each* $1 \leq p \leq \infty$
- $\mathcal{L}_{\infty e} \subset \mathcal{L}_{2e} \subset \mathcal{L}_{1e}$ *but* $\mathcal{L}_\infty \not\subseteq \mathcal{L}_2 \not\subseteq \mathcal{L}_1$
- *For any* $\boldsymbol{v} \in \mathcal{L}_{pe}$ $(1 \leq p \leq \infty)$*, the function* $f : \mathbb{R} \to \mathbb{R}$ *given by*

  $$f(T) := \|\Pi_T \boldsymbol{v}\|_p$$

  is a monotone non-decreasing *function, and for* $p = 2$ *it is also a* continuous *function. Furthermore*

  $$\lim_{T\to 0} f(T) = 0 \qquad \text{if } p \neq \infty$$
  $$\lim_{T\to\infty} f(T) = \begin{cases} \|\boldsymbol{v}\|_p & \text{if } \boldsymbol{v} \in \mathcal{L}_p \\ \infty & \text{otherwise} \end{cases}$$

- *Given a signal* $\boldsymbol{v} \in \mathcal{L}_{2e}$*, a time* T_1 *and a number* $k_1 \geq 0$ *such that* $\|\Pi_{T_1} \boldsymbol{v}\|_2 = k_1$*, then for any number* $0 \leq k_0 \leq k_1$ *there exists some time* T_0 *such that*

  $$\|\Pi_{T_0} \boldsymbol{v}\|_2 = k_0$$

  and furthermore

  $$\begin{aligned} 0 \leq \|\Pi_T \boldsymbol{v}\|_2 &\leq k_0 \quad \text{for any } 0 \leq T \leq T_0 \\ k_0 \leq \|\Pi_T \boldsymbol{v}\|_2 &\leq k_1 \quad \text{for any } T_0 \leq T \leq T_1 \end{aligned}$$

Remark

1. In the remainder of the thesis we shall consider only signals in $\mathcal{L}_{2e}$; this choice includes $\mathcal{L}_2$, $\mathcal{L}_{\infty e}$ and $\mathcal{L}_\infty$, the spaces of continuous signals, magnitude-limited signals and rate-limited signals, and all combinations (intersections and unions) of these spaces.

2.1.3 Linear time-invariant operators

Let $\mathcal{R}_p^{n\times m}$ denote the space of rational proper transfer functions of size n by m. Given a set of finite-dimensional linear time-invariant ordinary differential equations of the form

$$\begin{aligned} \frac{d\boldsymbol{x}}{dt} &= A\boldsymbol{x} + B\boldsymbol{u}; \qquad \boldsymbol{x}(0) = \boldsymbol{x}_0 \\ \boldsymbol{y} &= C\boldsymbol{x} + D\boldsymbol{u} \end{aligned}$$

(which is often denoted by $\left[\begin{array}{c|c} A & B \\ \hline C & D \end{array}\right]$), and with the assumption that $\boldsymbol{x}_0 = 0$, then the operator which maps $\boldsymbol{u} \in \mathcal{L}_{2e}^m$ to $\boldsymbol{y} \in \mathcal{L}_{2e}^n$ may be represented by an element $G \in \mathcal{R}_p^{n\times m}$ with transfer function $G(s) = D + C(sI - A)^{-1}B$.

G is said to be *stable* if all the eigenvalues of A have strictly negative real part (equivalently, if they are in the open left half-plane) and *unstable* otherwise.

We use the standard notation $\mathcal{RH}_\infty^{n\times m} \subset \mathcal{R}_p^{n\times m}$ for the space of stable real-rational transfer functions of size n by m, and $\mathcal{RH}_2^{n\times m} \subset \mathcal{RH}_\infty^{n\times m}$ for the space of stable, strictly-proper, real-rational transfer functions of size n by m. We denote the usual norms on these spaces by $\|.\|_\infty$ and $\|.\|_2$ respectively:

$$\|G\|_\infty := \sup_{\omega\in\mathbb{R}\cup\infty} \sqrt{\lambda_{\max}\big(G^*(j\omega)G(j\omega)\big)} \tag{2.3}$$

$$\|G\|_2 := \sqrt{\frac{1}{2\pi}\int_{-\infty}^{\infty} \operatorname{Trace}\big(G^*(j\omega)G(j\omega)\big)\,d\omega} \tag{2.4}$$

The following induced norms from $\mathcal{L}_2^m$ to $\mathcal{L}_2^n$ and from $\mathcal{L}_\infty^1$ to $\mathcal{L}_\infty^1$ are standard (eg Zhou *et al* [ZDG96]):

Proposition 2.2
If $G \in \mathcal{RH}_\infty^{n\times m}$ then

$$\sup_{\boldsymbol{v}\in\mathcal{L}_2^m, \|\boldsymbol{v}\|_2\neq 0} \frac{\|G\boldsymbol{v}\|_2}{\|\boldsymbol{v}\|_2} = \|G\|_\infty$$

If $g(t) \in \mathcal{L}_1^1$ and $G(s) = \int_0^\infty g(t)e^{-st}\,dt$ then

$$\sup_{v\in\mathcal{L}_\infty^1, \|v\|_\infty\neq 0} \frac{\|Gv\|_\infty}{\|v\|_\infty} = \|g(t)\|_1$$

Remark

1. We will sometimes write $\|G(s)\|_1$ to mean $\|g(t)\|_1$ where $G(s) = \int_0^\infty g(t)e^{-st}\,dt$, assuming that some such $g \in \mathcal{L}_1$ exists.

The following Proposition gives the induced norm from $\mathcal{L}_2^m$ to $\mathcal{L}_\infty^n$, taking the $\mathcal{L}_\infty$-norm in both its temporal and spatial senses; a proof is included for completeness, since although the result is well-known it is often omitted from standard textbooks.

Proposition 2.3

If $G = \begin{bmatrix} G_1 \\ G_2 \\ \vdots \\ G_n \end{bmatrix}$ *with each* $G_i \in \mathcal{RH}_2^{1\times m}$, *then*

$$\sup_{\boldsymbol{v}\in\mathcal{L}_2^m, \|\boldsymbol{v}\|_2\neq 0} \frac{\max_i \|G_i\boldsymbol{v}\|_\infty}{\|\boldsymbol{v}\|_2} = \max_i \|G_i\|_2 \leq \|G\|_2$$

PROOF OF PROPOSITION 2.3:

We show only the case for $n = 1$; the general multivariable case follows immediately.

The proof relies on the fact that $\mathcal{L}_2^m$ is an inner product space with inner product defined as

$$< \boldsymbol{x}, \boldsymbol{y} >: = \int_0^\infty \{\boldsymbol{x}(\tau)\}^T \boldsymbol{y}(\tau)\, d\tau$$

This inner product satisfies $< \boldsymbol{x}, \boldsymbol{y} >= \|\boldsymbol{x}\|_2 \|\boldsymbol{y}\|_2 \cos(\theta)$ where θ is the "angle" between $\boldsymbol{x}$ and $\boldsymbol{y}$, and hence also $< \boldsymbol{x}, \boldsymbol{x} >= \|\boldsymbol{x}\|_2^2$.

Now assume that $G \in \mathcal{RH}_2^{1\times m}$, $\boldsymbol{v} \in \mathcal{L}_2^m$ and $w = G\boldsymbol{v}$. Then for any $t \geq 0$

$$w(t) = \int_0^t \boldsymbol{g}(t-\tau)\boldsymbol{v}(\tau)\, d\tau$$

where $\boldsymbol{g}(\tau)$ is the impulse response of $G(s)$, and hence

$$w(t) =< \boldsymbol{g}_t^*, \boldsymbol{v} >$$

where $\boldsymbol{g}_t^*$ is a time-shifted, time-reversed transpose of $\boldsymbol{g}$ projected onto positive time, defined by

$$\boldsymbol{g}_t^*(\tau) := \begin{cases} 0 & \text{for } \tau < 0 \\ \{\boldsymbol{g}(t-\tau)\}^T & \text{for } \tau \geq 0 \end{cases}$$

It is now clear that

$$\sup_{\boldsymbol{v}\in\mathcal{L}_2^m, \|\boldsymbol{v}\|_2\neq 0} \frac{|w(t)|}{\|\boldsymbol{v}\|_2} = \|\boldsymbol{g}_t^*\|_2 = \|\Pi_t \boldsymbol{g}\|_2$$

holds for all $t \geq 0$; tightness is shown by setting $\boldsymbol{v} = \boldsymbol{g}_t^*$.

Finally, recalling that $\|w\|_\infty := \sup_{t\geq 0} |w(t)|$

$$\sup_{\boldsymbol{v}\in\mathcal{L}_2^m, \|\boldsymbol{v}\|_2\neq 0} \frac{\sup_{t\geq 0} |w(t)|}{\|\boldsymbol{v}\|_2} = \sup_{t\geq 0} \left\{ \sup_{\boldsymbol{v}\in\mathcal{L}_2^m, \|\boldsymbol{v}\|_2\neq 0} \frac{|w(t)|}{\|\boldsymbol{v}\|_2} \right\} = \sup_{t\geq 0} \|\Pi_t \boldsymbol{g}\|_2 = \|\boldsymbol{g}\|_2 = \|G\|_2$$

gives the desired result. ∎

Coprime factorisations

One useful, and tractable, way of looking at linear systems is in terms of coprime factorisations (we restrict attention to coprime factors which are real-rational — this is not strictly necessary, but for real-rational linear systems there is little or no point in considering coprime factors which are not themselves real-rational):

Definition 2.1 (Coprime factorisations)
$M_0 \in \mathcal{RH}_\infty^{m\times p}$ and $N_0 \in \mathcal{RH}_\infty^{n\times p}$ are said to be right-coprime *if there exist $X_r \in \mathcal{RH}_\infty^{p\times m}$ and $Y_r \in \mathcal{RH}_\infty^{p\times n}$ such that*

$$X_r M_0 + Y_r N_0 = I_p$$

If, in addition, M_0 is square and non-singular, and

$$P = N_0 M_0^{-1}$$

for some $P \in \mathcal{R}_p^{n\times m}$, then $N_0 M_0^{-1}$ is said to be a right-coprime factorisation *of P.*

Similarly, $\tilde{M}_0 \in \mathcal{RH}_\infty^{q\times n}$ and $\tilde{N}_0 \in \mathcal{RH}_\infty^{q\times m}$ are said to be left-coprime *if there exist $X_l \in \mathcal{RH}_\infty^{n\times q}$ and $Y_l \in \mathcal{RH}_\infty^{m\times q}$ such that*

$$\tilde{M}_0 X_l + \tilde{N}_0 Y_l = I_q$$

If, in addition, $\tilde{M}_0$ is square and non-singular, and

$$P = \tilde{M}_0^{-1} \tilde{N}_0$$

for some $P \in \mathcal{R}_p^{n\times m}$, then $\tilde{M}_0^{-1} \tilde{N}_0$ is said to be a left-coprime factorisation *of P.*

Remark

1. Right-coprime factorisations are unique up to right-multiplication by a unit in $\mathcal{RH}_\infty^{p\times p}$ (see eg. Vidyasagar [Vid85]). Let $\mathcal{Q}$ denote the set of units in $\mathcal{RH}_\infty$:

$$\mathcal{Q} := \left\{ Q : Q, Q^{-1} \in \mathcal{RH}_\infty \right\} \tag{2.5}$$

   If $P = N_0 M_0^{-1}$ is a right-coprime factorisation, and $Q \in \mathcal{Q}^{p\times p}$, then

$$P = \{N_0 Q^{-1}\}\{M_0 Q^{-1}\}^{-1}$$

   is also a right-coprime factorisation. Furthermore, *all* real-rational right-coprime factorisations of P can be generated from any given right-coprime factorisation in this way.

   Similarly, left-coprime factorisations are unique up to left-multiplication by a unit in $\mathcal{RH}_\infty^{q\times q}$.

Hence, if $P = N_0 M_0^{-1}$ and $C = \tilde{V}_0^{-1} \tilde{U}_0$ are right- and left-coprime factorisations of P and C respectively, normalised such that

$$\tilde{V}_0 M_0 + \tilde{U}_0 N_0 = I$$

then all such normalised coprime factorisations of P and C are given by

$$\begin{bmatrix} M(s) \\ N(s) \end{bmatrix} = \begin{bmatrix} M_0(s) \\ N_0(s) \end{bmatrix} Q^{-1}(s)$$

$$\begin{bmatrix} \tilde{V}(s) & \tilde{U}(s) \end{bmatrix} = Q(s) \begin{bmatrix} \tilde{V}_0(s) & \tilde{U}_0(s) \end{bmatrix}$$

where $Q \in \mathcal{Q}$.

Theorem 2.4 gives lower bounds on some typical norm minimisation problems related to coprime factorisations. The results stated are for right-coprime factorisations, but by duality are also applicable to left-coprime factorisations, with obvious modifications.

Theorem 2.4 *If $P \in \mathcal{R}_p$ is a proper real-rational transfer function with open right half-plane poles p_i, and if $P = N_0 M_0^{-1}$ is any right-coprime factorisation of P, then*

$$\inf_{Q \in \mathcal{Q}} \left\| I - M_0 Q^{-1} \right\|_\infty^2 = \begin{cases} 0 & \text{if } P \in \mathcal{RH}_\infty \\ 1 & \text{otherwise} \end{cases} \tag{2.6}$$

$$\inf_{Q \in \mathcal{Q}: Q(\infty) = M_0(\infty)} \left\| I - M_0 Q^{-1} \right\|_2^2 = \begin{cases} 0 & \text{if } P \in \mathcal{RH}_\infty \\ 2 \sum p_i & \text{if } P \notin \mathcal{RH}_\infty \text{ has no } j\omega\text{-axis poles} \end{cases} \tag{2.7}$$

Remark

1. If P has one or more $j\omega$-axis poles then it seems likely that these poles contribute zero to the infimum in Equation 2.7, especially in light of the result by Ren et al. [RQC99] which is referred to in the proof below, however it is not clear that their infimum holds with the additional restriction that $Q \in \mathcal{RH}_\infty$.

PROOF OF THEOREM 2.4:

Taking Equation 2.6 first, it is clear that if P has no closed rhp poles, then we can take $Q = M_0$, and hence achieve $\|I - M_0 Q^{-1}\|_\infty = 0$. Otherwise, there will be an interpolation constraint that $M_0(p_i) Q^{-1}(p_i) = 0$ at each closed rhp pole; hence $\|I - M_0 Q^{-1}\|_\infty \geq 1$. Since this constraint does not affect the achievable infimum in any other way (eg Vinnicombe [Vin00] Theorem 1.29) we conclude that the infimum is unity.

Moving on to Equation 2.7, it is again clear that if P has no closed rhp poles, then we can achieve a zero norm with $Q = M_0$. Otherwise, it is shown by Ren et al. [RQC99] that[6]

$$\inf_{Q^{-1}\in\mathcal{RH}_\infty, Q(\infty)=M_0(\infty)} \left\|I - M_0Q^{-1}\right\|_2^2 = 2\sum p_i \quad \text{if } P \notin \mathcal{RH}_\infty$$

This result gives a lower bound on the infimum, since we require also that $Q \in \mathcal{RH}_\infty$. We now show that this infimum is achievable if P has no $j\omega$-axis poles: 0 Assume that P has no $j\omega$-axis poles and that $\left[\begin{array}{c|c} A & B \\ \hline C & D \end{array}\right]$ is a stabilisable realisation of P. Then (by Zhou et al. [ZDG96], Theorem 13.34) a right-coprime factorisation $P = NM_{\text{ap}}^{-1}$ exists where M_{ap} is an all-pass factor given by

$$M_{\text{ap}} = \left[\begin{array}{c|c} A + BF & B \\ \hline F & I \end{array}\right] \quad \text{with} \quad M_{\text{ap}}^{-1} = \left[\begin{array}{c|c} A & -B \\ \hline F & I \end{array}\right]$$

where $F = -B^*X$ and $X = X^* \geq 0$ is the solution to

$$A^*X + XA - XBB^*X = 0$$

Calculating the $\mathcal{H}_2$-norm gives (by [ZDG96], Lemma 4.6)

$$\|I - M_{\text{ap}}\|_2^2 = \left\| \left[\begin{array}{c|c} A + BF & B \\ \hline -F & 0 \end{array}\right] \right\|_2^2 = \text{Trace}(B^*L_oB)$$

where $L_o = L_o^* \geq 0$ is the observability Gramian, which is the solution to

$$(A + BF)^*L_o + L_o(A + BF) + F^*F = 0$$

It is simple algebra to verify that $L_o = X$ solves this equation, and hence that

$$\begin{aligned} \|I - M_{\text{ap}}\|_2^2 &= \text{Trace}(B^*L_oB) \\ &= \text{Trace}(-FB) \\ &= \text{Trace}(A) - \text{Trace}(A + BF) \end{aligned}$$

Now, since for any square matrix H, Trace(H) is equal to the sum of the eigenvalues of H, we see that

$$\begin{aligned} \|I - M_{\text{ap}}\|_2^2 &= \text{Trace}(A) - \text{Trace}(A + BF) \\ &= \sum p_i + \sum p_i \end{aligned}$$

since the contribution from any stable poles of M_{ap}^{-1} is exactly cancelled out by an identical negative contribution from the stable poles of M_{ap} — otherwise M_{ap} would not be an all-pass transfer function.

Finally, taking[7] $Q := M_{\text{ap}}^{-1}M_0$ gives $I - M_0Q^{-1} = I - M_{\text{ap}}$ and hence achieves the infimum of Equation 2.7. ∎

[6] Actually the left-coprime case is considered in that paper; however, since $P^T = M_0^{-T}N_0^T$ is a left-coprime factorisation of P^T, and both P and P^T have the same poles, the result carries over immediately to the right-coprime case.

[7] Note that this calculation involves an unstable pole/zero cancellation for each p_i.

2.1.4 Nonlinear and/or time-varying operators

In this thesis we will use the term *nonlinear* to mean "not necessarily linear and/or time-invariant". For such operators (here denoted by $\Delta : X \to Y$, for some spaces of signals X and Y, and assumed to map the zero signal to itself) we can identify a number of different concepts of "gain"; regardless of X and Y we take the underlying signal space to be $\mathcal{L}_{2e}$. The definitions given are based on those of Willems [Wil71]:

- An operator $\Delta : X \to Y$ has *uniform instantaneous gain at time* T given by the supremum over all $\delta > 0$ of the greatest lower bound of all numbers M_T satisfying the following inequality for all $\boldsymbol{v}, \boldsymbol{w} \in X \cap \mathcal{L}_{2e}$ and some number $K_T < \infty$:

$$\left\|(\Pi_{T+\delta} - \Pi_T)(\Delta\boldsymbol{v} - \Delta\boldsymbol{w})\right\|_2 \leq K_T \left\|\Pi_T(\boldsymbol{v} - \boldsymbol{w})\right\|_2 + M_T \left\|(\Pi_{T+\delta} - \Pi_T)(\boldsymbol{v} - \boldsymbol{w})\right\|_2$$

- An operator $\Delta : X \to Y$ has *instantaneous gain at time* T given by

$$\inf_{\delta>0} \sup_{\boldsymbol{v},\boldsymbol{w} \in X \cap \mathcal{L}_{2e}, \|\Pi_T(\boldsymbol{v}-\boldsymbol{w})\|_2 = 0, \|\Pi_{T+\delta}(\boldsymbol{v}-\boldsymbol{w})\|_2 \neq 0} \frac{\left\|\Pi_{T+\delta}(\Delta\boldsymbol{v} - \Delta\boldsymbol{w})\right\|_2}{\left\|\Pi_{T+\delta}(\boldsymbol{v} - \boldsymbol{w})\right\|_2}$$

- An operator $\Delta : X \to Y$ is said to be *Lipschitz* if there exists a finite scalar k such that for all $\boldsymbol{v}, \boldsymbol{w} \in X \cap \mathcal{L}_2$

$$\left\|\Delta\boldsymbol{v} - \Delta\boldsymbol{w}\right\|_2 \leq k \left\|\boldsymbol{v} - \boldsymbol{w}\right\|_2$$

- An operator $\Delta : X \to Y$ is said to have *finite gain* if

$$\boldsymbol{v} \in X \cap \mathcal{L}_2 \Longrightarrow \Delta\boldsymbol{v} \in Y \cap \mathcal{L}_2 \quad \text{and} \quad \sup_{\boldsymbol{v} \in X \cap \mathcal{L}_2, \|\boldsymbol{v}\|_2 \neq 0} \frac{\left\|\Delta\boldsymbol{v}\right\|_2}{\left\|\boldsymbol{v}\right\|_2} < \infty$$

  in which case we denote this quantity by $\|\Delta\|$.

- A function $\Delta : X \to Y$ is said to be in the sector $[a, b]$ if for any $\boldsymbol{v} \in X \cap \mathcal{L}_2$

$$\int_0^\infty \big((\Delta\boldsymbol{v})(t) - a\boldsymbol{v}(t)\big)^* \big((\Delta\boldsymbol{v})(t) - b\boldsymbol{v}(t)\big)\, dt \leq 0$$

2.2 Saturation and deadzone functions

2.2.1 Definitions and properties

Saturation and deadzone functions will be important throughout this work. The basic definition is standard:

Definition 2.2 (Saturation function)
An odd Lipschitz function $\sigma : \mathbb{R} \to \mathbb{R}$ is said to be a saturation function *if there exist $a > 0$, $0 < b \leq 1$ and $c \geq 1$ such that for any $v \in \mathbb{R}$*

$$\min\left\{a, b\,|v|\,\right\} \leq |\sigma(v)| \leq c\,|v|$$

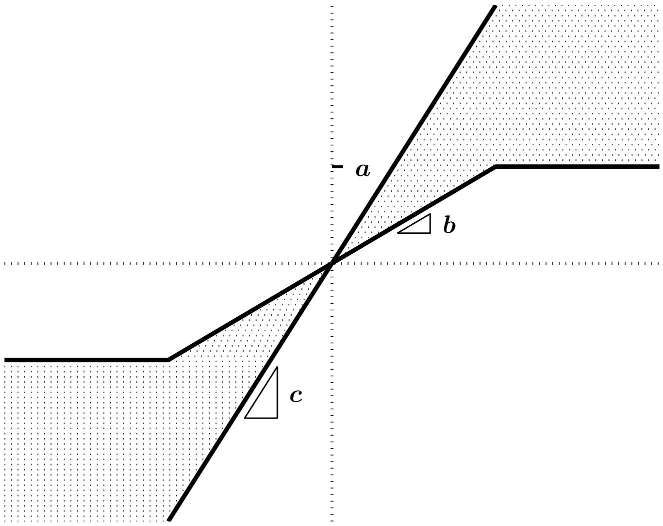

Figure 2.1: Saturation function

Remarks

1. Graphically, a saturation function lies in the shaded region of Figure 2.1.

2. Note that there is no loss of generality in choosing $b \leq 1 \leq c$, since any function satisfying the condition in Definition 2.2 only for $b \leq k \leq c$ (for some $k > 0$) can be made to satisfy the Definition by simple scaling.

   Note also that the identity operator $\sigma(v) = v$ is included in this definition.

Clearly the ideal saturation function $\mathrm{Sat}_a : \mathbb{R} \to \mathbb{R}$, for $a > 0$, defined as

$$\mathrm{Sat}_a(v) := \begin{cases} a & \text{if } v > a \\ v & \text{if } |v| \leq a \\ -a & \text{if } v < -a \end{cases} \tag{2.8}$$

satisfies Definition 2.2. This function is shown in Figure 2.2 (a).

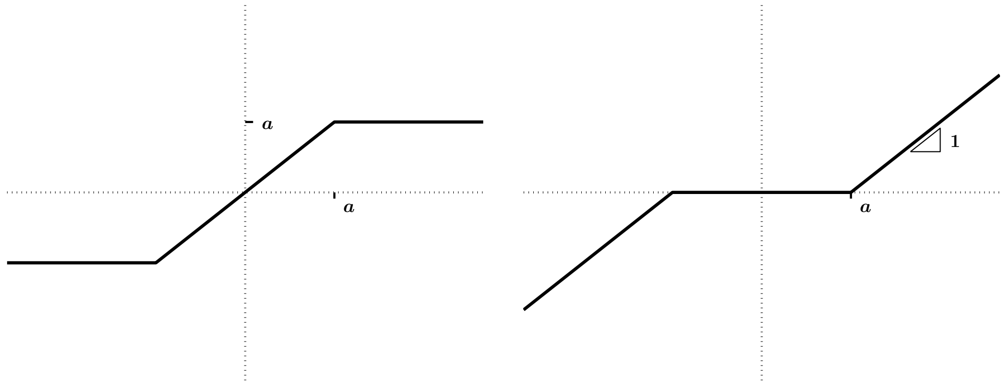

(a) Ideal saturation function (b) Ideal deadzone function

Figure 2.2: Ideal saturation and ideal deadzone functions

The ideal deadzone function $\mathrm{Dzn}_a : \mathbb{R} \to \mathbb{R}$, defined as

$$\mathrm{Dzn}_a(v) := \begin{cases} v - a & \text{if } v > a \\ 0 & \text{if } |v| \leq a \\ v + a & \text{if } v < -a \end{cases} \tag{2.9}$$

is the natural complement of the ideal saturation function, in the sense that for any $a > 0$ and $v \in \mathbb{R}$

$$\mathrm{Sat}_a(v) + \mathrm{Dzn}_a(v) = v \tag{2.10}$$

This function is shown in Figure 2.2 (b). We will use Sat(.) and Dzn(.) to denote the unity saturation and deadzone functions $\mathrm{Sat}_1(.)$ and $\mathrm{Dzn}_1(.)$, respectively.

The signum relation $\mathrm{Sgn} : \mathbb{R} \to \mathbb{R}$, defined as[8]

$$\mathrm{Sgn}(v) = \begin{cases} 1 & \text{if } v > 0 \\ \in [-1, 1] & \text{if } v = 0 \\ -1 & \text{if } v < 0 \end{cases} \tag{2.11}$$

is closely related to the ideal deadzone function, in the sense that for any $a > 0$ and $v \in \mathbb{R}$

$$\mathrm{Dzn}_a\big(v + a\,\mathrm{Sgn}(v)\big) = v \tag{2.12}$$

It is clear that the signum relation can be approximated by an ideal saturation function with high gain, ie that for any $a > 0$

$$a\,\mathrm{Sgn}(v) \approx \mathrm{Sat}_a(kv)$$

for some $k \gg 1$, as shown in Figure 2.3.

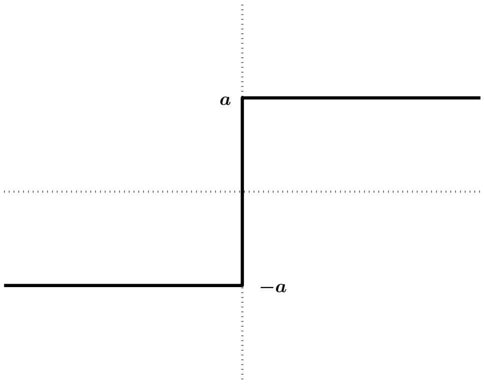

(a) $a\,\mathrm{Sgn}(v)$

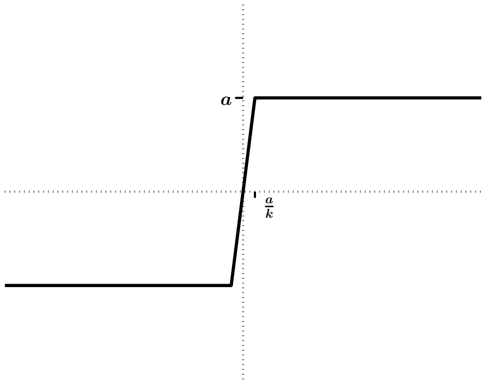

(b) $\mathrm{Sat}_a(kv)$

Figure 2.3: Signum relation and high-gain saturation function

It is easily verified that for any $a > 0$ and any $v \in \mathbb{R}$

$$\mathrm{Sat}_a(av) = a\,\mathrm{Sat}(v) \tag{2.13}$$
$$\mathrm{Dzn}_a(av) = a\,\mathrm{Dzn}(v) \tag{2.14}$$

[8]Note that we do not use the alternative definition $\mathrm{Sgn}(v) = 0$ if $v = 0$.

The multivariable equivalent of a saturation function is taken to be[9] as follows:

Definition 2.3 (Multivariable saturation function)
A function $\boldsymbol{\sigma} : \mathbb{R}^n \to \mathbb{R}^n$ is said to be a saturation function *if it is decentralised, with each component σ_i itself being a saturation function (as in Definition 2.2.)*

Given a diagonal matrix $A = \mathrm{Diag}\{a_1, a_2, \cdots, a_n\}$, $A > 0$, we denote by $\mathbf{Sat}_A : \mathbb{R}^n \to \mathbb{R}^n$ and $\mathbf{Dzn}_A : \mathbb{R}^n \to \mathbb{R}^n$ the component-wise multivariable saturation and deadzone functions, ie

$$\mathbf{Sat}_A(\boldsymbol{v}) := \begin{bmatrix} \mathrm{Sat}_{a_1}(v_1) \\ \mathrm{Sat}_{a_2}(v_2) \\ \vdots \\ \mathrm{Sat}_{a_n}(v_n) \end{bmatrix} \tag{2.15}$$

$$\mathbf{Dzn}_A(\boldsymbol{v}) := \begin{bmatrix} \mathrm{Dzn}_{a_1}(v_1) \\ \mathrm{Dzn}_{a_2}(v_2) \\ \vdots \\ \mathrm{Dzn}_{a_n}(v_n) \end{bmatrix} \tag{2.16}$$

and if $A = I$ we shall drop the subscript. Similarly, the component-wise multivariable signum function $\mathbf{Sgn} : \mathbb{R}^n \to \mathbb{R}^n$ is given by

$$\mathbf{Sgn}(\boldsymbol{v}) := \begin{bmatrix} \mathrm{Sgn}(v_1) \\ \mathrm{Sgn}(v_2) \\ \vdots \\ \mathrm{Sgn}(v_n) \end{bmatrix} \tag{2.17}$$

Analogous to Equations 2.10, 2.12, 2.13 and 2.14 we have that for any diagonal matrix $A > 0$ and any $\boldsymbol{v} \in \mathbb{R}^n$

$$\mathbf{Sat}_A(\boldsymbol{v}) + \mathbf{Dzn}_A(\boldsymbol{v}) = \boldsymbol{v} \tag{2.18}$$

$$\mathbf{Dzn}_A\big(\boldsymbol{v} + A\mathbf{Sgn}(\boldsymbol{v})\big) = \boldsymbol{v} \tag{2.19}$$

$$\mathbf{Sat}_A(A\boldsymbol{v}) = A\mathbf{Sat}(\boldsymbol{v}) \tag{2.20}$$

$$\mathbf{Dzn}_A(A\boldsymbol{v}) = A\mathbf{Dzn}(\boldsymbol{v}) \tag{2.21}$$

[9] Note that this is not the only way to define a multivariable saturation function; however, the restriction to decentralised functions clearly makes sense in most practical cases.

A couple of useful features about the ideal deadzone are summarised in the following Lemma and its immediate Corollary:

Lemma 2.5

For any diagonal matrix $A > 0$ and any $\boldsymbol{x}, \boldsymbol{y} \in \mathbb{R}^n$

$$\|\mathbf{Dzn}_A(\boldsymbol{x}+\boldsymbol{y})\| \leq \|\mathbf{Dzn}_A(\boldsymbol{x})\| + \|\boldsymbol{y}\|$$

and hence for any $\boldsymbol{v}, \boldsymbol{w} \in \mathcal{L}_2^n$

$$\|\mathbf{Dzn}_A(\boldsymbol{v}+\boldsymbol{w})\|_2 \leq \|\mathbf{Dzn}_A(\boldsymbol{v})\|_2 + \|\boldsymbol{w}\|_2$$

Corollary 2.6

For any diagonal matrix $A > 0$ and any $\boldsymbol{x}, \boldsymbol{y} \in \mathbb{R}^n$

$$\left\|\mathbf{Dzn}_A\big(A\mathbf{Sgn}(\boldsymbol{x})+\boldsymbol{y}\big)\right\| \leq \|\boldsymbol{y}\|$$

and hence for any $\boldsymbol{v}, \boldsymbol{w} \in \mathcal{L}_2^n$

$$\left\|\mathbf{Dzn}_A\big(A\mathbf{Sgn}(\boldsymbol{v})+\boldsymbol{w}\big)\right\|_2 \leq \|\boldsymbol{w}\|_2$$

PROOF OF LEMMA 2.5:

We only show the static result for the scalar case, from which the two multivariable results given follow immediately. Directly from the definition of Dzn we have that

$$\mathrm{Dzn}_a(x+y) := \begin{cases} (x-a)+(y) & \text{if } x > a \text{ and } y > a-x \\ (0)+(x-a+y) & \text{if } -a \leq x \leq a \text{ and } y > a-x \\ (x+a)+(y-2a) & \text{if } x < -a \text{ and } y > a-x \\ 0 & \text{if } -a \leq x+y \leq a \\ (x-a)+(y+2a) & \text{if } x > a \text{ and } y < -a-x \\ (0)+(x+a+y) & \text{if } -a \leq x \leq a \text{ and } y < -a-x \\ (x+a)+(y) & \text{if } x < -a \text{ and } y < -a-x \end{cases}$$

Examining these in turn

1 $\mathrm{Dzn}_a(x+y) = \mathrm{Dzn}_a(x) + y$

2 $y > a-x \geq 0$ so $y \geq y-(a-x) > 0$

3 $y > a-x > 2a$ so $y > y-2a > 0$

4 Trivial!

5 $y < -a-x < -2a$ so $y < y+2a < 0$

6 $y < -a-x \leq 0$ so $y \leq y+(a+x) < 0$

7 $\mathrm{Dzn}_a(x+y) = \mathrm{Dzn}_a(x) + y$

leads to the conclusion that $|\mathrm{Dzn}_a(x+y)| \leq |\mathrm{Dzn}_a(x)| + |y|$. ∎

The following Lemma establishes a "nonlinear sector" result for the ideal unity deadzone function, which will be central to the results presented in Section 3.4.1:

Lemma 2.7

For any $\boldsymbol{v} \in \mathcal{L}_{2e}^n$ *and* $\boldsymbol{w}(t) = \mathbf{Dzn}\big(\boldsymbol{v}(t)\big)$, *and any* $T > 0$

$$\max_i \|\Pi_T v_i\|_\infty \leq 1 \quad \Longrightarrow \quad \|\Pi_T \boldsymbol{w}\|_2 = 0 \tag{2.22}$$

$$\max_i \|\Pi_T v_i\|_\infty > 1 \quad \Longrightarrow \quad \|\Pi_T \boldsymbol{w}\|_2 \leq \left(1 - \tfrac{1}{\max_i \|\Pi_T v_i\|_\infty}\right) \|\Pi_T \boldsymbol{v}\|_2 \tag{2.23}$$

Furthermore, for any $\beta \in (0, 1)$

$$\|\Pi_T \boldsymbol{w}\|_2 \geq \beta \, \|\Pi_T \boldsymbol{v}\|_2 > 0 \quad \Longrightarrow \quad \max_i \|\Pi_T v_i\|_\infty \geq \frac{1}{1-\beta} \tag{2.24}$$

Remark

1. The first part of this Lemma is a slightly weaker version of a well-known result (eg Hindi & Boyd [HB98]; Miyamoto & Vinnicombe [MV96a] and Kothare *et al* [KM95], [KM99]) which states that if $\boldsymbol{v}$ is known to satisfy $\max_i \|v_i\|_\infty \leq r$, then the deadzone nonlinearity can be assumed to be in sector $[0, 1 - \frac{1}{r}]$ instead of $[0, 1]$. (A similar deduction applies to the saturation nonlinearity.)

   In one sense this Lemma is rather conservative, since it takes into account neither (a) different saturation levels on each channel, nor (b) the individual $\|\Pi_T v_i\|_\infty$. However, it is difficult to see how an equivalent statement to Equation 2.24 could be formulated for either of these cases.

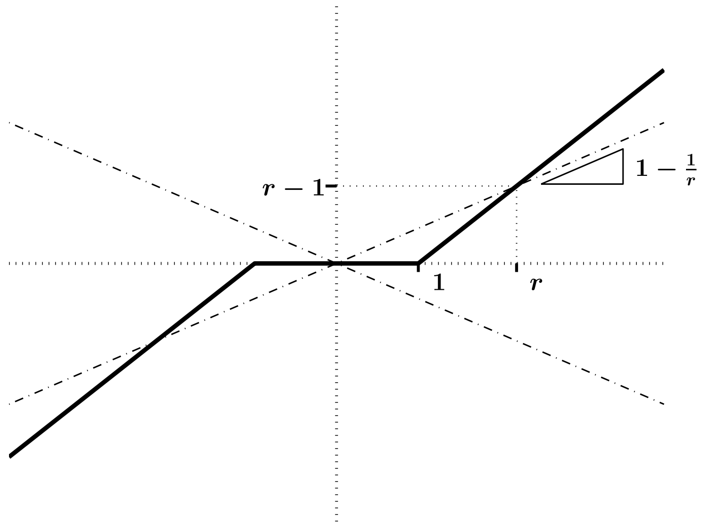

Figure 2.4: Ideal deadzone function showing "nonlinear sector" bound

PROOF OF LEMMA 2.7:

Equations 2.22 and 2.23 are best understood with reference to Figure 2.4, which shows the ideal scalar deadzone function of Equation 2.9; we show the result only for the scalar ($n = 1$) case, since the multivariable case follows immediately.

If $|v(t)| \leq 1$ for all $t \in [0, T]$ then clearly $w(t) = 0$ for all $t \in [0, T]$, from which Equation 2.22 follows immediately.

Similarly, if $|v(t)| \leq r$ for all $t \in [0, T]$, for some $r > 1$, then it is clear from the diagram that $|w(t)| \leq (1 - \frac{1}{r})\, |v(t)|$ for all $t \in [0, T]$, from which Equation 2.23 follows immediately.

To obtain Equation 2.24, we first note that Equation 2.22 implies

$$\|\Pi_T w\|_2 > 0 \quad \Longrightarrow \quad \|\Pi_T v\|_\infty > 1$$

We then substitute $\|\Pi_T w\|_2 \geq \beta \|\Pi_T v\|_2$ into the right-hand-side of Equation 2.23, giving

$$\beta \|\Pi_T v\|_2 \leq (1 - \tfrac{1}{\|\Pi_T v\|_\infty}) \|\Pi_T v\|_2$$

from which we can eliminate $\|\Pi_T v\|_2 \neq 0$ and rearrange to give Equation 2.24. ∎

The following definition characterises those scalar nonlinearities for which a "nonlinear sector" result similar to Lemma 2.7 holds:

Definition 2.4 ($\boldsymbol{\Delta}_\psi$)

Given a bijective function $\psi : (r_0, \infty) \to (\beta_0, \beta_1)$ which has finite nonzero derivative everywhere, for some scalars $r_0 \geq 0$ and $\beta_1 > \beta_0 \geq 0$, let $\boldsymbol{\Delta}_\psi$ be defined to be the family of scalar nonlinearities such that for any $\Delta \in \boldsymbol{\Delta}_\psi$

- *$\Delta : \mathcal{L}_{2e} \to \mathcal{L}_{2e}$ is causal with finite gain and finite uniform instantaneous gain*
- *For any $r > r_0$, any $v \in \mathcal{L}_2$ and $w = \Delta v$*

$$\|v\|_\infty < r \Longrightarrow \|w\|_2 < \psi(r) \|v\|_2$$

Remarks

1. Note that $\|\Delta\|_{\mathcal{L}_2 - \mathcal{L}_2} \leq \beta_1$, and that by careful choice of ψ, it should be possible to achieve equality, or almost, in this relation.

2. One interpretation of these classes of functions is that they are a generalisation of the ideal deadzone function Dzn(.), in the same way that the class of functions satisfying Definition 2.2 are a generalisation of the ideal saturation function Sat(.).

The following Lemma, which is a generalisation of Lemma 2.7, will be central to the results presented in Section 3.4.2:

Lemma 2.8

If $\boldsymbol{\Delta} = \mathrm{Diag}\{\Delta_1, \Delta_2, \cdots, \Delta_n\}$ *with* $\Delta_i \in \boldsymbol{\Delta}_\psi$ *for each* i*, for some suitable function* $\psi : (r_0, \infty) \to (\beta_0, \beta_1)$*, then for any* $\boldsymbol{v} \in \mathcal{L}_{2e}^n$ *and* $\boldsymbol{w} = \boldsymbol{\Delta v}$*, and any* $T > 0$

$$\max_i \|\Pi_T v_i\|_\infty \leq r_0 \Longrightarrow \|\Pi_T \boldsymbol{w}\|_2 \leq \beta_0 \|\Pi_T \boldsymbol{v}\|_2 \tag{2.25}$$

$$\max_i \|\Pi_T v_i\|_\infty > r_0 \Longrightarrow \|\Pi_T \boldsymbol{w}\|_2 \leq \psi(\max_i \|\Pi_T v_i\|_\infty) \|\Pi_T \boldsymbol{v}\|_2 \tag{2.26}$$

Furthermore, for any $\beta \in (\beta_0, \beta_1)$

$$\|\Pi_T \boldsymbol{w}\|_2 \geq \beta \|\Pi_T \boldsymbol{v}\|_2 > 0 \Longrightarrow \max_i \|\Pi_T v_i\|_\infty \geq \psi^{-1}(\beta) \tag{2.27}$$

Remark

1. This Lemma is again conservative, in the same sense as Lemma 2.7, and there are the same difficulties formulating an equivalent statement to Equation 2.27 which takes into account each of $\|v_i\|_\infty$ and the properties of Δ_i.

PROOF OF LEMMA 2.8:

We again show only the scalar case:

Equations 2.25 and 2.26 are clear from Definition 2.4. To obtain Equation 2.27, we first note that Equation 2.25 implies

$$\|\Pi_T w\|_2 > \beta_0 \|\Pi_T v\|_2 \quad \Longrightarrow \quad \|\Pi_T v\|_\infty > r_0$$

We then substitute $\|\Pi_T w\|_2 \geq \beta \|\Pi_T v\|_2$ into the right-hand-side of Equation 2.26, giving

$$\beta \|\Pi_T v\|_2 \leq \psi(\|\Pi_T v\|_\infty) \|\Pi_T v\|_2$$

from which we can eliminate $\|\Pi_T v\|_2 \neq 0$ and invert to give Equation 2.27. ∎

We give two scalar examples, in order to illustrate these families of nonlinear functions:

Examples

1. Consider $\psi : (1, \infty) \to (0, 1)$ given by $\psi(r) = 1 - \frac{1}{r}$

   This ψ is shown in Figure 2.5 (a). The set $\mathbf{\Delta}_\psi$ then contains (amongst others) all memoryless, Lipschitz nonlinearities which lie in the shaded "sector" of Figure 2.5 (b).

   One particular memoryless nonlinearity included in the set $\mathbf{\Delta}_\psi$ is the (ideal, unity) deadzone nonlinearity Dzn(.), shown in Figure 2.5 (c). We see that this nonlinearity coincides with the boundary of the shaded area of Figure 2.5 (b); this suggests that the relations given in Lemma 2.8 will be (relatively) non-conservative for this nonlinearity.

   In fact, the set $\mathbf{\Delta}_\psi$ contains *all* ideal deadzone functions Dzn_a with $a > 1$, as in Figure 2.5 (d). However, each of these nonlinearities is well within the shaded area of Figure 2.5 (b); this suggests that the relations given in Lemma 2.8 will be (relatively) conservative for these nonlinearities, and become progressively worse for larger a.

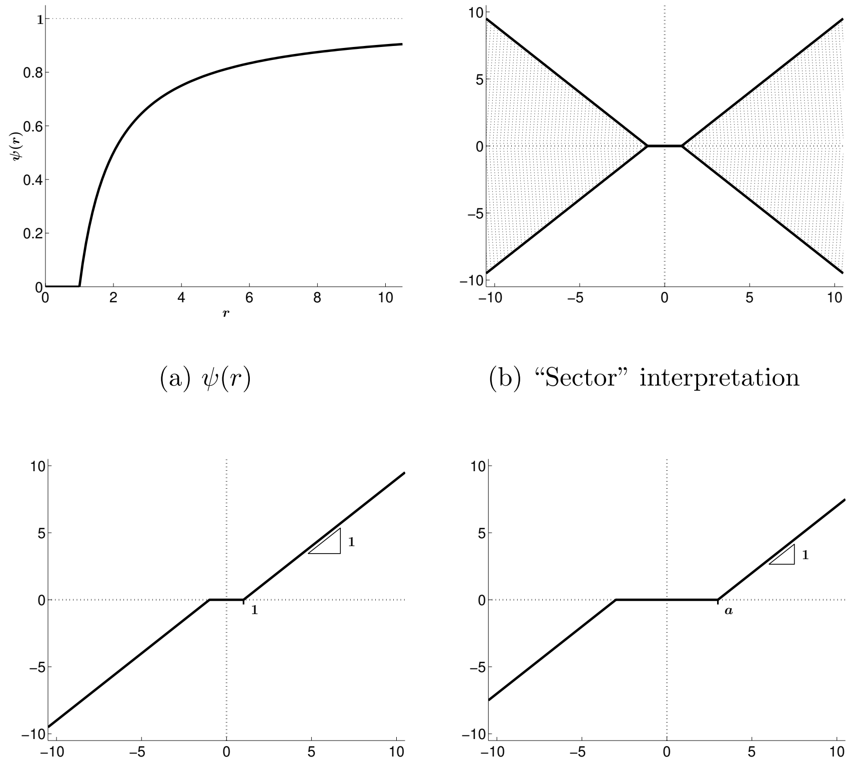

(a) $\psi(r)$ (b) "Sector" interpretation

(c) Unity deadzone (d) Dzn_a

Figure 2.5: $\mathbf{\Delta}_\psi$: Example 1

2. Consider $\psi : (0,\infty) \to (0, M+1)$ given by $\psi(r) = \begin{cases} r & \text{if } r \leq M \\ M + \frac{r-M}{r-M+1} & \text{if } r > M \end{cases}$

   This ψ is shown (for $M = 10$) in Figure 2.6 (a). The set $\mathbf{\Delta}_\psi$ then contains (amongst others) all memoryless, Lipschitz nonlinearities which lie in the shaded "sector" of Figure 2.6 (b).

   One particular memoryless nonlinearity included in the set $\mathbf{\Delta}_\psi$ is the "saturated squaring" function $w(t) := \left\{ \mathrm{Sat}_M \left(v(t) \right) \right\}^2$, shown in Figure 2.6 (c). We see that this nonlinearity coincides, for the most part, with the boundary of the shaded area of Figure 2.6 (b); this suggests that the relations given in Lemma 2.8 will be (relatively) non-conservative for this nonlinearity.

   In fact, $\mathbf{\Delta}_\psi$ also contains any ideal deadzone function Dzn_a with $a \geq \frac{1}{4}$, as in Figure 2.6 (d). However, each of these is well within the shaded area of Figure 2.6 (b); this suggests that the relations given in Lemma 2.8 will be (relatively) conservative for these nonlinearities, and become progressively worse for larger a.

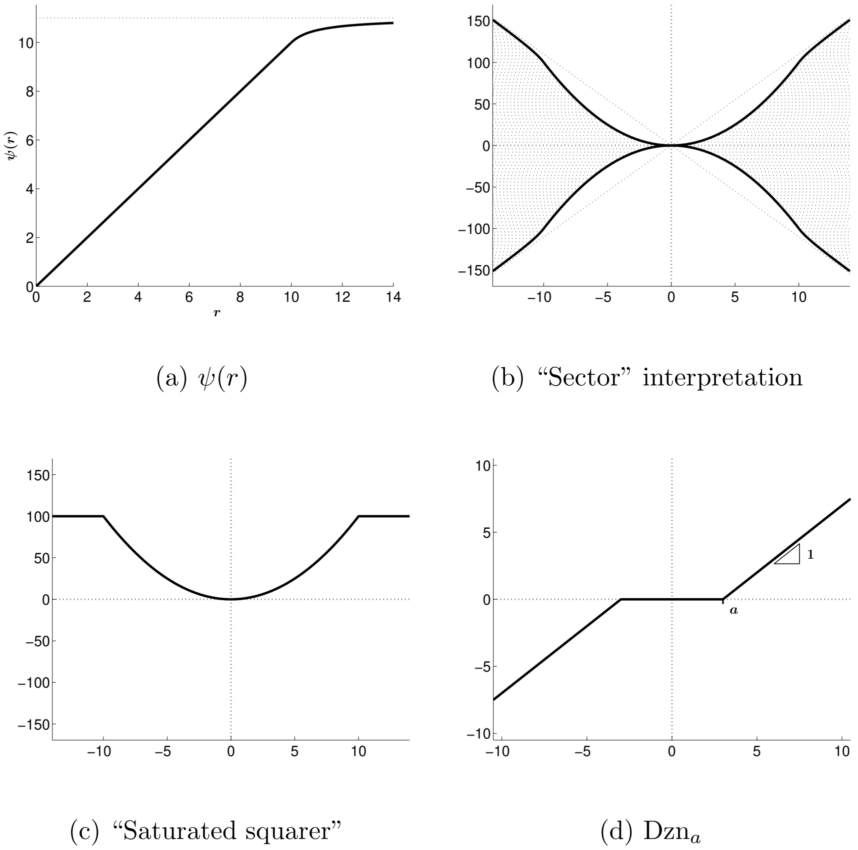

(a) $\psi(r)$ (b) "Sector" interpretation

(c) "Saturated squarer" (d) Dzn_a

Figure 2.6: $\mathbf{\Delta}_\psi$: Example 2

2.3 Mixed $\mathcal{H}_2$-$\mathcal{H}_\infty$ problems

2.3.1 Approximate solutions using linear matrix inequalities

The problem of simulaneously optimising the $\mathcal{H}_2$- and $\mathcal{H}_\infty$-norms of two (possibly identical) transfer functions has been, and remains, a topic of some interest. Much of the early work in this field (see, for example, Bernstein & Haddad [BH89]; Khargonekar & Rotea [KR91] and Zhou *et al* [ZGBD94]) considered minimising an upper bound on the $\mathcal{H}_2$-norm; more recent methods using the true $\mathcal{H}_2$-norm are given in Scherer [Sch95]; Sznaier [Szn94]; Hassibi *et al* [HHK97], [HK98] and Gahinet *et al* [GNLC95].

We consider the following version of the problem

$$\min_{Q\in\mathcal{RH}_\infty : \|L+MQ\|_\infty<\gamma} \|G+HQ\|_2$$

for some $\gamma > 0$ and compatible $L, M, G, H \in \mathcal{RH}_\infty$, which is a relatively simple special case, since the free variable Q enters affinely into both the objective and constraint transfer functions.

Our approach in Theorem 2.9 will be, given a feasible initial guess Q_i (ie one satisfying the $\mathcal{H}_\infty$-constraint), to fix the denominator of Q and to consider optimising over the numerator. This approach is similar to that of Scherer [Sch95] in that it uses a finite basis to approximate the whole of $\mathcal{RH}_\infty$; the algorithm presented does not have the guaranteed optimality properties of the algorithm described in [Sch95], but it has the advantage of being simple and ready to implement.

It might appear that this formulation gives only an incremental improvement over the initial guess Q_i, since the solution will share its denominator with Q_i. However, there is no reason why Q_i should not have a number of "extra" states which are redundant in Q_i — for example, if the initial guess in a scalar case were $Q_i = 1$, the actual state-space representation chosen could be

$$Q_i = \left[\begin{array}{c|c} \begin{bmatrix} -5 & 1 & 0 & 0 & 0 \\ -10 & 0 & 1 & 0 & 0 \\ -10 & 0 & 0 & 1 & 0 \\ -5 & 0 & 0 & 0 & 1 \\ -1 & 0 & 0 & 0 & 0 \end{bmatrix} & \begin{bmatrix} 0 \\ 0 \\ 0 \\ 0 \\ 0 \end{bmatrix} \\ \hline \begin{bmatrix} 1 & 0 & 0 & 0 & 0 \end{bmatrix} & \begin{bmatrix} 1 \end{bmatrix} \end{array}\right] = \frac{(s+1)^5}{(s+1)^5}$$

which will permit the algorithm to search over all transfer functions with denominator $(s+1)^5$.

By choosing a sufficiently high-order denominator with suitable poles, one would hope to obtain a solution which is close enough[10] to the true minimum for any practical purpose, but note that it is well-known (eg Megretski [Meg94]) that optimal solutions to mixed-norm problems over $\mathcal{H}_\infty$ can be irrational.

We show that our approximate problem has a convex LMI formulation, and hence that the minimum value of the $\mathcal{H}_2$-objective subject to the $\mathcal{H}_\infty$-constraint over this subset of $\mathcal{RH}_\infty$ may be approached arbitrarily closely (and with reasonable computating time) provided that a feasible initial guess Q_i satisfying $\|L + MQ_i\|_\infty < \gamma$ and $G + HQ_i \in \mathcal{RH}_2$ is given.[11]

Theorem 2.9

Given positive integers $u, y_2, y_\infty, y_q, x_g, x_h, x_l, x_m$ and x_q, a real number $\gamma > 0$ and transfer functions

$$
\begin{aligned}
G &= \left[\begin{array}{c|c} A_g & B_g \\ \hline C_g & D_g \end{array}\right] \in \mathcal{RH}_\infty^{y_2\times u}; \quad A_g \in \mathbb{R}^{x_g\times x_g} \\
H &= \left[\begin{array}{c|c} A_h & B_h \\ \hline C_h & D_h \end{array}\right] \in \mathcal{RH}_\infty^{y_2\times y_q}; \quad A_h \in \mathbb{R}^{x_h\times x_h} \\
L &= \left[\begin{array}{c|c} A_l & B_l \\ \hline C_l & D_l \end{array}\right] \in \mathcal{RH}_\infty^{y_\infty\times u}; \quad A_l \in \mathbb{R}^{x_l\times x_l} \\
M &= \left[\begin{array}{c|c} A_m & B_m \\ \hline C_m & D_m \end{array}\right] \in \mathcal{RH}_\infty^{y_\infty\times y_q}; \quad A_m \in \mathbb{R}^{x_m\times x_m} \qquad \textit{and} \\
Q_i &= \left[\begin{array}{c|c} A_{q_i} & B_{q_i} \\ \hline C_{q_i} & D_{q_i} \end{array}\right] \in \mathcal{RH}_\infty^{y_q\times u}; \quad A_{q_i} \in \mathbb{R}^{x_q\times x_q}
\end{aligned}
$$

such that $G + HQ_i \in \mathcal{RH}_2^{y_2\times u}$ and $\|L + MQ_i\|_\infty < \gamma$, denote by $\boldsymbol{v}_1, \boldsymbol{v}_2, \cdots, \boldsymbol{v}_j$ the (possibly empty) set of linearly independent vectors spanning the kernel of D_h and let

$$
V := \begin{bmatrix} \boldsymbol{v}_1 & \boldsymbol{v}_2 & \cdots & \boldsymbol{v}_j \end{bmatrix}
$$

$$
\begin{bmatrix} A_2 & B_2 & E_2 & F_2 \\ C_2 & & & \end{bmatrix} := \begin{bmatrix} \begin{bmatrix} A_g & 0 & 0 \\ 0 & A_h & B_hC_{q_i} \\ 0 & 0 & A_{q_i} \end{bmatrix} & \begin{bmatrix} B_g \\ B_hD_{q_i} \\ 0 \end{bmatrix} & \begin{bmatrix} 0 \\ B_hV \\ 0 \end{bmatrix} & \begin{bmatrix} 0 \\ 0 \\ I \end{bmatrix} \\ \begin{bmatrix} C_g & C_h & D_hC_{q_i} \end{bmatrix} & & & \end{bmatrix}
$$

$$
\begin{bmatrix} A_\infty & B_\infty & E_\infty & F_\infty \\ C_\infty & D_\infty & & \end{bmatrix} := \begin{bmatrix} \begin{bmatrix} A_l & 0 & 0 \\ 0 & A_m & B_mC_{q_i} \\ 0 & 0 & A_{q_i} \end{bmatrix} & \begin{bmatrix} B_l \\ B_mD_{q_i} \\ 0 \end{bmatrix} & \begin{bmatrix} 0 \\ B_mV \\ 0 \end{bmatrix} & \begin{bmatrix} 0 \\ 0 \\ I \end{bmatrix} \\ \begin{bmatrix} C_l & C_m & D_mC_{q_i} \end{bmatrix} & \begin{bmatrix} D_l + D_mD_{q_i} \end{bmatrix} & & \end{bmatrix}
$$

[10] In discrete-time we can closely approximate any stable (finite or infinite) impulse response with a sufficiently long finite impulse response, and by application of the Möbius transformation we might expect to closely approximate any continuous-time impulse response by a rational polynomial with a sufficiently high-order denominator. While this is not true for general $\mathcal{H}_\infty$ functions, it is shown by Scherer [Sch95] that such fixed-order real-rational functions suffice for problems over $\mathcal{RH}_\infty$.

[11] If the initial guess does not satisfy the $\mathcal{H}_\infty$-constraint then the algorithm is not certain to find a feasible solution, although it will always find one if it exists.

An approximate solution to the mixed-norm minimisation problem

$$\min_{Q \in \mathcal{RH}_\infty^{y_q \times u} \,:\, G+HQ \in \mathcal{RH}_2^{y_2 \times u},\ L+MQ \in \mathcal{RH}_\infty^{y_\infty \times u} \text{ and } \|L+MQ\|_\infty < \gamma} \|G+HQ\|_2$$

is then given by the solution to the following convex LMI optimisation: minimise $\mathrm{Trace}(Q_2)$ *over the LMI variables*

$$\begin{aligned} X_2 = X_2^T &\in \mathbb{R}^{(x_g+x_h+x_q)\times(x_g+x_h+x_q)} \\ Q_2 = Q_2^T &\in \mathbb{R}^{y_2 \times y_2} \\ X_\infty = X_\infty^T &\in \mathbb{R}^{(x_l+x_m+x_q)\times(x_l+x_m+x_q)} \\ B_q &\in \mathbb{R}^{x_q \times u} \\ \Lambda &\in \mathbb{R}^{j \times u} \end{aligned}$$

subject to

$$\begin{aligned} \begin{bmatrix} A_2X_2 + X_2A_2^T & B_2 + E_2\Lambda + F_2B_q \\ B_2^T + \Lambda^T E_2^T + B_q^T F_2^T & -I \end{bmatrix} &< 0 \\ \begin{bmatrix} Q_2 & C_2X_2 \\ X_2C_2^T & X_2 \end{bmatrix} &> 0 \\ \begin{bmatrix} A_\infty X_\infty + X_\infty A_\infty^T & B_\infty + E_\infty\Lambda + F_\infty B_q & X_\infty C_\infty^T \\ B_\infty^T + \Lambda^T E_\infty^T + B_q^T F_\infty^T & -I & D_\infty^T + \Lambda^T V^T D_m^T \\ C_\infty X_\infty & D_\infty + D_m V \Lambda & -\gamma^2 I \end{bmatrix} &< 0 \\ X_\infty &> 0 \end{aligned}$$

Denoting by X_2^*, Q_2^* *etc the optimal values of the LMI variables, the approximate solution* Q^* *is then given by*

$$Q^* = \left[\begin{array}{c|c} A_{q_i} & B_q^* \\ \hline C_{q_i} & D_{q_i} + V\Lambda^* \end{array}\right] \tag{2.28}$$

with corresponding $G + HQ^*$ *and* $L + MQ^*$ *given by*

$$G + HQ^* = \left[\begin{array}{c|c} A_2 & B_2 + E_2\Lambda^* + F_2B_q^* \\ \hline C_2 & 0 \end{array}\right] \tag{2.29}$$

$$L + MQ^* = \left[\begin{array}{c|c} A_\infty & B_\infty + E_\infty\Lambda^* + F_\infty B_q^* \\ \hline C_\infty & D_\infty + D_m V \Lambda^* \end{array}\right] \tag{2.30}$$

and satisfying $\|G + HQ^*\|_2 = \sqrt{\mathrm{Trace}(Q_2^*)}$ *and* $\|L + MQ^*\|_\infty < \gamma$.

The following Corollary, which is a special case of Theorem 2.9, considers a simpler problem which is related to the norm minimisation results given in Theorem 2.4:

Corollary 2.10

Given positive integers u, x_m and x_q, a real number $\gamma > 0$ and transfer functions

$$M_0 = \left[\begin{array}{c|c} A+BF & B \\ \hline F & I \end{array}\right] \in \mathcal{RH}_\infty^{u\times u}; \quad A \in \mathbb{R}^{x_m \times x_m}$$

$$Q_i = \left[\begin{array}{c|c} A_{q_i} & B_{q_i} \\ \hline C_{q_i} & I \end{array}\right] \in \mathcal{RH}_\infty^{u\times u}; \quad A_{q_i} \in \mathbb{R}^{x_q \times x_q}$$

such that $\|I - M_0 Q_i\|_\infty < \gamma$, let

$$\begin{bmatrix} A_2 & B_2 & F_2 \\ C_2 & & \end{bmatrix} := \begin{bmatrix} \begin{bmatrix} A+BF & BC_{q_i} \\ 0 & A_{q_i} \end{bmatrix} & \begin{bmatrix} B \\ 0 \end{bmatrix} & \begin{bmatrix} 0 \\ I \end{bmatrix} \\ \begin{bmatrix} -F & -C_{q_i} \end{bmatrix} & & \end{bmatrix}$$

An approximate solution to the mixed-norm minimisation problem

$$\min_{Q \in \mathcal{RH}_\infty^{u\times u} \,:\, I - M_0 Q \in \mathcal{RH}_2^{u\times u},\; I - M_0 Q \in \mathcal{RH}_\infty^{u\times u} \text{ and } \|I - M_0 Q\|_\infty < \gamma} \|I - M_0 Q\|_2$$

is then given by the solution to the following convex LMI optimisation: minimise Trace(Q_2) *over the LMI variables*

$$\begin{aligned} X_2 = X_2^T &\in \mathbb{R}^{(x_m+x_q)\times(x_m+x_q)} \\ Q_2 = Q_2^T &\in \mathbb{R}^{u\times u} \\ B_q &\in \mathbb{R}^{x_q \times u} \end{aligned}$$

subject to

$$\begin{bmatrix} Q_2 & C_2 X_2 \\ X_2 C_2^T & X_2 \end{bmatrix} > 0$$

$$\begin{bmatrix} A_2 X_2 + X_2 A_2^T & B_2 + F_2 B_q & X_2 C_2^T \\ B_2^T + B_q^T F_2^T & -I & 0 \\ C_2 X_2 & 0 & -\gamma^2 I \end{bmatrix} < 0$$

$$X_2 > 0$$

Denoting by X_2^*, Q_2^* etc the optimal values of the LMI variables, the approximate solution Q^* and corresponding $I - M_0 Q^*$ are then given by

$$Q^* = \left[\begin{array}{c|c} A_{q_i} & B_q^* \\ \hline C_{q_i} & I \end{array}\right]$$

$$I - M_0 Q^* = \left[\begin{array}{c|c} A_2 & B_2 + F_2 B_q^* \\ \hline C_2 & 0 \end{array}\right] = \left[\begin{array}{c|c} \begin{bmatrix} A+BF & BC_{q_i} \\ 0 & A_{q_i} \end{bmatrix} & \begin{bmatrix} B \\ B_q^* \end{bmatrix} \\ \hline \begin{bmatrix} -F & -C_{q_i} \end{bmatrix} & 0 \end{array}\right]$$

and satisfy $\|I - M_0 Q^*\|_2 = \sqrt{\mathrm{Trace}(Q_2^*)}$ and $\|I - M_0 Q^*\|_\infty < \gamma$.

Remarks

1. This Corollary is clearly directly applicable to the coprime-factor results given in Theorem 2.4. The main difference is that we do not (cannot!) restrict Q to be a unit in $\mathcal{RH}_\infty$ in Theorem 2.9. Nevertheless, in preliminary numerical tests the optimal Q^* has so far always been a unit in $\mathcal{RH}_\infty$.[12]

2. One sensible starting point for using this result would be, given an unstable transfer function P with stabilisable state-space realisation $= \left[\begin{array}{c|c} A & B \\ \hline C & D \end{array}\right]$, to take

$$M_0 = \left[\begin{array}{c|c} A+BF & B \\ \hline F & I \end{array}\right] \quad \text{and} \quad Q_i = \left[\begin{array}{c|c} A_{q_i} & 0 \\ \hline C_{q_i} & I \end{array}\right]$$

   with $F = -B^*X$ where X is the solution to

$$A^*X + XA - XBB^*X = 0$$

   In this case $\|I - M_0Q_i\|_\infty = 2$ and $\|I - M_0Q_i\|_2$ is the infimum given in Equation 2.7 of Theorem 2.4.

   With a suitable choice of A_{q_i} and C_{q_i} it should then be possible to set $1 < \gamma < 2$ and solve for a better $\mathcal{H}_\infty$-norm at the expense of an increase in $\mathcal{H}_2$-norm. Repeating this process should give a suitable compromise solution Q.

PROOF OF THEOREM 2.9:

This is a standard application of linear matrix inequalities. There are only two points of any interest:

Firstly, how to determine suitable $Q(\infty)$: we are given Q_i such that $G + HQ_i$ is strictly proper, ie

$$D_g + D_hD_{q_i} = 0$$

If $Q(\infty) = Q_d$, then the requirement that $G + HQ$ be strictly proper is equivalent to

$$D_h(D_q - D_{q_i}) = 0$$

ie that $(D_q - D_{q_i})$ is in the kernel of D_h. Hence $(D_q - D_{q_i})$ may be expressed as $V\Lambda$ where V is a matrix containing the vectors spanning the kernel of D_h and Λ is an arbitrary matrix of suitable dimensions.

Secondly, we need to ensure that $G + HQ$ and $L + MQ$ are affine in the free variables B_q and Λ. This is clear from the expressions given in Equations 2.29 and 2.30. ∎

PROOF OF COROLLARY 2.10:

Immediate from Theorem 2.9. ∎

[12] One possible theory as to why the numerical solution does not pick non-minimum-phase Q^* is that such choices do not offer any improvement in the minimum achievable. For the global infimum as $\gamma \to \infty$ this is provable — see Theorem 2.4 — but in other cases it is not so clear.

2.4 Summary and suggestions for further work

2.4.1 Summary

In this chapter we have

- Discussed spaces of constants, signals and operators relevant to the work presented in the remainder of this thesis.
- Defined and discussed saturation and deadzone functions, highlighting some useful properties of such functions, and proposing a class of "generalised deadzones" which satisfy a nonlinear sector bound relationship.
- Given an algorithm for obtaining approximate solutions to fairly general $\mathcal{H}_2$-$\mathcal{H}_\infty$ mixed norm problems, using Linear Matrix Inequalities.

2.4.2 Suggestions for further work

Mixed $\mathcal{H}_2$-$\mathcal{H}_\infty$ problems

The algorithms given in Section 2.3 should be considered only as an incremental step towards a general and robust method for solving such problems using Linear Matrix Inequalities. Some preliminary, but by no means exhaustive, testing of the procedures given in Theorem 2.9 and Corollary 2.10 has been undertaken, and the results have been promising; nevertheless, there remain significant points which should be addressed, such as the effects of

- common terms in the state-space matrices (eg if $A_g = A_h$),
- non-minimum-phase zeros, and
- non-minimal realisations of G, H, L or M.

Furthermore, the conjecture that the infimum may be approached closely using a continuous-time analogy of a sufficiently long Finite Impulse Response remains unproven. Moreover, it is quite clear that the number of terms necessary to obtain a particular level of performance will be dependent on the choice of denominator — no guidelines for choosing A_{q_i} (or C_{q_i}) can be given at the present time.

Chapter 3

Stability analysis of nonlinear systems

3.1 Introduction

3.1.1 Background and motivation

Stability analysis forms the foundation for almost the entire field of control engineering, with applications ranging from space travel to financial modelling. We now know almost everything there is to learn about the stability of linear, time-invariant differential (and difference) equations — although there are outstanding questions relating to the *synthesis* of LTI systems to perform in a pre-specified way.

In complete contrast, the analysis of *nonlinear* and/or *time-varying* systems remains a popular research area for control engineers (and mathematicians, and economists, and chemists...) Even the most benign-looking interconnections have yet to succumb to a complete understanding, although new results continue to accumulate (almost on a weekly basis!) Unfortunately, it is clear that the world around us is inherently nonlinear, and hence such research is extremely valuable to both theoretical and practicing engineers.

Modelling of real systems for stability analysis

In order to render real-world problems at least marginally tractable, we often assume that any system can be nominally modelled by linear, time-invariant differential (or difference) equations, perturbed by some nonlinear element(s). These nominal LTI dynamics need not be physically motivated; the important thing is that the real behaviour deviates from the nominal behaviour by some small amount (at least during such observations as we may make.)

We then also make some suitable assumptions about the behaviour of the nonlinear perturbation, for example, that it can be described by an unknown but sector-bounded time-varying gain. Once again, these assumptions may or may not be physically motivated; indeed, they may not even be correct if we have made too few observations...

The final step in preparing our model for analysis is to determine suitable entry points for external disturbances (since there will always be some unmodelled behaviour) and, equally importantly, suitable exit points for the "outputs". Putting all of this together gives an interconnection similar to Figure 3.1 on page 40, which is the system which we will be considering in this chapter.

Prior work on stability analysis

There has been so much prior work on analysing stability that to attempt to document even a small fraction would be almost impossible. Instead, we focus on those results which are most relevant to the work presented in the remainder of this chapter. State-space and input-output methods and results are often treated separately:

- In a state-space setting, stability is usually interpreted as requiring that the system states converge to the origin, starting from any arbitrary initial state $\boldsymbol{x}(0)$. (In the linear time-invariant case this question is trivial: the "A" matrix should be Hurwitz for stability.)

  We do not, in fact, consider state-space systems in the remainder of this thesis, however it is worth pointing out that certain input-output results have equivalent (or almost equivalent) state-space interpretations.

- Many well-known nonlinear input-output stability results are essentially due to the small-gain and passivity theorems (usually attributed to Zames [Zam66a]) By considering "multipliers" and loop transformations, these concepts have been extended far beyond their original domain (see, for example, Kothare *et al* [KM99]; Boyd *et al* [BGFB94] or Balakrishnan [Bal95]) Such transformations usually require the problem to be formulated as an LMI feasibility or optimisation problem, for which computationally efficient algorithms are now widely available.

It is interesting to note that some authors (eg the anti-windup work of Park & Choi [PC95]; Edwards & Postlethwaite [EP98] and Miyamoto & Vinnicombe [MV96b]) continue to base synthesis results directly on the small-gain theorem, even for problems which may admit a less conservative formulation using such multipliers and loop transformations. One likely reason for this, given the modern emphasis on "optimality" in all things, is that (assuming some fictional system which depends on a transfer function $H(s) = \left[\begin{array}{c|c} A & B \\ \hline C & D \end{array}\right]$) a typical small-gain result:

The system is stable if $\|H(s)\|_\infty < 1$.

is intuitively appealing compared to a typical LMI-based result:

The system is stable if there exists a matrix $X = X^T > 0$ *such that*

$$\begin{bmatrix} A^T X + XA & XB & C^T \\ B^T X & -I & D^T \\ C & D & -I \end{bmatrix} < 0$$

The former condition offers clear hints as to which H result in a stable system, but the latter relies on an iterative computation to give an answer. A small change to the transfer function H requires one to run the computation from scratch, even though it may be obvious (from, for example, a Bode or Nyquist plot) that the change makes no significant difference to the $\mathcal{H}_\infty$-norm.

In many cases, particularly if synthesising a controller by a similar iterative process, the computational method is acceptable and desirable; in others, the intuitive nature of the small gain approach can help with understanding the underlying problem.

One other interesting approach, which is growing in popularity, is the use of so-called Integral Quadratic Constraints (IQCs) pioneered by Megretski & Rantzer [MR97], [RM96] etc. Based on work done in the 1960s, IQCs are an extremely general way of relating signals to one another. Many well-known relationships (such as gain, sector bounds, passivity) can be written in the IQC framework; this approach has also motivated a number of novel relationships (see, for example, Megretski [Meg99])

Prior work on local stability analysis

Stability analysis in a local sense (ie for inital states or external inputs restricted in some way) is a much smaller field than in the global sense. We again consider state-space and input-output results separately:

- In a state-space setting the problem of local stability can be interpreted in a number of ways. One common problem is to find the set of all admissable initial states $\boldsymbol{x}(0)$ such that the state converges to zero. Even for a supposedly simple system — planar LTI dynamics with saturated state feedback — this problem has proved exceedingly intractable (see, for example Hu & Lin [HL99]; Alvarez *et al* [ASA93]) and remains a topic of some interest.

  There are also some synthesis methods which attempt to optimise such "regions of attraction", particularly those of Lin *et al* [LB98], [Lin97], [LS93]

- Local stability in an input-output context has not been considered widely, excepting that practically all global results (for causal systems) hold on truncated time intervals.

  One notable exception was a recent paper by Hindi and Boyd [HB98], which builds on well-understood LMI methods of stability analysis. (see, for example, Boyd *et al* [BGFB94]) The questions posed in this paper are broadly similar to those considered in Section 3.4, however the methods utilised are completely different.

Input-output stability

In the remainder of this chapter we will be considering only input-output stability of continuous-time systems, and in particular those systems which can be written in the form of a linear transfer matrix and a single nonlinear block.

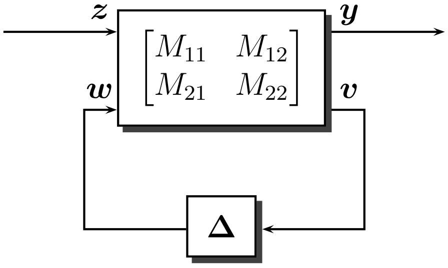

Figure 3.1: Interconnection for stability analysis

Consider the interconnection (shown in Figure 3.1)

$$\begin{bmatrix} \boldsymbol{y} \\ \boldsymbol{v} \end{bmatrix} = \begin{bmatrix} M_{11} & M_{12} \\ M_{21} & M_{22} \end{bmatrix} \begin{bmatrix} \boldsymbol{z} \\ \boldsymbol{w} \end{bmatrix}$$
$$\boldsymbol{w} = \boldsymbol{\Delta v}$$

where it is assumed that M_{11}, M_{12}, M_{21} and M_{22} are linear, time-invariant transfer functions of arbitrary (but compatible) sizes, and $\boldsymbol{\Delta}$ is a causal nonlinear operator of compatible size. As noted earlier, this interconnection is an appropriate model for many "real" physical systems.

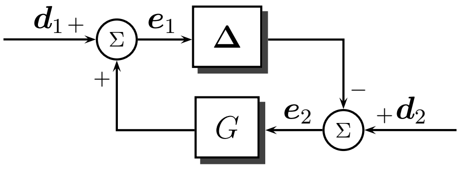

Figure 3.2: Interconnection for "absolute stability" problem

Note that this formulation includes the classical "absolute stability" problem (see eg Willems [Wil71] and references therein) — shown in Figure 3.2 — as a special case, with $\boldsymbol{z} = \begin{bmatrix} \boldsymbol{d}_1 \\ \boldsymbol{d}_2 \end{bmatrix}$, $\boldsymbol{y} = \begin{bmatrix} \boldsymbol{e}_1 \\ \boldsymbol{e}_2 \end{bmatrix}$ and $\begin{bmatrix} M_{11} & M_{12} \\ M_{21} & M_{22} \end{bmatrix} = \begin{bmatrix} \begin{bmatrix} I & G \\ 0 & I \end{bmatrix} & \begin{bmatrix} -G \\ -I \end{bmatrix} \\ \begin{bmatrix} I & G \end{bmatrix} & \begin{bmatrix} -G \end{bmatrix} \end{bmatrix}$.

In the majority of cases the goal has been to determine sufficient conditions on the elements of Figure 3.1 under which the interconnection is *globally stable*, which can be loosely interpreted as:

- **Global stability**: do bounded inputs produce bounded outputs?

It is normal, although by no means universal, to consider signals bounded in $\mathcal{L}_2$-norm (alternatives include considering signals bounded in the $\mathcal{L}_\infty$- or $\mathcal{L}_1$-norms.)

Inevitably, there are interconnections for which all of the various conditions for global stability fail. In these cases we consider a weaker question:

- **Local stability**: what is the largest class of bounded inputs (that we can determine) such that all inputs in this class produce bounded outputs?

In the first instance, it is expected that one would consider classes of signals which form "balls" in $\mathcal{L}_2$, ie with $\mathcal{L}_2$-norm bounded by some given finite number. Restricting attention to such classes should be more tractable, at the expense of possible conservatism.

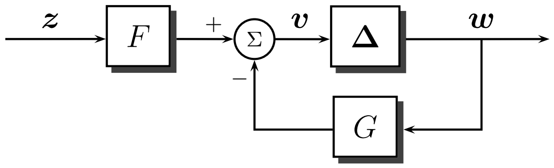

Figure 3.3: Simple nonlinear feedback system

If we assume that

$$\begin{bmatrix} M_{11} & M_{12} \\ M_{21} & M_{22} \end{bmatrix} \in \mathcal{RH}_\infty$$

ie, that the linear part of the interconnection is internally stable[1], then we may simplify the problem somewhat, by noting that $\boldsymbol{z}, \boldsymbol{w} \in \mathcal{L}_2 \Longrightarrow \boldsymbol{y} \in \mathcal{L}_2$. Hence we may temporarily ignore $\boldsymbol{y}$, and consider only the simpler interconnection (shown in Figure 3.3)

$$\begin{aligned} \boldsymbol{v} &= F\boldsymbol{z} - G\boldsymbol{w} \\ \boldsymbol{w} &= \boldsymbol{\Delta}\boldsymbol{v} \end{aligned}$$

where $F = M_{21}$ and $G = -M_{22}$. (Note that we take a negative feedback, for commonality with the "absolute stability" problem and the various well-known theorems associated with it.)

[1]This assumption is not strictly necessary for either local or global stability of the closed-loop, but such an assumption does make sense:

If we are to consider the nonlinearity Δ as being a perturbation from some nominal linear behaviour, then we will necessarily wish to consider the case $\boldsymbol{w} \equiv 0$. In this case, if either of M_{11} or M_{21} is unstable, then (at least) one of $\boldsymbol{v}$ or $\boldsymbol{y}$ will be unbounded for arbitrarily small $\boldsymbol{z}$.

Equally, if we consider $\boldsymbol{z} \equiv 0$, and if either of M_{12} or M_{22} is unstable, then (at least) one of $\boldsymbol{v}$ or $\boldsymbol{y}$ will be unbounded for an arbitrarily small disturbance at $\boldsymbol{w}$.

3.2 Mathematical preliminaries

3.2.1 Generalised $\mathcal{H}_\infty$-norms

The results of Section 3.4 will rely on the following simple way to calculate the induced norm of a partitioned $\mathcal{RH}_\infty$ transfer function with respect to the $\mathcal{L}_2$-norms of the individual elements of the input:

Given $\boldsymbol{M} \in \mathcal{RH}_\infty$ partitioned as $\begin{bmatrix} M_1 & M_2 & \cdots & M_n \end{bmatrix}$, and $\boldsymbol{\phi} \in \mathbb{R}^n_+$, let

$$\mathrm{Sq}_{\boldsymbol{M}}(\boldsymbol{\phi}) := \inf_{\alpha_i \in (0,\infty)} \sqrt{\left\| \begin{bmatrix} \frac{M_1}{\alpha_1} & \frac{M_2}{\alpha_2} & \cdots & \frac{M_n}{\alpha_n} \end{bmatrix} \right\|_\infty^2 \sum_{i=1}^{n} \alpha_i^2 \phi_i^2} \tag{3.1}$$

noting that each M_i may be of any width, provided the partitioning works correctly.

Theorem 3.1

For any $\boldsymbol{M} \in \mathcal{RH}_\infty$ partitioned as $\begin{bmatrix} M_1 & M_2 & \cdots & M_n \end{bmatrix}$, and $\boldsymbol{\phi} \in \mathbb{R}^n_+$

$$\sup_{\|d_i\|_2 \le \phi_i} \|\boldsymbol{M}\boldsymbol{d}\|_2 = \mathrm{Sq}_{\boldsymbol{M}}(\boldsymbol{\phi})$$

where $\boldsymbol{d} = \begin{bmatrix} d_1^T & d_2^T & \cdots & d_n^T \end{bmatrix}^T$ is assumed to be of suitable dimension and partitioned compatibly with $\boldsymbol{M}$.

PROOF OF THEOREM 3.1:

It is shown by D'Andrea in [D'A96] (as a special case of Theorem 3.6), that the following two statements are equivalent:

I. The following supremum is satisfied

$$\sup_{\|d_i\|_2 \le 1} \left\| \begin{bmatrix} \frac{\phi_1}{\gamma} M_1 & \frac{\phi_2}{\gamma} M_2 & \cdots & \frac{\phi_n}{\gamma} M_n \end{bmatrix} \begin{bmatrix} d_1 \\ d_2 \\ \vdots \\ d_n \end{bmatrix} \right\|_2 < 1$$

II. There exist scalars $x_1, x_2, \cdots, x_n > 0$ and $y > 0$ such that

$$x_1 + x_2 + \cdots + x_n < 1$$
$$y < 1 \quad \text{and}$$
$$\left\| \frac{1}{\sqrt{y}} I \begin{bmatrix} \frac{\phi_1}{\gamma} M_1 & \frac{\phi_2}{\gamma} M_2 & \cdots & \frac{\phi_n}{\gamma} M_n \end{bmatrix} \begin{bmatrix} \frac{1}{\sqrt{x_1}} I & 0 & \cdots & 0 \\ 0 & \frac{1}{\sqrt{x_2}} I & \cdots & 0 \\ \vdots & \vdots & \ddots & \vdots \\ 0 & 0 & \cdots & \frac{1}{\sqrt{x_n}} I \end{bmatrix} \right\|_\infty < 1$$

The relationship between the free variables $(\alpha_1, \alpha_2, \cdots, \alpha_n)$ in $\mathrm{Sq}_{\boldsymbol{M}}$ and the free variables $(x_1, x_2, \cdots, x_n$ and $y)$ in statement **II** is then $x_i = \frac{\alpha_i^2 \phi_i^2}{\alpha_1^2\phi_1^2 + \alpha_2^2\phi_2^2 + \cdots + \alpha_n^2\phi_n^2}$ for each $i \in \{1, 2, \cdots, n\}$ and $y = 1$. ∎

Given $\boldsymbol{M} \in \mathcal{RH}_\infty$ partitioned as $\begin{bmatrix} M_1 & M_2 & \cdots & M_n \end{bmatrix}$, and $\boldsymbol{\phi} \in \mathbb{R}^n_+$, let

$$\mathrm{Sq}_{[\mathrm{upper}]}(\boldsymbol{\phi}) := \sum_{i=1}^{n} \|M_i\|_\infty \phi_i \tag{3.2}$$

$$\mathrm{Sq}_{[\mathrm{lower}]}(\boldsymbol{\phi}) := \sqrt{\sum_{i=1}^{n} \|M_i\|_\infty^2 \phi_i^2} \tag{3.3}$$

Lemma 3.2

For any $\boldsymbol{M} \in \mathcal{RH}_\infty$ partitioned as $\begin{bmatrix} M_1 & M_2 & \cdots & M_n \end{bmatrix}$ and $\boldsymbol{\phi} \in \mathbb{R}^n_+$

$$\mathrm{Sq}_{[lower]}(\boldsymbol{\phi}) \le \mathrm{Sq}_{\boldsymbol{M}}(\boldsymbol{\phi}) \le \mathrm{Sq}_{[upper]}(\boldsymbol{\phi})$$

where each inequality is tight, in the sense that

1. *if $\boldsymbol{M} = \begin{bmatrix} M_1 & M_2 & \cdots & M_n \end{bmatrix}$ is such that*

$$\left\| \begin{bmatrix} \frac{M_1}{\|M_1\|_\infty} & \frac{M_2}{\|M_2\|_\infty} & \cdots & \frac{M_n}{\|M_n\|_\infty} \end{bmatrix} \right\|_\infty = \sqrt{n}$$

   then $\mathrm{Sq}_{\boldsymbol{M}}(\boldsymbol{\phi}) = \mathrm{Sq}_{[upper]}(\boldsymbol{\phi})$ for all $\boldsymbol{\phi} \in \mathbb{R}^n_+$.

2. *if $\boldsymbol{M} = \begin{bmatrix} M_1 & M_2 & \cdots & M_n \end{bmatrix}$ is such that*

$$\left\| \begin{bmatrix} \frac{M_1}{\|M_1\|_\infty} & \frac{M_2}{\|M_2\|_\infty} & \cdots & \frac{M_n}{\|M_n\|_\infty} \end{bmatrix} \right\|_\infty = 1$$

   then $\mathrm{Sq}_{\boldsymbol{M}}(\boldsymbol{\phi}) = \mathrm{Sq}_{[lower]}(\boldsymbol{\phi})$ for all $\boldsymbol{\phi} \in \mathbb{R}^n_+$.

Remarks

1. The condition for the upper bound to be achieved is equivalent to the existence of a single frequency at which $M_1, M_2, \cdots, M_n$ all achieve their individual $\mathcal{H}_\infty$-norms.

   For example, this bound is achieved if $M_i = k_i M_1$ for all $i \in \{2, \cdots, n\}$ and arbitrary scalars $k_2, \cdots, k_n$.

   The condition for the lower bound to be achieved requires at least that each of $M_2(j\omega), \cdots, M_n(j\omega)$ contributes exactly zero at any frequency ω at which M_1 achieves its $\mathcal{H}_\infty$-norm, and similarly for each of $M_2, \cdots, M_n$, which implies some (perhaps many) $j\omega$ axis zeros.

   For example, this bound is achieved if $\boldsymbol{M}(s) = \begin{bmatrix} \frac{s}{s+c} & \frac{c}{s+c} \end{bmatrix}$ for some $c > 0$.

PROOF OF LEMMA 3.2:

We assume throughout the proof that each M_i and ϕ_i is nonzero: it may be readily verified that if $M_i = 0$ or $\phi_i = 0$ then α_i may take any value in $(0, \infty)$ without affecting the infimum, however in the proof which follows, α_i will *appear* to be zero, infinity or undefined in the cases $M_i = 0$, $\phi_i = 0$ or $M_i = 0$ & $\phi_i = 0$ respectively.

For the upper bound, note that

$$\left\| \begin{bmatrix} \frac{M_1}{\alpha_1} & \frac{M_2}{\alpha_2} & \cdots & \frac{M_n}{\alpha_n} \end{bmatrix} \right\|_\infty^2 \leq \sum_{i=1}^{n} \left\| \frac{M_i}{\alpha_i} \right\|_\infty^2$$

so

$$\mathrm{Sq}_{\boldsymbol{M}}(\boldsymbol{\phi}) \leq \inf_{\alpha_i \in (0,\infty)} \sqrt{\left(\sum_{i=1}^{n} \left\| \frac{M_i}{\alpha_i} \right\|_\infty \right)^2 \sum_{j=1}^{n} \left(\alpha_j^2 \phi_j^2 \right)} = \sum_{i=1}^{n} \|M_i\|_\infty \phi_i$$

where we have minimised the expression under the square root by setting $\alpha_i = \alpha_1 \sqrt{\frac{\|M_i\|_\infty}{\phi_i}}$ for each $i \in \{2, \cdots, n\}$, with α_1 an arbitrary positive constant.

For the lower bound, note that

$$\left\| \begin{bmatrix} \frac{M_1}{\alpha_1} & \frac{M_2}{\alpha_2} & \cdots & \frac{M_n}{\alpha_n} \end{bmatrix} \right\|_\infty^2 \geq \max_i \left\| \frac{M_i}{\alpha_i} \right\|_\infty^2$$

so

$$\mathrm{Sq}_{\boldsymbol{M}}(\boldsymbol{\phi}) \geq \inf_{\alpha_i \in (0,\infty)} \sqrt{\left(\max_i \left\| \frac{M_i}{\alpha_i} \right\|_\infty \right)^2 \sum_{j=1}^{n} \left(\alpha_j^2 \phi_j^2 \right)} = \sqrt{\sum_{i=1}^{n} \|M_i\|_\infty^2 \phi_i^2}$$

where we have minimised the expression under the square root by setting $\alpha_i = \alpha_1 \|M_i\|_\infty$ for each $i \in \{2, \cdots, n\}$, with α_1 an arbitrary positive constant.

The conditions for tightness of the inequalities are then quite clear. ∎

We shall mainly be interested in the case $n = 2$, ie $\boldsymbol{M} = \begin{bmatrix} F & G \end{bmatrix}$. For simplicity we define shorthand versions of $\mathrm{Sq}_{\boldsymbol{M}}$, $\mathrm{Sq}_{[\text{lower}]}$ and $\mathrm{Sq}_{[\text{upper}]}$ for *nonzero* F and G:

Definition 3.1 ($\Gamma_{[F,G]}$, $\Gamma_{[\text{lower}]}$ **and** $\Gamma_{[\text{upper}]}$)

Given nonzero $F, G \in \mathcal{RH}_\infty$, $\boldsymbol{M} = \begin{bmatrix} F & G \end{bmatrix}$ *and* $\lambda \in [0, \infty)$, *let*

$$\Gamma_{[F,G]}(\lambda) := \mathrm{Sq}_{\boldsymbol{M}}\left(\begin{bmatrix} \|F\|_\infty^{-1} \\ \lambda \end{bmatrix} \right) = \inf_{\alpha \in (0,\infty)} \left\| \begin{bmatrix} \frac{1}{\alpha} F & G \end{bmatrix} \right\|_\infty \sqrt{\frac{\alpha^2}{\|F\|_\infty^2} + \lambda^2} \tag{3.4}$$

$$\Gamma_{[upper]}(\lambda) := \mathrm{Sq}_{[upper]}\left(\begin{bmatrix} \|F\|_\infty^{-1} \\ \lambda \end{bmatrix} \right) = 1 + \|G\|_\infty \lambda \tag{3.5}$$

$$\Gamma_{[lower]}(\lambda) := \mathrm{Sq}_{[lower]}\left(\begin{bmatrix} \|F\|_\infty^{-1} \\ \lambda \end{bmatrix} \right) = \sqrt{1 + \|G\|_\infty^2 \lambda^2} \tag{3.6}$$

where $\mathrm{Sq}_{\boldsymbol{M}}$, $\mathrm{Sq}_{[upper]}$ *and* $\mathrm{Sq}_{[lower]}$ *are as defined in Equations 3.1, 3.2 and 3.3 respectively.*

Remark

1. Note that the functions $\Gamma_{[\text{upper}]}$ and $\Gamma_{[\text{lower}]}$ depend *only* on $\|G\|_\infty$, ie other properties of the pair F, G have no effect (although clearly $\Gamma_{[F,G]}$ *is* dependent on the interplay between $F(j\omega)$ and $G(j\omega)$)

   This feature, which will significantly simplify notation in Section 3.4, comes at the expense of slightly clumsy notation for the definition of $\Gamma_{[F,G]}$, and also in the induced norm result given in Corollary 3.3:

Corollary 3.3

For any nonzero $F, G \in \mathcal{RH}_\infty$ and $\lambda \in [0, \infty)$

$$\sup_{\substack{\|\boldsymbol{z}\|_2 \leq \|F\|_\infty^{-1} \\ \|\boldsymbol{w}\|_2 \leq \lambda}} \|F\boldsymbol{z} + G\boldsymbol{w}\|_2 = \Gamma_{[F,G]}(\lambda)$$

Remark

1. One useful interpretation of this inequality (which may be deduced by simple rearrangement) is: for any $\boldsymbol{w}, \boldsymbol{z} \in \mathcal{L}_2$ such that $\|\boldsymbol{z}\|_2 > 0$

$$\|F\boldsymbol{z} + G\boldsymbol{w}\|_2 \leq \Gamma_{[F,G]}\left(\tfrac{\|\boldsymbol{w}\|_2}{\|F\|_\infty \|\boldsymbol{z}\|_2}\right) \|F\|_\infty \|\boldsymbol{z}\|_2$$

PROOF OF COROLLARY 3.3:

Immediate from Theorem 3.1. ∎

Lemma 3.4

For any nonzero $F, G \in \mathcal{RH}_\infty$

- *For any $\lambda \in [0, \infty)$ and $\delta > 0$*

$$\Gamma_{[F,G]}(\lambda) < \Gamma_{[F,G]}(\lambda + \delta) \leq \Gamma_{[F,G]}(\lambda) + \|G\|_\infty \delta$$

- *For each of $\Gamma_{[F,G]}$, $\Gamma_{[upper]}$ and $\Gamma_{[lower]}$, $\Gamma : [0, \infty) \mapsto [1, \infty)$ is bijective, with both Γ and Γ^{-1} continuous and strictly increasing.*

- *For any $\lambda \in [0, \infty)$*

$$\Gamma_{[lower]}(\lambda) \leq \Gamma_{[F,G]}(\lambda) \leq \Gamma_{[upper]}(\lambda)$$

  where each inequality is tight (in the sense of Lemma 3.2)

- *For any $\beta \in [1, \infty)$*

$$\Gamma^{-1}_{[upper]}(\beta) \leq \Gamma^{-1}_{[F,G]}(\beta) \leq \Gamma^{-1}_{[lower]}(\beta)$$

  where each inequality is tight (in the sense of Lemma 3.2)

PROOF OF LEMMA 3.4:

First, consider $\left\{\Gamma_{[F,G]}(\lambda+\delta)\right\}^2$:

$$\begin{aligned}
\left\{\Gamma_{[F,G]}(\lambda+\delta)\right\}^2 &= \inf_{\alpha\in(0,\infty)} \left\|\begin{bmatrix}\frac{1}{\alpha}F & G\end{bmatrix}\right\|_\infty^2 \left\{\tfrac{\alpha^2}{\|F\|_\infty^2} + (\lambda+\delta)^2\right\} \\
&\geq \inf_{\alpha\in(0,\infty)} \left\|\begin{bmatrix}\frac{1}{\alpha}F & G\end{bmatrix}\right\|_\infty^2 \left\{\tfrac{\alpha^2}{\|F\|_\infty^2} + \lambda^2\right\} \\
&\qquad + \inf_{\alpha\in(0,\infty)} \left\|\begin{bmatrix}\frac{1}{\alpha}F & G\end{bmatrix}\right\|_\infty^2 \left\{\delta(2\lambda+\delta)\right\} \\
&= \left\{\Gamma_{[F,G]}(\lambda)\right\}^2 + \|G\|_\infty^2\, \delta(2\lambda+\delta)
\end{aligned}$$

which shows that $\Gamma_{[F,G]}(\lambda+\delta) > \Gamma_{[F,G]}(\lambda)$.

Secondly, consider $\Gamma_{[F,G]}(\lambda+\delta)$:

$$\begin{aligned}
\Gamma_{[F,G]}(\lambda+\delta) &= \sup_{\substack{\|\boldsymbol{z}\|_2 \leq \|F\|_\infty^{-1} \\ \|\boldsymbol{w}\|_2 \leq \lambda+\delta}} \|F\boldsymbol{z} + G\boldsymbol{w}\|_2 \\
&= \sup_{\substack{\|\boldsymbol{z}\|_2 \leq \|F\|_\infty^{-1} \\ \|\boldsymbol{w}\|_2 \leq 1}} \|F\boldsymbol{z} + (\lambda+\delta)G\boldsymbol{w}\|_2 \\
&\leq \sup_{\substack{\|\boldsymbol{z}\|_2 \leq \|F\|_\infty^{-1} \\ \|\boldsymbol{w}\|_2 \leq 1}} \left\{ \|F\boldsymbol{z} + \lambda G\boldsymbol{w}\|_2 + \|\delta G\boldsymbol{w}\|_2 \right\} \\
&\leq \sup_{\substack{\|\boldsymbol{z}\|_2 \leq \|F\|_\infty^{-1} \\ \|\boldsymbol{w}\|_2 \leq 1}} \|F\boldsymbol{z} + \lambda G\boldsymbol{w}\|_2 + \sup_{\substack{\|\boldsymbol{z}\|_2 \leq \|F\|_\infty^{-1} \\ \|\boldsymbol{w}\|_2 \leq 1}} \|\delta G\boldsymbol{w}\|_2 \\
&= \sup_{\substack{\|\boldsymbol{z}\|_2 \leq \|F\|_\infty^{-1} \\ \|\boldsymbol{w}\|_2 \leq \lambda}} \|F\boldsymbol{z} + G\boldsymbol{w}\|_2 + \sup_{\|\boldsymbol{w}\|_2\leq\delta} \|G\boldsymbol{w}\|_2 \\
&= \Gamma_{[F,G]}(\lambda) + \|G\|_\infty \delta
\end{aligned}$$

which shows that $\Gamma_{[F,G]}(\lambda+\delta) \leq \Gamma_{[F,G]}(\lambda) + \|G\|_\infty \delta$.

Hence $\Gamma_{[F,G]}$ is continuous and strictly increasing, which implies that it is bijective, and furthermore that its inverse is continuous and strictly increasing. (That $\Gamma_{[\text{upper}]}$ and $\Gamma_{[\text{lower}]}$ share these properties follows trivially from Definition 3.1)

The inequalities then follow by Lemma 3.2 and monotonicity. ∎

Definition 3.2 ($\gamma_{[F,G]}$, $\gamma_{[\text{lower}]}$ and $\gamma_{[\text{upper}]}$)
Given nonzero $F, G \in \mathcal{RH}_\infty$ and $\lambda \in [0, \infty)$, let

$$\gamma_{[F,G]}(\lambda) := \frac{\lambda}{\Gamma_{[F,G]}(\lambda)} \tag{3.7}$$

$$\gamma_{[upper]}(\lambda) := \frac{\lambda}{\Gamma_{[upper]}(\lambda)} \tag{3.8}$$

$$\gamma_{[lower]}(\lambda) := \frac{\lambda}{\Gamma_{[lower]}(\lambda)} \tag{3.9}$$

where $\Gamma_{[F,G]}$, $\Gamma_{[upper]}$ and $\Gamma_{[lower]}$ are as in Definition 3.1.

Remark

1. Note that the functions $\gamma_{[\text{upper}]}$ and $\gamma_{[\text{lower}]}$ depend *only* on $\|G\|_\infty$, ie other properties of the pair F, G have no effect (although clearly $\gamma_{[F,G]}$ *is* dependent on the interplay between $F(j\omega)$ and $G(j\omega)$)

Lemma 3.5
For any nonzero $F, G \in \mathcal{RH}_\infty$

- *For any $\lambda \in [0, \infty)$ and $\delta > 0$*

$$\gamma_{[F,G]}(\lambda + \delta) \geq \gamma_{[F,G]}(\lambda) + \left(1 - \|G\|_\infty \gamma_{[F,G]}(\lambda)\right) \frac{\delta}{\Gamma_{[F,G]}(\lambda)} - \mathcal{O}(\delta^2)$$

$$\gamma_{[F,G]}(\lambda + \delta) < \gamma_{[F,G]}(\lambda) + \frac{\delta}{\Gamma_{[F,G]}(\lambda)}$$

- *For each of $\gamma_{[F,G]}$, $\gamma_{[upper]}$ and $\gamma_{[lower]}$, $\gamma : [0, \infty) \mapsto [1, \infty)$ is bijective, with both γ and γ^{-1} continuous and strictly increasing.*

- *For any $\lambda \in [0, \infty)$*

$$\gamma_{[upper]}(\lambda) \leq \gamma_{[F,G]}(\lambda) \leq \gamma_{[lower]}(\lambda)$$

where each inequality is tight (in the sense of Lemma 3.2)

- *For any $\beta \in [0, \frac{1}{\|G\|_\infty})$*

$$\gamma^{-1}_{[lower]}(\beta) \leq \gamma^{-1}_{[F,G]}(\beta) \leq \gamma^{-1}_{[upper]}(\beta)$$

where each inequality is tight (in the sense of Lemma 3.2)

PROOF OF LEMMA 3.5:

First recall from Lemma 3.4 that

$$0 < \Gamma_{[F,G]}(\lambda) < \Gamma_{[F,G]}(\lambda + \delta) \le \Gamma_{[F,G]}(\lambda) + \|G\|_\infty \delta$$

and hence that

$$\frac{\lambda+\delta}{\Gamma_{[F,G]}(\lambda)} > \frac{\lambda+\delta}{\Gamma_{[F,G]}(\lambda+\delta)} \ge \frac{\lambda+\delta}{\Gamma_{[F,G]}(\lambda) + \|G\|_\infty \delta}$$

ie

$$\gamma_{[F,G]}(\lambda) + \frac{1}{\Gamma_{[F,G]}(\lambda)}\delta > \gamma_{[F,G]}(\lambda+\delta) \ge \gamma_{[F,G]}(\lambda) + \frac{1 - \|G\|_\infty \gamma_{[F,G]}(\lambda)}{\Gamma_{[F,G]}(\lambda) + \|G\|_\infty \delta}\delta$$

from which the first two inequalities follow easily.

Hence $\gamma_{[F,G]}$ is continuous and strictly increasing, which implies that it is bijective, and furthermore that its inverse is continuous and strictly increasing. (That $\gamma_{[\text{upper}]}$ and $\gamma_{[\text{lower}]}$ share these properties follows trivially from Definition 3.2)

The inequalities then follow by Lemma 3.4 and monotonicity. ∎

We end this discussion with some representative examples of the various functions defined above:

Examples

We illustrate the behaviour of $\Gamma_{[F,G]}$ and $\gamma_{[F,G]}$ by setting $G = \frac{\pm 2}{s+2}$. This immediately fixes $\Gamma_{[\text{upper}]}$, $\Gamma_{[\text{lower}]}$, $\gamma_{[\text{upper}]}$ and $\gamma_{[\text{lower}]}$:

$$\begin{aligned} \Gamma_{[\text{upper}]}(\lambda) &= 1+\lambda \\ \Gamma_{[\text{lower}]}(\lambda) &= \sqrt{1+\lambda^2} \\ \gamma_{[\text{upper}]}(\lambda) &= \frac{\lambda}{1+\lambda} \\ \gamma_{[\text{lower}]}(\lambda) &= \frac{\lambda}{\sqrt{1+\lambda^2}} \end{aligned}$$

By considering various F such that $\|F\|_\infty = 1$, we will see how $\Gamma_{[F,G]}$ depends on the interaction between $F(j\omega)$ and $G(j\omega)$. In Figure 3.4 we show $\Gamma_{[F,G]}$ ($\gamma_{[F,G]}$) as a solid line and $\Gamma_{[\text{upper}]}$, $\Gamma_{[\text{lower}]}$ ($\gamma_{[\text{upper}]}$, $\gamma_{[\text{lower}]}$) as dotted lines.

1. For $F = \frac{\pm 2}{s+2}$:

$$\left\| \begin{bmatrix} F & G \end{bmatrix} \right\|_\infty = \sqrt{2}$$

which implies (by Lemma 3.2) that $\Gamma_{[F,G]} = \Gamma_{[\text{upper}]}$ and $\gamma_{[F,G]} = \gamma_{[\text{upper}]}$, as shown in Figure 3.4, (a) and (b) respectively.

2. For $F = \frac{\pm s}{s+2}$:

$$\left\| \begin{bmatrix} F & G \end{bmatrix} \right\|_\infty = 1$$

which implies (by Lemma 3.2) that $\Gamma_{[F,G]} = \Gamma_{[\text{lower}]}$ and $\gamma_{[F,G]} = \gamma_{[\text{lower}]}$, as shown in Figure 3.4, (c) and (d) respectively.

3. For $F = \frac{\pm 4s}{(s+2)^2}$:

$$\begin{aligned} &\Gamma_{[\text{lower}]} < \Gamma_{[F,G]} < \Gamma_{[\text{upper}]} \quad \text{and} \\ &\gamma_{[\text{upper}]} < \gamma_{[F,G]} < \gamma_{[\text{lower}]} \end{aligned}$$

as shown in Figure 3.4, (e) and (f) respectively.

Although these examples utilise only very simple transfer functions, they nevertheless demonstrate all of the important aspects of the functions $\Gamma_{[F,G]}$, $\gamma_{[F,G]}$ and their upper and lower bounds.

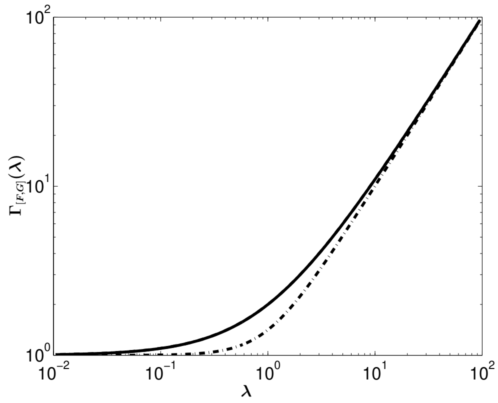

(a) $\Gamma_{[F,G]}$ for $F = \frac{\pm 2}{s+2}$ and $G = \frac{\pm 2}{s+2}$

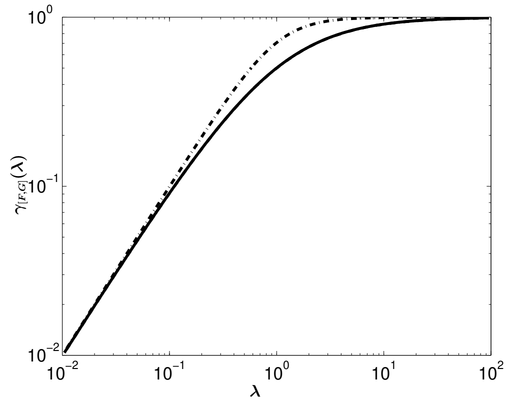

(b) $\gamma_{[F,G]}$ for $F = \frac{\pm 2}{s+2}$ and $G = \frac{\pm 2}{s+2}$

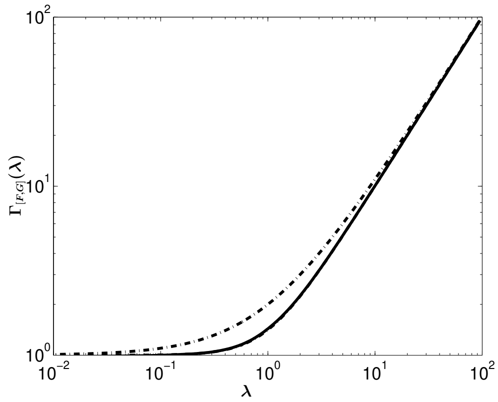

(c) $\Gamma_{[F,G]}$ for $F = \frac{\pm s}{s+2}$ and $G = \frac{\pm 2}{s+2}$

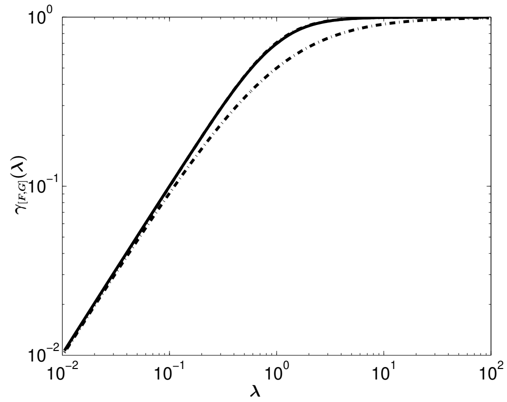

(d) $\gamma_{[F,G]}$ for $F = \frac{\pm s}{s+2}$ and $G = \frac{\pm 2}{s+2}$

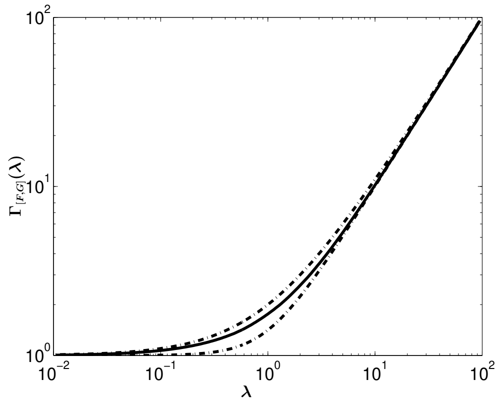

(e) $\Gamma_{[F,G]}$ for $F = \frac{\pm 4s}{(s+2)^2}$ and $G = \frac{\pm 2}{s+2}$

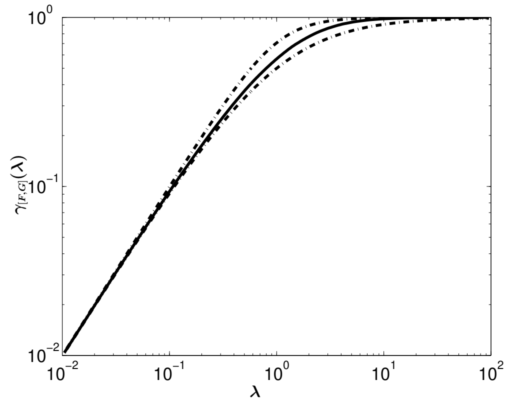

(f) $\gamma_{[F,G]}$ for $F = \frac{\pm 4s}{(s+2)^2}$ and $G = \frac{\pm 2}{s+2}$

Figure 3.4: Examples of generalised $\mathcal{H}_\infty$-norms

3.3 Global stability analysis

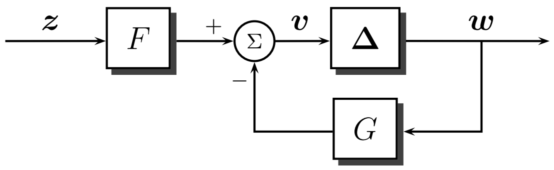

Figure 3.5: Linear system with nonlinearity $\boldsymbol{\Delta}$

Consider the interconnection

$$\boldsymbol{v} = F\boldsymbol{z} - G\boldsymbol{w} \tag{3.10}$$

$$\boldsymbol{w} = \boldsymbol{\Delta v} \tag{3.11}$$

shown in Figure 3.5. For integers $m, n, p \geq 1$ we make the following assumptions on the elements of Figure 3.5:

1. $\boldsymbol{z} \in \mathcal{L}_{2e}^{m}$ is a real-valued (vector or scalar) input
2. $F \in \mathcal{RH}_{\infty}^{n\times m}$ is a stable, proper real-rational transfer function
3. $G \in \mathcal{RH}_{2}^{n\times p}$ is a stable, strictly proper real-rational transfer function
4. $\boldsymbol{\Delta} : \mathcal{L}_{2e}^{n} \to \mathcal{L}_{2e}^{p}$ is a causal operator which
   - maps 0 to 0 (ie if $\boldsymbol{v}(t) = 0 \quad \forall t \geq 0$ then $(\boldsymbol{\Delta v})(t) = 0 \quad \forall t \geq 0$)
   - has finite $\mathcal{L}_2$-$\mathcal{L}_2$ gain, denoted by $\|\boldsymbol{\Delta}\|$
   - has finite uniform instantaneous gain (as defined earlier)

Given such F and G, let

$$\mu := \|G\|_{\infty} \tag{3.12}$$

$$\rho := \frac{\|F\|_{\infty}\,\|G\|_{2}}{\|F\|_{2}} \quad \text{if } F \text{ is strictly proper} \tag{3.13}$$

We shall claim, in light of the results of this chapter, that these two simple quantities (in conjunction with information about the nonlinearity $\boldsymbol{\Delta}$) can be used to predict a number of qualitative and quantitative properties of this interconnection. Firstly, however, we need to ensure that Equations 3.10 and 3.11 describe a suitable and sensible interconnection.

Well-posedness is a necessary property of any system which we wish to analyse - basically it ensures that the equations have unique, well-defined and robust solutions, which must be true for any physical process (and should be true of any model of such a process!) The following definition is standard and taken from Willems [Wil71]:

Definition 3.3 (Well-posedness)
The interconnection of Equations 3.10 and 3.11 is said to be well-posed *if*

1. *for any* $\boldsymbol{z} \in \mathcal{L}_{2e}^m$*, there exist unique solutions* $\boldsymbol{v} \in \mathcal{L}_{2e}^n$ *and* $\boldsymbol{w} \in \mathcal{L}_{2e}^p$
2. *on any finite interval* $[0, T]$ *the solutions* $\boldsymbol{v}$ *and* $\boldsymbol{w}$ *depend on* $\boldsymbol{z}$ *in a causal and Lipschitz-continuous way*
3. *the solutions* $\boldsymbol{v}, \boldsymbol{w}$ *are insensitive to modelling errors, in a sense defined by Willems [Wil71]*

Remark

1. Note that well-posedness implies, for any $T \geq 0$, that if $\|\Pi_T \boldsymbol{z}\|_2 = 0$ then $\|\Pi_T \boldsymbol{w}\|_2 = \|\Pi_T \boldsymbol{v}\|_2 = 0$, since this is clearly a valid (and hence unique) solution (all three of F, G and $\boldsymbol{\Delta}$ map 0 to 0)

Proposition 3.6
The interconnection of Equations 3.10 and 3.11 is well-posed.

PROOF OF PROPOSITION 3.6:
By Willems ([Wil71]), the interconnection is well-posed if the product of the uniform instantaneous gains of G and $\boldsymbol{\Delta}$ is bounded away from unity at any time $T \in [0, \infty)$.
But G is strictly proper, so has zero uniform instantaneous gain. The result then follows provided $\boldsymbol{\Delta}$ has finite uniform instantaneous gain at all times. ∎

We now define (global) stability in a standard way: "bounded inputs produce bounded outputs":

Definition 3.4 (Stability)
The interconnection of Equations 3.10 and 3.11 is said to be stable *if for any* $\boldsymbol{z} \in \mathcal{L}_2^m$

- $\boldsymbol{v} \in \mathcal{L}_2^n$ *and* $\boldsymbol{w} \in \mathcal{L}_2^p$

If the interconnection is not stable, it is said to be unstable.

As noted in the introduction, it will not always be possible to guarantee stability; with these cases in mind we define a form of local stability: "inputs in some restricted set produce bounded outputs":

Definition 3.5 (Local stability)

Given some set $\mathcal{Z} \subseteq \mathcal{L}_2^m$, the interconnection of Equations 3.10 and 3.11 is said to be locally stable with respect to $\mathcal{Z}$ *if for any $\boldsymbol{z} \in \mathcal{Z}$*

- $\boldsymbol{v} \in \mathcal{L}_2^n$ *and* $\boldsymbol{w} \in \mathcal{L}_2^p$

Remark

1. Note that our definition of *stability* is sometimes called "bounded-input bounded-output" (BIBO) stability, to distinguish it from, for example "finite-gain" stability:

   The interconnection of Equations 3.10 and 3.11 is said to be finite-gain stable *if there exist constants $K_1, K_2 < \infty$ such that for any $\boldsymbol{z} \in \mathcal{L}_2^m$*

   - $\|\boldsymbol{v}\|_2 < K_1 \|\boldsymbol{z}\|_2$ *and* $\|\boldsymbol{w}\|_2 < K_2 \|\boldsymbol{z}\|_2$

   which is a slightly stronger concept than (BIBO) *stability.*

   Also, note the equivalence between *local stability with respect to $\mathcal{L}_2^m$* and (BIBO) *stability.*

The following Proposition, based on the well-known small gain theorem attributed to Zames [Zam66a] gives a simple sufficient condition for stability of the interconnection, and in addition, shows that there is finite gain from $\|\boldsymbol{z}\|_2$ to $\|\boldsymbol{w}\|_2$ & $\|\boldsymbol{v}\|_2$ (and, if F is strictly proper, to $\|\boldsymbol{v}\|_\infty$):

Proposition 3.7 (Small-gain theorem)

The interconnection of Equations 3.10 and 3.11 is stable *if $\mu \|\boldsymbol{\Delta}\| < 1$.*
Furthermore, for any $\boldsymbol{z} \in \mathcal{L}_2^m$, and provided this condition is satisfied, then

$$\|\boldsymbol{w}\|_2 \leq \left\{ \frac{\|\boldsymbol{\Delta}\|}{1 - \mu \|\boldsymbol{\Delta}\|} \right\} \|F\|_\infty \|\boldsymbol{z}\|_2 \tag{3.14}$$

$$\|\boldsymbol{v}\|_2 \leq \left\{ \frac{1}{1 - \mu \|\boldsymbol{\Delta}\|} \right\} \|F\|_\infty \|\boldsymbol{z}\|_2 \tag{3.15}$$

$$\max_i \|v\|_\infty \leq \left\{ 1 + \rho \frac{\|\boldsymbol{\Delta}\|}{1 - \mu \|\boldsymbol{\Delta}\|} \right\} \|F\|_2 \|\boldsymbol{z}\|_2 \quad \text{if } F \in \mathcal{RH}_2 \tag{3.16}$$

Remark

1. Note the equivalent statement implicit in Proposition 3.7:

   If the interconnection of Equations 3.10 and 3.11 is unstable *then $\mu \|\boldsymbol{\Delta}\| \geq 1$.*

2. Recalling our earlier comment about the usefulness of μ and ρ, we see that (in conjunction with $\|\boldsymbol{\Delta}\|$), we can use them to find a sufficient condition for stability of the interconnection, and providing the condition is satisfied, to determine norm bounds on $\boldsymbol{v}$ and $\boldsymbol{w}$ in terms of $\|F\|_\infty \|\boldsymbol{z}\|_2$ and $\|F\|_2 \|\boldsymbol{z}\|_2$.

   In the remainder of this chapter we will state a number of gain results comparable to Equations 3.14, 3.15 and 3.16, on both finite and infinite horizons, and for restricted and unrestricted $\boldsymbol{z}$.

PROOF OF PROPOSITION 3.7:

The main statement is standard (eg Zames [Zam66a]); the norm bounds then follow by Propositions 2.2 and 2.3 (and some simple rearrangement) ∎

There are a great many other tests for stability, which can be significantly less conservative if some more information about $\mathbf{\Delta}$ is given. One such test, which is a special case of "D-scaling" (eg Zhou *et al* [ZDG96], chapter 11), is applicable when $\mathbf{\Delta}$ has a diagonal structure:

Proposition 3.8 (Diagonally-structured small gain theorem)

The interconnection of Equations 3.10 and 3.11 is stable *if* $\mathbf{\Delta}$ *has a diagonal structure*

$$\mathbf{\Delta} = \begin{bmatrix} \Delta_1 & 0 & \cdots & 0 \\ 0 & \Delta_2 & \cdots & 0 \\ \vdots & \vdots & \ddots & \vdots \\ 0 & 0 & \cdots & \Delta_{n_\Delta} \end{bmatrix}$$

for some $n_\Delta \geq 1$*, and there exists a compatibly partitioned, strictly positive diagonal matrix* $H = \mathrm{Diag}\{h_1 I, h_2 I, \cdots, h_{n_\Delta} I\}$ *such that*

$$\left\| H^{-1} \,\mathrm{Diag}\left\{ \|\Delta_1\| \, I, \|\Delta_2\| \, I, \cdots, \|\Delta_{n_\Delta}\| \, I \right\} G H \right\|_\infty < 1$$

PROOF OF PROPOSITION 3.8:

Consider applying Proposition 3.7 to the equivalent interconnection

$$\begin{aligned} \tilde{\boldsymbol{v}} &= H^{-1} D F \boldsymbol{z} + H^{-1} D G H \tilde{\boldsymbol{w}} \\ \tilde{\boldsymbol{w}} &= H^{-1} \mathbf{\Delta} D^{-1} H \tilde{\boldsymbol{v}} \end{aligned}$$

where $D = \mathrm{Diag}\left\{ \|\Delta_1\| \, I, \|\Delta_2\| \, I, \cdots, \|\Delta_{n_\Delta}\| \, I \right\}$ and $\|\mathbf{\Delta} D^{-1}\| = \|H^{-1} \mathbf{\Delta} D^{-1} H\| = 1$. ∎

Another stability test, which is related to the well-known circle criterion, is applicable when $\mathbf{\Delta}$ is a square nonlinearity in sector $[0, 1]$:

Theorem 3.9

The interconnection of Equations 3.10 and 3.11 is stable *if* $\mathbf{\Delta}$ *is a square nonlinearity in sector* $[0, 1]$ *and there exists a diagonal matrix* $A = \mathrm{Diag}\{a_1, a_2, \cdots, a_n\}$ *with* $a_i \in (0, 2)$ *for each* $i \in \{1, 2, \cdots, n\}$*, such that*

$$\|A(G + I) - I\|_\infty < 1$$

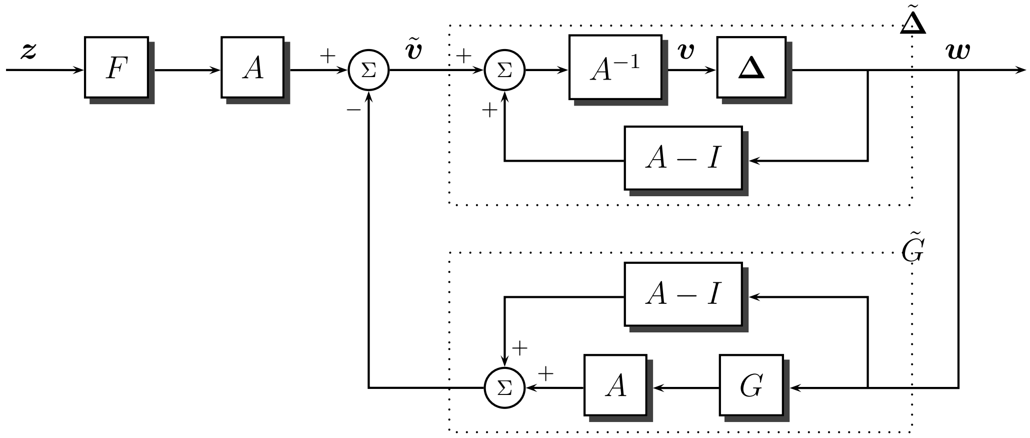

Figure 3.6: Equivalent representation of Figure 3.5

PROOF OF THEOREM 3.9:

Consider the interconnection in Figure 3.6, which is equivalent to that in Figure 3.5. The dotted lines outline two new operators, which we denote by $\tilde{G}$ and $\tilde{\boldsymbol{\Delta}}$, so that the interconnection may be represented as

$$\begin{aligned}\tilde{\boldsymbol{v}} &= AF\boldsymbol{z} + \tilde{G}\boldsymbol{w}\\ \boldsymbol{w} &= \tilde{\boldsymbol{\Delta}}\tilde{\boldsymbol{v}}\end{aligned}$$

where it is simple to see that $\tilde{G}$ is a linear transfer function:

$$\tilde{G} = A(G+I) - I$$

with $\tilde{G}(\infty) = A - I$.

We assume that $\boldsymbol{\Delta}$ is in sector $[0,1]$, ie

$$\int_0^\infty \boldsymbol{w}^*(\boldsymbol{w}-\boldsymbol{v})\,dt = \int_0^\infty \sum_{i=1}^n \big(w_i^*(w_i - v_i)\big)\,dt \le 0$$

and note that $\tilde{\boldsymbol{v}} = A\boldsymbol{v} - (A-I)\boldsymbol{w}$. If we consider

$$\begin{aligned}\int_0^\infty \boldsymbol{w}^*(\boldsymbol{w}-\tilde{\boldsymbol{v}})\,dt &= \int_0^\infty \boldsymbol{w}^* A(\boldsymbol{w}-\boldsymbol{v})\,dt\\ &= \int_0^\infty \sum_{i=1}^n \big(a_i w_i^*(w_i - v_i)\big)\,dt\end{aligned}$$

it is clear that $\tilde{\boldsymbol{\Delta}}$ is also in sector $[0,1]$ for any diagonal matrix $A > 0$.

For well-posedness of this new representation, however, we require that $\|A-I\| < 1$, ie that $a_i \in (0,2)$ for each $i \in \{1,2,\cdots,n\}$. The stability condition is then immediate, by Proposition 3.7. ∎

The following Corollary shows that, if the nonlinearity is an ideal unity deadzone, we can also bound the size of $\|\boldsymbol{w}\|_2$:

Corollary 3.10

The interconnection of Equations 3.10 and 3.11 with $\boldsymbol{\Delta} = \mathbf{Dzn}$ *is* stable *if there exists a diagonal matrix* $A = \mathrm{Diag}\{a_1, a_2, \cdots, a_n\}$ *with* $a_i \in (0, 2)$ *for each* $i \in \{1, 2, \cdots, n\}$*, such that*

$$\|A(G+I) - I\|_\infty < 1$$

Furthermore, in this case, for any $\boldsymbol{z} \in \mathcal{L}_2^m$

$$\|\boldsymbol{w}\|_2 \leq \frac{\|A\|}{1 - \|A(G+I) - I\|_\infty} \|\mathbf{Dzn}(F\boldsymbol{z})\|_2$$

PROOF OF COROLLARY 3.10:

Applying the same loop transformation used in the proof of Theorem 3.9, we find that

$$\tilde{\boldsymbol{\Delta}} = \mathbf{Dzn}_A$$

By Lemma 2.5 we can then deduce that

$$\begin{aligned}\|\boldsymbol{w}\|_2 &\leq \|\mathbf{Dzn}_A(AF\boldsymbol{z})\|_2 + \|A(G+I) - I\|_\infty \|\boldsymbol{w}\|_2 \\ &\leq \frac{\|\mathbf{Dzn}_A(AF\boldsymbol{z})\|_2}{1 - \|A(G+I) - I\|_\infty}\end{aligned}$$

provided that the stability condition of Theorem 3.9 is satisfied. But

$$\mathbf{Dzn}_A(AF\boldsymbol{z}) = A\mathbf{Dzn}(F\boldsymbol{z})$$

and so the bound follows immediately. ∎

3.4 Local stability analysis

3.4.1 Ideal deadzone nonlinearity

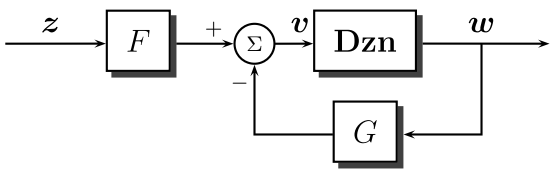

Figure 3.7: Linear system with unity deadzone nonlinearity

We consider the interconnection of Section 3.3, in the case that the nonlinearity $\boldsymbol{\Delta}$ is the ideal unity[2] deadzone function of Equation 2.9, ie

$$\boldsymbol{v} = F\boldsymbol{z} - G\boldsymbol{w} \tag{3.17}$$

$$\boldsymbol{w}(t) = \mathbf{Dzn}\big(\boldsymbol{v}(t)\big) \tag{3.18}$$

with $p = n$, ie $\boldsymbol{v}, \boldsymbol{w} \in \mathcal{L}^n_{2e}$.

We make one extra assumption in addition to those in Section 3.3:

5. F is *strictly* proper.[3]

and recall that we defined $\mu := \|G\|_\infty$ and $\rho := \frac{\|F\|_\infty \|G\|_2}{\|F\|_2}$ in the previous section.

There are two main results in this section, which apply to both stable and unstable interconnections: firstly (Theorem 3.11) that it is possible to obtain a lower bound on the local nonlinear "gain" from $\|\Pi_T \boldsymbol{z}\|_2$ to each of $\|\Pi_T \boldsymbol{w}\|_2$, $\|\Pi_T \boldsymbol{v}\|_2$ & $\max_i \|\Pi_T v_i\|_\infty$, and secondly (Theorem 3.16 & Corollary 3.19) that these local results are guaranteed to be applicable to a wider range of $\|\Pi_T \boldsymbol{z}\|_2$ than the "nominal" (and obvious) local result

$$\|\Pi_T \boldsymbol{w}\|_2 = 0 \quad \text{if } \|\Pi_T \boldsymbol{z}\|_2 \le \tfrac{1}{\|F\|_2}$$

provided either that $\mu < 1$ (which, of course, implies global stability) or $\rho < 1$.

Firstly, however, we need a few definitions: let

$$\lambda^0_{[F,G]} := 0 \tag{3.19}$$

$$\lambda^1_{[F,G]} := \begin{cases} \gamma^{-1}_{[F,G]}(1) & \text{if } \mu < 1 \\ \infty & \text{if } \mu \ge 1 \end{cases} \tag{3.20}$$

where $\gamma_{[F,G]}$ is as in Definition 3.2.

[2]The assumption of unity saturation level entails no significant loss of generality.

[3]One unfortunate effect of this assumption is that the "absolute stability" problem of Figure 3.2 (and, indeed, any other interconnection with biproper F) is excluded from the local analysis method. This may sometimes be rectified by considering, for example, a sequence $F_\varepsilon = \frac{1}{1+\varepsilon s}F$ and letting $\varepsilon \to 0$. There are more comments on this topic in the summary at the end of this chapter.

Then let

$$\begin{aligned}\boldsymbol{\Lambda}_{[F,G]} &:= \Big\{\lambda \in (0,\infty) : \gamma_{[F,G]}(\lambda) \in (0,1)\Big\} \\ &= (\lambda^0_{[F,G]}, \lambda^1_{[F,G]})\end{aligned} \tag{3.21}$$

so that $\lambda \in \boldsymbol{\Lambda}_{[F,G]} \iff \gamma_{[F,G]}(\lambda) \in (0,1) \iff \frac{1}{1-\gamma_{[F,G]}(\lambda)} \in (1,\infty)$

Theorem 3.11

For any $\lambda \in \boldsymbol{\Lambda}_{[F,G]}$*, any* $T > 0$ *and* $\boldsymbol{z} \in \mathcal{L}^m_{2e}$ *such that*

$$\|\Pi_T \boldsymbol{z}\|_2 < \frac{1}{\|F\|_2} \frac{1}{\big\{1+\rho\lambda\big\}\big\{1-\gamma_{[F,G]}(\lambda)\big\}}$$

then on the interval $[0,T]$ *the unique solutions* $\boldsymbol{v}, \boldsymbol{w} \in \mathcal{L}^n_{2e}$ *to Equations 3.17 and 3.18 satisfy*

$$\begin{aligned}\|\Pi_T \boldsymbol{w}\|_2 &< \big\{\lambda\big\}\, \|F\|_\infty \|\Pi_T \boldsymbol{z}\|_2 \\ \|\Pi_T \boldsymbol{v}\|_2 &< \big\{\Gamma_{[F,G]}(\lambda)\big\}\, \|F\|_\infty \|\Pi_T \boldsymbol{z}\|_2 \\ \max_i \|\Pi_T v_i\|_\infty &< \big\{1+\rho\lambda\big\}\, \|F\|_2 \|\Pi_T \boldsymbol{z}\|_2 \left(< \frac{1}{1-\gamma_{[F,G]}(\lambda)}\right)\end{aligned}$$

Remark

1. We clarify this result with a simple scalar example: take $F = \frac{\pm 4s}{(s+2)^2}$ and $G = \frac{\pm 2.2}{s+2}$ in Equations 3.17 and 3.18, for which $\boldsymbol{\Lambda}_{[F,G]} = (0,\infty)$.

   Taking $\lambda = 2$, for example, the Theorem then states that

   $$\text{If } \|\Pi_T z\|_2 < 1 \text{ then} \quad \left\{\begin{array}{ll} \|\Pi_T w\|_2 & < 2\,\|\Pi_T z\|_2 \\ \|\Pi_T v\|_2 & < 2.6\,\|\Pi_T z\|_2 \\ \|\Pi_T v\|_\infty & < 1.6\,\|\Pi_T z\|_2 \end{array}\right.$$

   This relationship between $\|\Pi_T z\|_2$ and $\|\Pi_T w\|_2$ may be shown graphically as in Figure 3.8 (a): at no time $T \geq 0$ may the point given by

   $$\big[\|\Pi_T z\|_2 \quad \|\Pi_T w\|_2\big]$$

   be within the shaded region, ie that area to the left of $\frac{1}{\|F\|_2}\frac{1}{\big\{1+\rho\lambda\big\}\big\{1-\gamma_{[F,G]}(\lambda)\big\}}$ $(=1)$ and above the line with gradient $\lambda \|F\|_\infty$ $(=2)$.

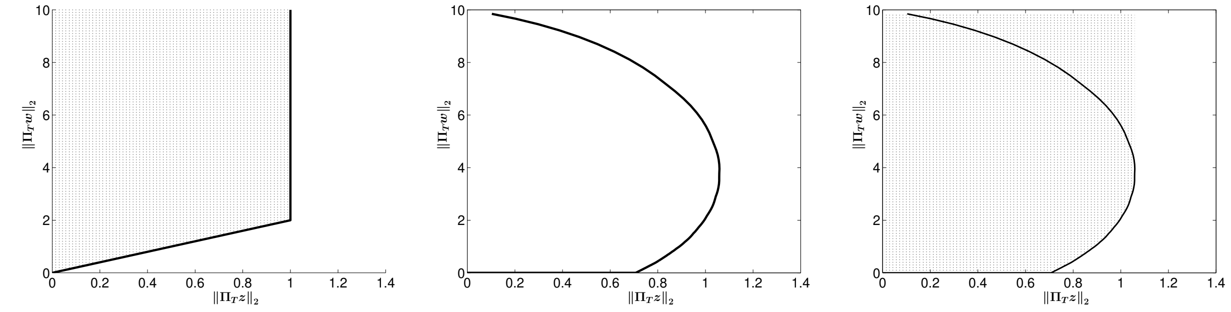

(a) (b) (c)

Figure 3.8: Graphical interpretation of Theorem 3.11 (shown for $F = \frac{\pm 4s}{(s+2)^2}$ and $G = \frac{\pm 2.2}{s+2}$)

Noting that this "forbidden region" is defined by its corner point, and that the Theorem gives one such region for each $\lambda \in \mathbf{\Lambda}_{[F,G]}$, we plot the continuous curve defined by the union of all of these corner points, ie

$$\left[\frac{1}{\|F\|_2} \frac{1}{\left\{1+\rho\lambda\right\}\left\{1-\gamma_{[F,G]}(\lambda)\right\}} \quad \frac{\|F\|_\infty \lambda}{\|F\|_2} \frac{1}{\left\{1+\rho\lambda\right\}\left\{1-\gamma_{[F,G]}(\lambda)\right\}} \right]$$

as shown in Figure 3.8 (b). We shall refer to this curve as the "characteristic bounding curve", since it contains *all* the information which can be obtained from Theorem 3.11 (relating $\|\Pi_T w\|_2$ to $\|\Pi_T z\|_2$)

Finally, the overall "forbidden region" (ie the union over all $\lambda \in \mathbf{\Lambda}_{[F,G]}$ of the individual forbidden regions) is shown in Figure 3.8 (c). It may be seen that this region can be determined from only the lower half of the "characteristic bounding curve", ie that portion of the curve which is increasing in the x-direction.

Figures 3.8 (b) or (c) may then be used to determine (conservatively) the local stability properties of the interconnection, in the sense that the following quantities may be read off the plot:

(a) A lower bound on the largest permissible $\|\Pi_T z\|_2$ which guarantees that $\Pi_T w \in \mathcal{L}_2$

(b) An upper bound on the nonlinear "gain" from $\|\Pi_T z\|_2$ to $\|\Pi_T w\|_2$, as a function of $\|\Pi_T z\|_2$ (provided that $\|\Pi_T z\|_2$ is no greater than the largest permitted value determined in (a))

Similar graphical interpretations hold for the relationships between $\|\Pi_T z\|_2$ & $\|\Pi_T v\|_2$ and between $\|\Pi_T z\|_2$ & $\|\Pi_T v\|_\infty$.

Proof of Theorem 3.11 will require the following Lemma:

Lemma 3.12

For any $\boldsymbol{z} \in \mathcal{L}_{2e}^m$ and $T > 0$ with $\|\Pi_T \boldsymbol{z}\|_2 \neq 0$ there exists some $T_0 \in (0, T]$ such that the unique solutions $\boldsymbol{v}, \boldsymbol{w} \in \mathcal{L}_{2e}^n$ to Equations 3.17 and 3.18 satisfy

$$\begin{aligned} \|\Pi_{T_0} \boldsymbol{z}\|_2 &\neq 0 \quad \textit{and} \\ \|\Pi_{T_0} \boldsymbol{w}\|_2 &= 0 \end{aligned}$$

PROOF OF LEMMA 3.12:

We use proof by contradiction: assume that there exists some $\boldsymbol{z} \in \mathcal{L}_{2e}^m$ and $T > 0$ with $\|\Pi_T \boldsymbol{z}\|_2 \neq 0$ such that for all $T_0 \in (0, T]$ either

$$\begin{aligned} \|\Pi_{T_0} \boldsymbol{z}\|_2 &= 0 \quad \big(\implies \|\Pi_{T_0} \boldsymbol{w}\|_2 = 0\big) \quad \text{or} \\ \|\Pi_{T_0} \boldsymbol{w}\|_2 &\neq 0 \quad \big(\implies \|\Pi_{T_0} \boldsymbol{z}\|_2 \neq 0\big) \end{aligned}$$

ie $\|\Pi_{T_0} \boldsymbol{z}\|_2$ and $\|\Pi_{T_0} \boldsymbol{w}\|_2$ are either both zero or both non-zero.

There exists (by Proposition 2.1) some $T_1 \in (0, T]$ such that

$$0 < \|\Pi_{T_1} \boldsymbol{z}\|_2 < \tfrac{1}{2\|F\|_2} \quad \big(\implies \|\Pi_{T_1} \boldsymbol{w}\|_2 > 0\big)$$

and similarly some $T_2 \in (0, T]$ such that

$$0 < \|\Pi_{T_2} \boldsymbol{w}\|_2 < \tfrac{1}{2\|G\|_2} \quad \big(\implies \|\Pi_{T_2} \boldsymbol{z}\|_2 > 0\big)$$

so letting $T_0 := \min\{T_1, T_2\}$ we see immediately that

$$0 < \|\Pi_{T_0} \boldsymbol{z}\|_2 < \tfrac{1}{2\|F\|_2} \quad \text{and} \quad 0 < \|\Pi_{T_0} \boldsymbol{w}\|_2 < \tfrac{1}{2\|G\|_2}$$

Hence by Proposition 2.3

$$\begin{aligned} \max_i \|\Pi_{T_0} v_i\|_\infty &\leq \|F\|_2 \|\Pi_{T_0} \boldsymbol{z}\|_2 + \|G\|_2 \|\Pi_{T_0} \boldsymbol{w}\|_2 \\ &< 1 \end{aligned}$$

But this implies (by Lemma 2.7) that $\|\Pi_{T_0} \boldsymbol{w}\|_2 = 0$, contradicting our assumption. Hence the Lemma is true. ∎

We can now prove Theorem 3.11:

PROOF OF THEOREM 3.11:

Consider the first inequality: it is clear that $\|\Pi_T \boldsymbol{z}\|_2 = 0 \Longrightarrow \|\Pi_T \boldsymbol{w}\|_2 = 0$, so assume that $\|\Pi_T \boldsymbol{z}\|_2 \neq 0$ and

$$\|\Pi_T \boldsymbol{w}\|_2 \geq \lambda \|F\|_\infty \|\Pi_T \boldsymbol{z}\|_2$$

By Lemma 3.12 there exists some $T_0 \in (0, T]$ such that $\|\Pi_{T_0} \boldsymbol{z}\|_2 \neq 0$ and

$$\|\Pi_{T_0} \boldsymbol{w}\|_2 = 0$$

so by Proposition 2.1 there exists some $T_1 \in (T_0, T]$ such that $\|\Pi_{T_1} \boldsymbol{z}\|_2 \neq 0$ and

$$\|\Pi_{T_1} \boldsymbol{w}\|_2 = \lambda \|F\|_\infty \|\Pi_{T_1} \boldsymbol{z}\|_2$$

By Corollary 3.3 we have that

$$\begin{aligned}&\|\Pi_{T_1} \boldsymbol{v}\|_2 \leq \Gamma_{[F,G]}(\lambda) \|F\|_\infty \|\Pi_{T_1} \boldsymbol{z}\|_2 = \frac{\Gamma_{[F,G]}(\lambda)}{\lambda} \|\Pi_{T_1} \boldsymbol{w}\|_2 \quad \text{ie} \\ &\|\Pi_{T_1} \boldsymbol{w}\|_2 \geq \gamma_{[F,G]}(\lambda) \|\Pi_{T_1} \boldsymbol{v}\|_2\end{aligned}$$

so by Lemma 2.7

$$\max_i \|\Pi_{T_1} v_i\|_\infty \geq \frac{1}{1 - \gamma_{[F,G]}(\lambda)}$$

By Proposition 2.3 we have that

$$\begin{aligned}\max_i \|\Pi_{T_1} v_i\|_\infty &\leq \|F\|_2 \|\Pi_{T_1} \boldsymbol{z}\|_2 + \|G\|_2 \|\Pi_{T_1} \boldsymbol{w}\|_2 \\ &= \big\{ \|F\|_2 + \|G\|_2 \|F\|_\infty \lambda \big\} \|\Pi_{T_1} \boldsymbol{z}\|_2 \\ &= \big\{1 + \rho\lambda\big\} \|F\|_2 \|\Pi_{T_1} \boldsymbol{z}\|_2\end{aligned}$$

so we have shown that $\|\Pi_T \boldsymbol{w}\|_2 \geq \lambda \|F\|_\infty \|\Pi_T \boldsymbol{z}\|_2$ implies

$$\|F\|_2 \|\Pi_T \boldsymbol{z}\|_2 \geq \|F\|_2 \|\Pi_{T_1} \boldsymbol{z}\|_2 \geq \frac{1}{\big\{1 + \rho\lambda\big\}\big\{1 - \gamma_{[F,G]}(\lambda)\big\}}$$

which is equivalent to the first inequality. The bounds on $\|\Pi_T \boldsymbol{v}\|_2$ and $\max_i \|\Pi_T v_i\|_\infty$ follow immediately by Corollary 3.3 and Propositions 2.2 and 2.3. ∎

In the remainder of the section we state a number of results which are all essentially derived from Theorem 3.11; for clarity of presentation we make the following definitions: for $\lambda \in \boldsymbol{\Lambda}_{[\boldsymbol{F},\boldsymbol{G}]}$ let

$$Z_{[F,G]}(\lambda) := \frac{1}{\left\{1+\rho\lambda\right\}\left\{1-\gamma_{[F,G]}(\lambda)\right\}} \tag{3.22}$$

and, since the largest such value will clearly be informative, let

$$Z^{\text{opt}}_{[F,G]} := \sup_{\lambda \in \boldsymbol{\Lambda}_{[\boldsymbol{F},\boldsymbol{G}]}} Z_{[F,G]}(\lambda) \tag{3.23}$$

Corollary 3.13 gives a straightforward infinite-horizon interpretation of Theorem 3.11, and Corollary 3.14 gives the "best" such result:

Corollary 3.13

For any $\lambda \in \boldsymbol{\Lambda}_{[\boldsymbol{F},\boldsymbol{G}]}$ the interconnection of Equations 3.17 and 3.18 is locally stable with respect to the set

$$\mathbb{Z}_{[F,G]}(\lambda) = \left\{\boldsymbol{z} : \|\boldsymbol{z}\|_2 < \tfrac{1}{\|F\|_2} Z_{[F,G]}(\lambda)\right\}$$

Furthermore for any $\boldsymbol{z} \in \mathbb{Z}_{[F,G]}(\lambda)$ the solutions $\boldsymbol{v}, \boldsymbol{w} \in \mathcal{L}_2^n$ to Equations 3.17 and 3.18 satisfy

$$\begin{aligned} \|\boldsymbol{w}\|_2 &< \left\{\lambda\right\} \|F\|_\infty \|\boldsymbol{z}\|_2 \\ \|\boldsymbol{v}\|_2 &< \left\{\Gamma_{[F,G]}(\lambda)\right\} \|F\|_\infty \|\boldsymbol{z}\|_2 \\ \max_i \|v_i\|_\infty &< \left\{1+\rho\lambda\right\} \|F\|_2 \|\boldsymbol{z}\|_2 \left(< \frac{1}{1-\gamma_{[F,G]}(\lambda)}\right) \end{aligned}$$

PROOF OF COROLLARY 3.13:

Directly from Theorem 3.11. ∎

Corollary 3.14

The interconnection of Equations 3.17 and 3.18 is locally stable with respect to the set

$$\mathbb{Z}^{opt}_{[F,G]} = \left\{\boldsymbol{z} : \|\boldsymbol{z}\|_2 < \tfrac{1}{\|F\|_2} Z^{opt}_{[F,G]}\right\}$$

Remark

1. Returning to Figure 3.8 (c), we see that this corresponds to the point

$$\left[\left\|\Pi_T \boldsymbol{z}\right\|_2 \quad \left\|\Pi_T \boldsymbol{w}\right\|_2\right]$$

remaining under the shaded region for all $T \geq 0$.

As mentioned in the Remarks following Theorem 3.11, a useful way to determine $Z^{\text{opt}}_{[F,G]}$ is to read it from the "characteristic bounding curve" (Figure 3.8 (b))

PROOF OF COROLLARY 3.14:
Directly from Corollary 3.13 and the definition of $Z^{\text{opt}}_{[F,G]}$. ∎

The limiting case as $\lambda \searrow 0$ in Corollary 3.13 is interesting, as it corresponds to the deadzone nonlinearity being inactive, ie $\boldsymbol{w} \equiv 0$. Let

$$Z^0_{[F,G]} := \lim_{\lambda \searrow 0} Z_{[F,G]}(\lambda) = 1 \tag{3.24}$$

Corollary 3.15
The interconnection of Equations 3.17 and 3.18 is locally stable with respect to the set

$$\mathbb{Z}^0_{[F,G]} = \left\{\boldsymbol{z} : \left\|\boldsymbol{z}\right\|_2 \leq \tfrac{1}{\|F\|_2} Z^0_{[F,G]}\right\}$$

Furthermore, for any $\boldsymbol{z} \in \mathbb{Z}^0_{[F,G]}$ the solutions $\boldsymbol{v}, \boldsymbol{w} \in \mathcal{L}_2^n$ to Equations 3.17 and 3.18 satisfy

$$\begin{aligned} \left\|\boldsymbol{w}\right\|_2 &= 0 \\ \left\|\boldsymbol{v}\right\|_2 &\leq \left\|F\right\|_\infty \left\|\boldsymbol{z}\right\|_2 \\ \max_i \left\|v_i\right\|_\infty &\leq \left\|F\right\|_2 \left\|\boldsymbol{z}\right\|_2 \Big(\leq 1\Big) \end{aligned}$$

Remarks

1. This result is not really surprising - in fact it is exactly what one would expect. However, the equivalent result in the general case (Corollary 3.25) will not be so obvious!
2. It is clear from this result that $Z^{\text{opt}}_{[F,G]} > Z^0_{[F,G]}$ is desirable, since otherwise there will be nothing more to gain from Corollaries 3.13 or 3.14.

   If the interconnection can be shown to be stable (ie, in the case $\mu < 1$), then this inequality will be trivially satisfied; otherwise (ie, in the case $\mu \geq 1$) we shall show in Corollary 3.19 that $\rho < 1$ is a sufficient condition to guarantee that $Z^{\text{opt}}_{[F,G]} > Z^0_{[F,G]}$.

PROOF OF COROLLARY 3.15:
Directly from Corollary 3.13 by considering $\lambda \searrow 0$. ∎

We now consider the cases $\mu < 1$ and $\mu \geq 1$ separately:

Case (a): $\mu < 1$, stability is assured

If $\mu < 1$ then we know already (by Proposition 3.7) that the interconnection must be *stable*. The same deduction may be made from Corollary 3.13:

Theorem 3.16

If $\mu < 1$ then

$$Z^{opt}_{[F,G]} = \infty$$

and the interconnection of Equations 3.17 and 3.18 is therefore ***stable****.*

Furthermore, for any $\boldsymbol{z} \in \mathcal{L}_2^m$ the solutions $\boldsymbol{v}, \boldsymbol{w} \in \mathcal{L}_2^n$ to Equations 3.17 and 3.18 satisfy

$$\|\boldsymbol{w}\|_2 \leq \left\{\gamma^{-1}_{[F,G]}(1)\right\} \|F\|_\infty \|\boldsymbol{z}\|_2 \tag{3.25}$$

$$\|\boldsymbol{v}\|_2 \leq \left\{\gamma^{-1}_{[F,G]}(1)\right\} \|F\|_\infty \|\boldsymbol{z}\|_2 \tag{3.26}$$

$$\max_i \|v_i\|_\infty \leq \left\{1 + \rho\gamma^{-1}_{[F,G]}(1)\right\} \|F\|_2 \|\boldsymbol{z}\|_2 \tag{3.27}$$

Moreover, $\gamma^{-1}_{[F,G]}(1)$ is bounded above and below by

$$\gamma^{-1}_{[lower]}(1) \leq \gamma^{-1}_{[F,G]}(1) \leq \gamma^{-1}_{[upper]}(1)$$

where each of these inequalities is tight (in the sense of Lemma 3.2) and

$$\gamma^{-1}_{[lower]}(1) = \frac{1}{\sqrt{1-\mu^2}} \qquad \gamma^{-1}_{[upper]}(1) = \frac{1}{1-\mu}$$

Hence the inequalities in Equations 3.25, 3.26 and 3.27 are no weaker than, and may be significantly stronger than, Equations 3.14, 3.15 and 3.16 in Proposition 3.7.

Remark

1. This result gives only the global gain bounds; it may still be useful sometimes to calculate the local gain bounds of Corollary 3.13 in order to see how the performance varies with $\|\boldsymbol{z}\|_2$.

PROOF OF THEOREM 3.16:

Directly from Corollary 3.13 by considering $\lambda \nearrow \gamma^{-1}_{[F,G]}(1)$, and noting that $\mu < 1$ implies $\gamma^{-1}_{[F,G]}(1) < \infty$. ∎

Case (b): $\mu \geq 1$, stability *may* be assured if $\mu = 1$, and is *not* assured if $\mu > 1$

Define, for $\lambda \in (0, \infty)$

$$Z_{[\text{lower}]}(\lambda) := \frac{1}{\{1+\rho\lambda\}\{1-\gamma_{[\text{lower}]}(\lambda)\}} \tag{3.28}$$

$$Z_{[\text{upper}]}(\lambda) := \frac{1}{\{1+\rho\lambda\}\{1-\gamma_{[\text{upper}]}(\lambda)\}} \tag{3.29}$$

and let $Z^{\text{opt}}_{[\text{lower}]}$ and $Z^{\text{opt}}_{[\text{upper}]}$ be defined analogously to Equation 3.23. Note that by Lemma 3.5

$$Z^{\text{opt}}_{[\text{upper}]} \leq Z^{\text{opt}}_{[F,G]} \leq Z^{\text{opt}}_{[\text{lower}]} \tag{3.30}$$

where each of these inequalities is tight (in the sense of Lemma 3.2)

If $\mu = 1$ then it is possible, although not certain, that we can guarantee stability:

Theorem 3.17

If $\mu = 1$ then

$$Z^{opt}_{[upper]} = \begin{cases} \frac{1}{\rho}\Big(> 1\Big) & \text{if } \rho < 1 \\ 1 & \text{if } \rho \geq 1 \end{cases}$$

and

$$Z^{opt}_{[lower]} = \infty$$

*Hence it is possible that $\mathbb{Z}^{opt}_{[F,G]}$ in Corollary 3.14 is the whole of $\mathcal{L}_2^m$, in which case the interconnection of Equations 3.17 and 3.18 is **stable**.*

Remarks

1. Note that this is *only* BIBO stability: it is not possible to state finite gain results similar to Theorem 3.11. The reason for this is that the result comes from considering $\lambda \to \infty$ in Corollary 3.13.

2. So, by Lemma 3.4, the interconnection is stable if $\|G\|_\infty = 1$ and $\left\| \begin{bmatrix} \frac{F}{\|F\|_\infty} & G \end{bmatrix} \right\|_\infty = 1$

PROOF OF THEOREM 3.17:

In the case $\mu = 1$ it is possible to find $Z^{\text{opt}}_{[\text{upper}]}$ by standard methods; we cannot find $Z^{\text{opt}}_{[\text{lower}]}$, but we can show that $Z_{[\text{lower}]}(\lambda) \to \infty$ as $\lambda \to \infty$.

Then, by Equation 3.30, we see that $Z^{\text{opt}}_{[F,G]} = Z^{\text{opt}}_{[\text{lower}]} = \infty$ is possible, in which case the interconnection would (by Corollary 3.14) be locally stable with respect to $\mathcal{L}_2^m$. But, by Definitions 3.4 and 3.5, local stability with respect to $\mathcal{L}_2^m$ is equivalent to stability. ∎

If $\mu > 1$ then we cannot guarantee stability:

Theorem 3.18
If $\mu > 1$ then

$$Z^{opt}_{[upper]} = \begin{cases} \left(\frac{\sqrt{\rho(\mu-1)}+\sqrt{\mu-\rho}}{\sqrt{\rho(\mu-\rho)}+\sqrt{\mu-1}}\right)^2 \in (1, \frac{1}{\rho}) & \text{if } \rho < 1 \\ 1 & \text{otherwise} \end{cases}$$

and

$$Z^{opt}_{[lower]} = \begin{cases} \in [\frac{\mu^3}{\mu(\mu^2-1)+\rho\sqrt{\mu^2-1}}, \frac{\mu}{\mu-1}] \subset (1, \infty) & \text{if } \rho < \frac{\mu}{\sqrt{\mu^2-1}} \\ 1 & \text{otherwise} \end{cases}$$

*Hence it is **not** possible that $\mathbb{Z}^{opt}_{[F,G]}$ in Corollary 3.14 is the whole of $\mathcal{L}_2^m$, so we **cannot** guarantee stability of the interconnection of Equations 3.17 and 3.18.*

Remarks

1. Note that $\mu > 1$ **does not** imply that the interconnection is *unstable*, merely that in this case the largest local stability region identified by this method is strictly smaller than the whole of $\mathcal{L}_2^m$.

2. Note also that $Z^{\text{opt}}_{[\text{upper}]} < \frac{1}{\rho}$ for any $\mu > 1$ and $\rho < 1$, ie that reducing μ to unity cannot increase $Z^{\text{opt}}_{[\text{upper}]}$ past $\frac{1}{\rho}$.

   However, the lower bound for $Z^{\text{opt}}_{[\text{lower}]}$ *can* be made arbitrarily large by making μ close to unity (provided always that $\rho < \frac{\mu}{\sqrt{\mu^2-1}}$, which ceases to be a problem as $\mu \to 1$)

   Hence, as $\mu \to 1$, we see that $Z^{\text{opt}}_{[F,G]}$ is bounded below by a number which is slightly less than $\frac{1}{\rho}$, and bounded above by a number which is arbitrarily large. Recall that both of these bounds are tight (in the sense of Lemma 3.2, ie for each bound there exist F and G achieving equality.) This suggests that we cannot make any stronger deductions without more analysis.

   If, however, it is possible to manipulate F such that $\left\| \begin{bmatrix} \frac{F}{\|F\|_\infty} & \frac{G}{\|G\|_\infty} \end{bmatrix} \right\|_\infty = 1$, then $Z^{\text{opt}}_{[F,G]} = Z^{\text{opt}}_{[\text{lower}]}$ will be achieved, and hence (provided both F and G can be manipulated to this extent — sometimes F and/or G will be fixed *a priori*), it is possible to obtain *semi-global* stability, in the sense that the interconnection will be locally stable with respect to an arbitrarily large subset of $\mathcal{L}_2^m$.

PROOF OF THEOREM 3.18:

In the case $\mu > 1$ we cannot solve for $Z^{\text{opt}}_{[\text{lower}]}$ analytically; we can, however, find $Z^{\text{opt}}_{[\text{upper}]}$ and show that if $\rho \geq \frac{\mu}{\sqrt{\mu^2-1}}$ then there are no λ such that $Z_{[\text{lower}]}(\lambda) > 1$.

For $\rho < \frac{\mu}{\sqrt{\mu^2-1}}$ we can only find upper and lower bounds for $Z^{\text{opt}}_{[\text{lower}]}$. The lower bound comes from simply considering a particular value of λ in $Z_{[\text{lower}]}$:

$$Z_{[\text{lower}]}\left(\tfrac{1}{\mu\sqrt{\mu^2-1}}\right) = \frac{\mu^3}{\mu(\mu^2-1) + \rho\sqrt{\mu^2-1}}$$

Noting that for all $\lambda \in \mathbf{\Lambda}_{[F,G]}$

$$\frac{1}{\{1+\rho\lambda\}\{1-\gamma_{[\text{lower}]}(\lambda)\}} < \frac{1}{1-\gamma_{[\text{lower}]}(\lambda)} < \frac{1}{1-\frac{1}{\mu}}$$

gives the upper bound. ∎

If $1 < Z^{\text{opt}}_{[F,G]} < \infty$ then let

$$\lambda^{\text{opt}}_{[F,G]} := \arg\max_{\lambda\in\mathbf{\Lambda}_{[F,G]}} Z_{[F,G]}(\lambda) \tag{3.31}$$

(which is guaranteed to exist, since the function is continuous and does not achieve its supremum at an endpoint)

Corollary 3.19

If $\mu \geq 1$ and $1 < Z^{opt}_{[F,G]} < \infty$ then the interconnection of Equations 3.17 and 3.18 is locally stable with respect to the set

$$\mathbb{Z}^{opt}_{[F,G]} = \left\{\boldsymbol{z} : \|\boldsymbol{z}\|_2 < \tfrac{1}{\|F\|_2} Z^{opt}_{[F,G]}\right\}$$

Furthermore, for any $\boldsymbol{z} \in \mathbb{Z}^{opt}_{[F,G]}$ the solutions $\boldsymbol{v}, \boldsymbol{w} \in \mathcal{L}_2^n$ satisfy

$$\begin{aligned}
\|\boldsymbol{w}\|_2 &< \left\{\lambda^{opt}_{[F,G]}\right\} \|F\|_\infty \|\boldsymbol{z}\|_2 \\
\|\boldsymbol{v}\|_2 &< \left\{\Gamma_{[F,G]}(\lambda^{opt}_{[F,G]})\right\} \|F\|_\infty \|\boldsymbol{z}\|_2 \\
\max_i \|v_i\|_\infty &< \left\{1+\rho\lambda^{opt}_{[F,G]}\right\} \|F\|_2 \|\boldsymbol{z}\|_2 \left(< \frac{1}{1-\gamma_{[F,G]}(\lambda^{opt}_{[F,G]})}\right)
\end{aligned}$$

Moreover

- *if $\mu > 1$ and $\rho \geq \frac{\mu}{\sqrt{\mu^2-1}}$ then it is certain that $Z^{opt}_{[F,G]} = Z^{opt}_{[lower]} = 1$*
- *if $\mu > 1$ then it is certain that $Z^{opt}_{[F,G]} \leq Z^{opt}_{[lower]} < \infty$*
- *if $\mu \geq 1$ and $\rho < 1$ then it is certain that $1 < Z^{opt}_{[upper]} \leq Z^{opt}_{[F,G]}$*

Remarks

1. If $Z^{\mathrm{opt}}_{[F,G]} = 1$ then Corollary 3.15 gives the best result available, and the possibility that $Z^{\mathrm{opt}}_{[F,G]} = \infty$ has already been discussed in Theorem 3.17.

2. The conditions stated in the final paragraph of this result may be quite conservative. However, they are based on achievable inequalities, and hence are, in some way, the best possible given the basic information μ and ρ only.

PROOF OF COROLLARY 3.19:

Simply putting together results from Corollary 3.14, Theorem 3.17 and Theorem 3.18. ■

This concludes the local stability analysis in the scalar deadzone case; a more general class of scalar nonlinearities is considered in the following section. An illustrative scalar example now follows:

Example

1. We consider the interconnection of Equations 3.17 and 3.18 with $F = \frac{\pm 4s}{(s+2)^2}$ and $G = k\frac{\pm 2}{s+2}$, for various values of k.

   By Corollary 3.15, we deduce immediately that $w \equiv 0$ if z is such that

   $$\|z\|_2 \leq \frac{1}{\|F\|_2} = 0.7071$$

   independently of k. We now consider the cases $k < 1$, $k > 1$ and $k = 1$ separately:

$k < 1$ For any $k < 1$ the interconnection is *stable*: three representative "characteristic bounding curves" (see Theorem 3.11, Figure 3.8 and the associated remarks) are shown in Figure 3.9 (a), (b) and (c) for $k = 0.8$, $k = 0.9$ and $k = 0.99$

We see that as k approaches zero, these bounding curves lose their curvature near the origin, as may be seen in the enlargements in Figure 3.9 (d), (e) and (f).

$k > 1$ For any $k > 1$, we cannot show stability: three representative "characteristic bounding curves" are shown in Figure 3.9 (g), (h) and (i) for $k = 1.01$, $k = 1.1$ and $k = 1.2$

We see that as k approaches 1, the bounding curves extend further to the right, ie the interconnection is *locally stable* with respect to progressively larger $\|z\|_2$.

$k = 1$ For the case when k is exactly unity, the algorithm used to generate the graphical plot runs into numerical difficulties. It is not clear whether this case is in fact BIBO stable or not.

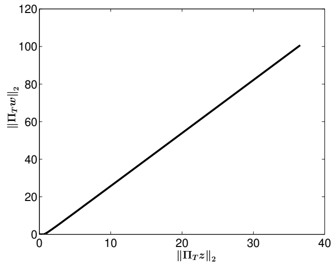

(a) $k = 0.80$

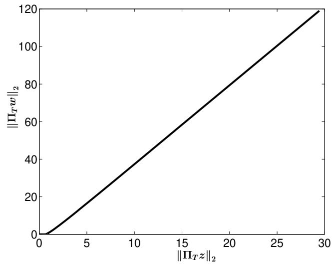

(b) $k = 0.90$

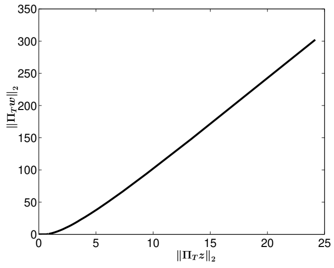

(c) $k = 0.99$

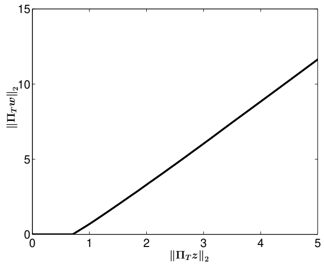

(d) $k = 0.80$ (zoom)

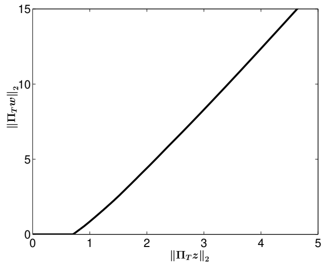

(e) $k = 0.90$ (zoom)

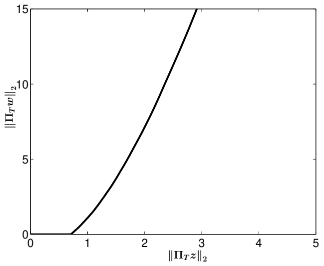

(f) $k = 0.99$ (zoom)

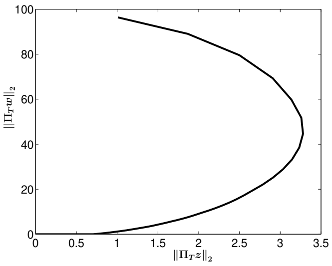

(g) $k = 1.01$

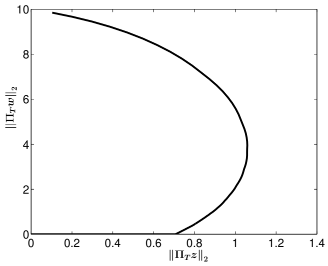

(h) $k = 1.10$

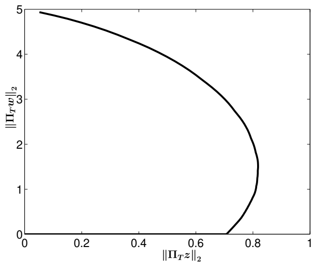

(i) $k = 1.20$

Figure 3.9: Local stability analysis: Example 1

3.4.2 A general class of nonlinearities

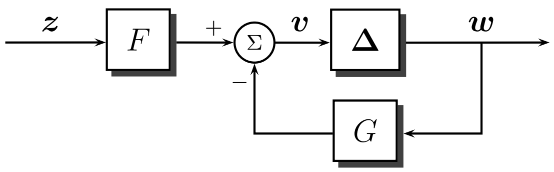

Figure 3.10: Linear system with diagonal nonlinearity $\mathbf{\Delta}$

We now consider the general interconnection (shown in Figure 3.10)

$$\boldsymbol{v} = F\boldsymbol{z} - G\boldsymbol{w} \tag{3.32}$$

$$\boldsymbol{w} = \mathbf{\Delta}\boldsymbol{v} \tag{3.33}$$

where the diagonal nonlinearity $\mathbf{\Delta} = \mathrm{Diag}\{\Delta_1, \Delta_2, \cdots, \Delta_n\}$ satisfies $\Delta_i \in \mathbf{\Delta}_\psi$ (see Definition 2.4) for each i and some suitable $\psi : (r_0, \infty) \to (\beta_0, \beta_1)$.

We make two extra assumptions in addition to those in Section 3.3:

5. F is *strictly* proper

6. $\mu\beta_0 < 1$

recalling that $\mu := \|G\|_\infty$ and $\rho := \frac{\|F\|_\infty \|G\|_2}{\|F\|_2}$.

Assumption 6 is desirable, as it indicates that the "loop gain" $\|\mathbf{\Delta}\| \, \|G\|$ is less than one for sufficiently small $\max\limits_i \|v_i\|_\infty$, and it will in fact be needed in the proof of the local stability results.

There are two main results in this section, which are analogous to those in the previous section: firstly (Theorem 3.20) that it is possible to obtain a lower bound on the local nonlinear "gain" from $\|\Pi_T \boldsymbol{z}\|_2$ to each of $\|\Pi_T \boldsymbol{w}\|_2$, $\|\Pi_T \boldsymbol{v}\|_2$ & $\max\limits_i \|\Pi_T v_i\|_\infty$, and secondly (Theorems 3.26 & 3.29) that these local results are guaranteed to be applicable to a wider range of $\|\Pi_T \boldsymbol{z}\|_2$ than a "nominal" result[4] provided either that $\beta_1\mu < 1$ (which, of course, implies global stability) or that ρ satisfies a simple sufficient condition which is given in terms of μ and the properties of ψ.

As in Section 3.4.1, let

$$\lambda^0_{[F,G]} := \begin{cases} 0 & \text{if } \mu\beta_0 = 0 \\ \gamma^{-1}_{[F,G]}(\beta_0) & \text{if } \mu\beta_0 \in (0,1) \end{cases} \tag{3.34}$$

$$\lambda^1_{[F,G]} := \begin{cases} \gamma^{-1}_{[F,G]}(\beta_1) & \text{if } \mu\beta_1 \in (0,1) \\ \infty & \text{if } \mu\beta_1 \geq 1 \end{cases} \tag{3.35}$$

where $\gamma_{[F,G]}$ is as in Definition 3.2.

[4] which may be obtained using small gain arguments, given that the "gain" of $\mathbf{\Delta}$ is no greater than β_0 if $\max\limits_i \|v_i\|_\infty \leq r_0$.

Then let

$$\begin{aligned}\boldsymbol{\Lambda}_{[\boldsymbol{F},\boldsymbol{G}]} &:= \Big\{\lambda \in (0,\infty) : \gamma_{[F,G]}(\lambda) \in (\beta_0,\beta_1)\Big\} \\ &= (\lambda^0_{[F,G]}, \lambda^1_{[F,G]})\end{aligned} \tag{3.36}$$

so that $\lambda \in \boldsymbol{\Lambda}_{[\boldsymbol{F},\boldsymbol{G}]} \iff \gamma_{[F,G]}(\lambda) \in (\beta_0,\beta_1) \iff \psi^{-1}\big(\gamma_{[F,G]}(\lambda)\big) \in (r_0,\infty)$

For $\lambda \in \boldsymbol{\Lambda}_{[\boldsymbol{F},\boldsymbol{G}]}$ we then define

$$Z_{[F,G]}(\lambda) := \frac{\psi^{-1}\big(\gamma_{[F,G]}(\lambda)\big)}{\big\{1+\rho\lambda\big\}} \tag{3.37}$$

and also
$$Z^0_{[F,G]} := \lim_{\lambda \searrow \lambda^0_{[F,G]}} Z_{[F,G]}(\lambda) = \frac{r_0}{\big\{1+\rho\lambda^0_{[F,G]}\big\}} \tag{3.38}$$

$$Z^{\mathrm{opt}}_{[F,G]} := \sup_{\lambda \in \boldsymbol{\Lambda}_{[\boldsymbol{F},\boldsymbol{G}]}} Z_{[F,G]}(\lambda) \tag{3.39}$$

In addition, we will utilise the functions $\gamma_{\text{[lower]}}$ and $\gamma_{\text{[upper]}}$ (discussed in Section 3.2.1) to provide some upper and lower bounds for the functions and constants defined in Equations 3.34 to 3.39.

For $\heartsuit$ being either [upper] or [lower], let

$$\lambda^0_\heartsuit := \begin{cases} 0 & \text{if } \mu\beta_0 = 0 \\ \gamma^{-1}_\heartsuit(\beta_0) & \text{if } \mu\beta_0 \in (0,1)\end{cases} \tag{3.40}$$

$$\lambda^1_\heartsuit := \begin{cases} \gamma^{-1}_\heartsuit(\beta_1) & \text{if } \mu\beta_1 \in (0,1) \\ \infty & \text{if } \mu\beta_1 \geq 1\end{cases} \tag{3.41}$$

where $\gamma_{\text{[upper]}}$ and $\gamma_{\text{[lower]}}$ are as in Definition 3.2. Then let

$$\begin{aligned}\boldsymbol{\Lambda}_\heartsuit &:= \Big\{\lambda \in (0,\infty) : \gamma_\heartsuit(\lambda) \in (\beta_0,\beta_1)\Big\} \\ &= (\lambda^0_\heartsuit, \lambda^1_\heartsuit)\end{aligned} \tag{3.42}$$

so that $\lambda \in \boldsymbol{\Lambda}_\heartsuit \iff \gamma_\heartsuit(\lambda) \in (\beta_0,\beta_1) \iff \psi^{-1}\big(\gamma_\heartsuit(\lambda)\big) \in (r_0,\infty)$

For $\lambda \in \boldsymbol{\Lambda}_\heartsuit$ we then define

$$Z_\heartsuit(\lambda) := \frac{\psi^{-1}\big(\gamma_\heartsuit(\lambda)\big)}{\big\{1+\rho\lambda\big\}} \tag{3.43}$$

and also
$$Z^0_\heartsuit := \lim_{\lambda \searrow \lambda^0_\heartsuit} Z_\heartsuit(\lambda) = \frac{r_0}{\big\{1+\rho\lambda^0_\heartsuit\big\}} \tag{3.44}$$

$$Z^{\mathrm{opt}}_\heartsuit = \sup_{\lambda \in \boldsymbol{\Lambda}_\heartsuit} Z_\heartsuit(\lambda) \tag{3.45}$$

Remark

1. Note that all of the functions and constants indexed by [upper] or [lower] depend only on μ and ρ, unlike those indexed by $[F,G]$, which depend on the interaction of F and G in $\big[F(j\omega) \quad G(j\omega)\big]$.

Theorem 3.20

For any $\lambda \in \boldsymbol{\Lambda}_{[\boldsymbol{F},\boldsymbol{G}]}$, any $T > 0$ and $\boldsymbol{z} \in \mathcal{L}_{2e}$ such that

$$\|\Pi_T \boldsymbol{z}\|_2 < \tfrac{1}{\|F\|_2} Z_{[F,G]}(\lambda)$$

then on the interval $[0,T]$ the unique solutions $\boldsymbol{v}, \boldsymbol{w} \in \mathcal{L}_{2e}^n$ to Equations 3.32 and 3.33 satisfy

$$\begin{aligned} \|\Pi_T \boldsymbol{w}\|_2 &< \left\{\lambda\right\} \|F\|_\infty \|\Pi_T \boldsymbol{z}\|_2 \\ \|\Pi_T \boldsymbol{v}\|_2 &< \left\{\Gamma_{[F,G]}(\lambda)\right\} \|F\|_\infty \|\Pi_T \boldsymbol{z}\|_2 \\ \max_i \|\Pi_T v_i\|_\infty &< \left\{1 + \rho\lambda\right\} \|F\|_2 \|\Pi_T \boldsymbol{z}\|_2 \left(< \psi^{-1}\big(\gamma_{[F,G]}(\lambda)\big)\right) \end{aligned}$$

Furthermore, if $\mu\beta_0 = 0$ and/or $\mu\beta_1 \geq 1$ then[5]

$$\begin{aligned} 0 \leq Z^0_{[upper]} \leq Z^0_{[F,G]} < Z_{[lower]}(\lambda) < \infty \qquad & \text{for } \lambda \in (\lambda^0_{[lower]}, \lambda^0_{[F,G]}] \\ 0 \leq Z^0_{[upper]} < Z_{[F,G]}(\lambda) \leq Z_{[lower]}(\lambda) < \infty \qquad & \text{for } \lambda \in (\lambda^0_{[F,G]}, \lambda^0_{[upper]}] \\ 0 < Z_{[upper]}(\lambda) \leq Z_{[F,G]}(\lambda) \leq Z_{[lower]}(\lambda) < \infty \qquad & \text{for } \lambda \in (\lambda^0_{[upper]}, \lambda^1_{[lower]}) \\ 0 < Z_{[upper]}(\lambda) \leq Z_{[F,G]}(\lambda) < \infty \qquad & \text{for } \lambda \in [\lambda^1_{[lower]}, \lambda^1_{[F,G]}) \\ 0 < Z_{[upper]}(\lambda) < \infty \qquad & \text{for } \lambda \in [\lambda^1_{[F,G]}, \lambda^1_{[upper]}) \end{aligned}$$

where every non-strict inequality is tight (in the sense of Lemma 3.2)

Remark

1. We clarify this result with the same simple example as in Section 3.4.1: take $F = \frac{\pm 4s}{(s+2)^2}$ and $G = \frac{\pm 2.2}{s+2}$ in Equations 3.32 and 3.33, and let $\psi : (1,\infty) \to (0,1)$ be given by

$$\psi(r) = 1 - \frac{1}{r}$$

In this case $\boldsymbol{\Lambda}_\heartsuit = (0,\infty)$ for $\heartsuit$ being each of $_{[F,G]}$, $_{[\text{lower}]}$ or $_{[\text{upper}]}$.

Taking $\lambda = 2$, for example, the Theorem then states that

$$\text{If } \|\Pi_T z\|_2 < 1 \text{ then } \quad \left\{ \begin{array}{ll} \|\Pi_T w\|_2 & < 2\,\|\Pi_T z\|_2 \\ \|\Pi_T v\|_2 & < 2.6\,\|\Pi_T z\|_2 \\ \|\Pi_T v\|_\infty & < 1.6\,\|\Pi_T z\|_2 \end{array} \right.$$

This relationship between $\|\Pi_T z\|_2$ and $\|\Pi_T w\|_2$ may be shown graphically as in Figure 3.11 (a): at no time $T \geq 0$ may the point given by

$$\big[\|\Pi_T z\|_2 \quad \|\Pi_T w\|_2\big]$$

be within the shaded region, ie that area to the left of $\frac{1}{\|F\|_2} Z_{[F,G]}(\lambda)$ ($= 1$ in this example) and above the line with gradient $\lambda \|F\|_\infty$ ($= 2$ in the example).

[5] These five inequalities simply imply that the three "characteristic bounding curves" indexed by $_{[\text{upper}]}$, $_{[F,G]}$ and $_{[\text{lower}]}$ are nested, ie one inside the other.

The equivalent statement in the case $0 < \mu\beta_0 < \mu\beta_1 < 1$ is omitted for reasons of comprehensibility, since the three intervals $\boldsymbol{\Lambda}_{[\text{lower}]}$, $\boldsymbol{\Lambda}_{[\boldsymbol{F},\boldsymbol{G}]}$ and $\boldsymbol{\Lambda}_{[\text{upper}]}$ may intersect, or not, in any possible combination, subject only to the inequalities given in items 1 and 2 of Lemma 3.22 (which simply state that the *endpoints* of these intervals are ordered)

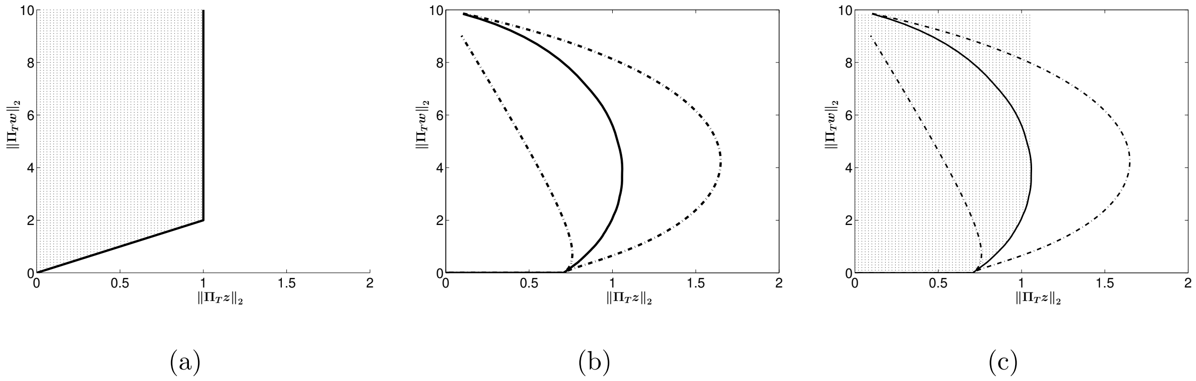

Figure 3.11: Graphical interpretation of Theorem 3.20 (shown for $F = \frac{\pm 4s}{(s+2)^2}$ and $G = \frac{\pm 2.2}{s+2}$)

Noting that this "forbidden region" is defined by its corner point, and that the Theorem gives one such region for each $\lambda \in \mathbf{\Lambda}_{[F,G]}$, we plot the continuous curve defined by the union of all of these corner points, ie

$$\left[\frac{1}{\|F\|_2} Z_{[F,G]}(\lambda) \quad \frac{\|F\|_\infty \lambda}{\|F\|_2} Z_{[F,G]}(\lambda)\right]$$

as shown (solid line) in Figure 3.11 (b). This is the "characteristic bounding curve".

Furthermore, the second part of the theorem states that the characteristic bounding curves indexed by $_{\text{[upper]}}$ and $_{\text{[lower]}}$ are such that the three curves are nested, in the sense that the curve indexed by $_{\text{[upper]}}$ is conservative, and that indexed by $_{\text{[lower]}}$ is optimistic (and note that these are tight bounds, in the sense of Lemma 3.2) These curves are shown as dotted lines in Figure 3.11 (b).

Finally, the overall "forbidden region" (ie the union over all $\lambda \in \mathbf{\Lambda}_{[F,G]}$ of the individual forbidden regions) is shown in Figure 3.11 (c). It may be seen that this region can be determined from only the lower half of the "characteristic bounding curve", ie that portion of the curve which is increasing in the x-direction.

Figures 3.11 (b) or (c) may then be used to determine (conservatively) the local stability properties of the interconnection, in the sense that the following quantities may be read off the plot:

(a) A lower bound on the largest permissible $\|\Pi_T z\|_2$ which guarantees that $\Pi_T w \in \mathcal{L}_2$

(b) An upper bound on the nonlinear "gain" from $\|\Pi_T z\|_2$ to $\|\Pi_T w\|_2$, as a function of $\|\Pi_T z\|_2$ (provided that $\|\Pi_T z\|_2$ is no greater than the largest permitted value determined in (a))

and, moreover, tight upper and lower bounds on each of these may be determined from the dotted lines in Figure 3.11 (b).

Similar graphical interpretations hold for the relationships between $\|\Pi_T z\|_2$ & $\|\Pi_T v\|_2$ and between $\|\Pi_T z\|_2$ & $\|\Pi_T v\|_\infty$.

Proof of Theorem 3.20 will require the following two Lemmas:

Lemma 3.21

For any $\boldsymbol{z} \in \mathcal{L}_{2e}$ and $T > 0$ with $\|\Pi_T \boldsymbol{z}\|_2 \neq 0$ there exists some $T_0 \in (0, T]$ such that the unique solutions $\boldsymbol{v}, \boldsymbol{w} \in \mathcal{L}_{2e}^n$ to Equations 3.32 and 3.33 satisfy

$$\begin{aligned} &\|\Pi_{T_0} \boldsymbol{z}\|_2 \neq 0 \quad \textit{and} \\ &\|\Pi_{T_0} \boldsymbol{w}\|_2 \leq \lambda^0_{[F,G]} \|F\|_\infty \|\Pi_{T_0} \boldsymbol{z}\|_2 \end{aligned}$$

Lemma 3.22

1.

$$\lambda^0_{[lower]} \leq \lambda^0_{[F,G]} \leq \lambda^0_{[upper]} \quad \textit{with all three equal iff } \beta_0 \mu = 0$$

2.

$$\lambda^1_{[lower]} \leq \lambda^1_{[F,G]} \leq \lambda^1_{[upper]} \quad \textit{with all three equal iff } \beta_1 \mu \geq 1$$

3.

$$Z^0_{[upper]} \leq Z^0_{[F,G]} \leq Z^0_{[lower]} \quad \textit{with all three equal iff } \beta_0 \mu = 0 \textit{ or } r_0 = 0$$

4.

$$Z^{opt}_{[upper]} \leq Z^{opt}_{[F,G]} \leq Z^{opt}_{[lower]} \quad \textit{with all three equal if } \beta_1 \mu < 1 \textit{ and only if } \beta_1 \mu \leq 1$$

5. if $\lambda^0_{[upper]} < \lambda < \lambda^1_{[F,G]}$ then

$$\begin{aligned} \beta_0 < \gamma_{[upper]}(\lambda) \leq \gamma_{[F,G]}(\lambda) < \beta_1 \quad \textit{and} \\ Z_{[upper]}(\lambda) \leq Z_{[F,G]}(\lambda) \end{aligned}$$

6. if $\lambda^0_{[F,G]} < \lambda < \lambda^1_{[lower]}$ then

$$\begin{aligned} \beta_0 < \gamma_{[F,G]}(\lambda) \leq \gamma_{[lower]}(\lambda) < \beta_1 \quad \textit{and} \\ Z_{[F,G]}(\lambda) \leq Z_{[lower]}(\lambda) \end{aligned}$$

7. if $\lambda \in (\lambda^0_{[lower]}, \lambda^1_{[lower]})$ and $\lambda \leq \lambda^0_{[F,G]}$ then

$$\begin{aligned} \beta_0 < \gamma_{[lower]}(\lambda) < \beta_1 \quad \textit{and} \\ Z^0_{[F,G]} < Z_{[lower]}(\lambda) \end{aligned}$$

8. if $\lambda \in (\lambda^0_{[F,G]}, \lambda^1_{[F,G]})$ and $\lambda \leq \lambda^0_{[upper]}$ then

$$\begin{aligned} \beta_0 < \gamma_{[F,G]}(\lambda) < \beta_1 \quad \textit{and} \\ Z^0_{[upper]} < Z_{[F,G]}(\lambda) \end{aligned}$$

Furthermore, the non-strict inequalities in items 1 – 6 are tight (in the sense of Lemma 3.2)

PROOF OF LEMMA 3.21:

We use proof by contradiction: assume that there exists some $\boldsymbol{z} \in \mathcal{L}_{2e}$ and $T > 0$ with $\|\Pi_T \boldsymbol{z}\|_2 \neq 0$ such that for all $T_0 \in (0, T]$ either

$$\begin{aligned} \|\Pi_{T_0}\boldsymbol{z}\|_2 = 0 \quad &\big(\Longrightarrow \|\Pi_{T_0}\boldsymbol{w}\|_2 = 0\big) \quad \text{or} \\ \|\Pi_{T_0}\boldsymbol{w}\|_2 > \lambda^0_{[F,G]}\,\|F\|_\infty\,\|\Pi_{T_0}\boldsymbol{z}\|_2 \geq 0 \quad &\big(\Longrightarrow \|\Pi_{T_0}\boldsymbol{z}\|_2 \neq 0\big) \end{aligned}$$

ie $\|\Pi_{T_0}\boldsymbol{z}\|_2$ and $\|\Pi_{T_0}\boldsymbol{w}\|_2$ are either both zero or both non-zero.

For any $r > r_0 \geq 0$ there exists (by Proposition 2.1) some $T_1 \in (0, T]$ such that

$$0 < \|\Pi_{T_1}\boldsymbol{z}\|_2 < \tfrac{r}{2\|F\|_2} \quad \big(\Longrightarrow \|\Pi_{T_1}\boldsymbol{w}\|_2 > 0\big)$$

and similarly some $T_2 \in (0, T]$ such that

$$0 < \|\Pi_{T_2}\boldsymbol{w}\|_2 < \tfrac{r}{2\|G\|_2} \quad \big(\Longrightarrow \|\Pi_{T_2}\boldsymbol{z}\|_2 > 0\big)$$

so letting $T_0 := \min\{T_1, T_2\}$ we see immediately that

$$0 < \|\Pi_{T_0}\boldsymbol{z}\|_2 < \tfrac{r}{2\|F\|_2} \quad \text{and} \quad 0 < \|\Pi_{T_0}\boldsymbol{w}\|_2 < \tfrac{r}{2\|G\|_2}$$

Hence by Proposition 2.3

$$\begin{aligned} \max_i \|\Pi_{T_0} v_i\|_\infty &\leq \|F\|_2\,\|\Pi_{T_0}\boldsymbol{z}\|_2 + \|G\|_2\,\|\Pi_{T_0}\boldsymbol{w}\|_2 \\ &< r \end{aligned}$$

Since this is true for any $r > r_0$, we deduce that $\max_i \|\Pi_{T_0} v_i\|_\infty \leq r_0$. But this implies (by Lemma 2.8) that $\|\Pi_{T_0}\boldsymbol{w}\|_2 \leq \beta_0\,\|\Pi_{T_0}\boldsymbol{v}\|_2$.

But then by Corollary 3.3

$$\begin{aligned} \|\Pi_{T_0}\boldsymbol{w}\|_2 &\leq \beta_0\,\|\Pi_{T_0}\boldsymbol{v}\|_\infty \\ &\leq \beta_0 \Gamma_{[F,G]}\Bigg(\frac{\|\Pi_{T_0}\boldsymbol{w}\|_2}{\|F\|_\infty \|\Pi_{T_0}\boldsymbol{z}\|_2}\Bigg)\,\|F\|_\infty\,\|\Pi_{T_0}\boldsymbol{z}\|_2 \\ &= \frac{\beta_0}{\gamma_{[F,G]}\Big(\frac{\|\Pi_{T_0}\boldsymbol{w}\|_2}{\|F\|_\infty \|\Pi_{T_0}\boldsymbol{z}\|_2}\Big)}\,\|\Pi_{T_0}\boldsymbol{w}\|_2 \end{aligned}$$

which implies that

$$\gamma_{[F,G]}\Bigg(\frac{\|\Pi_{T_0}\boldsymbol{w}\|_2}{\|F\|_\infty \|\Pi_{T_0}\boldsymbol{z}\|_2}\Bigg) \leq \beta_0$$

but we assumed that $\|\Pi_{T_0}\boldsymbol{w}\|_2 > \lambda^0_{[F,G]}\,\|F\|_\infty\,\|\Pi_{T_0}\boldsymbol{z}\|_2$, which means that

$$\gamma_{[F,G]}\Bigg(\frac{\|\Pi_{T_0}\boldsymbol{w}\|_2}{\|F\|_\infty \|\Pi_{T_0}\boldsymbol{z}\|_2}\Bigg) > \beta_0$$

This is contradictory, so the Lemma must be true. ∎

PROOF OF LEMMA 3.22:

Items one to six, and the first parts of items seven and eight follow directly form the definitions of $\gamma_\heartsuit$, $\lambda_\heartsuit$ and $Z_\heartsuit$, and Lemma 3.5.

For the second part of the seventh item, consider

$$Z_{[\text{lower}]}(\lambda) = \frac{\psi^{-1}\big(\gamma_{[\text{lower}]}(\lambda)\big)}{1+\rho\lambda} > \frac{r_0}{1+\rho\lambda} \geq \frac{r_0}{1+\rho\lambda^0_{[F,G]}} = Z^0_{[F,G]}$$

The second part of the eighth item follows in a similar manner. ∎

We can now prove Theorem 3.20:

PROOF OF THEOREM 3.20:

Consider the first inequality: it is clear that $\|\Pi_T \boldsymbol{z}\|_2 = 0 \implies \|\Pi_T \boldsymbol{w}\|_2 = 0$, so assume that $\|\Pi_T \boldsymbol{z}\|_2 \neq 0$ and

$$\|\Pi_T \boldsymbol{w}\|_2 \geq \lambda \|F\|_\infty \|\Pi_T \boldsymbol{z}\|_2$$

By Lemma 3.21 there exists some $T_0 \in (0, T]$ such that $\|\Pi_{T_0} \boldsymbol{z}\|_2 \neq 0$ and

$$\|\Pi_{T_0} \boldsymbol{w}\|_2 \leq \lambda^0_{[F,G]} \|\Pi_{T_0} \boldsymbol{z}\|_2$$

so by Proposition 2.1 there exists some $T_1 \in (T_0, T]$ such that $\|\Pi_{T_1} \boldsymbol{z}\|_2 \neq 0$ and

$$\|\Pi_{T_1} \boldsymbol{w}\|_2 = \lambda \|F\|_\infty \|\Pi_{T_1} \boldsymbol{z}\|_2$$

By Corollary 3.3 we have that

$$\begin{aligned}
&\|\Pi_{T_1} \boldsymbol{v}\|_2 \leq \Gamma_{[F,G]}(\lambda) \|F\|_\infty \|\Pi_{T_1} \boldsymbol{z}\|_2 = \frac{\Gamma_{[F,G]}(\lambda)}{\lambda} \|\Pi_{T_1} \boldsymbol{w}\|_2 \quad \text{ie} \\
&\|\Pi_{T_1} \boldsymbol{w}\|_2 \geq \gamma_{[F,G]}(\lambda) \|\Pi_{T_1} \boldsymbol{v}\|_2
\end{aligned}$$

so by Lemma 2.8

$$\max_i \|\Pi_{T_1} v_i\|_\infty \geq \psi^{-1}\big(\gamma_{[F,G]}(\lambda)\big)$$

By Proposition 2.3 we then have that

$$\begin{aligned}
\max_i \|\Pi_{T_1} v_i\|_\infty &\leq \|F\|_2 \|\Pi_{T_1} \boldsymbol{z}\|_2 + \|G\|_2 \|\Pi_{T_1} \boldsymbol{w}\|_2 \\
&= \big\{ \|F\|_2 + \|G\|_2 \|F\|_\infty \lambda \big\} \|\Pi_{T_1} \boldsymbol{z}\|_2 \\
&= \big\{ 1 + \rho\lambda \big\} \|F\|_2 \|\Pi_{T_1} \boldsymbol{z}\|_2
\end{aligned}$$

so we have shown that $\|\Pi_T \boldsymbol{w}\|_2 \geq \lambda \|F\|_\infty \|\Pi_T \boldsymbol{z}\|_2$ implies

$$\|F\|_2 \|\Pi_T \boldsymbol{z}\|_2 \geq \|F\|_2 \|\Pi_{T_1} \boldsymbol{z}\|_2 \geq \frac{\psi^{-1}\big(\gamma_{[F,G]}(\lambda)\big)}{\big\{1+\rho\lambda\big\}}$$

which is equivalent to the first inequality. The bounds on $\|\Pi_T \boldsymbol{v}\|_2$ and $\max_i \|\Pi_T v_i\|_\infty$ follow immediately by Corollary 3.3 and Propositions 2.2 and 2.3.

The inequalities in the final paragraph follow directly from Lemma 3.22. ∎

In the remainder of the section we state a number of results which are all essentially derived from Theorem 3.20.

Corollary 3.23 gives a straightforward infinite-horizon interpretation of Theorem 3.20, and Corollary 3.24 gives the "best" such result:

Corollary 3.23

For any $\lambda \in \mathbf{\Lambda}_{[F,G]}$ the interconnection of Equations 3.32 and 3.33 is locally stable with respect to the set

$$\mathbb{Z}_{[F,G]}(\lambda) = \left\{ \boldsymbol{z} : \|\boldsymbol{z}\|_2 < \tfrac{1}{\|F\|_2} Z_{[F,G]}(\lambda) \right\}$$

Furthermore for any $\boldsymbol{z} \in \mathbb{Z}_{[F,G]}(\lambda)$ the solutions $\boldsymbol{v}, \boldsymbol{w} \in \mathcal{L}_2^n$ to Equations 3.32 and 3.33 satisfy

$$\begin{aligned} \|\boldsymbol{w}\|_2 &< \left\{\lambda\right\} \|F\|_\infty \|\boldsymbol{z}\|_2 \\ \|\boldsymbol{v}\|_2 &< \left\{\Gamma_{[F,G]}(\lambda)\right\} \|F\|_\infty \|\boldsymbol{z}\|_2 \\ \max_i \|v_i\|_\infty &< \left\{1 + \rho\lambda\right\} \|F\|_2 \|\boldsymbol{z}\|_2 \left(< \psi^{-1}\big(\gamma_{[F,G]}(\lambda)\big)\right) \end{aligned}$$

PROOF OF COROLLARY 3.23:

Directly from Theorem 3.20. ∎

Corollary 3.24

The interconnection of Equations 3.32 and 3.33 is locally stable with respect to the set

$$\mathbb{Z}_{[F,G]}^{opt} = \left\{ \boldsymbol{z} : \|\boldsymbol{z}\|_2 < \tfrac{1}{\|F\|_2} Z_{[F,G]}^{opt} \right\}$$

Remark

1. Returning to Figure 3.11 (c), we see that this corresponds to the point

$$\begin{bmatrix} \|\Pi_T \boldsymbol{z}\|_2 & \|\Pi_T \boldsymbol{w}\|_2 \end{bmatrix}$$

remaining under the shaded region for all $T \geq 0$.

As mentioned in the Remarks following Theorem 3.20, a useful way to determine $Z_{[F,G]}^{\text{opt}}$ is to read it from the "characteristic bounding curve" (Figure 3.11 (b))

PROOF OF COROLLARY 3.24:

Directly from Corollary 3.23 and the definition of $Z_{[F,G]}^{\text{opt}}$. ∎

Considering the limiting case as $\lambda \searrow \lambda^0_{[F,G]}$ gives a simple result that holds for all interconnections. Recall that for $\heartsuit$ being any of ${}_{[F,G]}$, ${}_{[\text{upper}]}$ or ${}_{[\text{lower}]}$

$$Z^0_{\heartsuit} := \lim_{\lambda \searrow \lambda^0_{\heartsuit}} Z_{\heartsuit}(\lambda) = \frac{r_0}{1 + \rho\lambda^0_{\heartsuit}}$$

Corollary 3.25

The interconnection of Equations 3.32 and 3.33 is locally stable with respect to the set

$$\mathbb{Z}^0_{[F,G]} = \left\{ \boldsymbol{z} : \|\boldsymbol{z}\|_2 \leq \tfrac{1}{\|F\|_2} Z^0_{[F,G]} \right\}$$

Furthermore, for any $\boldsymbol{z} \in \mathbb{Z}^0_{[F,G]}$ the solutions $\boldsymbol{v}, \boldsymbol{w} \in \mathcal{L}_2^n$ to Equations 3.32 and 3.33 satisfy

$$\begin{aligned} \|\boldsymbol{w}\|_2 &\leq \left\{\lambda^0_{[F,G]}\right\} \|F\|_\infty \|\boldsymbol{z}\|_2 \\ \|\boldsymbol{v}\|_2 &\leq \left\{\Gamma_{[F,G]}(\lambda^0_{[F,G]})\right\} \|F\|_\infty \|\boldsymbol{z}\|_2 \\ \max_i \|v_i\|_\infty &\leq \left\{1 + \rho\lambda^0_{[F,G]}\right\} \|F\|_2 \|\boldsymbol{z}\|_2 \Big(\leq r_0 \Big) \end{aligned}$$

Moreover, $Z^0_{[F,G]}$, $\lambda^0_{[F,G]}$ and $\Gamma_{[F,G]}(\lambda^0_{[F,G]})$ are bounded above and below by

$$\begin{aligned} Z^0_{[upper]} &\leq Z^0_{[F,G]} \leq Z^0_{[lower]} \\ \lambda^0_{[lower]} &\leq \lambda^0_{[F,G]} \leq \lambda^0_{[upper]} \\ \Gamma_{[lower]}(\lambda^0_{[lower]}) &\leq \Gamma_{[F,G]}(\lambda^0_{[F,G]}) \leq \Gamma_{[upper]}(\lambda^0_{[upper]}) \end{aligned}$$

where each of these inequalities is tight (in the sense of Lemma 3.2) and

$$\begin{aligned} Z^0_{[lower]} &= \frac{r_0\sqrt{1-\beta_0^2\mu^2}}{\rho\beta_0 + \sqrt{1-\beta_0^2\mu^2}} & Z^0_{[upper]} &= \frac{r_0(1-\beta_0\mu)}{\rho\beta_0 + (1-\beta_0\mu)} \\ \lambda^0_{[lower]} &= \frac{\beta_0}{\sqrt{1-\beta_0^2\mu^2}} & \lambda^0_{[upper]} &= \frac{\beta_0}{1-\beta_0\mu} \\ \Gamma_{[lower]}(\lambda^0_{[lower]}) &= \frac{1}{\sqrt{1-\beta_0^2\mu^2}} & \Gamma_{[upper]}(\lambda^0_{[upper]}) &= \frac{1}{1-\beta_0\mu} \end{aligned}$$

Remark

1. It is quite possible that r_0 may be zero, in which case this is a very small set of signals!
2. Note that the various bounds in the final paragraph ($Z^0_{[\text{lower}]}$ etc) depend only on ρ & μ (representing F & G), and on r_0 & β_0 (representing $\boldsymbol{\Delta}$)

PROOF OF COROLLARY 3.25:

Directly from Corollary 3.23 by considering $\lambda \searrow \lambda^0_{[F,G]}$. ∎

We now consider the cases $\beta_1\mu < 1$ and $\beta_1\mu \geq 1$ separately:

Case (a): $\beta_1\mu < 1$**, stability is assured**

If $\beta_1\mu < 1$ then we know already (by Proposition 3.7, and because $\|\boldsymbol{\Delta}\| \leq \beta_1$) that the interconnection must be *stable*. The same deduction may be made from Corollary 3.23:

Theorem 3.26

If $\beta_1\mu < 1$ *then*

$$Z^{opt}_{[F,G]} = \infty$$

and the interconnection of Equations 3.32 and 3.33 is therefore ***stable****.*

Furthermore, for any $\boldsymbol{z} \in \mathcal{L}_2^m$ *the solutions* $\boldsymbol{v}, \boldsymbol{w} \in \mathcal{L}_2^n$ *to Equations 3.32 and 3.33 satisfy*

$$\|\boldsymbol{w}\|_2 \leq \left\{\lambda^1_{[F,G]}\right\} \|F\|_\infty \|\boldsymbol{z}\|_2 \tag{3.46}$$

$$\|\boldsymbol{v}\|_2 \leq \left\{\tfrac{\lambda^1_{[F,G]}}{\beta_1}\right\} \|F\|_\infty \|\boldsymbol{z}\|_2 \tag{3.47}$$

$$\max_i \|v_i\|_\infty \leq \left\{1 + \rho\lambda^1_{[F,G]}\right\} \|F\|_2 \|\boldsymbol{z}\|_2 \tag{3.48}$$

Moreover, $\lambda^1_{[F,G]}$ *is bounded above and below by*

$$\lambda^1_{[lower]} \leq \lambda^1_{[F,G]} \leq \lambda^1_{[upper]}$$

where each of these inequalities is tight (in the sense of Lemma 3.2) and

$$\lambda^1_{[upper]} = \frac{\beta_1}{1-\beta_1\mu} \qquad \lambda^1_{[lower]} = \frac{\beta_1}{\sqrt{1-\beta_1^2\mu^2}}$$

Hence if $\|\boldsymbol{\Delta}\| = \beta_1$ *then the inequalities in Equations 3.46, 3.47 and 3.48 are no weaker than, and may be significantly stronger than, Equations 3.14, 3.15 and 3.16 in Proposition 3.7.*

Remark

1. If $\|\boldsymbol{\Delta}\| < \beta_1$ then the relationship between these inequalities and those in Proposition 3.7 is not so clear; it depends on quite how much larger β_1 is than $\|\boldsymbol{\Delta}\|$. However, if the least conservative ψ is used, then the difference between β_1 and $\|\boldsymbol{\Delta}\|$ will often be small.

2. Note that the bounds $\lambda^1_{[\text{lower}]}$ and $\lambda^1_{[\text{upper}]}$ depend only on μ (representing F & G), and on β_1 (representing $\boldsymbol{\Delta}$)

PROOF OF THEOREM 3.26:

Directly from Corollary 3.23 by considering $\lambda \nearrow \lambda^1_{[F,G]}$, and noting that $\beta_1\mu < 1$ implies $\lambda^1_{[\text{lower}]} \leq \lambda^1_{[F,G]} \leq \lambda^1_{[\text{upper}]} < \infty$. ∎

Case (b): $\beta_1\mu \geq 1$, stability *may* be assured if $\beta_1\mu = 1$, and is *not* assured if $\beta_1\mu > 1$

For $\heartsuit$ being any of ${}_{[F,G]}$, ${}_{[\text{lower}]}$, ${}_{[\text{upper}]}$, recall that

$$Z_{\heartsuit}^{\text{opt}} := \sup_{\lambda \in \mathbf{\Lambda}_{\heartsuit}} Z_{\heartsuit}(\lambda)$$

and that

$$Z_{[\text{upper}]}^{\text{opt}} \leq Z_{[F,G]}^{\text{opt}} \leq Z_{[\text{lower}]}^{\text{opt}} \tag{3.49}$$

where each of these inequalities is tight (in the sense of Lemma 3.2)

If $\beta_1\mu = 1$ then it is possible, although not certain, that we can guarantee stability:

Theorem 3.27

If $\beta_1\mu = 1$ then

1. *The following are equivalent*
   - $Z_{[lower]}^{opt} = \infty$ *(ie $Z_{[lower]}(\lambda) \to \infty$ as $\lambda \nearrow \infty$)*
   - *There exists some $\alpha > \frac{1}{2}$ and (possibly infinite) $k > 0$ such that*

   $$\left(\tfrac{1}{\mu} - r\right)^{\alpha} \psi^{-1}(r) \to k \quad \text{as } r \nearrow \tfrac{1}{\mu}$$

2. *The following are equivalent*
   - $Z_{[upper]}^{opt} = \infty$ *(ie $Z_{[upper]}(\lambda) \to \infty$ as $\lambda \nearrow \infty$)*
   - *There exists some $\alpha > 1$ and (possibly infinite) $k > 0$ such that*

   $$\left(\tfrac{1}{\mu} - r\right)^{\alpha} \psi^{-1}(r) \to k \quad \text{as } r \nearrow \tfrac{1}{\mu}$$

Hence it is possible that $\mathbb{Z}_{[F,G]}^{opt}$ in Corollary 3.24 is the whole of $\mathcal{L}_2^m$, in which case the interconnection of Equations 3.32 and 3.33 is ***stable****.*

Remarks

1. Note that this is *only* BIBO stability: it is not possible to state finite gain results similar to Theorem 3.20. The reason for this is that the result comes from considering $\lambda \to \infty$ in Corollary 3.23.

2. Clearly, if $Z_{[\text{upper}]}^{\text{opt}} = \infty$, then stability is guaranteed. On the other hand, if $Z_{[\text{lower}]}^{\text{opt}} < \infty$, then stability cannot be guaranteed.

   The final case, where $Z_{[\text{upper}]}^{\text{opt}} < \infty$ and $Z_{[\text{lower}]}^{\text{opt}} = \infty$, is more interesting. The upper bound $Z_{[F,G]}^{\text{opt}} \leq Z_{[\text{lower}]}^{\text{opt}}$ *is* achievable but so is the lower bound $Z_{[F,G]}^{\text{opt}} \geq Z_{[\text{upper}]}^{\text{opt}}$.

   Nevertheless, relaxing the upper bound to infinity is still a useful result!

PROOF OF THEOREM 3.27:

Note that $\frac{1}{\mu} - \gamma_{[\text{lower}]}$ has a zero of order 2 at infinity, and $\frac{1}{1+\rho\lambda}$ has a zero of order 1 at infinity. If α, the order of the singularity of ψ at $\frac{1}{\mu}$, is such that $2\alpha > 1$ then $Z_{[\text{lower}]}$ will have a pole at infinity.

A similar argument applies to $Z_{[\text{upper}]}$, where $\frac{1}{\mu} - \gamma_{[\text{upper}]}$ has a zero of order 1 at infinity.

Then, by Equation 3.49, we see that $Z^{\text{opt}}_{[F,G]} = \infty$ is therefore possible, in which case the interconnection would (by Corollary 3.24) be locally stable with respect to $\mathcal{L}_2^m$. But, by Definitions 3.4 and 3.5, local stability with respect to $\mathcal{L}_2^m$ is equivalent to stability. ∎

If $\beta_1\mu > 1$ then we cannot guarantee stability:

Theorem 3.28

If $\beta_1\mu > 1$ then

$$Z^{opt}_{[lower]} < \infty$$

*Hence it is **not** possible that $\mathbb{Z}^{opt}_{[F,G]}$ in Corollary 3.24 is the whole of $\mathcal{L}_2^m$, so we **cannot** guarantee stability of the interconnection of Equations 3.32 and 3.33.*

Remarks

1. Note that $\beta_1\mu > 1$ **does not** imply that the interconnection is *unstable*, merely that in this case the largest local stability region identified by this method is strictly smaller than the whole of $\mathcal{L}_2^m$.
2. In Theorem 3.18 we were able to make $Z^{\text{opt}}_{[\text{lower}]}$ arbitrarily large by making $\beta_1\mu$ approach 1. One would *hope* that the same procedure would apply in the general case (because the process which generates $Z^{\text{opt}}_{[\text{lower}]}$ appears to be quite well-behaved), but this remains unproven.

PROOF OF THEOREM 3.28:

If $\beta_1\mu > 1$ then from Lemma 3.5 we see that $\gamma_{[F,G]}(\lambda) < \frac{1}{\mu} < \beta_1$ for all $\lambda \in \mathbf{\Lambda}_{[F,G]}$. So

$$\frac{\psi^{-1}\big(\gamma_{[F,G]}(\lambda)\big)}{\big\{1+\rho\lambda\big\}} < \psi^{-1}\big(\gamma_{[F,G]}(\lambda)\big) < \psi^{-1}\big(\tfrac{1}{\mu}\big)$$

for any $\lambda \in \mathbf{\Lambda}_{[F,G]}$, and hence $Z^{\text{opt}}_{[F,G]} \leq \psi^{-1}\big(\frac{1}{\mu}\big) < \infty$. ∎

If $Z^0_{[F,G]} < Z^{\text{opt}}_{[F,G]} < \infty$ then let

$$\lambda^{\text{opt}}_{[F,G]} := \arg\max_{\lambda \in \mathbf{\Lambda}_{[F,G]}} Z_{[F,G]}(\lambda) \tag{3.50}$$

(which is guaranteed to exist, since the function is continuous and does not achieve its supremum at an endpoint)

Theorem 3.29

If $\beta_1\mu \geq 1$ *and* $Z^0_{[F,G]} < Z^{opt}_{[F,G]} < \infty$ *then the interconnection of Equations 3.32 and 3.33 is locally stable with respect to the set*

$$\mathbb{Z}^{opt}_{[F,G]} = \left\{ \boldsymbol{z} : \|\boldsymbol{z}\|_2 < \tfrac{1}{\|F\|_2} Z^{opt}_{[F,G]} \right\}$$

Furthermore, for any $\boldsymbol{z} \in \mathbb{Z}^{opt}_{[F,G]}$ *the solutions* $\boldsymbol{v}, \boldsymbol{w} \in \mathcal{L}_2^n$ *satisfy*

$$\begin{aligned} \|\boldsymbol{w}\|_2 &< \left\{ \lambda^{opt}_{[F,G]} \right\} \|F\|_\infty \|\boldsymbol{z}\|_2 \\ \|\boldsymbol{v}\|_2 &< \left\{ \Gamma_{[F,G]}(\lambda^{opt}_{[F,G]}) \right\} \|F\|_\infty \|\boldsymbol{z}\|_2 \\ \max_i \|v_i\|_\infty &< \left\{ 1 + \rho\lambda^{opt}_{[F,G]} \right\} \|F\|_2 \|\boldsymbol{z}\|_2 \left(< \frac{1}{1 - \gamma_{[F,G]}(\lambda^{opt}_{[F,G]})} \right) \end{aligned}$$

Moreover

- *if* $\beta_1\mu > 1$ *then it is certain that* $Z^{opt}_{[F,G]} \leq Z^{opt}_{[lower]} < \infty$
- *if* $\beta_1\mu \geq 1$ *and*

$$r_0\psi'(r_0^+)\rho < \frac{(1 + \rho\lambda^0_{[F,G]})(1 - \beta_0\mu)}{\Gamma_{[F,G]}(\lambda^0_{[F,G]})}$$

  where $\psi'(r_0^+)$ *means the right-derivative* $\frac{d\psi}{dr}$ *evaluated at* r_0*, then it is certain that* $Z^0_{[F,G]} < Z^{opt}_{[F,G]}$.

Remarks

1. If $Z^{\mathrm{opt}}_{[F,G]} = Z^0_{[F,G]}$ then Corollary 3.25 gives the best result available, and the possibility that $Z^{\mathrm{opt}}_{[F,G]} = \infty$ has already been discussed in Theorem 3.27.
2. The following simple deductions, which depend only on μ and ρ (ie they do not depend on the interaction of $F(j\omega)$ and $G(j\omega)$) are immediate from the stated (sufficient) condition for $Z^0_{[F,G]} < Z^{\mathrm{opt}}_{[F,G]}$ in the case $\beta_1\mu \geq 1$:
   - If either r_0 or $\psi'(r_0^+)$ is zero then the condition is **always** satisfied.
   - If $\mu\beta_0 = 0$ then the condition simplifies to $r_0\psi'(r_0^+)\rho < 1$
   - If $\mu\beta_0 \in (0,1)$, and $r_0\psi'(r_0^+) > 0$, then the condition is satisfied by any of the following

$$\begin{aligned} r_0\psi'(r_0^+)\rho &< (1 - \beta_0\mu + \rho\beta_0)(1 - \beta_0\mu) \\ r_0\psi'(r_0^+)\rho &< (1 - \beta_0\mu)^2 \\ r_0\psi'(r_0^+) &< \beta_0(1 - \beta_0\mu) \end{aligned}$$

3. The stated (sufficient) condition for $Z^0_{[F,G]} < Z^{\mathrm{opt}}_{[F,G]}$ may be *extremely* conservative. For a specific (given) ψ, it is often possible to calculate $Z^{\mathrm{opt}}_{[\mathrm{upper}]}$ and $Z^{\mathrm{opt}}_{[\mathrm{lower}]}$ analytically, and hence using the relation in Equation 3.49 one may obtain a less conservative sufficient condition, and possibly also a necessary condition.

PROOF OF THEOREM 3.29:

Apart from the very last condition, this is simply putting together results from Corollary 3.24, Theorem 3.27 and Theorem 3.28.

The final part — the condition for $Z^0_{[F,G]} < Z^{\mathrm{opt}}_{[F,G]}$ — involves finding sufficient conditions for the existence of some $\delta > 0$ such that

$$\frac{\psi^{-1}\big(\gamma_{[F,G]}(\lambda^0_{[F,G]}+\delta)\big)}{1+\rho(\lambda^0_{[F,G]}+\delta)} = Z_{[F,G]}(\lambda^0_{[F,G]}+\delta) > Z^0_{[F,G]} = \frac{r_0}{1+\rho\lambda^0_{[F,G]}}$$

or equivalently, noting that $\psi(.)$ is monotonic

$$\gamma_{[F,G]}(\lambda^0_{[F,G]}+\delta) > \psi\left(r_0 + \frac{r_0\rho\delta}{1+\rho\lambda^0_{[F,G]}}\right)$$

Since ψ is differentiable (by assumption), it is clear that

$$\psi(r_0+\delta r) \leq \psi(r_0) + \psi'(r_0^+)\delta r + \mathcal{O}(\delta r^2)$$

ie that

$$\psi\left(r_0 + \frac{r_0\rho\delta}{1+\rho\lambda^0_{[F,G]}}\right) \leq \psi(r_0) + \psi'(r_0^+)\frac{r_0\rho\delta}{1+\rho\lambda^0_{[F,G]}} + \mathcal{O}(\delta^2)$$

and Lemma 3.5 states that

$$\gamma_{[F,G]}(\lambda^0_{[F,G]}+\delta) \geq \gamma_{[F,G]}(\lambda^0_{[F,G]}) + \big(1-\mu\gamma_{[F,G]}(\lambda^0_{[F,G]})\big)\frac{\delta}{\Gamma_{[F,G]}(\lambda^0_{[F,G]})} - \mathcal{O}(\delta^2)$$

Substituting $\gamma_{[F,G]}(\lambda^0_{[F,G]}) = \psi(r_0) = \beta_0$ into these two inequalities, and subtracting, we see that $Z_{[F,G]}(\lambda^0_{[F,G]}+\delta) > Z^0_{[F,G]}$ if

$$\left\{\frac{(1-\beta_0\mu)}{\Gamma_{[F,G]}(\lambda^0_{[F,G]})} - \frac{r_0\psi'(r_0^+)\rho}{1+\rho\lambda^0_{[F,G]}}\right\}\delta - \mathcal{O}(\delta^2) > 0$$

which is clearly true for some sufficiently small δ if the quantity in the braces is positive. ∎

This concludes the local stability analysis in the general scalar case; some examples now follow:

Examples

1a. Consider $\psi : (1, \infty) \to (0, 1)$ given by

$$\psi(r) = 1 - \frac{1}{r}$$

which we used as Example 1 in Section 2.2, and which is shown in Figure 3.12 (a). For this particular ψ the family of nonlinearities $\mathbf{\Delta}_\psi$ contains the ideal unity deadzone function, which is shown in Figure 3.12 (b).

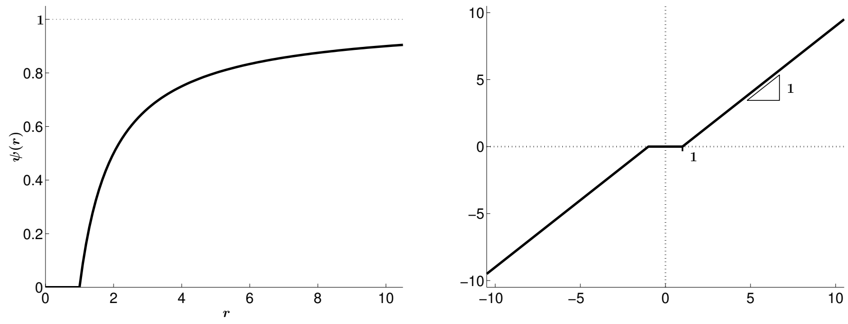

(a) $\psi(r)$ (b) Unity deadzone

Figure 3.12: ψ for local stability Example 1

In fact, the results from using this ψ are identical to those obtained in Section 3.4.1. However, in Section 3.4.1 we did not discuss fully the bounds obtained by using $Z_{\text{[upper]}}$ and $Z_{\text{[lower]}}$.

Figure 3.13 shows, for the same F and G as in Example 1 in Section 3.4.1, the "real" characteristic bounding curves of Figure 3.9 as bold lines, and those obtained using $Z_{\text{[lower]}}$ and $Z_{\text{[upper]}}$ as dashed lines.

It may be seen, in this particular case, that the "real" curve lies almost midway between the bounds; this is to be expected if we look at $\Gamma_{[F,G]}$ and $\gamma_{[F,G]}$ (and their bounds) which were shown in Figure 3.4 (e) and (f). If we were to repeat the example using $F = \frac{\pm 2}{s+2}$ then the "real" curve would coincide with the curve obtained using $\gamma_{\text{[upper]}}$; if we were to repeat the example with $F = \frac{\pm s}{s+2}$ then we might hope that the "real" curve would coincide with that obtained using $\gamma_{\text{[lower]}}$ — unfortunately this F is not strictly proper, so the analysis method cannot be applied.

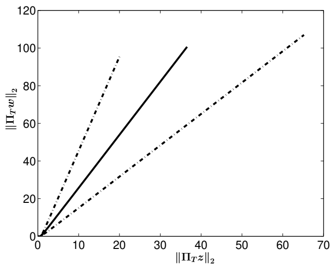

(a) $k = 0.80$

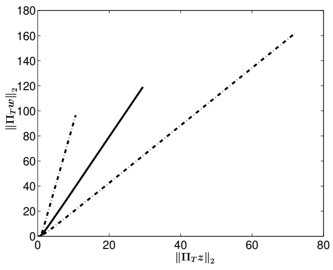

(b) $k = 0.90$

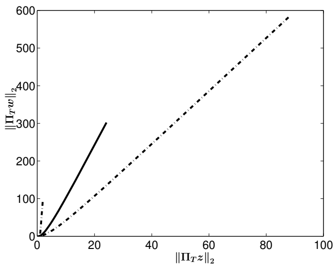

(c) $k = 0.99$

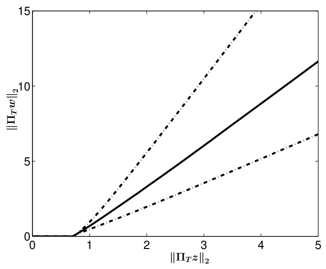

(d) $k = 0.80$ (zoom)

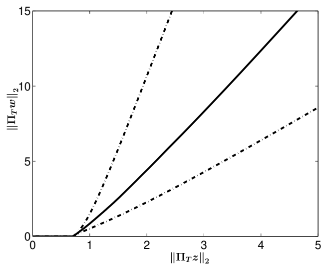

(e) $k = 0.90$ (zoom)

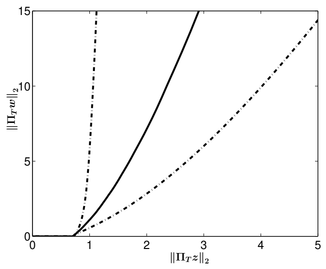

(f) $k = 0.99$ (zoom)

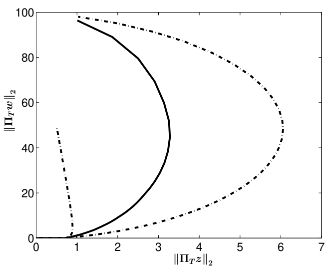

(g) $k = 1.01$

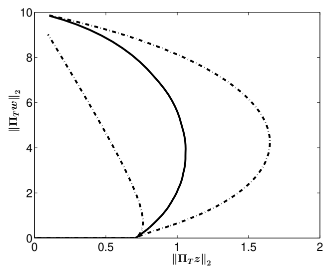

(h) $k = 1.10$

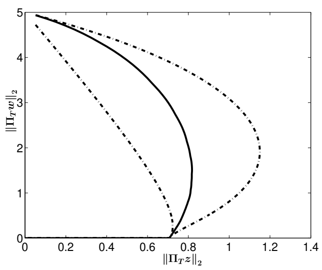

(i) $k = 1.20$

Figure 3.13: Local stability analysis: Example 1a

1b. In fact, for $\psi : (1,\infty) \to (0,1)$ given by

$$\psi(r) = 1 - \frac{1}{r}$$

(and hence for the case of the ideal deadzone nonlinearity) it is possible to identify *all* possible "shapes" for the "characteristic bounding curves" obtained using the bounds $\gamma_{[\text{upper}]}$ and $\gamma_{[\text{lower}]}$. Figure 3.14 shows[6] representative examples of all the possibilities (dependent upon μ and ρ)

The various possibilities depend on μ and ρ in the following ways (as taken from Theorem 3.16 and Corollary 3.19)

- For $\mu < 1$ we have $Z^{\text{opt}}_{[\text{upper}]} = \infty$ and $Z^{\text{opt}}_{[\text{lower}]} = \infty$
- For $\mu = 1$ we have $Z^{\text{opt}}_{[\text{upper}]} = \max\{1, \frac{1}{\rho}\}$ and $Z^{\text{opt}}_{[\text{lower}]} = \infty$
- For $\mu > 1$ we have $Z^{\text{opt}}_{[\text{upper}]} > 1$ if $\rho < 1$, with $Z^{\text{opt}}_{[\text{upper}]} = 1$ otherwise
  and $Z^{\text{opt}}_{[\text{lower}]} > 1$ if $\rho < \frac{\mu}{\sqrt{\mu^2-1}}$, with $Z^{\text{opt}}_{[\text{lower}]} = 1$ otherwise

The "real" characteristic bounding curve obtained using $\gamma_{[F,G]}$ always lies somewhere between the two bounds, depending on the precise relationship between $F(j\omega)$ and $G(j\omega)$.

Note that some of these curves (Figure 3.14 (c), (f) & (i)) have an odd feature: they appear to allow "non-graceful degradation", in the sense that $\|\Pi_T \boldsymbol{w}\|_2$ may increase rapidly for a small change in $\|\Pi_T \boldsymbol{z}\|_2$ (for $\|\Pi_T \boldsymbol{z}\|_2 > \frac{1}{\|F\|_2}$)

In practice, one would not expect such "non-graceful degradation" to occur, and in fact we hope that by applying the analysis to a whole family of loop-transformed systems, and superimposing all of the results onto a single plot, that such features will be eliminated. It is not clear, however, whether this claim could be proven in general.

[6] In this figure the x-axis has been scaled by $\|F\|_2$ and the y-axis scaled by $\frac{\|F\|_2}{\|F\|_\infty}$ so that the curves plotted are simply

$$\begin{bmatrix} Z_{[\text{upper}]}(\lambda) & \lambda Z_{[\text{upper}]}(\lambda) \end{bmatrix} \quad \text{and} \quad \begin{bmatrix} Z_{[\text{lower}]}(\lambda) & \lambda Z_{[\text{lower}]}(\lambda) \end{bmatrix}$$

over $\lambda \in \boldsymbol{\Lambda}_{[\text{upper}]}$ and $\lambda \in \boldsymbol{\Lambda}_{[\text{lower}]}$ respectively. For the purposes of qualitatively showing the possible "shapes" of these bounding curves the scaling due to $\|F\|$ is not important.

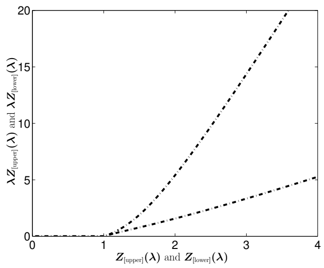

(a) $\mu = 0.9$, $\rho = 0.5$

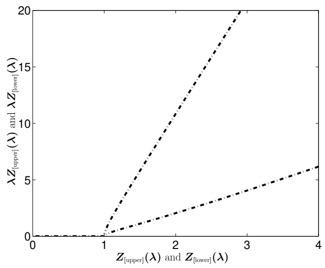

(b) $\mu = 0.9$, $\rho = 1$

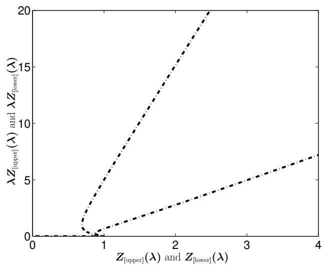

(c) $\mu = 0.9$, $\rho = 2$

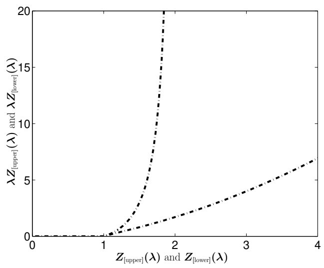

(d) $\mu = 1$, $\rho = 0.5$

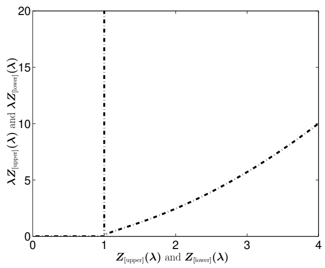

(e) $\mu = 1$, $\rho = 1$

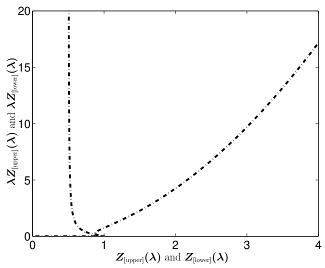

(f) $\mu = 1$, $\rho = 2$

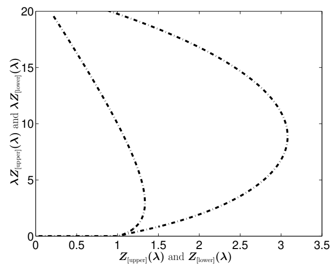

(g) $\mu = 1.1$, $\rho = 0.5$

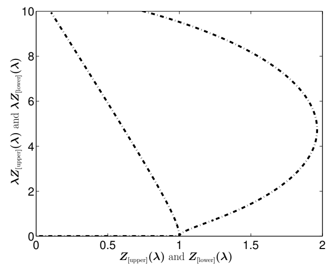

(h) $\mu = 1.1$, $\rho = 1$

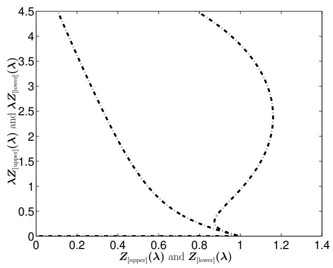

(i) $\mu = 1.1$, $\rho = 2$

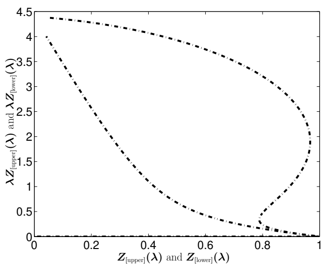

(j) $\mu = 1.1$, $\rho = 2.5$

Figure 3.14: Local stability analysis: Example 1b

2. Consider $\psi : (0, \infty) \to (0, M+1)$ given by

$$\psi(r) = \begin{cases} r & \text{if } r \leq M \\ M + \frac{r-M}{r-M+1} & \text{if } r > M \end{cases}$$

for some $M \gg 1$, which we used as Example 2 in Section 2.2, and which is shown in Figure 3.15 (a). For this particular ψ the family of nonlinearities $\boldsymbol{\Delta}_\psi$ contains the "saturated squaring" function[7]

$$w(t) := \left\{ \mathrm{Sat}_M \left(v(t) \right) \right\}^2$$

which is shown in Figure 3.15 (b).

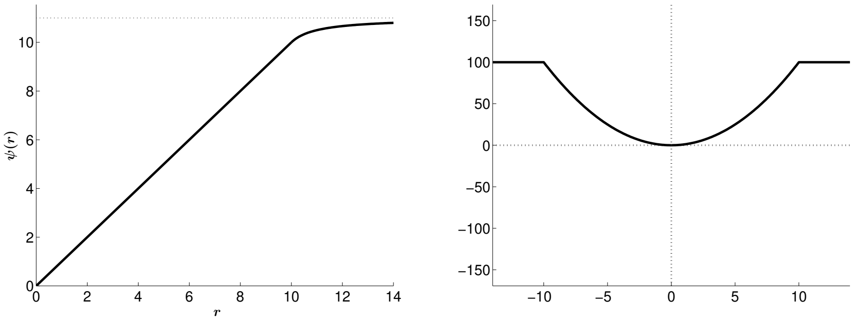

(a) $\psi(r)$ (b) "Saturated squarer"

Figure 3.15: ψ for local stability Example 2

Since $\beta_1 = M + 1 \gg 1$, it is not possible to guarantee stability of the interconnection for any G such that $\|G\|_\infty > \frac{1}{M+1}$. Indeed, if M is sufficiently large, and assuming a nonlinearity $\Delta \in \boldsymbol{\Delta}_\psi$ with $\|\Delta\| = \beta_1$, then it is not unlikely that the interconnection would be (globally) *unstable*.

[7]The motivation here is that as $M \to \infty$ the "saturated squarer" becomes almost indistinguishable from the "real squarer" $w(t) := |v(t)|^2$ — note that you can't actually consider the real squaring function directly, since it has infinitely large uniform instantaneous gain. Nevertheless, we expect that for sufficiently large M the results will be independent of M, and hence could be expected to hold for the "real squarer" (in so far as it is possible to find such a device in the real world)

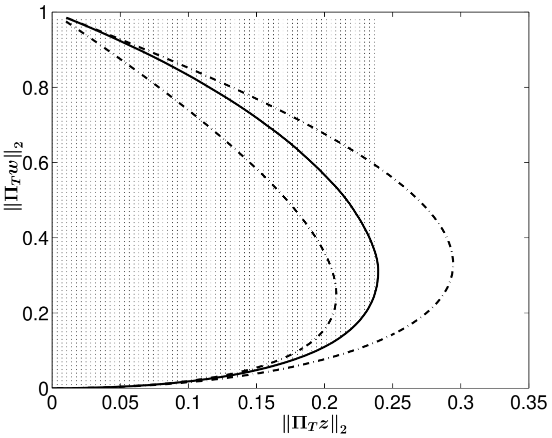

Figure 3.16: Local stability analysis: Example 2

Figure 3.16 shows the "characteristic bounding curve" and "forbidden region" obtained by applying the local stability analysis (Theorem 3.20) for

$$F = \tfrac{\pm 4s}{(s+2)^2} \quad \text{and} \quad G = \tfrac{\pm 2}{s+2}$$

(The solid line is the "real" characteristic bounding curve obtained using $\gamma_{[F,G]}$, and the dashed lines are those obtained using $\gamma_{[\text{upper}]}$ and $\gamma_{[\text{lower}]}$)

As it happens, it is possible in this case to find the upper and lower bounds on $Z^{\text{opt}}_{[F,G]}$ analytically, using standard algebraic methods, in which case we see an explicit and relatively simple dependence on μ and ρ.

Lemma 3.30 *For sufficiently large M, and $\psi : (0,\infty) \to (0, M+1)$ given by*

$$\psi(r) = \begin{cases} r & \text{if } r \le M \\ M + \frac{r-M}{r-M+1} & \text{if } r > M \end{cases}$$

and for any stable, strictly proper F and G with $\mu := \|G\|_\infty$ and $\rho := \frac{\|F\|_\infty \|G\|_2}{\|F\|_2}$

$$Z^{opt}_{[upper]} = \frac{1}{(\rho^{\frac{1}{2}} + \mu^{\frac{1}{2}})^2}$$

$$Z^{opt}_{[lower]} = \frac{1}{(\rho^{\frac{2}{3}} + \mu^{\frac{2}{3}})^{\frac{3}{2}}}$$

3.5 Summary and suggestions for further work

3.5.1 Summary

In this chapter we have

- Motivated the idea of analysing stability from both global and local perspectives.
- Given a simple $\mathcal{H}_\infty$-norm-based stability criterion for $[0,1]$ sector-bounded nonlinearities, which is related to the well-known Circle criterion.
- Derived a novel method for determining local stability properties of a simple nonlinear feedback system, and shown that $\mu := \|G\|_\infty$ and $\rho := \frac{\|F\|_\infty \|G\|_2}{\|F\|_2}$ are important factors in determining the local and global stability of such a feedback system.
- Demonstrated the features of this new analysis method with a number of examples.

3.5.2 Suggestions for further work

Biproper F in Section 3.4

The results of Section 3.4 cannot be applied directly to systems with a biproper transfer function $F(s)$ from the external input $\boldsymbol{z}$ to the nonlinearity $\boldsymbol{\Delta}$. However, by considering a sequence $F_\varepsilon = \frac{1}{\varepsilon s+1}F$, and letting $\varepsilon \to 0$, one would hope to get a meaningful result; no general results in this area have been obtained to date.

The main drawback to using this sequence of approximations is that $\frac{1}{\|F_\varepsilon\|_2}$ tends to zero as $\varepsilon \to 0$. If we recall that local stability is guaranteed for $\boldsymbol{z}$ such that

$$\|\boldsymbol{z}\|_2 < \tfrac{1}{\|F\|_2} Z^{\text{opt}}_{[F,G]}$$

then it is clear that non-trivial results will only be obtained in cases where $Z^{\text{opt}}_{[F_\varepsilon,G]}$ grows at least as fast as $\|F_\varepsilon\|_2$. Conditions under which this takes place have not, as yet, been determined.

Conservatism in the results of Section 3.4

It is expected (and accepted) that the results of Section 3.4 will often be quite conservative; *how* conservative remains an open question.

There are a number of avenues for combatting this conservatism: the most useful is to consider various “multipliers” and loop transformations, such as was used in the proof of Theorem 3.9. Such methods are widespread in the literature; good treatments and many common examples may be found in Balakrishnan [Bal95] and Kothare *et al* [KM99].

We mentioned in the preamble that Hindi & Boyd [HB98] have recently proposed a different method for determining a similar form of local stability. (This paper dealt exclusively with the ideal deadzone nonlinearity, but the approach could be easily generalised in a similar manner to Section 3.4.2.) We would expect that their method will give less conservative results than the method of Section 3.4, since it uses local generalisations of the Circle and Popov criteria.

However, as pointed out in the preamble, this method uses a “black box” numerical optimisation algorithm based on LMIs, which offers no intuition. By comparison, the main advantages claimed for our method are **simplicity** and **transparency**, in the sense that it is relatively easy to calculate the numerical results, and that there are clear indicators of the important (open-loop) properties affecting the results, specifically $\mu := \|G\|_\infty$ and $\rho := \frac{\|F\|_\infty \|G\|_2}{\|F\|_2}$.

Chapter 4

Systems with nonlinear actuators

4.1 Introduction

4.1.1 Background and motivation

It is clear from practical experience that all physical systems have limitations: structures are only designed to take certain stresses, pistons and valves have a restricted range of travel, and in fact all aspects of practical reality are limited in some way.

Equally, however, many systems can be modelled well by linear and time-invariant differential equations, provided that certain "signals" (which may be voltages, stresses, displacements, flow rates or whatever) remain within some nominal limits.

We unify these two observations by modelling the overall system in two parts: the "plant" (which has the LTI dynamics), and the "actuator(s)" (which are fundamentally nonlinear and/or time-varying.) This is a good way to represent many real systems, and has the added benefits that (i) a nominal LTI controller may often be designed which works well with the LTI plant (ignoring the limitations), and (ii) such a model can often be represented in the standard form of Figure 3.1 for the purpose of stability and/or performance analysis.

A motivating example: input saturation

As a motivating example let us consider the simple, and widely studied, case of a single-input system with a magnitude limitation in the input path. A model of such a system is often assumed to take the following form:

$$\begin{aligned} \tilde{u}(t) &= \mathrm{Sat}_a\big(u(t)\big) \\ y &= P_{\mathrm{lin}}\tilde{u} \end{aligned}$$

where $P_{\mathrm{lin}} \in \mathcal{R}_p$ is a LTI transfer function, and $a > 0$ denotes the limitation on $\tilde{u}(t)$.

Our final objective will be to implement some sort of compensation scheme to account for the nonlinearity: it therefore seems clear that we will need either a measurement or an estimate of $\tilde{u}(t)$; methods for obtaining this signal differ from author to author, however most fall into one of the following categories:

1. Assuming that an exact measurement of $\tilde{u}(t)$ may be made (Lin & Berg [LB98] actually claim that this is a reasonable assumption...)

2. Assuming that a filtered measurement $F\tilde{u}$ may be made, where the filter $F \in \mathcal{RH}_\infty$ is known exactly

3. Estimating $\tilde{u}$ by $\mathrm{Sat}_a\big(u(t)\big)$, assuming that the "real" nonlinearity is an ideal saturation function, and that the saturation level a is known exactly

We claim that none of these ideas makes good sense, for a number of reasons:

- There may not actually be a signal $\tilde{u}(t)$ in the physical system, or it may simply be impossible to make a measurement (for example, there may not be a suitable sensor, or sufficient space for the sensor, or sufficient bandwidth to transmit the measurement back to the controller)

- Any (filtered or unfiltered) measurement will inevitably be affected by noise

- A filtered measurement will be sensitive to errors in estimating the filter F

- An estimate will be sensitive to errors in estimating a, or by the "real" saturation function failing to be perfectly ideal.

- If the compensation scheme assumes the "real" saturation element to be the ideal function Sat_a, then the scheme may also be sensitive to errors in estimating a, or by the "real" saturation function failing to be perfectly ideal

Instead, we propose a fourth method

4. Ensure that $u(t)$ is such that $\tilde{u}(t) = u(t)$ for all t, and use $u(t)$ for compensation

Of course, if the model is correct, and we know a exactly, then it is clear *how* to do this: let $u(t)$ be the output of an ideal saturation function $\mathrm{Sat}_{\hat{a}}$, for any $\hat{a} \leq a$. What is not so obvious is *why* this is a better idea:

- The measurement/estimation problem is now solved: $u(t)$ is an internal signal of the *controller* implementation, and hence is available exactly (give or take the precision of the computer, in the case of a digital implementation!)

- Similarly, the compensation scheme is not sensitive to estimating the properties of the *implemented* nonlinearity, and is no more sensitive (and possibly *less* sensitive) to the "real" nonlinearity failing to be ideal *in the "linear" range* (we do not care what happens outside the range $[-a, a]$!)

  In other words, the "real" actuator needs only to satisfy the simple condition:

  $$\text{if } |u(t)| \leq \hat{a} \text{ then } \tilde{u}(t) = u(t)$$

  This condition is, of course, satisfied by the modelled actuator (the ideal saturation function Sat_a), but it actually permits the "real" nonlinearity to be any one of a wide class of functions, whose common feature is unity gain for small magnitude signals.

Essentially, what we propose is to model the magnitude-limited system by the equations

$$\tilde{u}(t) = \begin{cases} u(t) & \text{if } |u(t)| \leq a \\ \text{undefined} & \text{otherwise} \end{cases}$$
$$y = P_{\text{lin}}\tilde{u}$$

and to ensure that

$$u(t) = \text{Sat}_{\hat{a}}\left(\hat{u}(t)\right)$$

where $\hat{u}$ is the output of the combined control & compensation scheme, and $\hat{a} \leq a$.

We shall refer to this idea of "ensuring that u is within the limitations for the actuator" as *precompensation*. Note that we do not claim that this approach is novel, but rather that it has been tacitly ignored in most of the theoretical literature, while being implemented without question in practical applications!

This work is believed to be the first in-depth consideration of the general form of the problem, with the final objective being a framework which aids synthesis of Anti-Windup compensators.

Prior work on actuator modelling

There are only a handful of ideas in the existing literature about how to model a nonlinear actuator; the most common are briefly given below:

- **Magnitude-limited actuator**

  The simplest, and most widespread, model of a nonlinear actuator is, as stated earlier, based on saturation functions. The literature is split between those who consider the ideal saturation function **Sat** (Equation 2.15), and those who consider general saturation functions $\boldsymbol{\sigma}$ (satisfying, for example, Definitions 2.2 and/or 2.3)

  1. Ideal saturating actuators, ie

     $$\tilde{\boldsymbol{u}}(t) = \textbf{Sat}\Big(\boldsymbol{u}(t)\Big)$$

     are considered by, for example, Hui & Chan [HC99]; Lin & Berg [LB98]; Miyamoto & Vinnicombe [MV96b], [Miy97], [MV96a]; Aström & Rundqwist[AR89]; Park & Choi [PC95]; Peng *et al* [PVH96]; Weston & Postlethwaite [WP98] and Zheng *et al* [ZKM94].
  2. The general case, ie

     $$\tilde{\boldsymbol{u}}(t) = \boldsymbol{\sigma}\Big(\boldsymbol{u}(t)\Big)$$

     is considered by, for example, Kapila & Haddad [KH98]; Lin *et al* [Lin97], [LS93]; Saberi *et al* [SLT96]; Yakubovich *et al* [YNF99] and Teel & Kapoor [TK97].

     Note that our proposal in the motivating example above could be interpreted in such a way, although with the fairly strong assumption that small magnitude signals are not affected by the nonlinearity (eg $b_i = c_i = 1$ in Definitions 2.2 and 2.2) — this assumption is simlar to that made by Teel & Kapoor [TK97].

- **Rate-limited actuator**

  There are two common models for rate limitations; both models use either an ideal or generalised saturation function (we shall use the symbol $\boldsymbol{\sigma}$ to represent either of these possibilities) to limit the derivative, but they differ in the internal structure:

  1. One model differentiates the input, saturates the resulting signal, and then integrates, ie

     $$\frac{d\tilde{\boldsymbol{u}}}{dt} = \boldsymbol{\sigma}\Big(\frac{d\boldsymbol{u}}{dt}\Big)$$

     This model is considered by, for example, Kapila *et al* [KH98], [KPdQ99]; Hui & Chan [HC99] and Peng *et al* [PVH96].

     There are obvious problems with this model if $\boldsymbol{u}$ fails to be differentiable.

  2. The second model assumes a first-order dynamic for the actuator, ie

     $$\frac{d\tilde{\boldsymbol{u}}}{dt} = \boldsymbol{\sigma}\Big(\boldsymbol{u}(t) - \tilde{\boldsymbol{u}}(t)\Big); \quad \tilde{\boldsymbol{u}}(0) = 0$$

     This model is considered by, for example, Lin *et al* [LB98], [Lin97] and Rantzer & Megretski [RM97].

- **Rate- & magnitude-limited actuator**

  Actuators with both rate and magnitude limitation may be modelled by a simple series composition of a magnitude-limited model and a rate-limited model; there is, however, a choice to make here: which comes first?

  1. Kapila *et al* [KH98], [KPdQ99] model the saturation before the rate limiter — although it is interesting to note that they then propose to implement a precompensator which is the other way around.
  2. On the other hand, Hui & Chan [HC99] and Lin *et al* [LB98], [Lin97] model the rate limiter first.
  3. Finally, Peng *et al* [PVH96] do not make it clear which of these two choices they subscribe to. They say that $\tilde{\boldsymbol{u}}$ and $\frac{d\tilde{\boldsymbol{u}}}{dt}$ satisfy $\tilde{\boldsymbol{u}}(t) = \mathbf{Sat}\big(\boldsymbol{u}(t)\big)$ and $\frac{d\tilde{\boldsymbol{u}}}{dt} = \mathbf{Sat}\big(\frac{d\boldsymbol{u}}{dt}\big)$ simultaneously — but these two statements can be contradictory!

- **"Unknown" actuator**

  A significant number of papers simply assume that the nonlinearity is modelled by some "Δ", for example, Edwards & Postlethwaite [EP97] and Kothare *et al* [KCMN94], [KM95], [KM99].

  This is fine (for anti-windup synthesis), just so long as an exact measurement of the internal (and possibly non-existent!) signal $\tilde{\boldsymbol{u}}$ is available...

Prior work on precompensation (or similar concepts)

A small number of similar, although still significantly different, schemes have been proposed recently; each of these has been quite a brief treatment, without any strong physical or mathematical motivation.

1. Campo & Morari [CM90] (see also Park & Choi [PC95] and Peng *et al* [PVHW98]) consider an "artificial nonlinearity", which goes between the controller output and the actuator input; nevertheless, it is still assumed in these papers that the *actual* plant input ($\tilde{\boldsymbol{u}}$ in the above example) is measurable.

   Moreover, their "artificial nonlinearity" is more than a simple model of the real actuator: it actively modifies the input signal, for example to maintain the "direction" of the vector $\boldsymbol{u}(t)$. This seems a counter-intuitive proposal: if one actuator saturates, then it does not seem sensible to deliberately restrict the control authority in the remaining actuators.

2. Kapila *et al* [KH98], [KPdQ99] consider rate- & magnitude-limited actuators, and propose to produce the actuator input $\boldsymbol{u}(t)$ in the following way

$$\begin{aligned} \boldsymbol{u}(t) &= \mathbf{Sat}\big(\boldsymbol{v}(t)\big) \\ \tfrac{d\boldsymbol{v}}{dt} &= \mathbf{Sat}\big(\boldsymbol{w}(t)\big) \end{aligned}$$

   where $\boldsymbol{w}(t)$ is the output of the control & compensation scheme. This certainly ensures that the actuator input $\boldsymbol{u}(t)$ is within the constraints, however we would point out that there is no reason why $\boldsymbol{v}(t)$ should not become very large ("wind up"), which could have a detrimental effect, since $\boldsymbol{u}(t)$ might then remain saturated for an unnecessarily long time.

3. Hui & Chan [HC99] propose a similar scheme, but with $\boldsymbol{w}(t)$ being the *derivative* of the controller output. The previous comment about "windup" applies equally to this proposal.

4.1.2 Modelling of systems with limited-authority actuators

We assume that the system which we are trying to control can be modelled as two separate components, which we will refer to as the "plant" and "actuator".

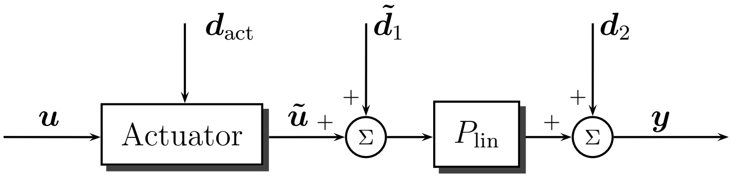

Figure 4.1: Model of limited-authority actuator and plant

This two-element model is shown in Figure 4.1, where $\boldsymbol{u} \in \mathcal{L}_{2e}^{n_u}$ is the input to the actuator, $\tilde{\boldsymbol{u}} \in \mathcal{L}_{2e}^{n_u}$ is the input to the plant, and $\boldsymbol{y} \in \mathcal{L}_{2e}^{n_y}$ is the measured output of the plant. Note that although $\boldsymbol{u}$ and $\boldsymbol{y}$ are real signals in the physical system, $\tilde{\boldsymbol{u}}$ may only be a feature of the system model.

We make the following assumptions about the behaviour of the plant and actuator:

- We assume that the plant can be modelled by a (possibly unstable) LTI transfer function $P_{\mathrm{lin}}(s) \in \mathcal{R}_p^{n_y \times n_u}$, with input- and output-additive disturbance signals ($\tilde{\boldsymbol{d}}_1 \in \mathcal{L}_{2e}^{n_u}$ and $\boldsymbol{d}_2 \in \mathcal{L}_{2e}^{n_y}$ respectively) to represent any unmodelled effects:

$$\boldsymbol{y} = P_{\mathrm{lin}}(\tilde{\boldsymbol{u}} + \tilde{\boldsymbol{d}}_1) + \boldsymbol{d}_2$$

- We assume that the actuator is square and decentralised (ie it may be represented as the diagonal composition of n_u individual scalar operators) and that it can be modelled by a nonlinear operator $\mathbb{A} : \boldsymbol{u} \mapsto \tilde{\boldsymbol{u}}$ satisfying the following two relationships for some given $\boldsymbol{\mathcal{U}}_{\mathrm{act}} \subset \mathcal{L}_{2e}^{n_u}$ (the *output constraint space*), $\boldsymbol{\mathcal{U}}_{\mathrm{nom}} \subset \mathcal{L}_{2e}^{n_u}$ (the *nominal input space*) and stable LTI transfer function $P_{\mathrm{act}}(s) \in \mathcal{RH}_\infty^{n_u \times n_u}$ (the *nominal dynamics*)

  A1 $\tilde{\boldsymbol{u}} \in \boldsymbol{\mathcal{U}}_{\mathrm{act}}$ for all $\boldsymbol{u} \in \mathcal{L}_{2e}^{n_u}$

  A2 if $\boldsymbol{u} \in \boldsymbol{\mathcal{U}}_{\mathrm{nom}}$ then $\tilde{\boldsymbol{u}} \equiv P_{\mathrm{act}}\boldsymbol{u}$

  with a disturbance signal ($\boldsymbol{d}_{\mathrm{act}}$) to represent any unmodelled effects, which we will assume to be output-additive, and hence absorb without further comment into $\tilde{\boldsymbol{d}}_1$. Note that we *cannot* model disturbances at the actuator input in this framework.

- We assume that the nominal input space $\boldsymbol{\mathcal{U}}_{\mathrm{nom}}$ comprises those inputs for which the nominal output does not violate the constraints, ie

$$\boldsymbol{\mathcal{U}}_{\mathrm{nom}} := \left\{ \boldsymbol{v} \in \mathcal{L}_{2e}^{n_u} : P_{\mathrm{act}}\boldsymbol{v} \in \boldsymbol{\mathcal{U}}_{\mathrm{act}} \right\}$$

  so that if $P_{\mathrm{act}}(s) = I$ then $\boldsymbol{\mathcal{U}}_{\mathrm{nom}} = \boldsymbol{\mathcal{U}}_{\mathrm{act}}$.

- Finally, we make a technical assumption that P_{act} does not cancel any unstable poles of P_{lin}.

In terms of an overall system model, these assumptions are equivalent to assuming that the following relationship between $\boldsymbol{u}$ and $\boldsymbol{y}$ holds:

$$\boldsymbol{y} = \begin{cases} P_{\text{lin}}(P_{\text{act}}\boldsymbol{u} + \tilde{\boldsymbol{d}}_1) + \boldsymbol{d}_2 & \text{if } P_{\text{act}}\boldsymbol{u} \in \boldsymbol{\mathcal{U}}_{\text{act}} \\ \text{undefined} & \text{otherwise} \end{cases} \tag{4.1}$$

It is now clear that a desirable goal is to ensure that the actuator input $\boldsymbol{u}$ satisfies $\boldsymbol{u} \in \boldsymbol{\mathcal{U}}_{\text{nom}}$ (ie $P_{\text{act}}\boldsymbol{u} \in \boldsymbol{\mathcal{U}}_{\text{act}}$), so that the behaviour of the actuator and plant can be assumed to be *linear and time-invariant.*

There is a strong physical motivation behind these assumptions, based on the observation that a limited-authority actuator (such as, for example, a valve, a hydraulic piston, a mass-spring-damper with endstops or an op-amp) behaves *linearly* until such time as its *output* violates the constraint(s). After this time the behaviour may become quite complex — but if this situation can be avoided, then it is unnecessary to attempt to model this complexity.

4.1.3 Precompensation for limited-authority actuators

We now propose to implement, *within* our combined control & compensation scheme, a "nonlinear precompensator" (which we denote by an operator $\mathbb{P}$), the purpose of which is to ensure that the actuator input is always a member of the nominal input space, ie that $\boldsymbol{u} \in \boldsymbol{\mathcal{U}}_{\text{nom}}$.

In addition, we desire that one or more signals containing information about the internal state of the precompensator should be available for use by the control & compensation scheme, for anti-windup purposes.

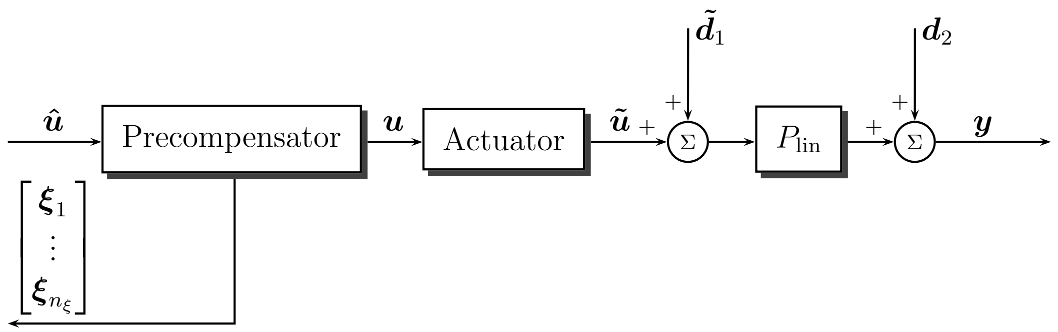

Figure 4.2: Precompensator, nonlinear actuator and linear plant

This idea is shown in Figure 4.2, where $\hat{\boldsymbol{u}} \in \mathcal{L}_{2e}^{n_u}$ is the input to the precompensator, $\boldsymbol{\xi}_1, \boldsymbol{\xi}_2, \cdots, \boldsymbol{\xi}_{n_\xi}$ are the additional feedback signals, and all other signals are as in Figure 4.1.

Since we may not know $\boldsymbol{\mathcal{U}}_{\text{nom}}$ perfectly, we state the requirements for the precompensator in terms of an *estimated* nominal input space $\hat{\boldsymbol{\mathcal{U}}}_{\text{nom}}$, which is assumed to satisfy

$$\hat{\boldsymbol{\mathcal{U}}}_{\text{nom}} \quad \text{is a subset of} \quad \boldsymbol{\mathcal{U}}_{\text{nom}} \tag{4.2}$$

The specific requirements which the precompensator must satisfy are listed below:

- to ensure, for any input $\hat{\boldsymbol{u}}(t)$, that its output $\boldsymbol{u}$ is always a member of $\hat{\boldsymbol{\mathcal{U}}}_{\text{nom}}$
- to pass *unchanged* any input $\hat{\boldsymbol{u}}$ which is a member of $\hat{\boldsymbol{\mathcal{U}}}_{\text{nom}}$
- to produce (one or more) feedback signals $\boldsymbol{\xi}_1 \cdots \boldsymbol{\xi}_{n_\xi}$ which contain useful information about the signals within the precompensator, satisfying

$$\boldsymbol{\xi}_1 \equiv \boldsymbol{\xi}_2 \cdots \boldsymbol{\xi}_{n_\xi} \equiv \hat{\boldsymbol{u}} \quad \text{if } \hat{\boldsymbol{u}} \in \hat{\boldsymbol{\mathcal{U}}}_{\text{nom}}$$

- to behave in a reasonable manner for $\hat{\boldsymbol{u}} \notin \hat{\boldsymbol{\mathcal{U}}}_{\text{nom}}$
- to be as simple as possible
- to be suitable for both implementation and analysis

Unfortunately, not all of these items can be quantified in a rigorous manner; those which can are given below, but we may still decide that an admissable precompensator is unacceptable for an unquantifiable reason (such as being overly complicated.)

Definition 4.1 (Precompensator admissibility)
Given $\hat{\boldsymbol{\mathcal{U}}}_{nom} \subseteq \mathcal{L}_{2e}^{n_u}$ and $n_\xi \geq 1$, a precompensator

$$\mathbb{P} : \hat{\boldsymbol{u}} \mapsto \begin{bmatrix} \boldsymbol{u} \\ \begin{bmatrix} \boldsymbol{\xi}_1 \\ \vdots \\ \boldsymbol{\xi}_{n_\xi} \end{bmatrix} \end{bmatrix}$$

is said to be admissible *if*

P0 $\mathbb{P}$ *is causal and well-defined (analogously to* well posedness*, Definition 3.3)*

P1 $\boldsymbol{u} \in \hat{\boldsymbol{\mathcal{U}}}_{nom}$ *for all* $\hat{\boldsymbol{u}} \in \mathcal{L}_{2e}^{n_u}$

P2 if $\hat{\boldsymbol{u}} \in \hat{\boldsymbol{\mathcal{U}}}_{nom}$ *then* $\boldsymbol{u} \equiv \hat{\boldsymbol{u}}$ *and* $\boldsymbol{\xi}_i \equiv \hat{\boldsymbol{u}}$ *for each* $i \in \{1, 2, \cdots, n_\xi\}$

Note the similarity between these requirements, and the assumptions we made about the behaviour of the actuator itself. In fact, although we have chosen *not* to model actuators in the "normal" way, each of our precompensators will be based on a standard model of a limited-authority actuator (recall from the introduction to this chapter that our proposed precompensator for the magnitude-limited system was a simple ideal saturation function.)

4.2 Mathematical preliminaries

4.2.1 Signal spaces with magnitude or rate constraints

Simple constraints

We denote by $\mathfrak{M}_a \subset \mathcal{L}_\infty$ those scalar signals which are bounded in magnitude by $a > 0$:

$$\mathfrak{M}_a := \Big\{ v \in \mathcal{L}_\infty : |v(t)| \leq a \quad \forall t \geq 0 \Big\} \tag{4.3}$$

The multivariable equivalent $\boldsymbol{\mathfrak{M}}_A \subset \mathcal{L}_\infty^n$ for a diagonal matrix $A > 0$ is then:

$$\boldsymbol{\mathfrak{M}}_A := \Big\{ \boldsymbol{v} \in \mathcal{L}_\infty^n : v_i \in \mathfrak{M}_{a_i} \quad \forall i \in \{1, 2, \cdots n\} \Big\} \tag{4.4}$$

Lemma 4.1

- *If* $A, \hat{A} > 0$ *are diagonal matrices such that*

$$A\hat{A}^{-1} \geq I$$

then $\boldsymbol{\mathfrak{M}}_{\hat{A}} \subseteq \boldsymbol{\mathfrak{M}}_A$.

PROOF OF LEMMA 4.1:
Immediate from Equations 4.3 and 4.4. ∎

We denote by $\mathcal{C} \subset \mathcal{L}_{\infty e}$ those signals which are continuous, and by $\mathcal{D}_+ \subset \mathcal{C}$ those signals which are also right-differentiable. Note that for any $\boldsymbol{v} \in \mathcal{C}$ and $T \geq 0$

$$\sup_{t \in [0,T]} \|\boldsymbol{v}(t)\| \quad \text{is finite}$$

ie that such signals are bounded, not just essentially bounded. Hence the truncated $\mathcal{L}_\infty$-norm $\|\Pi_T \boldsymbol{v}\|_\infty$ is the true magnitude supremum for any $\boldsymbol{v} \in \mathcal{C}$.

We then denote by $\mathfrak{R}_b \subset \mathcal{D}_+$ those scalar signals which are continuous and right-differentiable, with derivative bounded in magnitude by $b > 0$:

$$\mathfrak{R}_b := \Big\{ v \in \mathcal{D}_+ : \tfrac{dv}{dt} \in \mathfrak{M}_b \Big\} \tag{4.5}$$

The multivariable equivalent $\boldsymbol{\mathfrak{R}}_B \subset \mathcal{D}_+^n$ for a diagonal matrix $B > 0$ is then:

$$\boldsymbol{\mathfrak{R}}_B := \Big\{ \boldsymbol{v} \in \mathcal{D}_+^n : v_i \in \mathfrak{R}_{b_i} \quad \forall i \in \{1, 2, \cdots n\} \Big\} \tag{4.6}$$

Lemma 4.2

- *For any diagonal matrix $B > 0$*

$$\boldsymbol{\mathfrak{R}}_B = \left\{ \boldsymbol{v} \in \mathcal{D}_+^n : \boldsymbol{v}(t) = \boldsymbol{v}_0 + \int_0^t \boldsymbol{w}(\tau)\, d\tau, \quad \textit{for some } \boldsymbol{w} \in \boldsymbol{\mathfrak{M}}_B \textit{ and } \boldsymbol{v}_0 \in \mathbb{R}^n \right\}$$

- *If $B, \hat{B} > 0$ are diagonal matrices such that*

$$B\hat{B}^{-1} \geq I$$

then $\boldsymbol{\mathfrak{R}}_{\hat{B}} \subseteq \boldsymbol{\mathfrak{R}}_B$.

PROOF OF LEMMA 4.2:
Immediate from Equations 4.5 and 4.6. ∎

Dynamic constraints (first-order)

We denote by $\mathfrak{M}^1_{a,c} \subset \mathcal{L}_{\infty e}$ those scalar signals which, when passed through a first-order lag $\frac{c}{s+c}$ $(c > 0)$, produce an output which is bounded in magnitude by $a > 0$, ie

$$\mathfrak{M}^1_{a,c} := \left\{ v \in \mathcal{L}_{\infty e} : \tfrac{c}{s+c} v \in \mathfrak{M}_a \right\} \tag{4.7}$$

The multivariable equivalent $\boldsymbol{\mathfrak{M}^1}_{A,C} \subset \mathcal{L}^n_{\infty e}$ for diagonal matrices $A, C > 0$ is then:

$$\boldsymbol{\mathfrak{M}^1}_{A,C} := \left\{ \boldsymbol{v} \in \mathcal{L}^n_{\infty e} : v_i \in \mathfrak{M}^1_{a_i,c_i} \quad \forall i \in \{1, 2, \cdots n\} \right\} \tag{4.8}$$

Lemma 4.3

- *For any diagonal matrices $A, C > 0$*

$$\boldsymbol{\mathfrak{M}^1}_{A,C} = \left\{ \boldsymbol{v} \in \mathcal{L}^n_{\infty e} : \boldsymbol{v}(t) = \boldsymbol{x}(t) + C^{-1}\tfrac{d\boldsymbol{x}}{dt}, \quad \textit{for some } \boldsymbol{x} \in \mathcal{D}^n_+ \cap \boldsymbol{\mathfrak{M}}_A \right\}$$

- *If $A, C, \hat{A} > 0$ are diagonal matrices such that*

$$A\hat{A}^{-1} \geq I$$

then $\boldsymbol{\mathfrak{M}}_{\hat{A}} \subset \boldsymbol{\mathfrak{M}^1}_{A,C}$.

- *If $A, C, \hat{A}, \hat{C} > 0$ are diagonal matrices such that*

$$A\hat{A}^{-1} \geq I \quad \textit{and} \quad A\hat{A}^{-1} \geq 2C\hat{C}^{-1} - I$$

then $\boldsymbol{\mathfrak{M}^1}_{\hat{A},\hat{C}} \subseteq \boldsymbol{\mathfrak{M}^1}_{A,C}$.

Remark

1. Figure 4.3 shows the admissible ratios $\frac{a}{\hat{a}}$ and $\frac{c}{\hat{c}}$ such that $\mathfrak{M}^1_{\hat{a},\hat{c}} \subset \mathfrak{M}^1_{a,c}$.

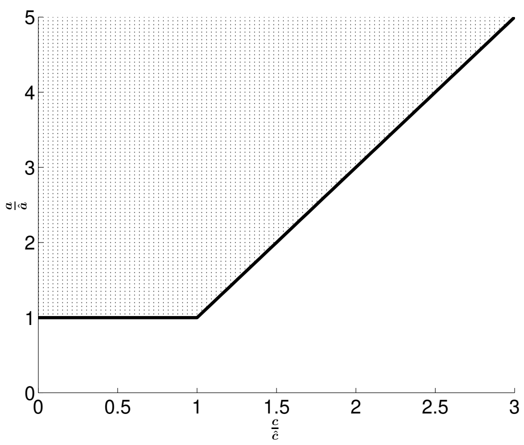

Figure 4.3: $\frac{a}{\hat{a}}$ and $\frac{c}{\hat{c}}$ such that $\mathfrak{M}^1_{\hat{a},\hat{c}} \subset \mathfrak{M}^1_{a,c}$

PROOF OF LEMMA 4.3:

We prove the results for the scalar case only; the multivariable case then follows immediately, since everything is defined component-wise.

Given $v \in \mathcal{L}_{\infty e}$, it is clear that $x = \frac{c}{s+c}v$ is the unique solution to the following differential equation (assuming $x(0) = 0$)

$$\tfrac{dx}{dt} = c\big(v(t) - x(t)\big)$$

or, equivalently, to the following unique decomposition of v

$$v(t) = x(t) + \tfrac{1}{c}.\tfrac{dx}{dt}$$

in which x is certain to be continuous and right-differentiable (for any $v \in \mathcal{L}_{\infty e}$), and must satisfy $x \in \mathfrak{M}_a$ if $v \in \mathfrak{M}^1_{a,c}$.

To show the first set inclusion result, note that if $v \in \mathfrak{M}_{\hat{a}}$ then

$$\|x\|_\infty \leq \left\|\tfrac{c}{s+c}\right\|_1 \|v\|_\infty \leq \hat{a}$$

Since x is continuous, its $\mathcal{L}_\infty$-norm is its true magnitude supremum, and so we deduce that $\frac{c}{s+c}v \in \mathfrak{M}_{\hat{a}}$. Lemma 4.1 then states that $\mathfrak{M}_{\hat{a}} \subseteq \mathfrak{M}_a$ if $\hat{a} \leq a$, in which case $\frac{c}{s+c}v \in \mathfrak{M}_a$.

For the second set inclusion result, consider $\hat{x} = \frac{\hat{c}}{s+\hat{c}}v$ and $x = \frac{c}{s+c}v$, and assume that v is such that $\hat{x} \in \mathfrak{M}_{\hat{a}}$, ie that $v \in \mathfrak{M}^1_{\hat{a},\hat{c}}$. By a simple rearrangement we see that

$$x = \left\{\tfrac{c}{\hat{c}} + \tfrac{\hat{c}-c}{\hat{c}}.\tfrac{c}{s+c}\right\}\hat{x}$$

and hence by Proposition 2.2 that

$$\begin{aligned}\|x\|_\infty &\leq \left\{\tfrac{c}{\hat{c}} + \tfrac{\hat{c}-c}{\hat{c}}.\left\|\tfrac{c}{s+c}\right\|_1\right\}\|\hat{x}\|_\infty \\ &= \tfrac{c+|\hat{c}-c|}{\hat{c}}\|\hat{x}\|_\infty \\ &\leq \tfrac{c+|\hat{c}-c|}{\hat{c}}\hat{a}\end{aligned}$$

The inequalities then follow by simple algebra, once again noting that the $\mathcal{L}_\infty$-norm of x is its true magnitude supremum. ∎

We denote by $\mathfrak{R}^1_{b,c} \subset \mathcal{L}_{\infty e}$ those scalar signals which, when passed through a first-order lag $\frac{c}{s+c}$ $(c > 0)$, produce an output with derivative bounded in magnitude by $b > 0$, ie

$$\mathfrak{R}^1_{b,c} := \left\{ v \in \mathcal{L}_{\infty e} : \tfrac{c}{s+c} v \in \mathfrak{R}_b \right\} \tag{4.9}$$

The multivariable equivalent $\boldsymbol{\mathfrak{R}}^{\mathbf{1}}{}_{B,C} \subset \mathcal{L}^n_{\infty e}$ for diagonal matrices $B, C > 0$ is then:

$$\boldsymbol{\mathfrak{R}}^{\mathbf{1}}{}_{B,C} := \left\{ \boldsymbol{v} \in \mathcal{L}^n_{\infty e} : v_i \in \mathfrak{R}^1_{b_i,c_i} \quad \forall i \in \{1, 2, \cdots n\} \right\} \tag{4.10}$$

Lemma 4.4

- *For any diagonal matrices $B, C > 0$*

$$\boldsymbol{\mathfrak{R}}^{\mathbf{1}}{}_{B,C} = \left\{ \boldsymbol{v} \in \mathcal{L}^n_{\infty e} : \boldsymbol{v}(t) = \int_0^t \boldsymbol{w}(\tau)\, d\tau + C^{-1}\boldsymbol{w}(t), \quad \textit{for some } \boldsymbol{w} \in \boldsymbol{\mathfrak{M}}_B \right\}$$

- *If $\hat{A}, B, C > 0$ are diagonal matrices such that*

$$BC^{-1} \geq 2\hat{A}$$

  then $\boldsymbol{\mathfrak{M}}_A \subset \boldsymbol{\mathfrak{R}}^{\mathbf{1}}{}_{B,C}$.

- *If $B, C, \hat{B}, \hat{C} > 0$ are diagonal matrices such that*

$$B\hat{B}^{-1} \geq I \quad \textit{and} \quad B\hat{B}^{-1} \geq 2C\hat{C}^{-1} - I$$

  then $\boldsymbol{\mathfrak{R}}^{\mathbf{1}}{}_{\hat{B},\hat{C}} \subseteq \boldsymbol{\mathfrak{R}}^{\mathbf{1}}{}_{B,C}$.

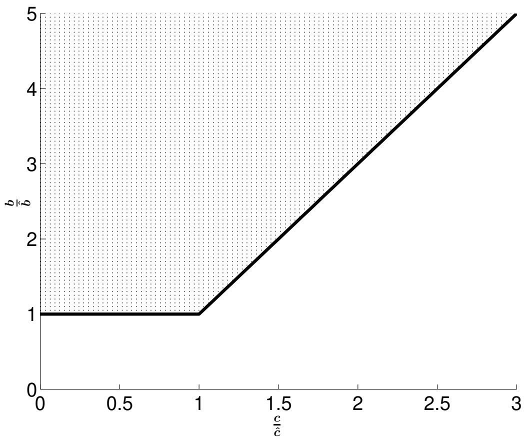

Figure 4.4: $\frac{b}{\hat{b}}$ and $\frac{c}{\hat{c}}$ such that $\mathfrak{R}^1_{\hat{b},\hat{c}} \subset \mathfrak{R}^1_{b,c}$

Remark

1. Figure 4.4 shows the admissible ratios $\frac{b}{\hat{b}}$ and $\frac{c}{\hat{c}}$ such that $\mathfrak{R}^1_{\hat{b},\hat{c}} \subset \mathfrak{R}^1_{b,c}$.

PROOF OF LEMMA 4.4:

We prove the results for the scalar case only; the multivariable case then follows immediately, since everything is defined component-wise.

Given $v \in \mathcal{L}_{\infty e}$, it is clear that $x = \frac{c}{s+c}v$ is the unique solution to the following differential equation (assuming $x(0) = 0$)

$$\tfrac{dx}{dt} = c\big(v(t) - x(t)\big)$$

or, equivalently, to the following unique decomposition of v

$$v(t) = x(t) + \tfrac{1}{c}.\tfrac{dx}{dt}$$

in which x is certain to be continuous and right-differentiable (for any $v \in \mathcal{L}_{\infty e}$) and must satisfy $x \in \mathfrak{R}_b$ if $v \in \mathfrak{R}^1_{b,c}$. Moreover, by Lemma 4.2, $x \in \mathfrak{R}_b$ iff

$$x(t) = \int_0^t w(\tau)\, d\tau$$

for some $w \in \mathfrak{M}_b$; note that $\frac{dx}{dt} = w(t)$.

For the first set inclusion result, note that if $v \in \mathfrak{M}_{\hat{a}}$ then

$$\|x\|_\infty \le \left\|\tfrac{c}{s+c}\right\|_1 \|v\|_\infty \le \hat{a}$$

and hence (by the triangle inequality) $\left\|\frac{dx}{dt}\right\|_\infty = \|c(v-x)\|_\infty \le 2\hat{a}c$. Noting that x has finite derivative indicates that $\frac{c}{s+c}v \in \mathfrak{R}_{2\hat{a}c}$, from which the inequality follows immediately.

For the second set inclusion result, consider $\hat{x} = \frac{\hat{c}}{s+\hat{c}}v$ and $x = \frac{c}{s+c}v$, and assume that v is such that $\frac{d\hat{x}}{dt} \in \mathfrak{M}_{\hat{b}}$, ie that $v \in \mathfrak{M}^1_{\hat{b},\hat{c}}$. By a simple rearrangement we see that

$$\tfrac{dx}{dt} = \left\{\tfrac{c}{\hat{c}} + \tfrac{\hat{c}-c}{\hat{c}}.\tfrac{c}{s+c}\right\}\tfrac{d\hat{x}}{dt}$$

and hence by Proposition 2.2 that

$$\begin{aligned}\left\|\tfrac{dx}{dt}\right\|_\infty &\le \left\{\tfrac{c}{\hat{c}} + \tfrac{\hat{c}-c}{\hat{c}}.\left\|\tfrac{c}{s+c}\right\|_1\right\}\left\|\tfrac{d\hat{x}}{dt}\right\|_\infty \\ &= \tfrac{c+|\hat{c}-c|}{\hat{c}}\left\|\tfrac{d\hat{x}}{dt}\right\|_\infty \\ &= \tfrac{c+|\hat{c}-c|}{\hat{c}}\hat{b}\end{aligned}$$

The inequalities then follow by simple algebra, once again noting that $\frac{dx}{dt}$ is finite. ∎

Dynamic constraints (general)

Lemma 4.5 gives a general result for essentially arbitrary dynamic constraints, although it must be stressed that the set inclusion may possibly be extremely conservative.

Lemma 4.5

If

$$P(s) = \mathrm{Diag}\left\{p_1(s), p_2(s), \cdots, p_n(s)\right\}$$

with $\|p_i(s)\|_1 \leq 1$ *for each* $i \in \{1, 2, \cdots, n\}$*, and if* $A, \hat{A} > 0$ *are diagonal matrices such that*

$$A\hat{A}^{-1} \geq I$$

then $\mathfrak{M}_{\hat{A}} \subseteq \left\{\boldsymbol{v} \in \mathcal{L}_{2e}^{n_u} : P\boldsymbol{v} \in \mathfrak{M}_A\right\}$

PROOF OF LEMMA 4.5:

In the scalar case, the result follows from Proposition 2.3; the multivariable case is then immediate. ∎

4.3 Precompensators for common nonlinear actuators

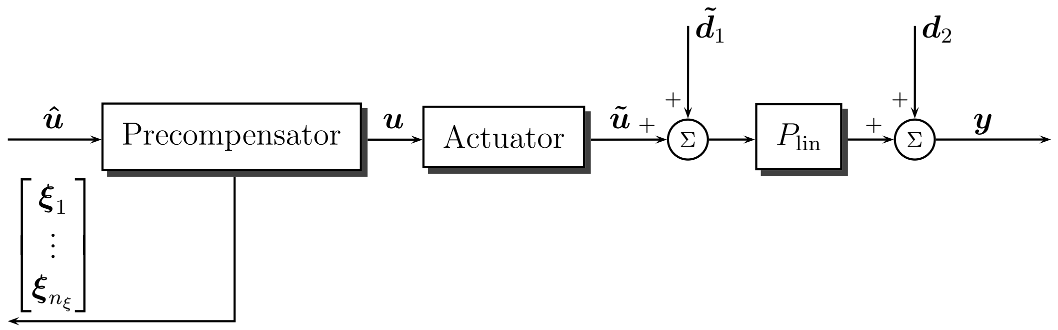

Figure 4.5: Precompensator, nonlinear actuator and linear plant

Figure 4.5 shows once again the series composition of precompensator, nonlinear actuator and linear plant. In the following sections we state the appropriate *output constraint space* $\boldsymbol{\mathcal{U}}_{\text{act}}$, *nominal dynamics* $P_{\text{act}}(s)$ and *nominal input space* $\boldsymbol{\mathcal{U}}_{\text{nom}}$ for a number of common actuator nonlinearities, and propose a suitable precompensator for each.

4.3.1 Magnitude-limited actuator

The simplest, and most common, form of limitation is clearly that of a magnitude constraint, for example that a valve can only be between 0% and 100% open. For simplicity, and without loss of generality, we shall assume that the allowable range for the ith input channel is symmetrical about zero, ie $[-a_i, a_i]$, for some $a_i > 0$.

The *output constraint space* for an actuator with magnitude limitation is then seen to be given by $\boldsymbol{\mathcal{U}}_{\text{act}} = \mathfrak{M}_A$, where $A = \text{Diag}\{a_1, a_2, \cdots, a_{n_u}\}$.

Actuator with unity nominal dynamics $P_{\textbf{act}}(s) = I$

We consider first the case of a static actuator with no nominal dynamics, and without loss of generality we assume that $P_{\text{act}}(s) = I$. Hence we see that the *nominal input space* is given by $\boldsymbol{\mathcal{U}}_{\text{nom}} = \boldsymbol{\mathcal{U}}_{\text{act}} = \mathfrak{M}_A$.

Now, by Lemma 4.1, if $\hat{A} > 0$ is a diagonal matrix such that

$$A\hat{A}^{-1} \geq I \tag{4.11}$$

then $\mathfrak{M}_{\hat{A}} \subseteq \mathfrak{M}_A$. So, we propose to take $\hat{\boldsymbol{\mathcal{U}}}_{\text{nom}} = \mathfrak{M}_{\hat{A}}$ as our estimate of $\boldsymbol{\mathcal{U}}_{\text{nom}}$.

It is clear that a suitable precompensator for $\hat{\boldsymbol{\mathcal{U}}}_{\text{nom}} = \mathfrak{M}_{\hat{A}}$ may be obtained using an ideal saturation function to limit the magnitude of $\boldsymbol{u}$. Note that this is precisely the same proposal as in the motivating example discussed in Section 4.1:

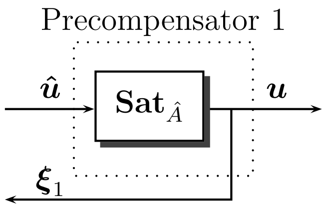

Figure 4.6: Precompensator 1

Precompensator 1 (for $\hat{\boldsymbol{\mathcal{U}}}_{\mathbf{nom}} = \mathfrak{M}_{\hat{A}}$)

Given a diagonal matrix $\hat{A} > 0$, let $\mathbb{P}_1^{\hat{A}} : \hat{\boldsymbol{u}} \mapsto \begin{bmatrix} \boldsymbol{u} \\ [\boldsymbol{\xi}_1] \end{bmatrix}$ be defined by

$$\begin{aligned} \boldsymbol{\xi}_1(t) &= \mathbf{Sat}_{\hat{A}}\big(\hat{\boldsymbol{u}}(t)\big) \\ \boldsymbol{u}(t) &= \boldsymbol{\xi}_1(t) \end{aligned}$$

Theorem 4.6

For any diagonal matrix $\hat{A} > 0$ and $\hat{\boldsymbol{\mathcal{U}}}_{nom} = \mathfrak{M}_{\hat{A}}$, the decentralised operator

$$\mathbb{P}_1^{\hat{A}} : \hat{\boldsymbol{u}} \mapsto \begin{bmatrix} \boldsymbol{u} \\ [\boldsymbol{\xi}_1] \end{bmatrix} \quad \textit{(Precompensator 1)}$$

satisfies Definition 4.1.

Furthermore, for any $T > 0$ and any $i \in \{1, 2, \cdots, n_u\}$

- *If $\hat{u}_i \in \mathcal{L}_{\infty e}$ then $\|\Pi_T u_i\|_\infty \leq \|\Pi_T \hat{u}_i\|_\infty$*
- *If $\hat{u}_i \in \mathcal{L}_{2e}$ then $\|\Pi_T(\hat{u}_i - u_i)\|_2 \leq \|\Pi_T \hat{u}_i\|_2$*

PROOF OF THEOREM 4.6:

It is clear from the definition of $\mathbf{Sat}(.)$ that conditions P0, P1 and P2 in Definition 4.1 are satisfied.

That $|u_i(t)| \leq |\hat{u}_i(t)|$ for each $i \in \{1, 2, \cdots, n_u\}$ and any time $t \geq 0$ is immediate, and since, by Equation 2.18

$$\hat{\boldsymbol{u}}(t) - \boldsymbol{u}(t) = \mathbf{Dzn}_{\hat{A}}\big(\hat{\boldsymbol{u}}(t)\big)$$

it is also true that $|\hat{u}_i(t) - u_i(t)| \leq |\hat{u}_i(t)|$ for each $i \in \{1, 2, \cdots, n_u\}$ and any time $t \geq 0$. Hence the two inequalities follow immediately. ∎

Precompensator 1 is simple and suitable for both implementation and analysis, and the feedback signal $\boldsymbol{\xi}_1$ provides the only possibly useful internal information. Furthermore, the behaviour of this operator is reasonable for $\hat{\boldsymbol{u}} \notin \hat{\boldsymbol{\mathcal{U}}}_{\text{nom}}$: note that the $\mathcal{L}_\infty$-$\mathcal{L}_\infty$ and $\mathcal{L}_2$-$\mathcal{L}_2$ norm bounds in Theorem 4.6 show that the output does not become arbitrarily larger than the input.

Hence we claim that Precompensator 1 provides appropriate precompensation for an actuator with magnitude limitation $\boldsymbol{\mathcal{U}}_{\text{nom}} = \mathfrak{M}_A$ and unity nominal dynamics $P_{\text{act}}(s) = I$, provided that the "matching condition" in Equation 4.11 is satisfied.

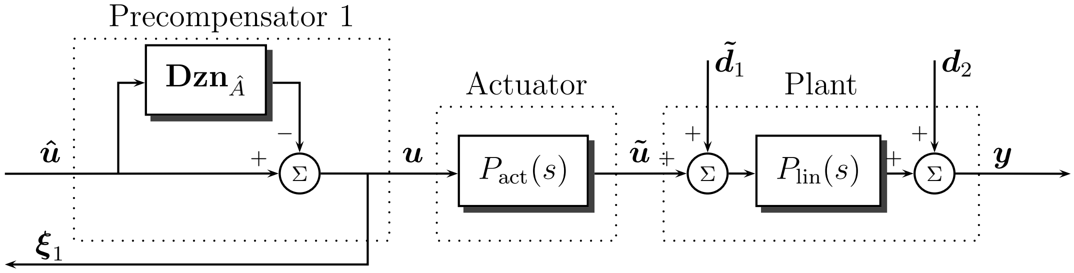

Figure 4.7: Precompensator 1, magnitude-limited actuator and linear plant

One useful consequence of Theorem 4.6 is that the series composition of Precompensator 1, magnitude-limited actuator and linear plant may be represented as shown in Figure 4.7, ie that the behaviour of the actuator can be considered to be *linear and time-invariant.*

Actuator with first-order nominal dynamics $P_{\text{act}}(s) = \text{Diag}\{\frac{c_i}{s+c_i}\}$

We now consider the simplest non-trivial nominal dynamic model - a first-order lag. We assume that

$$P_{\text{act}}(s) = \text{Diag}\{\tfrac{c_1}{s+c_1}, \tfrac{c_2}{s+c_2}, \cdots, \tfrac{c_{n_u}}{s+c_{n_u}}\}$$

for some $c_1, c_2, \cdots, c_{n_u} > 0$, and hence we see that the *nominal input space* is given by $\boldsymbol{\mathcal{U}}_{\text{nom}} = \mathfrak{M}^{\mathbf{1}}{}_{A,C}$, where $C = \text{Diag}\{c_1, c_2, \cdots, c_{n_u}\}$.

Now, by Lemma 4.3, if $\hat{A} > 0$ is a diagonal matrix satisfying Equation 4.11 then $\mathfrak{M}_{\hat{A}} \subseteq \mathfrak{M}^{\mathbf{1}}{}_{A,C}$. So, one possibility is to take $\hat{\boldsymbol{\mathcal{U}}}_{\text{nom}} = \mathfrak{M}_{\hat{A}}$ as our estimate of $\boldsymbol{\mathcal{U}}_{\text{nom}}$.

But this is precisely the same space $\hat{\boldsymbol{\mathcal{U}}}_{\text{nom}}$ for which we designed Precompensator 1! It may be thought that this solves our problem, since we already know that Precompensator 1 is appropriate for $\hat{\boldsymbol{\mathcal{U}}}_{\text{nom}} = \mathfrak{M}_{\hat{A}}$.

However, we have neglected the fact that $\mathfrak{M}_{\hat{A}}$ is a *strict* subset of $\mathfrak{M}^{\mathbf{1}}{}_{A,C}$. What this means is that there may be some conservatism due the fact that Precompensator 1 will modify some signals which would not actually violate the magnitude constraint.

We illustrate this conservatism with a simple scalar example:

Example

1. Assume that $\hat{a} = a$ and $\hat{c} = c$ (ie that the parameters of the actuator are known exactly), and let $\hat{u}$ be given by (Figure 4.8 (a), dotted line)

$$\hat{u}(t) = \begin{cases} at + \frac{a}{c} & \text{for } t < 1 \\ a & \text{for } t \geq 1 \end{cases}$$

In this case $u \neq \hat{u}$ is given by (Figure 4.8 (a), solid line)

$$u(t) = \begin{cases} at + \frac{a}{c} & \text{for } t < \min\{0, 1 - \frac{1}{c}\} \\ a & \text{for } t \geq \min\{0, 1 - \frac{1}{c}\} \end{cases}$$

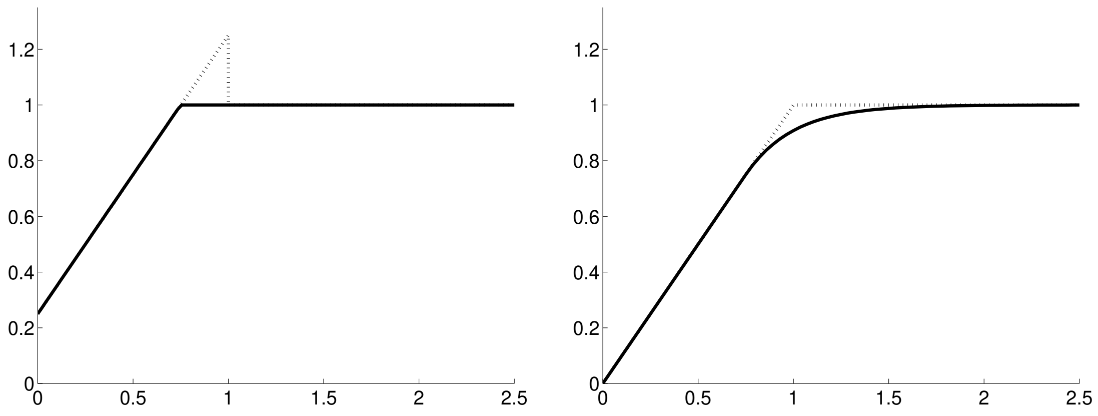

(a) $\hat{u}$ (dotted) and u (solid) (b) $\frac{c}{s+c}\hat{u}$ (dotted) and $\frac{c}{s+c}u$ (solid)

Figure 4.8: Example responses for $\boldsymbol{\mathcal{U}}_{\text{nom}} = \mathfrak{M}^1_{a,c}$ and Precompensator 1

Figure 4.8 (b) then shows $\frac{c}{s+c}\hat{u}$ and $\frac{c}{s+c}u$ as dotted and solid lines respectively. We observe from Figure 4.8 (b) that $\frac{c}{s+c}\hat{u}$ does not violate the magnitude constraint, and hence conclude that the precompensator is being overly conservative.

In an attempt to reduce this conservatism, we return to Lemma 4.3 to see that if $\hat{A}, \hat{C} > 0$ are diagonal matrices such that

$$A\hat{A}^{-1} \geq I \quad \text{and} \quad A\hat{A}^{-1} \geq 2C\hat{C}^{-1} - I$$

then $\boldsymbol{\mathfrak{M}^1}_{\hat{A},\hat{C}} \subseteq \boldsymbol{\mathfrak{M}^1}_{A,C}$. So, a second possibility is to take $\hat{\boldsymbol{\mathcal{U}}}_{\text{nom}} = \boldsymbol{\mathfrak{M}^1}_{\hat{A},\hat{C}}$ as our estimate of $\boldsymbol{\mathcal{U}}_{\text{nom}}$. Moreover, recall that a signal $\boldsymbol{v} \in \boldsymbol{\mathfrak{M}^1}_{\hat{A},\hat{C}}$ may be obtained as

$$\boldsymbol{v} = \boldsymbol{x} + \hat{C}^{-1}\frac{d\boldsymbol{x}}{dt}$$

for some right-differentiable $\boldsymbol{x} \in \boldsymbol{\mathfrak{M}}_{\hat{A}}$.

Based on this decomposition of elements of $\mathfrak{M}^{\mathbf{1}}{}_{\hat{A},\hat{C}}$, we might propose the following precompensator for $\hat{\boldsymbol{\mathcal{U}}}_{\text{nom}} = \mathfrak{M}^{\mathbf{1}}{}_{\hat{A},\hat{C}}$:

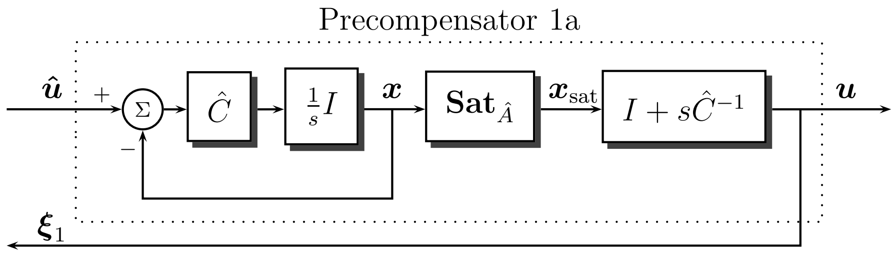

Figure 4.9: Precompensator 1a

Precompensator 1a (for $\hat{\boldsymbol{\mathcal{U}}}_{\mathbf{nom}} = \mathfrak{M}^{\mathbf{1}}{}_{\hat{A},\hat{C}}$)

Given diagonal matrices $\hat{A}, \hat{C} > 0$, let $\mathbb{P}_{1a}^{\hat{A},\hat{C}} : \hat{\boldsymbol{u}} \mapsto \begin{bmatrix} \boldsymbol{u} \\ [\boldsymbol{\xi}_1] \end{bmatrix}$ be defined by

$$\begin{aligned} \frac{d\boldsymbol{x}}{dt} &= \hat{C}\big(\hat{\boldsymbol{u}}(t) - \boldsymbol{x}(t)\big); \quad \boldsymbol{x}(0) = 0 \\ \boldsymbol{x}_{sat}(t) &= \mathbf{Sat}_{\hat{A}}\big(\boldsymbol{x}(t)\big) \\ \boldsymbol{\xi}_1(t) &= \boldsymbol{x}_{sat}(t) + \hat{C}^{-1}\tfrac{d\boldsymbol{x}_{sat}}{dt} \\ \boldsymbol{u}(t) &= \boldsymbol{\xi}_1(t) \end{aligned}$$

Precompensator 1a is quite simple, easily implementable (despite the differentiator) and amenable to analysis, and it imposes the required constraints on $\hat{\boldsymbol{u}}$. However the operator behaves in an unreasonable way, exhibiting "wind-up", in the sense that $\boldsymbol{x}(t)$ can become very large, preventing $\hat{\boldsymbol{u}}$ from correctly following $\boldsymbol{u}$. We illustrate this with a scalar example:

Example

1a. Assume that $\hat{a} = a$ and $\hat{c} = c$ (ie that the parameters of the actuator are known exactly), and let $\hat{u}$ be given by (Figure 4.10 (a), dotted line)

$$\hat{u}(t) = \begin{cases} at + \frac{a}{c} & \text{for } t < T \\ 0 & \text{for } t \geq T \end{cases}$$

for some $T \gg 1$. In this case u is given by (Figure 4.10 (a), solid line)

$$u(t) = \begin{cases} at + \frac{a}{c} & \text{for } t < 1 \\ a & \text{for } 1 \leq t < T + \frac{1}{c}\log(T) \\ 0 & \text{for } t \geq T + \frac{1}{c}\log(T) \end{cases}$$

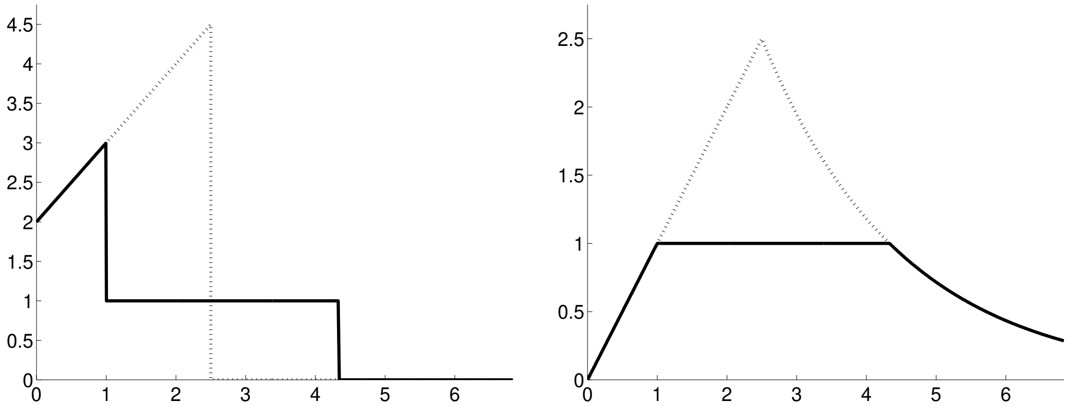

(a) $\hat{u}$ (dotted) and u (solid)

(b) $\frac{c}{s+c}\hat{u}$ (dotted) and $\frac{c}{s+c}u$ (solid)

Figure 4.10: Example responses for $\boldsymbol{\mathcal{U}}_{\text{nom}} = \mathfrak{M}^1_{a,c}$ and Precompensator 1a

Figure 4.10 (b) then shows $\frac{c}{s+c}\hat{u}$ $(= x)$ and $\frac{c}{s+c}u$ $(= x_{\text{sat}})$ as dotted and solid lines respectively. We observe from Figure 4.10 (a) that u continues to drive the actuator for a significant time after $\hat{u}$ has dropped to zero — this is due to x "winding up".

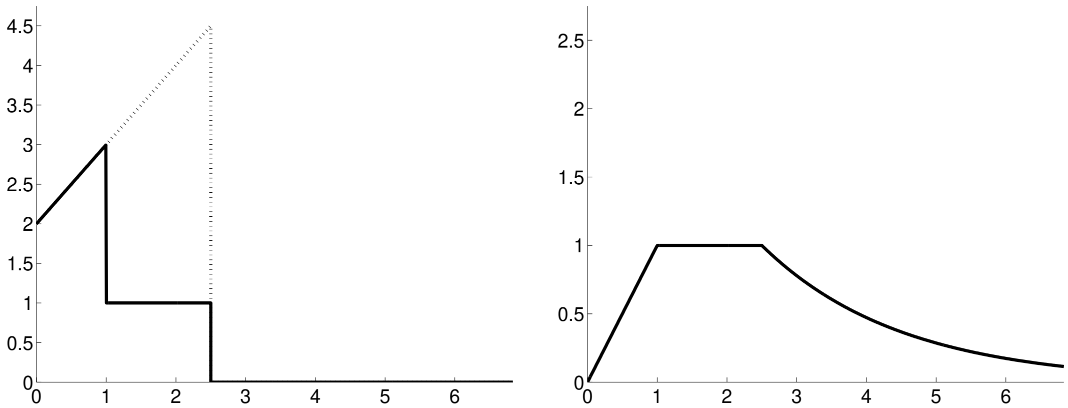

(a) $\hat{u}$ (dotted) and desirable u (solid)

(b) Desirable $\frac{c}{s+c}u$

Figure 4.11: Desirable responses for $\boldsymbol{\mathcal{U}}_{\text{nom}} = \mathfrak{M}^1_{a,c}$

A much more desirable actuator input u is shown in Figure 4.11 (a), and the corresponding desirable $\frac{c}{s+c}u$ in Figure 4.11 (b). In this figure we observe that u drops to zero at the same time as $\hat{u}$, and hence the actuator output $(\frac{c}{s+c}u)$ comes out of saturation as soon as possible.

The reason for Precompensator 1a exhibiting "wind-up" is clear: although $|x_{\mathrm{sat}}(t)| \leq \hat{a}$ is enforced by the saturation function, it is not possible to restrict the growth of x. An alternative precompensator for $\hat{\mathcal{U}}_{\mathrm{nom}} = \mathfrak{M}^{\mathbf{1}}{}_{\hat{A},\hat{C}}$ which does not suffer from "windup" is given below:

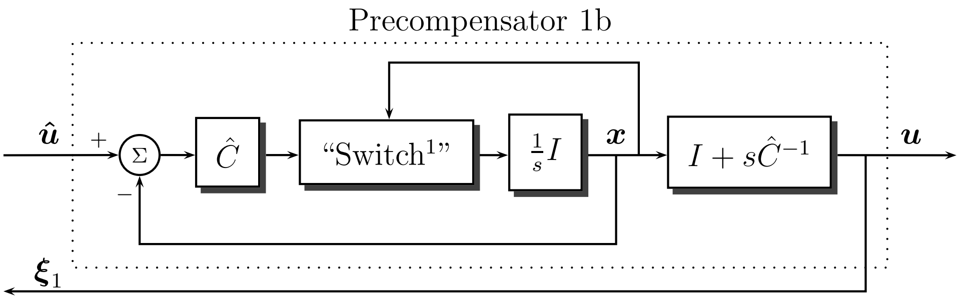

Figure 4.12: Precompensator 1b

Precompensator 1b (for $\hat{\mathcal{U}}_{\mathbf{nom}} = \mathfrak{M}^{\mathbf{1}}{}_{\hat{A},\hat{C}}$)

Given diagonal matrices $\hat{A}, \hat{C} > 0$, let $\mathbb{P}_{1b}^{\hat{A},\hat{C}} : \hat{\boldsymbol{u}} \mapsto \begin{bmatrix} \boldsymbol{u} \\ [\boldsymbol{\xi}_1] \end{bmatrix}$ be defined by

$$\frac{dx_i}{dt} = \begin{cases} 0 & \textit{if } x_i(t) \geq \hat{a}_i \textit{ and } \hat{u}_i(t) > x_i(t) \\ 0 & \textit{if } x_i(t) \leq -\hat{a}_i \textit{ and } \hat{u}_i(t) < x_i(t) \, ; \\ \hat{c}_i\big(\hat{u}_i(t) - x_i(t)\big) & \textit{otherwise} \end{cases} \quad x_i(0) = 0$$

$$\textit{for each } i \in \{1, 2, \cdots, u_n\}$$

$$\boldsymbol{\xi}_1(t) = \boldsymbol{x}(t) + \hat{C}^{-1}\tfrac{d\boldsymbol{x}}{dt}$$

$$\boldsymbol{u}(t) = \boldsymbol{\xi}_1(t)$$

Precompensator 1b is quite simple and implementable, it behaves in a reasonable manner, and it imposes the required constraints on $\boldsymbol{u}$. Moreover, it gives the "desirable" response of Figure 4.11 (a) and (b) for the same scalar input signal as previously, ie for

$$\hat{u}(t) = \begin{cases} at + \frac{a}{c} & \text{for } t < T \\ 0 & \text{for } t \geq T \end{cases}$$

One major drawback to this precompensator, however, is that it is not particularly amenable to analysis — in fact, it is not even clear that the operator $\mathbb{P}_{1b}^{\hat{A},\hat{C}}$ is well-posed, since the "switching" element introduces a non-Lipschitz nonlinearity into the feedback equations.

[1]As seen in the differential equations defining Precompensator 1b, this element stops integration in the ith channel whenever $|x_i(t)|$ is going to increase beyond $\hat{a}_i$: it is, in a way, a crude form of anti-windup.

After considering Precompensators 1a and 1b, we conclude that the conservatism due to using Precompensator 1 is probably an acceptable price to pay for simplicity and tractability. Hence we propose to use Precompensator 1 for the magnitude-limited actuator with first-order nominal dynamics, providing that the "matching condition" in Equation 4.11 is satisfied.

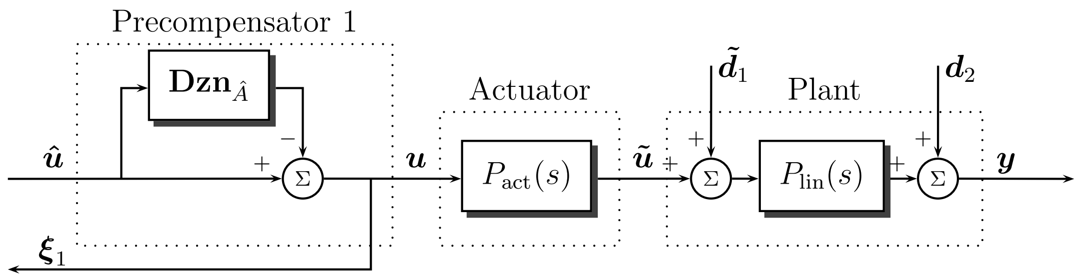

Figure 4.13: Precompensator 1, magnitude-limited actuator and linear plant

Moreover, we again see that the series composition of Precompensator 1, magnitude-limited actuator and linear plant may be represented as shown in Figure 4.13 (which is simply Figure 4.7 again), ie that the behaviour of the actuator can be considered to be *linear and time-invariant*. The nonlinear perturbation due to Precompensator 1 is again denoted by $\mathbf{Dzn}_{\hat{A}}$.

Actuator with *any* nominal dynamics $P_{\text{act}}(s)$

Finally, we consider the case of arbitrary $P_{\text{act}}(s)$. We make the mild assumption[2] that

$$P_{\text{act}}(s) = \text{Diag}\{p_1(s), p_2(s), \cdots, p_{n_u}(s)\}$$

with $\|p_i(s)\|_1 \leq 1$ for each $i \in \{1, 2, \cdots, n_u\}$.

Then, by Lemma 4.5, if $\hat{A} > 0$ is a diagonal matrix satisfying Equation 4.11

$$\mathfrak{M}_{\hat{A}} \subseteq \left\{ \boldsymbol{v} \in \mathcal{L}_{2e}^{n_u} : P_{\text{act}}\boldsymbol{v} \in \mathfrak{M}_A \right\}$$

which means that we can take $\hat{\boldsymbol{\mathcal{U}}}_{\text{nom}} = \mathfrak{M}_{\hat{A}}$ as our estimate of $\boldsymbol{\mathcal{U}}_{\text{nom}}$.

Hence we conclude that, subject to satisfying the "matching condition" in Equation 4.11, Precompensator 1 provides appropriate precompensation for *any* magnitude-limited actuator, although there may be some — possibly significant — conservatism (in the sense discussed previously in the first-order case)

Moreover, we again see that the series composition of Precompensator 1, magnitude-limited actuator and linear plant may be represented as shown in Figure 4.13, ie that the behaviour of the actuator can be considered to be *linear and time-invariant*.

[2]This assumption may often be trivially satisfied by transferring gain from the actuator to the plant or controller.

4.3.2 Rate-limited actuator

Another common limitation is that of a rate constraint, for example that a hydraulic ram has a maximum (instantaneous) velocity. More rigorously, this means that the actuator output $\tilde{\boldsymbol{u}}(t)$ should be right-differentiable, with derivative in some range. Without loss of generality we shall assume that the allowable range for the ith input channel is symmetrical about zero, ie $[-b_i, b_i]$, for some $b_i > 0$.

The *output constraint space* for an actuator with rate limitation is then seen to be given by $\boldsymbol{\mathcal{U}}_{\text{act}} = \mathfrak{R}_B$, where $B = \text{Diag}\{b_1, b_2, \cdots, b_{n_u}\}$.

Actuator with unity nominal dynamics $P_{\text{act}}(s) = I$

We consider first the case of a static actuator with no dynamics, and without loss of generality we assume that $P_{\text{act}}(s) = I$. Hence we see that the *nominal input space* is given by $\boldsymbol{\mathcal{U}}_{\text{nom}} = \boldsymbol{\mathcal{U}}_{\text{act}} = \mathfrak{R}_B$.

Now, by Lemma 4.2, if $\hat{B} > 0$ is a diagonal matrix such that

$$B\hat{B}^{-1} \geq I \tag{4.12}$$

then $\mathfrak{R}_{\hat{B}} \subseteq \mathfrak{R}_B$. So, we propose to take $\hat{\boldsymbol{\mathcal{U}}}_{\text{nom}} = \mathfrak{R}_{\hat{B}}$ as our estimate of $\boldsymbol{\mathcal{U}}_{\text{nom}}$.

The following precompensator for $\hat{\boldsymbol{\mathcal{U}}}_{\text{nom}} = \mathfrak{R}_{\hat{B}}$ is based on a model of a rate-limiting actuator which has been widely studied:

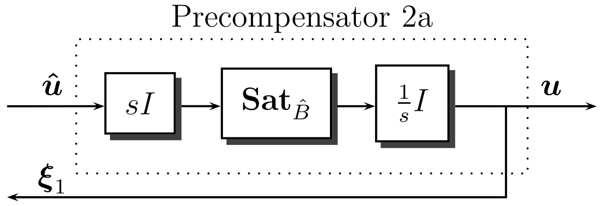

Figure 4.14: Precompensator 2a

Precompensator 2a (for $\hat{\boldsymbol{\mathcal{U}}}_{\text{nom}} = \mathfrak{R}_{\hat{B}}$)

Given a diagonal matrix $\hat{B} > 0$, let $\mathbb{P}_{2a}^{\hat{B}} : \hat{\boldsymbol{u}} \mapsto \begin{bmatrix} \boldsymbol{u} \\ [\boldsymbol{\xi}_1] \end{bmatrix}$ be defined by

$$\begin{aligned} \frac{d\boldsymbol{\xi}_1}{dt} &= \mathbf{Sat}_{\hat{B}}\Big(\frac{d\hat{\boldsymbol{u}}}{dt}\Big); \quad \boldsymbol{\xi}_1(0) = 0 \\ \boldsymbol{u}(t) &= \boldsymbol{\xi}_1(t) \end{aligned}$$

Precompensator 2a is quite simple and amenable to analysis (provided the input $\hat{\boldsymbol{u}}$ is right-differentiable), but it would be impossible to implement exactly due to the differentiation element.

Furthermore, although it *does* enforce the correct limitations on its output $\boldsymbol{u}$, it does not behave in a reasonable manner. For example, if there are regions of high gradient, then $\boldsymbol{u}$ completely fails to remain close to $\hat{\boldsymbol{u}}$, as the following scalar example demonstrates:

Example

2a. Assume that $\hat{b} = b$ (ie that the rate constraint is known exactly), and let $\hat{u}$ be given by a "sawtooth" (Figure 4.15 (a), dotted line)

$$\hat{u}(t) = \begin{cases} \hat{b}t & \text{for } t \in [0,1) \\ \hat{b} - (k-1)\hat{b}(t-1) & \text{for } t \in [1, 1+\frac{1}{k}) \\ \hat{b}(t-1) & \text{for } t \in [1+\frac{1}{k}, 2) \\ \hat{b} - (k-1)\hat{b}(t-2) & \text{for } t \in [2, 2+\frac{1}{k}) \\ \text{etc} & \end{cases}$$

for some $k \gg 1$. In this case u is given by (Figure 4.15 (a), solid line)

$$u(t) = \begin{cases} \hat{b}t & \text{for } t \in [0,1) \\ \hat{b} - \hat{b}(t-1) & \text{for } t \in [1, 1+\frac{1}{k}) \\ \hat{b}(1-\frac{2}{k}) + \hat{b}(t-1) & \text{for } t \in [1+\frac{1}{k}, 2) \\ \hat{b}(2-\frac{2}{k}) - \hat{b}(t-2) & \text{for } t \in [2, 2+\frac{1}{k}) \\ \text{etc} & \end{cases}$$

It is clear that u is quite unreasonable, since it continues to grow without bound, even though $|\hat{u}(t)| \leq 1$ for all t!

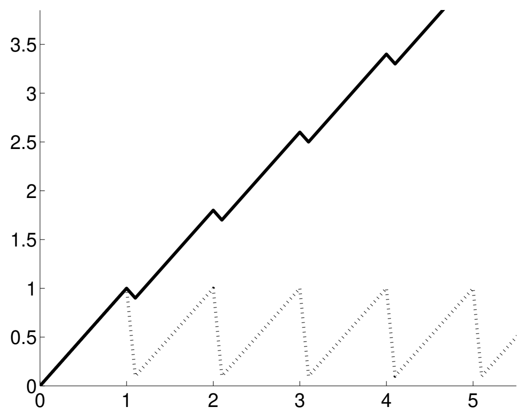

(a) $\hat{u}$ (dotted) and u (solid)

Figure 4.15: Example responses for $\hat{\boldsymbol{\mathcal{U}}}_{\text{nom}} = \mathfrak{R}_{\hat{B}}$ and Precompensator 2a

A much more desirable actuator input u is shown in Figure 4.16 (a): this signal remains close to $\hat{u}$ by converging at the maximum permitted rate whenever $u(t) \neq \hat{u}(t)$.

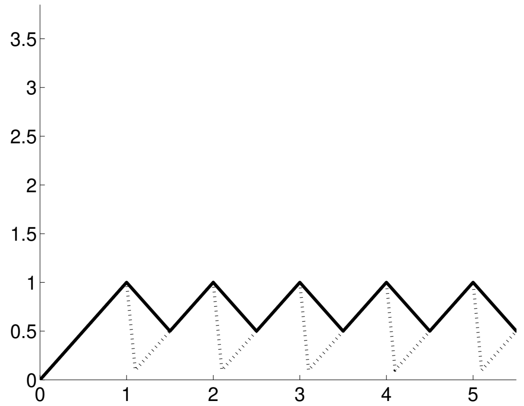

(a) $\hat{u}$ (dotted) and desirable u (solid)

Figure 4.16: Desirable responses for $\hat{\boldsymbol{\mathcal{U}}}_{\text{nom}} = \mathfrak{R}_{\hat{B}}$

The following alternative precompensator for $\hat{\boldsymbol{\mathcal{U}}}_{\text{nom}} = \mathfrak{R}_{\hat{B}}$ is modelled on an "ideal" rate-limiter:

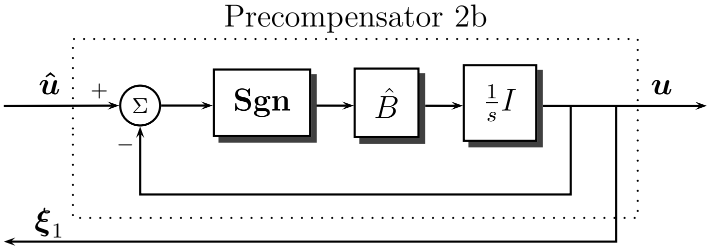

Figure 4.17: Precompensator 2b

Precompensator 2b (for $\hat{\boldsymbol{\mathcal{U}}}_{\text{nom}} = \mathfrak{R}_{\hat{B}}$)

Given a diagonal matrix $\hat{B} > 0$, let $\mathbb{P}_{2b}^{\hat{B}} : \hat{\boldsymbol{u}} \mapsto \begin{bmatrix} \boldsymbol{u} \\ [\boldsymbol{\xi}_1] \end{bmatrix}$ be defined by

$$\frac{d\boldsymbol{\xi}_1}{dt} = \hat{B}.\mathbf{Sgn}\big(\hat{\boldsymbol{u}}(t) - \boldsymbol{\xi}_1(t)\big); \quad \boldsymbol{\xi}_1(0) = 0$$
$$\boldsymbol{u}(t) = \boldsymbol{\xi}_1(t)$$

Precompensator 2b is quite simple, it imposes the required constraint on $\boldsymbol{u}$, and moreover it gives the "desirable" response of Figure 4.16 (a).

For implementation or analysis, however, the signum relation **Sgn** is not desirable.[3]

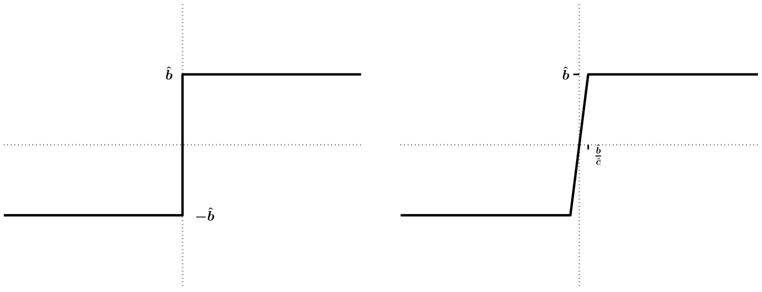

(a) $\hat{b}\,\mathrm{Sgn}(v)$ (b) $\mathrm{Sat}_{\hat{b}}(\hat{c}v)$

Figure 4.18: Signum relation and high-gain saturation function

Intuition suggests that this problem (and the associated problems of well-posedness and tractability) could be solved by approximating the signum relation with a high-gain saturation function, ie to change the feedback equation in the definition to

$$\frac{d\boldsymbol{\xi}_1}{dt} = \mathbf{Sat}_{\hat{B}}\Big(\hat{C}\big(\hat{\boldsymbol{u}}(t) - \boldsymbol{\xi}_1(t)\big)\Big)$$

with $\hat{c}_i \gg \hat{b}_i$ for each $i \in \{1, 2, \cdots, n_u\}$.

However, it is easily verified that this change results in

$$\hat{\boldsymbol{u}} \in \hat{\boldsymbol{\mathcal{U}}}_{\text{nom}} \quad \Longrightarrow \quad \boldsymbol{u} = \mathrm{Diag}\{\tfrac{c_i}{s+c_i}\}\hat{\boldsymbol{u}}$$

which does not satisfy Definition 4.1. This rules out using this approximation to Precompensator 2b directly.

We propose instead to consider the nominal dynamics as being first-order; note that this is a perfectly reasonable assumption in practice, since *all* real physical devices attenuate (sufficiently) high-frequency signals.

Moreover, it will become clear that the appropriate precompensator for a rate-limited actuator with first-order dynamics will be (in some sense) "close" to this approximation to Precompensator 2b, and hence also "close" to Precompensator 2b itself.

Actuator with first-order nominal dynamics $P_{\mathbf{act}}(s) = \mathrm{Diag}\{\frac{c_i}{s+c_i}\}$

We now consider the simplest non-trivial nominal dynamic model - a first-order lag. We assume that

$$P_{\text{act}}(s) = \mathrm{Diag}\{\tfrac{c_1}{s+c_1}, \tfrac{c_2}{s+c_2}, \cdots, \tfrac{c_{n_u}}{s+c_{n_u}}\}$$

for some $c_1, c_2, \cdots, c_{n_u} > 0$, and hence we see that the *nominal input space* is given by $\boldsymbol{\mathcal{U}}_{\text{nom}} = \mathfrak{R}^{\mathbf{1}}{}_{B,C}$, where $C = \mathrm{Diag}\{c_1, c_2, \cdots, c_{n_u}\}$.

[3]For example, if $\hat{\boldsymbol{u}} \in \hat{\boldsymbol{\mathcal{U}}}_{\text{nom}}$, then the solution ought to be $\boldsymbol{\xi}_1 = \boldsymbol{u} = \hat{\boldsymbol{u}}$ with $\hat{B}\mathbf{Sgn}(0) = \frac{d\hat{\boldsymbol{u}}}{dt}$ at each time instant — and it is not clear how one might implement this without prior knowledge of $\hat{\boldsymbol{u}}$.

Now, by Lemma 4.4, if $\hat{A} > 0$ is a diagonal matrix satisfying

$$\hat{A} \leq \tfrac{1}{2} B C^{-1}$$

then $\mathfrak{M}_{\hat{A}} \subseteq \mathfrak{R}^{\mathbf{1}}{}_{B,C}$. So, one possibility is to take $\hat{\boldsymbol{\mathcal{U}}}_{\text{nom}} = \mathfrak{M}_{\hat{A}}$ as our estimate of $\boldsymbol{\mathcal{U}}_{\text{nom}}$. This suggests once again that Precompensator 1 would be appropriate; this is, however, likely to be a very conservative choice.

Returning to Lemma 4.4, if $\hat{B}, \hat{C} > 0$ are diagonal matrices satisfying

$$B\hat{B}^{-1} \geq I \quad \text{and} \quad B\hat{B}^{-1} \geq 2C\hat{C}^{-1} - I \tag{4.13}$$

then $\mathfrak{R}^{\mathbf{1}}{}_{\hat{B},\hat{C}} \subseteq \mathfrak{R}^{\mathbf{1}}{}_{B,C}$. So, a second possibility is to take $\hat{\boldsymbol{\mathcal{U}}}_{\text{nom}} = \mathfrak{R}^{\mathbf{1}}{}_{\hat{B},\hat{C}}$ as our estimate of $\boldsymbol{\mathcal{U}}_{\text{nom}}$.

The following precompensator is based on a common model of a rate-limited actuator:

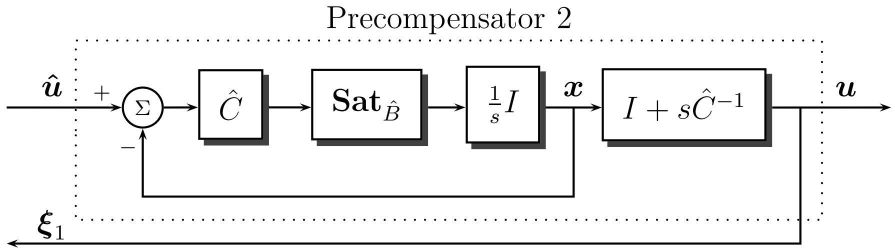

Figure 4.19: Precompensator 2

Precompensator 2 (for $\hat{\boldsymbol{\mathcal{U}}}_{\mathbf{nom}} = \mathfrak{R}^{\mathbf{1}}{}_{\hat{B},\hat{C}}$)

Given diagonal matrices $\hat{B}, \hat{C} > 0$, let $\mathbb{P}_2^{\hat{B},\hat{C}} : \hat{\boldsymbol{u}} \mapsto \begin{bmatrix} \boldsymbol{u} \\ [\boldsymbol{\xi}_1] \end{bmatrix}$ be defined by

$$\begin{aligned} \frac{d\boldsymbol{x}}{dt} &= \mathbf{Sat}_{\hat{B}}\Big(\hat{C}\big(\hat{\boldsymbol{u}}(t) - \boldsymbol{x}(t)\big)\Big); \quad \boldsymbol{x}(0) = 0 \\ \boldsymbol{\xi}_1(t) &= \boldsymbol{x}(t) + \hat{C}^{-1}\frac{d\boldsymbol{x}}{dt} \\ \boldsymbol{u}(t) &= \boldsymbol{\xi}_1(t) \end{aligned}$$

Note that if C is very large (ie $c_i \gg 1$ for each i), then Precompensator 2 is “similar” to Precompensator 2b, in the sense that

$$\begin{aligned} \mathbf{Sat}_{\hat{B}}\Big(\hat{C}\big(\hat{\boldsymbol{u}}(t) - \boldsymbol{x}(t)\big)\Big) &\approx \hat{B}.\mathbf{Sgn}\big(\hat{\boldsymbol{u}}(t) - \boldsymbol{x}(t)\big) \\ \text{and} \qquad I + s\hat{C}^{-1} &\approx I \end{aligned}$$

Theorem 4.7

For any diagonal matrices $\hat{B}, \hat{C} > 0$ and $\hat{\boldsymbol{\mathcal{U}}}_{nom} = \boldsymbol{\mathfrak{R}}^{\mathbf{1}}{}_{\hat{B},\hat{C}}$, the decentralised operator

$$\mathbb{P}_2^{\hat{B},\hat{C}} : \hat{\boldsymbol{u}} \mapsto \begin{bmatrix} \boldsymbol{u} \\ [\boldsymbol{\xi}_1] \end{bmatrix} \quad \textit{(Precompensator 2)}$$

satisfies Definition 4.1.

Furthermore, for any $T > 0$ and any $i \in \{1, 2, \cdots, n_u\}$

- *If $\hat{u}_i \in \mathcal{L}_{\infty e}$ then $\|\Pi_T u_i\|_\infty \leq \|\Pi_T \hat{u}_i\|_\infty$*
- *If $\hat{u}_i \in \mathcal{L}_{2e}$ then $\|\Pi_T(\hat{u}_i - u_i)\|_2 \leq (1 + \sqrt{2})\, \|\Pi_T \hat{u}_i\|_2$*

PROOF OF THEOREM 4.7:

The feedback loop is clearly well-posed, by Proposition 3.6, so condition P0 in Definition 4.1 is satisfied. Furthermore, since $\boldsymbol{x} \in \boldsymbol{\mathfrak{R}}_{\hat{B}}$, and using Lemma 4.4, $\boldsymbol{u} \in \mathfrak{R}^1_{\hat{B},\hat{C}}$, satisfying condition P1. Finally, if $\hat{\boldsymbol{u}} \in \mathfrak{R}^1_{\hat{B},\hat{C}}$ then a valid (and hence unique) solution $\boldsymbol{x} \in \boldsymbol{\mathfrak{R}}_{\hat{B}}$ to the differential equation would be given by

$$\boldsymbol{x} = \mathrm{Diag}\{\tfrac{c_i}{s+c_i}\}\hat{\boldsymbol{u}}$$

which satisfies the final condition in Definition 4.1.

For the $\mathcal{L}_\infty$-$\mathcal{L}_\infty$ norm inequality, assume that $\|\Pi_T \hat{u}_i\|_\infty = k_i$ for some $k_i > 0$. It is then immediate from the differential equations that

$$\begin{aligned} u_i(t_0) > k_i \quad &\Longrightarrow \tfrac{dx_i}{dt} < 0 \quad \text{and} \\ u_i(t_0) \geq k_i \quad &\Longrightarrow \tfrac{dx_i}{dt} \leq 0 \end{aligned}$$

By continuity of u_i, and the assumption that $u_i(0) = 0$, we conclude that $u_i(t) \leq k_i$ for all $t \in [0, T]$. A similar argument shows that $u_i(t) \geq -k_i$ for all $t \in [0, T]$.

For the $\mathcal{L}_2$-$\mathcal{L}_2$ norm inequality, it is shown by Megretski [Meg99] that for any $t_0 \in [0, T]$

$$\|\Pi_T u_i\|_2 \leq \sqrt{2}\, \|\Pi_T \hat{u}_i\|_2$$

for $\hat{u}_i \in \mathcal{L}_{2e}$, and hence the result follows by the triangle inequality. ∎

Precompensator 2 is simple, easily implementable (despite the differentiator) and amenable to analysis, and the feedback signal $\boldsymbol{\xi}_1$ is clearly sufficient to determine the current value of the only internal state ($\boldsymbol{x}$); furthermore, the behaviour of this operator is reasonable: note that the $\mathcal{L}_\infty$-$\mathcal{L}_\infty$ and $\mathcal{L}_2$-$\mathcal{L}_2$ norm bounds in Theorem 4.7 show that the output does not become arbitrarily larger than the input.

Hence we claim that Precompensator 2 provides appropriate precompensation for an actuator with rate limitation $\boldsymbol{\mathcal{U}}_{\text{nom}} = \mathfrak{R}_B$ and first-order nominal dynamics $P_{\text{act}}(s) = \text{Diag}\{\frac{c_i}{s+c_i}\}$, provided that the "matching condition" in Equation 4.13 is satisfied.

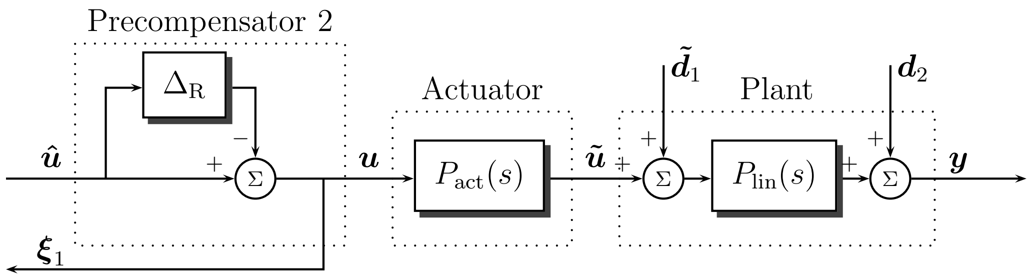

Figure 4.20: Precompensator 2, rate-limited actuator and linear plant

One useful consequence of Theorem 4.7 is that the series composition of Precompensator 2, magnitude-limited actuator and linear plant may be represented as shown in Figure 4.20, ie that the behaviour of the actuator can be considered to be *linear and time-invariant*. In this figure, the nonlinear perturbation due to Precompensator 2 is denoted by Δ_{R} (with $\|\Delta_{\text{R}}\| \leq 1 + \sqrt{2}$, by Theorem 4.7)

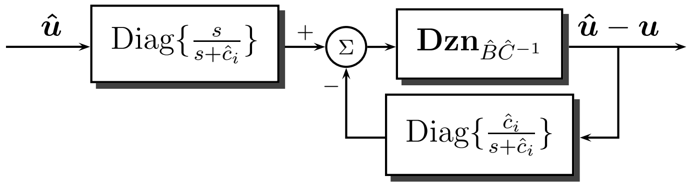

Figure 4.21: Alternative representation of Δ_{R}

Furthermore, the nonlinear perturbation Δ_{R} in Figure 4.20 may itself be represented in the form of a linear feedback around an ideal deadzone nonlinearity, as shown in Figure 4.21.

Actuator with other nominal dynamics

Finally, we demonstrate that Precompensator 2 is appropriate for rate-limited actuators with a wide, but not exhaustive, range of other nominal dynamics.

Specifically, we make the non-trivial assumption that, for some diagonal matrix $\hat{C} > 0$, the nominal dynamics $P_{\text{act}}(s)$ satisfy

$$\text{Diag}\{\tfrac{s+\hat{c}_i}{\hat{c}_i}\}P_{\text{act}}(s) = \text{Diag}\{q_1(s), q_2(s), \cdots, q_{n_u}(s)\}$$

with $\|q_i(s)\|_1 \leq 1$ for each $i \in \{1, 2, \cdots, n_u\}$. The interpretation of $\text{Diag}\{\frac{s+\hat{c}_i}{\hat{c}_i}\}P_{\text{act}}(s)$ is that it is the (nominal) transfer function relating $\text{Diag}\{\frac{\hat{c}_i}{s+\hat{c}_i}\}\boldsymbol{u}$ to $\tilde{\boldsymbol{u}}$.

This assumption means (by Lemma 4.5) that

$$\tfrac{d}{dt}\Big(\text{Diag}\{\tfrac{\hat{c}_i}{s+\hat{c}_i}\}\boldsymbol{u}\Big) \in \mathfrak{M}_{\hat{B}} \quad \Longrightarrow \quad \tfrac{d\tilde{\boldsymbol{u}}}{dt} \in \boldsymbol{\mathfrak{M}}_{\hat{B}}$$

which is equivalent to saying that $\boldsymbol{u} \in \boldsymbol{\mathfrak{R}^1}_{\hat{B},\hat{C}}$ implies $\tilde{\boldsymbol{u}} \in \boldsymbol{\mathfrak{R}}_{\hat{B}}$.

Hence we may take $\hat{\boldsymbol{\mathcal{U}}}_{\text{nom}} = \boldsymbol{\mathfrak{R}^1}_{\hat{B},\hat{C}}$ as our estimate of $\boldsymbol{\mathcal{U}}_{\text{nom}}$ for this actuator. This is precisely the nominal input space for which we designed Precompensator 2, and so we conclude that Precompensator 2 provides appropriate, although possibly quite conservative, precompensation for such a rate-limited actuator.

Moreover, we again see that the series composition of Precompensator 2, rate-limited actuator and linear plant may be represented as shown in Figure 4.20, ie that the behaviour of the actuator can be considered to be *linear and time-invariant*.

4.3.3 Rate- and magnitude-limited actuator

We are now in a position to consider an actuator subject to both magnitude and rate constraints. By direct comparison with Sections 4.3.1 and 4.3.2 we can state immediately that the output constraint space for an actuator with both rate- and magnitude-limitations is given by $\boldsymbol{\mathcal{U}}_{\text{act}} = \mathfrak{M}_A \cap \mathfrak{R}_B$ for some diagonal matrices $A, B > 0$ (which have the same interpretations as in Sections 4.3.1 and 4.3.2 respectively)

Actuator with unity nominal dynamics $P_{\textbf{act}}(s) = I$

In this case we see that $\boldsymbol{\mathcal{U}}_{\text{nom}} = \mathfrak{M}_A \cap \mathfrak{R}_B$.

Now, by Lemmas 4.1 and 4.2, if $\hat{A}, \hat{B} > 0$ are diagonal matrices such that

$$A\hat{A}^{-1} \geq I \quad \text{and} \quad B\hat{B}^{-1} \geq I$$

then $\mathfrak{M}_{\hat{A}} \subseteq \mathfrak{M}_A$ and $\mathfrak{R}_{\hat{B}} \subseteq \mathfrak{R}_B$. So, we may take $\hat{\boldsymbol{\mathcal{U}}}_{\text{nom}} = \mathfrak{M}_{\hat{A}} \cap \mathfrak{R}_{\hat{B}}$ as our estimate of $\boldsymbol{\mathcal{U}}_{\text{nom}}$.

But in the previous section we concluded that direct precompensation for $\hat{\boldsymbol{\mathcal{U}}}_{\text{nom}} = \mathfrak{R}_{\hat{B}}$ was not feasible, and that we should instead assume (with strong physical justification) that the nominal dynamics are given by a first-order lag. This case is considered below:

Actuator with first-order nominal dynamics $P_{\textbf{act}}(s) = \text{Diag}\{\frac{c_i}{s+c_i}\}$

In this case we see that $\boldsymbol{\mathcal{U}}_{\text{nom}} = \mathfrak{M}^{\mathbf{1}}{}_{A,C} \cap \mathfrak{R}^{\mathbf{1}}{}_{B,C}$

Now, by Lemmas 4.3 and 4.4, if $\hat{A} > 0$ is a diagonal matrix satisfying

$$A\hat{A}^{-1} \geq I \quad \text{and} \quad \hat{A} \leq \tfrac{1}{2}BC^{-1}$$

then $\mathfrak{M}_{\hat{A}}$ would be a subset of both $\mathfrak{M}^{\mathbf{1}}{}_{A,C}$ and $\mathfrak{R}^{\mathbf{1}}{}_{B,C}$. So, one possibility is to take $\hat{\boldsymbol{\mathcal{U}}}_{\text{nom}} = \mathfrak{M}_{\hat{A}}$ as our estimate of $\boldsymbol{\mathcal{U}}_{\text{nom}}$.

This means, yet again, that Precompensator 1 would be appropriate, and moreover, if $A = \hat{A}$ (ie the magnitude constraint is known exactly), there would be **no** conservatism.[4] This method of precompensation is to be recommended whenever the magnitude constraint is significantly more restrictive than the rate constraint.

If $c_i \gg 1$, then this method would not be appropriate ($\hat{A}$ would have to be extremely small, and hence the precompensator would be unnecessarily conservative.)

We return to Lemmas 4.3 and 4.4: if $\hat{A}, \hat{B}, \hat{C} > 0$ are diagonal matrices such that

$$A\hat{A}^{-1} \geq I \quad \text{and} \quad B\hat{B}^{-1} \geq I \quad \text{and} \quad B\hat{B}^{-1} \geq 2C\hat{C}^{-1} - I \tag{4.14}$$

then $\mathfrak{M}_{\hat{A}} \subseteq \mathfrak{M}^{\mathbf{1}}{}_{A,C}$ and $\mathfrak{R}^{\mathbf{1}}{}_{\hat{B},\hat{C}} \subseteq \mathfrak{R}^{\mathbf{1}}{}_{B,C}$. So, we conclude that a second possibility is to take $\hat{\boldsymbol{\mathcal{U}}}_{\text{nom}} = \mathfrak{M}_{\hat{A}} \cap \mathfrak{R}^{\mathbf{1}}{}_{\hat{B},\hat{C}}$ as our estimate of $\boldsymbol{\mathcal{U}}_{\text{nom}}$.

This suggests that a series composition of Precompensators 1 and 2 would be appropriate — we must, however, be careful to ensure that the series composition imposes *both* constraints simultaneously.

[4] This is because $\|u_i\|_\infty \leq a$ implies immediately that $\left\| \frac{d}{dt}(\frac{c_i}{s+c_i}u_i) \right\|_\infty \leq a$

We propose to put Precompensator 1 first, followed by Precompensator 2 (and note that, as mentioned in the preamble to this chapter, the anti-windup methods of both Kapila *et al* [KH98], [KPdQ99] and Hui & Chan [HC99] implement the converse scheme, with the saturation after the rate-limiter):

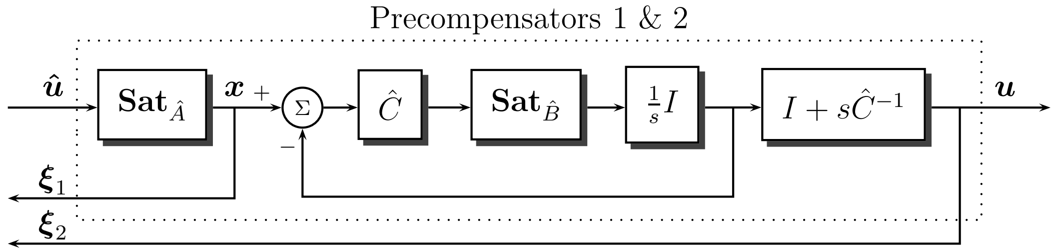

Figure 4.22: Precompensators 1 & 2

Precompensators 1 & 2 (for $\hat{\mathcal{U}}_{\mathbf{nom}} = \mathfrak{M}_{\hat{A}} \cap \mathfrak{R}_{\hat{B},\hat{C}}$)

Given diagonal matrices $\hat{A}, \hat{B}, \hat{C} > 0$ *, let* $\mathbb{P}_{1\&2}^{\hat{A},\hat{B},\hat{C}} : \hat{\boldsymbol{u}} \mapsto \begin{bmatrix} \boldsymbol{u} \\ \begin{bmatrix} \boldsymbol{\xi}_1 \\ \boldsymbol{\xi}_2 \end{bmatrix} \end{bmatrix}$ *be defined by*

$$\begin{bmatrix} \boldsymbol{x} \\ \boldsymbol{\xi}_1 \end{bmatrix} = \mathbb{P}_1^{\hat{A}}(\hat{\boldsymbol{u}}) \quad \textit{and} \quad \begin{bmatrix} \boldsymbol{u} \\ \boldsymbol{\xi}_2 \end{bmatrix} = \mathbb{P}_2^{\hat{B},\hat{C}}(\boldsymbol{x})$$

where $\mathbb{P}_1^{\hat{A}}$ *and* $\mathbb{P}_2^{\hat{B},\hat{C}}$ *are Precompensators 1 and 2 respectively.*

Theorem 4.8

For any diagonal matrices $\hat{A}, \hat{B}, \hat{C} > 0$ *and* $\hat{\mathcal{U}}_{nom} = \mathfrak{M}_{\hat{A}} \cap \mathfrak{R}^{\mathbf{1}}{}_{\hat{B},\hat{C}}$*, the decentralised operator*

$$\mathbb{P}_{1\&2}^{\hat{A},\hat{B},\hat{C}} : \hat{\boldsymbol{u}} \mapsto \begin{bmatrix} \boldsymbol{u} \\ \begin{bmatrix} \boldsymbol{\xi}_1 \\ \boldsymbol{\xi}_2 \end{bmatrix} \end{bmatrix} \qquad \textit{(Precompensators 1 \& 2)}$$

satisfies Definition 4.1.

Furthermore, for any $T > 0$ *and any* $i \in \{1, 2, \cdots, n_u\}$

- *if* $\hat{u}_i \in \mathcal{L}_{\infty e}$ *then* $\|\Pi_T u_i\|_\infty \leq \|\Pi_T \hat{u}_i\|_\infty$
- *if* $\hat{u}_i \in \mathcal{L}_{2e}$ *then*

$$\|\Pi_T(\hat{u}_i - [\xi_1]_i)\|_2 \leq \|\Pi_T \hat{u}_i\|_2$$
$$\|\Pi_T([\xi_1]_i - [\xi_2]_i)\|_2 \leq (1 + \sqrt{2})\, \|\Pi_T [\xi_1]_i\|_2$$

where $[\xi_1]_i$ *denotes the ith element of* ξ_1*, and similar for* ξ_2*.*

PROOF OF THEOREM 4.8:
Immediate from Theorems 4.6 and 4.7, noting in particular that for each $i \in \{1, 2, \cdots, n_u\}$ and $T > 0$

$$\|\Pi_T u_i\|_\infty \leq \|\Pi_T x_i\|_\infty$$

and hence, since $\boldsymbol{u}$ can be seen to be actually (rather than essentially) bounded, we conclude that $\boldsymbol{x} \in \mathfrak{M}_{\hat{A}} \Longrightarrow \boldsymbol{u} \in \mathfrak{M}_{\hat{A}}$. ∎

This composition of Precompensators 1 & 2 is clearly suitable (since both of its components are), and hence we claim that this series composition provides appropriate precompensation for an actuator with simultaneous rate and magnitude limitations, and first-order nominal dynamics $P_{\text{act}}(s) = \text{Diag}\{\frac{c_i}{s+c_i}\}$, provided that the "matching conditions" in Equation 4.14 are satisfied.

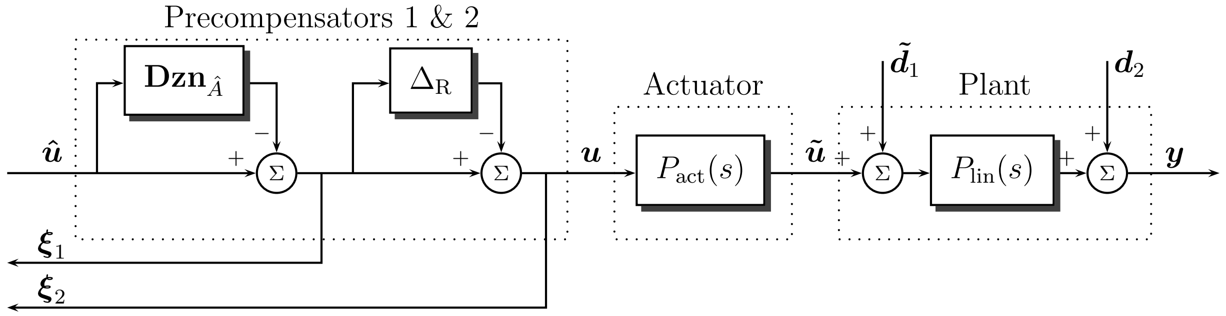

Figure 4.23: Precompensators 1 & 2 , rate- & magnitude-limited actuator and linear plant

One useful consequence of Theorem 4.8 is that the series composition of Precompensators 1 & 2, rate- & magnitude-limited actuator and linear plant may be represented as shown in Figure 4.23, ie that the behaviour of the actuator can be considered to be *linear and time-invariant*. In this figure, the nonlinear perturbations due to Precompensators 1 and 2 are respectively denoted by $\mathbf{Dzn}_{\hat{A}}$ and Δ_{R} (with $\|\Delta_{\text{R}}\| \leq 1 + \sqrt{2}$, by Theorem 4.7)

Actuator with other nominal dynamics

Combining the results of Sections 4.3.1 and 4.3.2 for actuators with other nominal dynamics, we conclude that the series composition of Precompensators 1 & 2 (as described above) provides appropriate precompensation for an actuator with simultaneous rate and magnitude limitations, subject to two conditions on $P_{\text{act}}(s)$:

$$P_{\text{act}}(s) = \text{Diag}\{p_1(s), p_2(s), \cdots, p_{n_u}(s)\} \quad \text{and}$$
$$\text{Diag}\{\tfrac{s+\hat{c}_i}{\hat{c}_i}\}P_{\text{act}}(s) = \text{Diag}\{q_1(s), q_2(s), \cdots, q_{n_u}(s)\}$$

with $\|p_i(s)\|_1 \leq 1$ and $\|q_i(s)\|_1 \leq 1$ for each $i \in \{1, 2, \cdots, n_u\}$.
Moreover, the representation in Figure 4.23 is still valid in such a case.

4.4 Summary and suggestions for further work

4.4.1 Summary

In this chapter we have

- Stated a general method for modelling actuator nonlinearities.
- Introduced the concept of *precompensation*, to ensure that
  1. the real actuator limitations are always inactive,
  2. the nonlinearity is known exactly, and
  3. suitable feedback signals are available for anti-windup compensation.
- Derived appropriate models and precompensators for a number of common actuator nonlinearities.
- Shown how the resulting interconnection can be represented in the form of a nominal linear, time-invariant plant subject to an input-additive, $\mathcal{L}_2$-norm-bounded perturbation.

4.4.2 Suggestions for further work

Actuators with different dynamics or limitations on each channel

Throughout the preceeding sections, we have assumed that each channel of the actuator has similar properties, in the sense that if one channel has a magnitude limitation and does not have a rate limitation, then the other channels also have only a magnitude limitation. Similarly, if one channel has a first-order nominal dynamic, then all other channels have first-order dynamics.

In the general case, it is quite likely that different channels will have different types of limitation or dynamics; indeed it may be approriate to assume that some channels have *no* limitations.

We have chosen here not to present such cases in their full generality, for reasons of space and clarity. Nevertheless, it should be clear from this chapter that the general case may be obtained by using the appropriate precompensator for "blocks" of channels which share the same properties.

Limitations on higher derivatives

We conjecture that a limitation on the second (or higher) derivative may often be modelled by either a rate- or magnitude- limitation by transferring some dynamics to the plant $P_{\text{lin}}(s)$ or controller $C(s)$. In such cases, the work described will be applicable.

In other cases, which we expect to be rare, it should be possible to derive a suitable model and precompensator using similar methods to those proposed in this chapter.

Non-ideal saturation functions

In our models, we assumed that the actuator behaviour was linear around the origin (or operating point, in general); it would be quite reasonable to consider other behaviours, however some care must be taken when designing a precompensator for such actuators.

As mentioned in the preamble, some authors have considered quite general actuator nonlinearities, such as magnitude limitations which only satisfy Definition 2.2. Clearly it is impossible to precompensate for a whole family of such functions; clearly also (as discussed previously) it is often unreasonable to assume that one may measure the true plant input.

We conjecture that the appropriate action would be to assume an ideal saturation function and hence use Precompensator 1 as usual. The actuator must then be modelled as P_{act} plus some *unmeasured* nonlinear perturbation (hopefully with small $\mathcal{L}_2$-$\mathcal{L}_2$ gain); a "good" anti-windup compensator should be able to cope with such a perturbation.

Other forms of limitation

We have considered only limitations which apply independently to each channel (and also actuator dynamics which are decentralised) Moreover, we have assumed that the plant $P_{\mathrm{lin}}(s)$ comprises the majority of the dynamical behaviour, which rules out, for example, trying to cope with a limitation on the plant output $\boldsymbol{y}$.

It is not inconceivable that a future extension to this work could generalise to arbitrary limitations; care will have to be taken in the case of unstable dynamics, however, since it will be appreciated that our precompensators are, in a sense, an open-loop observer of certain signals within the system.

"Optimal" precompensation

It may be possible to pose the question of "how to design a precompensator" in the form of an optimisation problem (see, for example, the discussion on "optimal artificial nonlinearities" in Peng *et al* [PVHW98].)

For example, one could consider minimising

$$\sup_{\hat{\boldsymbol{u}} \in \mathcal{L}_{2e}^{nu}} \|\Pi_T(\boldsymbol{u} - \hat{\boldsymbol{u}})\|$$

where $\hat{\boldsymbol{u}}$ is the control demand, $\boldsymbol{u}$ is the actuator input, and the norm (or, in general, some cost function) is defined in an appropriate manner. With suitable consideration of, for example, errors in the actuator model, this could be a powerful methodology; whether it would perform better in practice remains to be seen.

Chapter 5

Anti-windup compensators

5.1 Introduction

5.1.1 Background and motivation

The phenomenon of "windup" is, in its simplest form, simply the observation that the signal received at the plant input differs from the signal produced by the control system. The term windup comes from the application in which this phenomenon was first noticed: a plant with an input saturation nonlinearity in combination with a controller containing integral action. Under some circumstances, it is observed that the controller output continues to grow (wind up) far beyond the level of the input limitation, and hence the actuator continues to apply maximum effort long after the need has passed.

Over the years a number of ad-hoc schemes were devised to counter this problem, with varying levels of success, but it is only recently (Kothare *et al* [KCMN94]) that a suitably general framework has been formulated in which to consider *all* useful anti-windup schemes. In recent years there has been a vibrant effort in the area of synthesising "optimal" anti-windup schemes to guarantee global (or semi-global) stability and optimise performance (in a variety of senses.)

We should point out that synthesis of anti-windup controllers / compensators is not far removed from the general problem of nonlinear control (with the obvious restriction to saturation or similar nonlinearities); the usual convention is that the term *anti-windup* refers to schemes which try to maintain the nominal linear behaviour (ie, in the absence of the nonlinearity) around some operating point.

Prior work on control of systems with actuator nonlinearities

The field of nonlinear control is wide and varied; here we only discuss papers which specifically consider problems motivated by actuator nonlinearities (such as saturation or rate-limits.) There are two major areas of research: the design of *controllers* where any control input is acceptable, and the design of *compensators* which maintain some nominal linear behaviour (in these cases a nominal LTI controller is specified *a priori*.)

- In the more general case the recent emphasis has been on *unstable* systems, where it is well known that global stability cannot be achieved with any linear or nonlinear control scheme. A number of authors (eg Kapila *et al* [KPdQ99]; Lin *et al* [LS93]; Pare *et al* [PHHB98] Hu *et al* [HL99]) have considered synthesising controllers which achieve so-called *semi-global* stability, in the sense that the system states converge to the origin for any initial conditions in some arbitrarily large set.

  A few authors have also considered rate limitations in this framework, such as Kapila *et al* [KH98], [KPdQ99]; Hui & Chan [HC99] and Lin *et al* [LB98], [Lin98], [Lin97].

This sort of work is extremely valuable in indicating the fundamental limitations governing the control of nonlinear systems, but we would claim that (in most cases) a physical system can be modelled well by linear, time-invariant differential equations around an operating point, and hence that the control engineer should use some of the well-established and powerful *linear* design tools to synthesise a nominal controller. This suggests the use of Anti-Windup compensation:

- The problem of synthesising a compensator to cope with actuator nonlinearities while matching some nominal LTI behaviour around the normal operating point has received a great deal of attention over the last few decades. The following representative papers give a good overview of the progress to date, from the initial recognition of "windup" as a problem in real-world PID control, to the current unified framework of Kothare *et al* :

  Aström & Rundqwist [AR89]; Hanus *et al* [HKH87]; Edwards & Postlethwaite [EP98]; Kothare *et al* [KCMN94]; Miyamoto & Vinnicombe [MV96b]; Park & Choi [PC95]; Peng *et al* [PVH96], [PVHW98]; Teel & Kapoor [TK97]; Weston & Postlethwaite [WP98]; Walgama & Sternby [WS90]; Zheng *et al* [ZKM94] and Saberi [SLT96]

In the remainder of this chapter we shall be considering only those anti-windup schemes which maintain the nominal linear behaviour if the nonlinearity is not activated.

Anti-windup problem formulation

Figure 5.1 shows a nominal tracking problem where the signals $\boldsymbol{y}_{\text{ref}}$, $\boldsymbol{u}_{\text{lin}}$, $\boldsymbol{y}_{\text{lin}}$ and $\boldsymbol{e}_{\text{lin}}$ are the reference signal, controller output, plant output measurement and error signal respectively. The plant and controller are assumed to be linear, time-invariant systems with transfer functions $P(s)$ and $C(s)$ respectively.

Perturbations due to such factors as plant uncertainty and measurement errors are modelled as disturbances $\boldsymbol{d}_1$ and $\boldsymbol{d}_2$ at the plant input and output respectively.

As previously stated, we assume that the nominal controller $C(s)$ is specified in advance, having been designed using some (unspecified) method to guarantee some (also unspecified) properties of this linear interconnection.

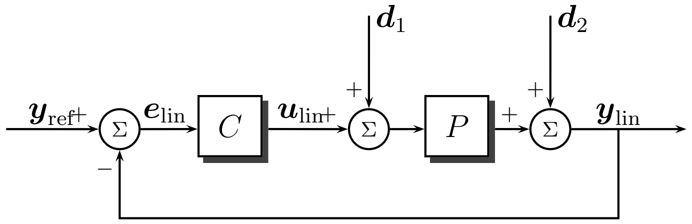

Figure 5.1: Nominal linear system

In particular, and as a minimum requirement, we assume that this nominal interconnection is internally stable. If we write the closed-loop relation for this system as

$$\begin{bmatrix} e_{\mathrm{lin}} \\ y_{\mathrm{lin}} \\ u_{\mathrm{lin}} \end{bmatrix} = \begin{bmatrix} S & -SP & -S \\ I-S & SP & S \\ CS & -CSP & -CS \end{bmatrix} \begin{bmatrix} y_{\mathrm{ref}} \\ d_1 \\ d_2 \end{bmatrix}$$

where $S := (I + PC)^{-1}$ is the sensitivity function, then internal stability is equivalent to each element in this transfer matrix being stable.

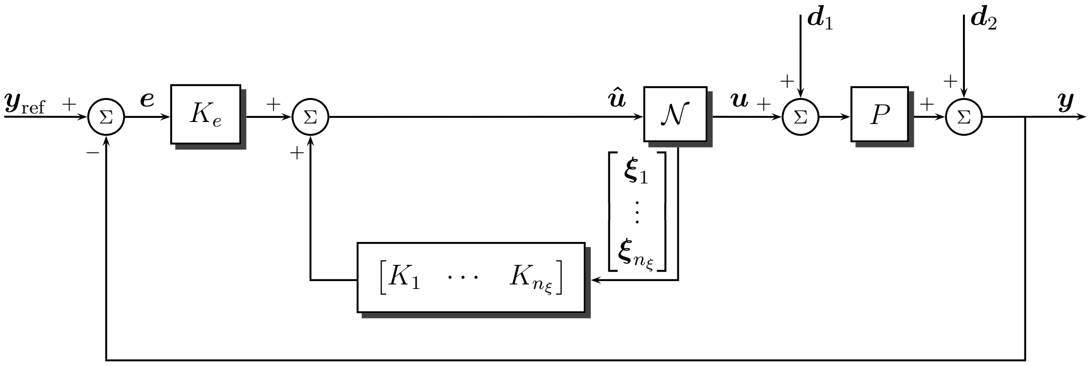

Figure 5.2: System with input nonlinearity

Figure 5.2 shows the tracking problem for the same plant $P(s)$, modified to take account of a nonlinearity $\mathcal{N}$ between the controller output and plant input. Here $\hat{u}$, u, y and e are the controller output, plant input, measured plant output and error signal respectively. We consider the *same* external signals y_{ref}, d_1 and d_2 as in Figure 5.1.

In this interconnection the nominal controller $C(s)$ has been replaced by a linear time-invariant controller $\begin{bmatrix} K_e & \begin{bmatrix} K_1 & \cdots & K_{n_\xi} \end{bmatrix} \end{bmatrix}$ which, in addition to the error signal $\boldsymbol{e}$, has access to one or more signals $\boldsymbol{\xi}_1, \cdots, \boldsymbol{\xi}_{n_\xi}$ (for some $n_\xi \geq 1$) from *within* the nonlinearity $\mathcal{N}$, so that the new controller output $\hat{\boldsymbol{u}}$ is given by

$$\hat{\boldsymbol{u}} = K_e \boldsymbol{e} + K_1 \boldsymbol{\xi}_1 + \cdots + K_{n_\xi} \boldsymbol{\xi}_{n_\xi}$$

We make the assumption that

- If $\boldsymbol{u} \equiv \hat{\boldsymbol{u}}$ then $\boldsymbol{\xi}_1 = \boldsymbol{\xi}_2 = \cdots = \boldsymbol{\xi}_{n_\xi} = \hat{\boldsymbol{u}}$

and recall that the precompensators which we proposed in Chapter 4 (cf Definition 4.1 and Figures 4.13, 4.20 and 4.23) were designed with this assumption in mind.

Parametrisation of anti-windup compensators

The purpose of the new controller $\begin{bmatrix} K_e & \begin{bmatrix} K_1 & \cdots & K_{n_\xi} \end{bmatrix} \end{bmatrix}$ is to mitigate the destabilising or performance-reducing effects of the nonlinearity $\mathcal{N}$, while ensuring that the nominal linear behaviour is recovered if the nonlinearity is not activated.

Rather than blindly searching over all possible $\begin{bmatrix} K_e & \begin{bmatrix} K_1 & \cdots & K_{n_\xi} \end{bmatrix} \end{bmatrix}$ until a suitable response is obtained, we propose to parametrise all "useful" anti-windup schemes, using a small number of simple parameters. Our parametrisation will have the following desirable features:

- The scheme will be simple and tractable
- The scheme will be implementable, and will not, for example, inherently cause internal instability (although, of course, it may not be possible to globally stabilise the resulting closed loop system)
- If $\boldsymbol{u} \equiv \hat{\boldsymbol{u}}$ in Figure 5.2 then the nominal linear behaviour of Figure 5.1 is recovered, ie

$$\begin{bmatrix} \boldsymbol{e} \\ \boldsymbol{y} \\ \hat{\boldsymbol{u}} \end{bmatrix} \equiv \begin{bmatrix} \boldsymbol{e}_{\text{lin}} \\ \boldsymbol{y}_{\text{lin}} \\ \boldsymbol{u}_{\text{lin}} \end{bmatrix} = \begin{bmatrix} S & -SP & -S \\ I-S & SP & S \\ CS & -CSP & -CS \end{bmatrix} \begin{bmatrix} \boldsymbol{y}_{\text{ref}} \\ \boldsymbol{d}_1 \\ \boldsymbol{d}_2 \end{bmatrix}$$

Synthesis of anti-windup compensators

The primary purpose of anti-windup is to ensure stability of the system in the face of actuator nonlinearity. This is formalised in the following problem statement:

Problem 5.1 (Anti-windup stabilisation problem)
Given a linear plant P, stabilising linear controller C and nonlinearity $\mathcal{N}$, to find an anti-windup controller $\begin{bmatrix} K_e & \begin{bmatrix} K_1 & K_2 & \cdots & K_{n_\xi} \end{bmatrix} \end{bmatrix}$ such that, for the interconnection of Figure 5.2

- *If $\boldsymbol{u} \equiv \hat{\boldsymbol{u}}$ then the nominal linear behaviour of Figure 5.1 is recovered, ie*

$$\begin{bmatrix} \boldsymbol{e} \\ \boldsymbol{y} \\ \hat{\boldsymbol{u}} \end{bmatrix} \equiv \begin{bmatrix} \boldsymbol{e}_{lin} \\ \boldsymbol{y}_{lin} \\ \boldsymbol{u}_{lin} \end{bmatrix} = \begin{bmatrix} S & -SP & -S \\ I-S & SP & S \\ CS & -CSP & -CS \end{bmatrix} \begin{bmatrix} \boldsymbol{y}_{ref} \\ \boldsymbol{d}_1 \\ \boldsymbol{d}_2 \end{bmatrix}$$

- $\boldsymbol{e}, \hat{\boldsymbol{u}}, \boldsymbol{u}, \boldsymbol{y} \in \mathcal{L}_2$ *for all* $\boldsymbol{y}_{ref}, \boldsymbol{d}_1, \boldsymbol{d}_2 \in \mathcal{L}_2$

Assuming that Problem 5.1 admits at least one solution, we may also wish to consider optimising a suitable performance measure.

If, however, Problem 5.1 may not be solved, we will consider the following local version of Problem 5.1:

Problem 5.2 (Local anti-windup stabilisation problem)
Given a linear plant P, stabilising linear controller C, nonlinearity $\mathcal{N}$ and sets $\mathcal{Z}_{\boldsymbol{y}_{ref}} \subseteq \mathcal{L}_2$, $\mathcal{Z}_{\boldsymbol{d}_1} \subseteq \mathcal{L}_2$ and $\mathcal{Z}_{\boldsymbol{d}_2} \subseteq \mathcal{L}_2$, to find an anti-windup controller $\begin{bmatrix} K_e & \begin{bmatrix} K_1 & K_2 & \cdots & K_{n_\xi} \end{bmatrix} \end{bmatrix}$ such that, for the interconnection of Figure 5.2

- *If $\boldsymbol{u} \equiv \hat{\boldsymbol{u}}$ then the nominal linear behaviour of Figure 5.1 is recovered, ie*

$$\begin{bmatrix} \boldsymbol{e} \\ \boldsymbol{y} \\ \hat{\boldsymbol{u}} \end{bmatrix} \equiv \begin{bmatrix} \boldsymbol{e}_{lin} \\ \boldsymbol{y}_{lin} \\ \boldsymbol{u}_{lin} \end{bmatrix} = \begin{bmatrix} S & -SP & -S \\ I-S & SP & S \\ CS & -CSP & -CS \end{bmatrix} \begin{bmatrix} \boldsymbol{y}_{ref} \\ \boldsymbol{d}_1 \\ \boldsymbol{d}_2 \end{bmatrix}$$

- $\boldsymbol{e}, \hat{\boldsymbol{u}}, \boldsymbol{u}, \boldsymbol{y} \in \mathcal{L}_2$ *for all* $\boldsymbol{y}_{ref} \in \mathcal{Z}_{\boldsymbol{y}_{ref}}$, $\boldsymbol{d}_1 \in \mathcal{Z}_{\boldsymbol{d}_1}$ *and* $\boldsymbol{d}_2 \in \mathcal{Z}_{\boldsymbol{d}_2}$

Remark

1. Note that in Problem 5.2 we assume that the disturbances at $\boldsymbol{d}_1$ and $\boldsymbol{d}_2$ are due to isolated external effects, and can no longer use these signals to represent persistent effects such as model uncertainty or systematic measurement errors.

As noted at the beginning of Chapter 1, our motivation for the local stability framework is that signals of bounded energy are suitable for modelling isolated disturbances. If we believe this to be the case, then it is not unreasonable to assume that only one disturbance occurs, at *either* $\boldsymbol{d}_1$ *or* $\boldsymbol{d}_2$ *or* $\boldsymbol{y}_{\mathrm{ref}}$, in a given period of time. Provided that the system is not destabilised by this disturbance, we may hope that the effect wears off before the next isolated disturbance occurs.

To determine the largest single disturbance on, say, $\boldsymbol{d}_1$ such that the system is not destabilised involves setting

$$\begin{aligned} \mathcal{Z}_{\boldsymbol{d}_1} &= \left\{\boldsymbol{z} : \|\boldsymbol{z}\|_2 \leq \varepsilon\right\} \\ \mathcal{Z}_{\boldsymbol{d}_2} &= \left\{\boldsymbol{z} : \boldsymbol{z} \equiv 0\right\} \quad \text{and} \\ \mathcal{Z}_{\boldsymbol{y}_{\mathrm{ref}}} &= \left\{\boldsymbol{z} : \boldsymbol{z} \equiv 0\right\} \end{aligned}$$

in Problem 5.2, and finding the largest ε such that the problem has a solution. The equivalent procedure can then be used for disturbances on $\boldsymbol{d}_2$ and $\boldsymbol{y}_{\mathrm{ref}}$.

Of course, there is no reason why one should not consider the combined effect of simultaneous disturbances on two or three of these external signals, but the results could well be overly conservative.

5.2 Parametrisation of anti-windup compensators

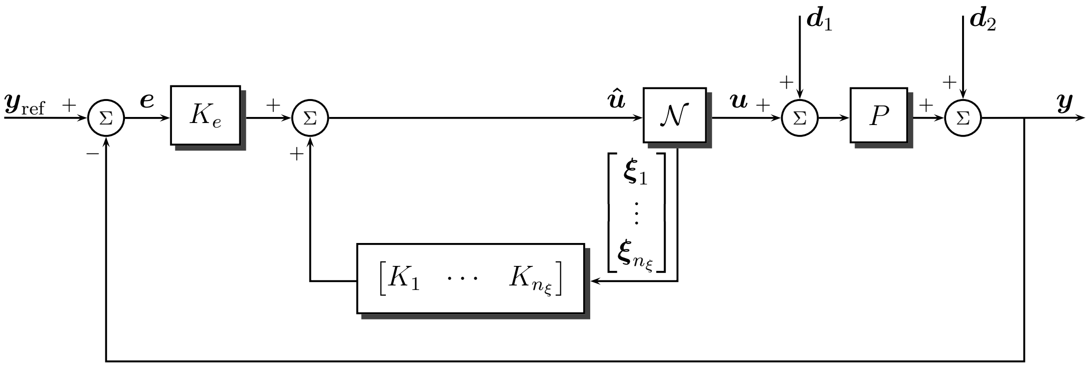

Figure 5.3: System with input nonlinearity

Figure 5.3 shows once again the nonlinear tracking problem, for some nonlinearity $\mathcal{N}$. In the following sections we propose a parametrisation of anti-windup compensation schemes, based on coprime factorisations of the plant $P(s)$ (or equivalently, as we shall show, of the nominal controller $C(s)$)

5.2.1 System with input saturation nonlinearity

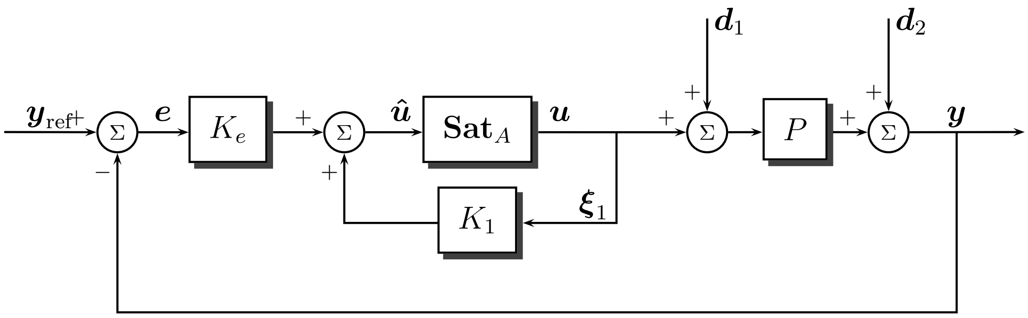

Figure 5.4: Anti-windup for saturation nonlinearity

The interconnection of Figure 5.2, in the case when the nonlinearity is given by an ideal saturation

$$u = \xi_1 = \mathbf{Sat}_{\hat{A}}(\hat{u})$$

is shown in Figure 5.4, where $\hat{A} = \text{diag}\{\hat{a}_1, \hat{a}_2, \cdots, \hat{a}_{n_u}\}$, $\hat{A} > 0$ indicates the saturation level for each channel. The anti-windup synthesis problem is then one of choosing $K_e(s)$ and $K_1(s)$.

This general framework has been shown to encompass many previously studied schemes, such as the following (see, for example, Kothare *et al* [KCMN94] for more details about these and other prior schemes):

- **no anti-windup:** $K_e = C$ and $K_1 = 0$
- **"conventional" scheme:** $K_e = (I + CC_F)^{-1}C$ and $K_1 = (I + CC_F)^{-1}CC_F$ where C_F is a tuning parameter
- **Hanus' conditioning scheme:** $K_e = C(\infty)$ and $K_1 = I - C(\infty)C^{-1}$ provided that C is biproper
- **Internal model (IMC) scheme:** $K_e = (I + CP)^{-1}C$ and $K_1 = (I + CP)^{-1}CP$ where it is assumed that P is stable

Coprime factor anti-windup parametrisation

A general framework, including almost all existing linear anti-windup schemes, has been proposed by Kothare *et al* [KCMN94] and elaborated upon by Miyamoto & Vinnicombe [MV96b]. These authors suggest that the controller should be given by

$$K_e(s) = \tilde{U}(s)$$
$$K_1(s) = I - \tilde{V}(s)$$

where $C = \tilde{V}^{-1}\tilde{U}$ is a left-coprime factorisation of C. In [KCMN94] the anti-windup controller was parametrised by all *fixed-order* coprime factors of C; it was later proposed in [MV96b] to use *all* coprime factors of C, which can be parametrised by

$$\begin{bmatrix}\tilde{V}(s) & \tilde{U}(s)\end{bmatrix} = Q(s)\begin{bmatrix}\tilde{V}_0(s) & \tilde{U}_0(s)\end{bmatrix}$$

with $Q \in \mathcal{Q}$ (Equation 2.5), where $C = \tilde{V}_0^{-1}\tilde{U}_0$ is any arbitrary left-coprime factorisation of C.

It is desirable, although not strictly essential, to have $\tilde{V}(\infty) = I$ so that there is not an algebraic loop in the controller implementation. If we choose initial left- and right-coprime factorisations $C = \tilde{V}_0^{-1}\tilde{U}_0$ and $P = N_0M_0^{-1}$ such that the following Bezout identity holds

$$\tilde{V}_0M_0 + \tilde{U}_0N_0 = I \tag{5.1}$$

and under the mild assumption that P is strictly proper, then this is equivalent to desiring that $M(\infty) = I$, ie that $Q(\infty) = M_0(\infty)$.

We now see that anti-windup synthesis can be interpreted as choosing a particular left-coprime factorisation of the linear controller

$$C = \tilde{V}^{-1}\tilde{U}; \quad \begin{bmatrix}\tilde{V}(s) & \tilde{U}(s)\end{bmatrix} = Q(s)\begin{bmatrix}\tilde{V}_0(s) & \tilde{U}_0(s)\end{bmatrix}$$

or a particular right-coprime factorisation of the linear plant

$$P = NM^{-1}; \quad \begin{bmatrix}M(s) \\ N(s)\end{bmatrix} = \begin{bmatrix}M_0(s) \\ N_0(s)\end{bmatrix}Q^{-1}(s)$$

or simply of choosing $Q \in \mathcal{Q}$ such that $Q(\infty) = M_0(\infty)$.

Closed-loop representation for stability and performance analysis

If we write the interconnection of Figure 5.4 with the saturation nonlinearity depicted as a perturbation from the identity, ie

$$\begin{aligned}\boldsymbol{u}(t) &= \mathbf{Sat}_{\hat{A}}\big(\hat{\boldsymbol{u}}(t)\big)\\ &= \hat{\boldsymbol{u}}(t) - \boldsymbol{\Delta}\big(\hat{\boldsymbol{u}}(t)\big)\end{aligned}$$

then it is clear that the perturbation $\boldsymbol{\Delta}$ is in fact an ideal deadzone $\mathbf{Dzn}_{\hat{A}}$.

With the given coprime factor anti-windup parametrisation, the interconnection can be represented as shown in Figure 5.5.

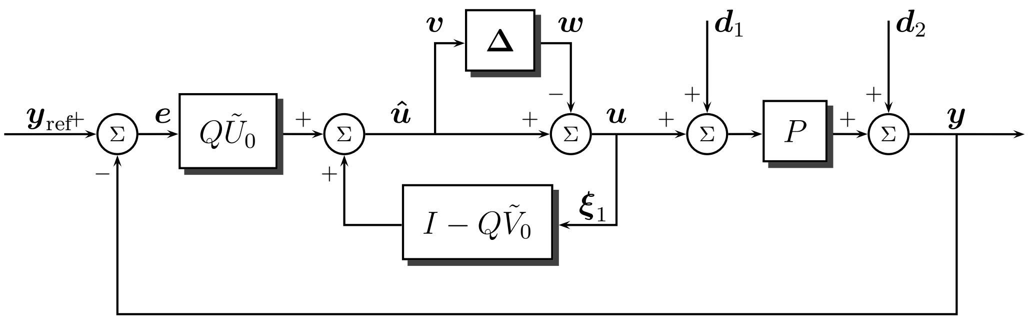

Figure 5.5: Alternative representation of Figure 5.4

Denote by $\boldsymbol{v}$ and $\boldsymbol{w}$ the signals at the input and output of the perturbation $\boldsymbol{\Delta}$. We can then express the interconnection with the following LFT on $\boldsymbol{\Delta}$

$$\begin{bmatrix}\begin{bmatrix}\boldsymbol{e}\\ \boldsymbol{y}\\ \boldsymbol{u}\end{bmatrix}\\ \boldsymbol{v}\end{bmatrix} = \begin{bmatrix}\begin{bmatrix}S & -SP & -S\\ I-S & SP & S\\ CS & -CSP & -CS\end{bmatrix} & \begin{bmatrix}N_0Q^{-1}\\ -N_0Q^{-1}\\ -M_0Q^{-1}\end{bmatrix}\\ \begin{bmatrix}CS & -CSP & -CS\end{bmatrix} & I - M_0Q^{-1}\end{bmatrix}\begin{bmatrix}\begin{bmatrix}\boldsymbol{y}_{\mathrm{ref}}\\ \boldsymbol{d}_1\\ \boldsymbol{d}_2\end{bmatrix}\\ \boldsymbol{w}\end{bmatrix}$$
$$\boldsymbol{w} = \boldsymbol{\Delta}\boldsymbol{v}$$

We see immediately that if $\boldsymbol{w} \equiv 0$, then the nominal linear behaviour of Figure 5.1 is recovered, as desired. Moreover, it is clear from Proposition 3.6 that the interconnection in Figure 5.5 (equivalently, the interconnection in Figure 5.4) is well-posed for any $Q \in \mathcal{Q}$ such that $Q(\infty) = M_0(\infty)$, since $\boldsymbol{\Delta}$ has finite uniform instantaneous gain and $(I - M_0Q^{-1}) \in \mathcal{RH}_2$.

Remarks

1. We can now see why $Q, Q^{-1} \in \mathcal{H}_\infty$ is a suitable restriction on the choice of Q:

   - If $Q \notin \mathcal{H}_\infty$, then (at least one of) $Q\tilde{V}_0$ and $Q\tilde{U}_0$ will be unstable, which is undesirable from the point-of-view of implementing the controller (this point has been made also by Miyamoto & Vinnicombe [MV96b] and Peng *et al* [PVHW98])

     Furthermore, allowing $Q \notin \mathcal{H}_\infty$ does not offer any improvement in the minimisation of either $\|M_0Q^{-1} - I\|_\infty$ or $\|M_0Q^{-1} - I\|_2$ (Miyamoto & Vinnicombe [MV96a] and Theorem 2.4 respectively), noting that both of these are reasonable synthesis objectives.

   - In contrast to the above, if P is *unstable*, then M_0 will be non-minimum-phase, and in this case allowing $Q^{-1} \notin \mathcal{H}_\infty$ *would* offer an improvement in the minimisation of $\|M_0Q^{-1} - I\|_\infty$. But it is well-known that for *unstable* P this closed-loop system **cannot** be stabilised in this manner.

     Furthermore, if $Q^{-1} \notin \mathcal{H}_\infty$ then (at least one of) M_0Q^{-1} and N_0Q^{-1} will be unstable and hence there will exist some arbitrarily small $\boldsymbol{w} \in \mathcal{L}_2$ such that either $\boldsymbol{y} \notin \mathcal{L}_2$ or $\boldsymbol{u} \notin \mathcal{L}_2$. Noting that it is possible to "back substitute" to find appropriate disturbances $\boldsymbol{d}_1$, $\boldsymbol{d}_2$ and $\boldsymbol{y}_{\text{ref}}$ which produce this $\boldsymbol{w}$, we conclude that $Q^{-1} \notin \mathcal{H}_\infty$ implies instability of the interconnection.

2. The four schemes mentioned earlier can often be considered as special cases of the coprime factor parametrisation:

   - **no anti-windup:** $Q = \tilde{V}_0^{-1}$
   - **"conventional" scheme:** $Q = (\tilde{V}_0 + \tilde{U}_0 C_F)^{-1}$
   - **Hanus' conditioning scheme:** $Q = C(\infty)\tilde{U}_0^{-1}$
   - **Internal model (IMC) scheme:** $Q = M_0$

   provided, of course, that in each case $Q \in \mathcal{Q}$. For example, the system with no anti-windup is a special case if C is stable, and the IMC scheme is a special case if P is stable.

5.2.2 System with a single input nonlinearity

A simple generalisation of the parametrisation for the input saturation case may be used whenever the nonlinearity $\mathcal{N}$ takes the form of the identity operator plus a single bounded perturbation

$$\boldsymbol{u} = \boldsymbol{\xi}_1 = (I - \Delta)\hat{\boldsymbol{u}}$$

where we assume that $\|\Delta\|$ is finite.

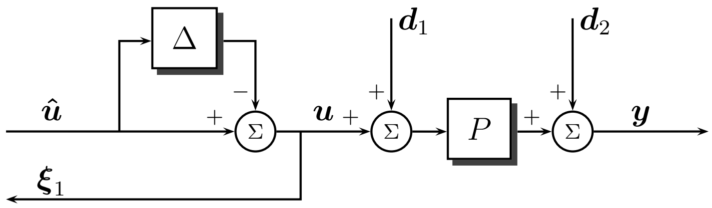

Figure 5.6: Single input nonlinearity

Figure 5.6 shows a nonlinearity of this form; the plant P and disturbances $\boldsymbol{d}_1$ and $\boldsymbol{d}_2$ are shown for clarity.

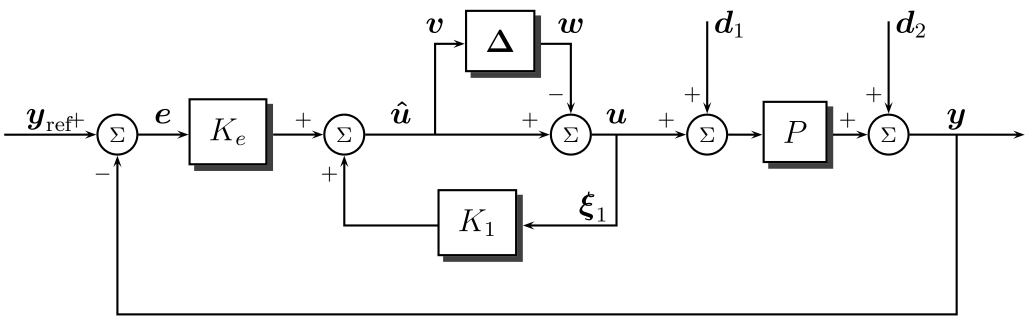

Figure 5.7: Anti-windup for single input nonlinearity

The anti-windup synthesis problem for this nonlinearity is one of choosing $K_e(s)$ and $K_1(s)$ in Figure 5.7, and it is clear from this figure that the coprime factorisation parametrisation of the previous section may be used without modification for such nonlinearities.

5.2.3 System with multiple (cascaded) input nonlinearities

We consider the interconnection of Figure 5.2 with a general class of cascade nonlinearity $\mathcal{N}$, of the form

$$\begin{aligned}
\boldsymbol{\xi}_1 &= (I-\Delta_1)\hat{\boldsymbol{u}} \\
\boldsymbol{\xi}_2 &= (I-\Delta_2)\boldsymbol{\xi}_1 \\
&\vdots \\
\boldsymbol{\xi}_{n_\xi-1} &= (I-\Delta_{n_\xi-1})\boldsymbol{\xi}_{n_\xi-2} \\
\boldsymbol{u} = \boldsymbol{\xi}_{n_\xi} &= (I-\Delta_{n_\xi})\boldsymbol{\xi}_{n_\xi-1}
\end{aligned}$$

for some $n_\xi \geq 1$. We assume that $\|\Delta_i\|$ is finite for each $i \in \{1, 2, \cdots, n_\xi\}$.

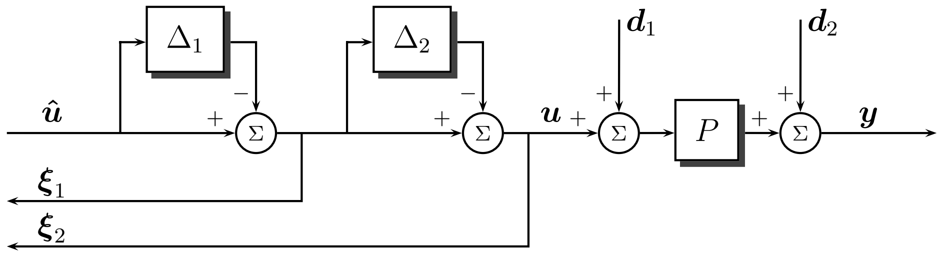

Figure 5.8: Multiple (cascaded) input nonlinearities (shown for $n_\xi = 2$)

Figure 5.8 shows a nonlinearity of this form, for $n_\xi = 2$; the plant P and disturbances $\boldsymbol{d}_1$ and $\boldsymbol{d}_2$ are shown for clarity.

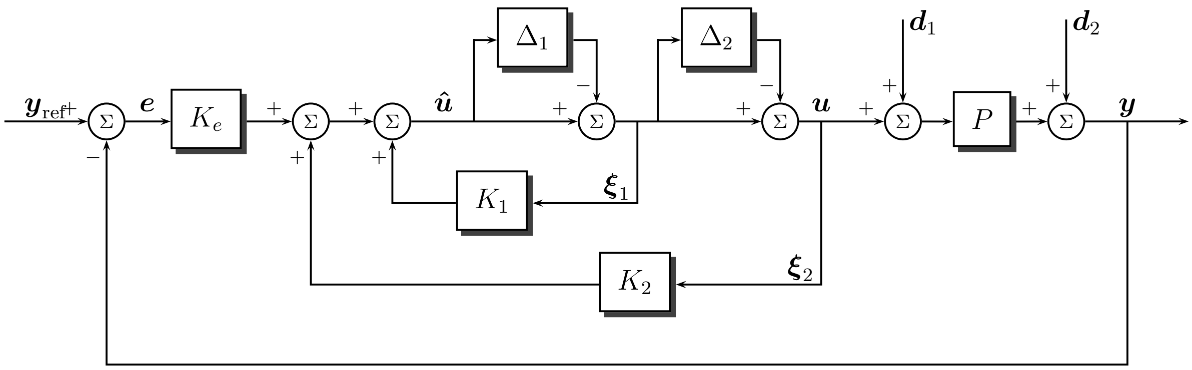

Figure 5.9: Anti-windup for multiple input nonlinearities (shown for $n_\xi = 2$)

The anti-windup synthesis problem for this nonlinearity is then one of choosing $K_e(s)$ and $K_1(s), \cdots, K_{n_\xi}(s)$ in Figure 5.9.

Coprime factor anti-windup parametrisation

We propose the following controller parametrisation, which is a generalisation of the coprime factor anti-windup parametrisation described in Section 5.2.1:

$$\begin{aligned} K_e &= Q_1 \tilde{U}_0 \\ K_i &= Q_1 (Q_i^{-1} - Q_{i+1}^{-1}) \quad \forall i \in \{1, 2, \cdots, (n_\xi - 1)\} \\ K_{n_\xi} &= Q_1 (Q_{n_\xi}^{-1} - \tilde{V}_0) \end{aligned}$$

with free parameters $Q_1 \ldots Q_{n_\xi}$ such that $Q_i \in \mathcal{Q}$ (Equation 2.5) for each $i \in \{1, 2, \cdots, n_\xi\}$.

It is desirable, although not strictly essential, to have

$$\begin{aligned} Q_{n_\xi}(\infty) = \cdots = Q_2(\infty) = Q_1(\infty) \quad \text{and} \\ Q_{n_\xi} \tilde{V}_0 = I \end{aligned}$$

so that there is not an algebraic loop in the controller implementation. If we choose initial left- and right-coprime factorisations $C = \tilde{V}_0^{-1} \tilde{U}_0$ and $P = N_0 M_0^{-1}$ such that the Bezout identity (Equation 5.1) holds, and under the mild assumption that P is strictly proper, then the second of these is equivalent to $M_{n_\xi}(\infty) = I$, ie that $Q_{n_\xi}(\infty) = M_0(\infty)$.

We now see that the problem of anti-windup synthesis can be interpreted as choosing n_ξ (not necessarily all different) left-coprime factorisations of the linear controller

$$C = \tilde{V}_i^{-1} \tilde{U}_i; \quad \begin{bmatrix} \tilde{V}_i(s) & \tilde{U}_i(s) \end{bmatrix} = Q_i(s) \begin{bmatrix} \tilde{V}_0(s) & \tilde{U}_0(s) \end{bmatrix} \quad \forall i \in \{1, 2, \cdots, n_\xi\}$$

or n_ξ right-coprime factorisations of the linear plant

$$P = N_i M_i^{-1}; \quad \begin{bmatrix} M_i(s) \\ N_i(s) \end{bmatrix} = \begin{bmatrix} M_0(s) \\ N_0(s) \end{bmatrix} Q_i^{-1}(s) \quad \forall i \in \{1, 2, \cdots, n_\xi\}$$

or simply of choosing $Q_1, Q_2, \cdots, Q_{n_\xi} \in \mathcal{Q}$ such that

$$Q_1(\infty) = Q_2(\infty) = \cdots = Q_{n_\xi}(\infty) = M_0(\infty)$$

Remark

1. If one or more of the signals $\boldsymbol{\xi}_i$ are not available (or, perhaps to reduce controller complexity, the designer chooses not to use them), then simply setting $Q_{i_0} = Q_{i_0+1}$ will make $\hat{\boldsymbol{u}}$ independent of $\boldsymbol{\xi}_{i_0}$ (and also reduce the number of free parameters by one.)

Closed-loop representation for stability and performance analysis

The interconnection of Figure 5.2, with a nonlinearity $\mathcal{N}$ of this form and with the stated controller parametrisation, can be represented as shown (for $n_\xi = 2$) in Figure 5.10.

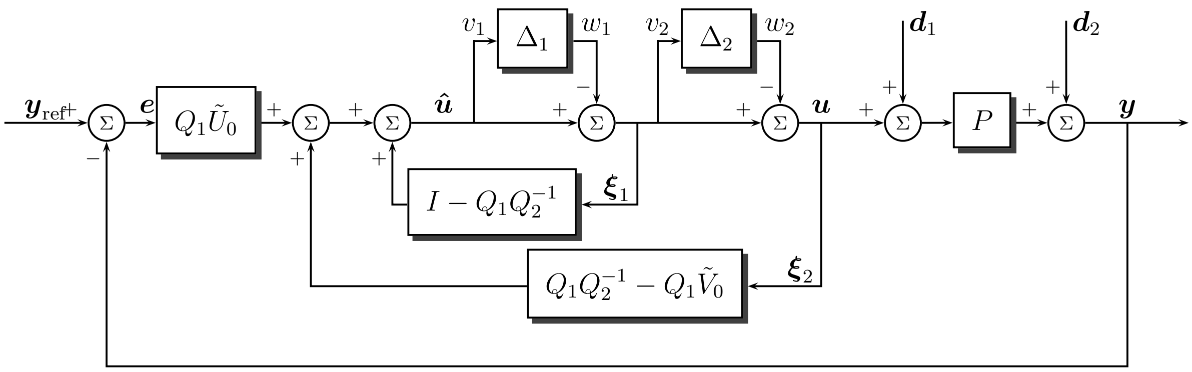

Figure 5.10: Alternative representation of Figure 5.9

Denote by v_i and w_i the signals[1] at the input and output of the i-th perturbation Δ_i, for each $i \in \{1, 2, \cdots, n_\xi\}$, and let

$$\boldsymbol{v} := \begin{bmatrix} v_1 \\ v_2 \\ \vdots \\ v_{n_\xi - 1} \\ v_{n_\xi} \end{bmatrix}, \quad \boldsymbol{w} := \begin{bmatrix} w_1 \\ w_2 \\ \vdots \\ w_{n_\xi - 1} \\ w_{n_\xi} \end{bmatrix}, \quad \boldsymbol{\Delta} := \begin{bmatrix} \Delta_1 & 0 & \cdots & 0 & 0 \\ 0 & \Delta_2 & \cdots & 0 & 0 \\ \vdots & \vdots & \ddots & \vdots & \vdots \\ 0 & 0 & \cdots & \Delta_{n_\xi - 1} & 0 \\ 0 & 0 & \cdots & 0 & \Delta_{n_\xi} \end{bmatrix}$$

In addition, define the following transfer matrices

$$X_{11} := \begin{bmatrix} S & -SP & -S \\ I - S & SP & S \\ CS & -CSP & -CS \end{bmatrix} \qquad X_{12} := \begin{bmatrix} N_1 & N_2 & \cdots & N_{n_\xi - 1} & N_{n_\xi} \\ -N_1 & -N_2 & \cdots & -N_{n_\xi - 1} & -N_{n_\xi} \\ -M_1 & -M_2 & \cdots & -M_{n_\xi - 1} & -M_{n_\xi} \end{bmatrix}$$

$$X_{21} := \begin{bmatrix} CS & -CSP & -CS \\ CS & -CSP & -CS \\ \vdots & \vdots & \vdots \\ CS & -CSP & -CS \\ CS & -CSP & -CS \end{bmatrix} \qquad X_{22} := \begin{bmatrix} I - M_1 & I - M_2 & \cdots & I - M_{n_\xi - 1} & I - M_{n_\xi} \\ -M_1 & I - M_2 & \cdots & I - M_{n_\xi - 1} & I - M_{n_\xi} \\ \vdots & \vdots & \ddots & \vdots & \vdots \\ -M_1 & -M_2 & \cdots & I - M_{n_\xi - 1} & I - M_{n_\xi} \\ -M_1 & -M_2 & \cdots & -M_{n_\xi - 1} & I - M_{n_\xi} \end{bmatrix}$$

[1] Note the break with our convention of using **bold**face for vectors. The reason is that we shall stack $v_1 \cdots v_{n_\xi}$ into a new vector $\boldsymbol{v}$.

We can then express the interconnection with the following LFT on $\boldsymbol{\Delta}$

$$\begin{bmatrix}\begin{bmatrix}\boldsymbol{e}\\ \boldsymbol{y}\\ \boldsymbol{u}\end{bmatrix}\\ \boldsymbol{v}\end{bmatrix} = \begin{bmatrix}X_{11} & X_{12}\\ X_{21} & X_{22}\end{bmatrix}\begin{bmatrix}\begin{bmatrix}\boldsymbol{y}_{\text{ref}}\\ \boldsymbol{d}_1\\ \boldsymbol{d}_2\end{bmatrix}\\ \boldsymbol{w}\end{bmatrix}$$
$$\boldsymbol{w} = \boldsymbol{\Delta}\boldsymbol{v}$$

and see immediately that if $\boldsymbol{w} \equiv 0$ then the nominal linear behaviour of Figure 5.1 is recovered, as desired.

We see also that this interconnection does not conform to the assumptions of Section 3.3 (since $X_{22} \notin \mathcal{RH}_2$), and hence well-posedness cannot be shown using Proposition 3.6. We show that the loop is well-posed using a variation on "D-scaling" (eg Zhou *et al* [ZDG96], Chapter 11):

Proposition 5.1

The interconnection shown in Figure 5.10 (equivalently, Figure 5.9) is well-posed for any $Q_1, Q_2, \cdots, Q_{n_\xi} \in \mathcal{Q}$ *such that* $Q_1(\infty) = Q_2(\infty) = \cdots = Q_{n_\xi}(\infty) = M_0(\infty)$.

PROOF OF PROPOSITION 5.1:

Consider the equivalent interconnection

$$\begin{bmatrix}\begin{bmatrix}\boldsymbol{e}\\ \boldsymbol{y}\\ \boldsymbol{u}\end{bmatrix}\\ \tilde{\boldsymbol{v}}\end{bmatrix} = \begin{bmatrix}X_{11} & X_{12}\\ H^{-1}X_{21} & H^{-1}X_{22}H\end{bmatrix}\begin{bmatrix}\begin{bmatrix}\boldsymbol{y}_{\text{ref}}\\ \boldsymbol{d}_1\\ \boldsymbol{d}_2\end{bmatrix}\\ \tilde{\boldsymbol{w}}\end{bmatrix}$$
$$\tilde{\boldsymbol{w}} = H^{-1}\boldsymbol{\Delta}H\tilde{\boldsymbol{v}}$$

where $H = \text{Diag}\{h_1 I, h_2 I, \cdots, h_{n_\xi} I\}$ is strictly positive.

By Willems ([Wil71]), this interconnection is well-posed if the product of the uniform instantaneous gains of $H^{-1}X_{22}H$ and $H^{-1}\boldsymbol{\Delta}H$ is bounded away from unity at any time $T \in [0, \infty)$. It is clear that the uniform instantaneous gains of $H^{-1}\boldsymbol{\Delta}H$ and $\boldsymbol{\Delta}$ are identical, and that the uniform instantaneous gain of $H^{-1}X_{22}H$ is simply given by

$$\left\|H^{-1}X_{22}H\right\| = \left\|\begin{bmatrix} 0 & 0 & \cdots & 0 & 0\\ -\frac{h_1}{h_2}I & 0 & \cdots & 0 & 0\\ \vdots & \vdots & \ddots & \vdots & \vdots\\ -\frac{h_1}{h_{n_\xi-1}}I & -\frac{h_2}{h_{n_\xi-1}}I & \cdots & 0 & 0\\ -\frac{h_1}{h_{n_\xi}}I & -\frac{h_2}{h_{n_\xi}}I & \cdots & -\frac{h_{n_\xi-1}}{h_{n_\xi}}I & 0\end{bmatrix}\right\|$$

which can be made arbitrarily small by suitable choice of H. Well-posedness then follows provided $\boldsymbol{\Delta}$ has finite uniform instantaneous gain. ∎

5.3 Synthesis of anti-windup compensators

5.3.1 System with magnitude-limited actuator

Implementation of nonlinear precompensator

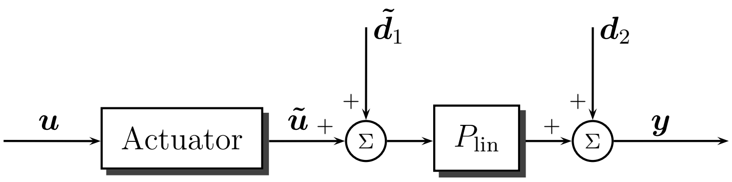

Figure 5.11: Model of magnitude-limited actuator and plant

Figure 5.11 shows our assumed model of a (possibly unstable) linear plant $P_{\text{lin}} \in \mathcal{R}_p^{n_y \times n_u}$ with magnitude-limited actuator. We make the same assumptions as in Sections 4.1.2 and 4.3.1, ie

$$\boldsymbol{y} = \begin{cases} P_{\text{lin}}(P_{\text{act}}\tilde{\boldsymbol{u}} + \tilde{\boldsymbol{d}}_1) + \boldsymbol{d}_2 & \text{if } P_{\text{act}}\boldsymbol{u} \in \mathfrak{M}_A \\ \text{undefined} & \text{otherwise} \end{cases}$$

for some (stable) nominal actuator dynamics $P_{\text{act}}(s) \in \mathcal{RH}_\infty^{n_u \times n_u}$ and diagonal matrix $A > 0$.

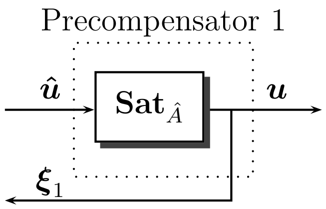

Figure 5.12: Precompensator 1

We saw in Section 4.3.1 that Precompensator 1 is a suitable precompensator for a magnitude-limited actuator with *any* nominal dynamics $P_{\text{act}} = \text{Diag}\{p_1, p_2, \cdots, p_{n_u}\}$, so long as $\|p_i(s)\|_1 \leq 1$ for each $i \in \{1, 2, \cdots, n_u\}$ and the diagonal matrix $\hat{A} > 0$ satisfies

$$A\hat{A}^{-1} \geq I$$

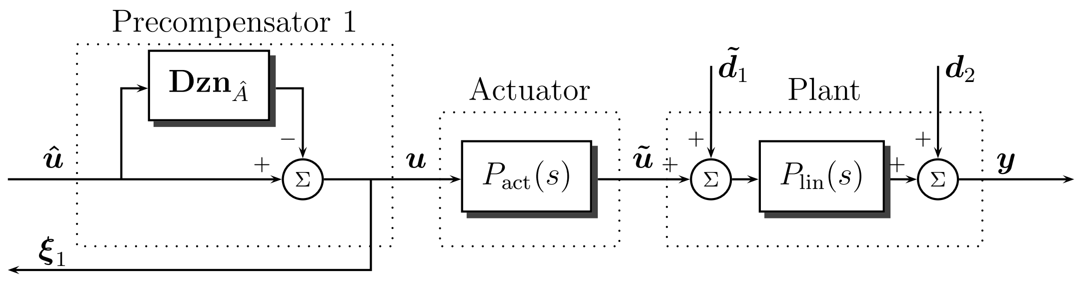

Figure 5.13: Precompensator 1, magnitude-limited actuator and linear plant

Since Precompensator 1 ensures that $P_{\mathrm{act}}\hat{\boldsymbol{u}} \in \mathfrak{M}_A$, we may represent the resulting interconnection of precompensator, actuator and plant as shown in Figure 5.13; note that this interconnection has only *one* nonlinear element, and that the signal $\boldsymbol{\xi}_1$ is exactly measurable.

To simplify the presentation of the synthesis results which follow, we assume (without loss of generality) that $\hat{A} = I$, which corresponds to unity saturation levels on each channel in the precompensator, and hence saturation levels of unity or greater in the real actuator.

Implementation of anti-windup compensator

If we were now to define $P(s) := P_{\mathrm{lin}}(s)P_{\mathrm{act}}(s)$ and $\boldsymbol{d}_1 := P_{\mathrm{act}}^{-1}\tilde{\boldsymbol{d}}_1$, and to consider $\boldsymbol{d}_1$ instead of $\tilde{\boldsymbol{d}}_1$, entering just *before* the actuator dynamics $P_{\mathrm{act}}(s)$, then we would have a system of the form considered in Section 5.2.2 (cf. Figure 5.6)

At first glance, this approach seems invalid, since it is unlikely that $P_{\mathrm{act}}(s)$ is invertible in $\mathcal{R}_p$; however, it will transpire that (in the final closed-loop relations) $\boldsymbol{d}_1$ will always appear in the form of $P\boldsymbol{d}_1$, which is the same as $P_{\mathrm{lin}}\tilde{\boldsymbol{d}}_1$. This sleight-of-hand simply motivates the use of the coprime factor anti-windup parametrisation, and could in theory be avoided completely by a simple re-definition of the plant and disturbances in Figure 5.6.

The important thing to remember, as mentioned in Section 4.1.2, is that we *do not* (indeed we *cannot*) consider disturbances entering at the actuator input.

In Section 5.2.2 we stated a coprime factor parametrisation of anti-windup controllers for this interconnection: given initial left- and right-coprime factorisations $C = \tilde{V}_0^{-1}\tilde{U}_0$ and $P = N_0 M_0^{-1}$ satisfying the Bezout identity (Equation 5.1), the anti-windup controller is given by

$$\hat{\boldsymbol{u}} = Q\tilde{U}_0\boldsymbol{e} + (I - Q\tilde{V}_0)\boldsymbol{\xi}_1$$

parametrised by $Q \in \mathcal{Q}$ (Equation 2.5) such that $Q(\infty) = M_0(\infty)$.

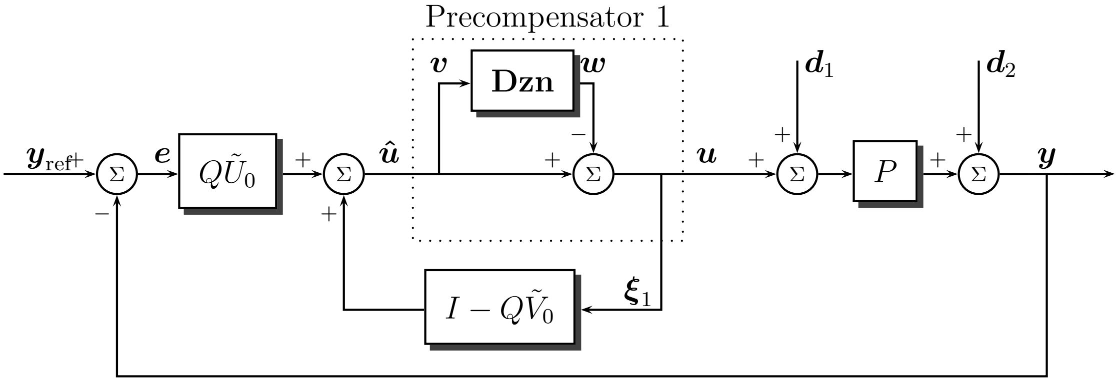

Figure 5.14: System with Precompensator 1 and coprime factor anti-windup controller

The resulting closed-loop interconnection, shown in Figure 5.14, can be described by the following LFT on **Dzn**:

$$\begin{bmatrix} \begin{bmatrix} \boldsymbol{e} \\ \boldsymbol{y} \\ \boldsymbol{u} \end{bmatrix} \\ \boldsymbol{v} \end{bmatrix} = \begin{bmatrix} \begin{bmatrix} S & -SP & -S \\ I-S & SP & S \\ CS & -CSP & -CS \end{bmatrix} & \begin{bmatrix} N_0Q^{-1} \\ -N_0Q^{-1} \\ -M_0Q^{-1} \end{bmatrix} \\ \begin{bmatrix} CS & -CSP & -CS \end{bmatrix} & I - M_0Q^{-1} \end{bmatrix} \begin{bmatrix} \begin{bmatrix} \boldsymbol{y}_{\text{ref}} \\ \boldsymbol{d}_1 \\ \boldsymbol{d}_2 \end{bmatrix} \\ \boldsymbol{w} \end{bmatrix}$$
$$\boldsymbol{w} = \mathbf{Dzn}(\boldsymbol{v})$$

where $S := (I + PC)^{-1}$. As mentioned, we see that $\boldsymbol{d}_1$ enters this relation as a multiple of $P\boldsymbol{d}_1$ which is equivalent to $P_{\text{lin}}\tilde{\boldsymbol{d}}_1$, and hence that an equivalent relation — using the real disturbance $\tilde{\boldsymbol{d}}_1$ — is given by

$$\begin{bmatrix} \begin{bmatrix} \boldsymbol{e} \\ \boldsymbol{y} \\ \boldsymbol{u} \end{bmatrix} \\ \boldsymbol{v} \end{bmatrix} = \begin{bmatrix} \begin{bmatrix} S & -SP_{\text{lin}} & -S \\ I-S & SP_{\text{lin}} & S \\ CS & -CSP_{\text{lin}} & -CS \end{bmatrix} & \begin{bmatrix} N_0Q^{-1} \\ -N_0Q^{-1} \\ -M_0Q^{-1} \end{bmatrix} \\ \begin{bmatrix} CS & -CSP_{\text{lin}} & -CS \end{bmatrix} & I - M_0Q^{-1} \end{bmatrix} \begin{bmatrix} \begin{bmatrix} \boldsymbol{y}_{\text{ref}} \\ \tilde{\boldsymbol{d}}_1 \\ \boldsymbol{d}_2 \end{bmatrix} \\ \boldsymbol{w} \end{bmatrix}$$
$$\boldsymbol{w} = \mathbf{Dzn}(\boldsymbol{v})$$

We see that we have, in a sense, come around in a full circle: Figure 5.14 shows precisely the same AWBT interconnection that is usually assumed in the literature (eg Miyamoto & Vinnicombe [MV96b]; Weston & Postlethwaite [WP98]; Peng *et al* [PVHW98] or Teel & Kapoor [TK97]), with the significant difference being that the saturation nonlinearity in our case is an *implemented* element, and hence that both the nonlinear perturbation **Dzn** and the feedback signal $\boldsymbol{\xi}_1$ are known exactly.

Anti-windup compensator synthesis

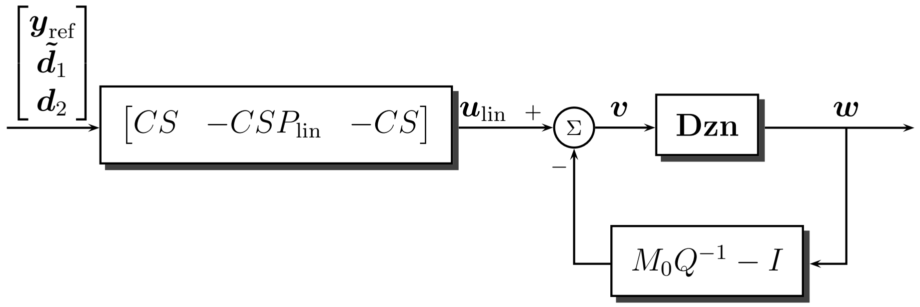

Figure 5.15: Representation of Figure 5.14 for stability analysis

For *stability* analysis, recalling the comments made in Section 3.3, and noting that each element in this transfer matrix is stable,[2] we need consider only the simpler interconnection of Figure 5.15. Note that the external input to this interconnection may be taken to be either $\begin{bmatrix} \boldsymbol{y}_{\text{ref}} \\ \tilde{\boldsymbol{d}}_1 \\ \boldsymbol{d}_2 \end{bmatrix}$ or simply $\boldsymbol{u}_{\text{lin}} := \begin{bmatrix} CS & CSP_{\text{lin}} & -CS \end{bmatrix} \begin{bmatrix} \boldsymbol{y}_{\text{ref}} \\ \tilde{\boldsymbol{d}}_1 \\ \boldsymbol{d}_2 \end{bmatrix}$, which may be seen to be independent of the anti-windup compensation scheme chosen. Both of these interpretations will be useful.

The signals $\boldsymbol{e}, \hat{\boldsymbol{u}}, \boldsymbol{u}$ and $\boldsymbol{y}$ in Figure 5.14 are then simply given in terms of the nominal linear response of Figure 5.1 and $\boldsymbol{w}$, the output of the deadzone nonlinearity in Figure 5.15:

$$\boldsymbol{e} - \boldsymbol{e}_{\text{lin}} = N_0 Q^{-1} \boldsymbol{w} \tag{5.2}$$
$$\hat{\boldsymbol{u}} - \boldsymbol{u}_{\text{lin}} = (I - M_0 Q^{-1}) \boldsymbol{w} \tag{5.3}$$
$$\boldsymbol{u} - \boldsymbol{u}_{\text{lin}} = -M_0 Q^{-1} \boldsymbol{w} \tag{5.4}$$
$$\boldsymbol{y} - \boldsymbol{y}_{\text{lin}} = -N_0 Q^{-1} \boldsymbol{w} \tag{5.5}$$

This characterisation of the behaviour in terms of the relatively simple nonlinear interconnection of Figure 5.15 has been previously identified by a small number of authors, notably Weston & Postlethwaite [WP98], Hui & Chan [HC99] and Crawshaw & Vinnicombe [CV98] (implicitly also by Miyamoto & Vinnicombe [MV96b], [MV96a], [Miy97])

Direct consideration of the difference in behaviour between the nominal and real behaviour (eg $\boldsymbol{y} - \boldsymbol{y}_{\text{lin}}$ etc) has been studied by those same authors, plus also Teel & Kapoor [TK97] (who discuss *nonlinear* anti-windup schemes, and hence do not identify the nonlinear feedback loop of Figure 5.15), and Rantzer [Ran99].

[2] This may not be obvious: if SP_{lin} (or CSP_{lin}) were unstable, and SP (resp. CSP) were stable, then of necessity P_{act} would have to cancel out the unstable pole(s) of SP_{lin} (resp. CSP_{lin}) However, since both S and CS are assumed to be stable, the only way this could occur would be for P_{act} to cancel out the unstable pole(s) of P_{lin}, which we assumed (in Section 4.1.2) was not the case.

Proposition 5.2 and Theorem 5.3 are important results which indicate the fundamental limitations to the anti-windup synthesis problem:

Proposition 5.2
Given $C = \tilde{V}_0^{-1}\tilde{U}_0$ and $P = N_0 M_0^{-1}$ satisfying the Bezout identity (Equation 5.1), and with respect to the interconnection of Figure 5.14:

- *If **all** poles of P are in the open left half-plane then there exists at least one $Q \in \mathcal{Q}$ which solves Problem 5.1 and which satisfies $Q(\infty) = M_0(\infty)$*
- *If **any** poles of P are in the open right half-plane then there does not exist any $Q \in \mathcal{Q}$ which solves Problem 5.1 and which satisfies $Q(\infty) = M_0(\infty)$*

PROOF OF PROPOSITION 5.2:
If *all* poles of P are in the open left half-plane then it is clear, by Proposition 3.7, that the interconnection can be stabilised by choosing $Q = M_0$.
If *any* poles of P are in the open right half-plane then it is well known (eg Sussmann *et al* [SSY94]) that the interconnection cannot be stabilised by *any* bounded control input. ∎

Theorem 5.3
Given $C = \tilde{V}_0^{-1}\tilde{U}_0$ and $P = N_0 M_0^{-1}$ satisfying the Bezout identity (Equation 5.1) and any $Q \in \mathcal{Q}$ such that $Q(\infty) = M_0(\infty)$, and for any $\varepsilon > 0$ and $\gamma < \|P\|_\infty$, there exists $\boldsymbol{u}_{lin} \in \mathcal{L}_{2e}$ and $T \geq 0$ with

$$\begin{aligned} \|\mathbf{Dzn}(\boldsymbol{u}_{lin})\|_2 &< \varepsilon \\ \boldsymbol{u}_{lin}(t) &= 0 \quad \textit{for all } t > T \end{aligned}$$

such that in the interconnection of Figure 5.14

$$\begin{aligned} \|\boldsymbol{u} - \boldsymbol{u}_{lin}\|_2 &\geq \|\mathbf{Dzn}(\boldsymbol{u}_{lin})\|_2 \quad \textit{and} \\ \|\boldsymbol{y} - \boldsymbol{y}_{lin}\|_2 &> \gamma \|\mathbf{Dzn}(\boldsymbol{u}_{lin})\|_2 \end{aligned}$$

PROOF OF THEOREM 5.3:
Given any $\varepsilon > 0$ and $\gamma < \|P\|_\infty$, there exists $\boldsymbol{r} \in \mathcal{L}_{2e}$ and $T \geq 0$ such that

$$\begin{aligned} \|\Pi_T \boldsymbol{r}\|_2 &< \varepsilon \quad \text{and} \\ \|\Pi_T P \boldsymbol{r}\|_2 &> \gamma \|\Pi_T \boldsymbol{r}\|_2 \end{aligned}$$

(otherwise $\gamma < \|P\|_\infty$ would not be true) Now, let $\boldsymbol{u}_{\text{lin}}$ be given by

$$\boldsymbol{u}_{\text{lin}} = \Pi_T\Big(\boldsymbol{r} + \mathbf{Sgn}(Q M_0^{-1} \boldsymbol{r})\Big)$$

in which case it may be verified that $\Pi_T \boldsymbol{w} = \Pi_T Q M_0^{-1} \boldsymbol{r}$ and hence that

$$\begin{aligned} \Pi_T(\boldsymbol{u} - \boldsymbol{u}_{\text{lin}}) &= -\Pi_T \boldsymbol{r} \quad \text{and} \\ \Pi_T(\boldsymbol{y} - \boldsymbol{y}_{\text{lin}}) &= -\Pi_T P \boldsymbol{r} \end{aligned}$$

Finally, by Corollary 2.6, $\|\mathbf{Dzn}(\boldsymbol{u}_{\text{lin}})\|_2 \leq \|\Pi_T \boldsymbol{r}\|_2$ which completes the proof. ∎

Remark

1. In the case that P is "critically stable" (having one or more $j\omega$-axis poles but no open right half-plane poles), we conclude from Proposition 5.2 and Theorem 5.3 that *finite gain* stability with respect to $\|\mathbf{Dzn}(\boldsymbol{u}_{\text{lin}})\|_2$ cannot be achieved with any $Q \in \mathcal{Q}$, but that *bounded-input bounded-output* stability is not necessarily impossible.[3]

Case I: stable P

Proposition 5.2 indicates that for any stable P, there is at least one solution to Problem 5.1; we now consider synthesising Q to optimise a suitable performance measure while guaranteeing global stability of the interconnection. We consider two possible performance criteria:

- Miyamoto & Vinnicombe [MV96b] propose to minimise the $\mathcal{L}_2$ gain from $\hat{\boldsymbol{u}} - \boldsymbol{u}$ $(=\boldsymbol{w})$ to the difference between the actual and nominal outputs $\boldsymbol{y} - \boldsymbol{y}_{\text{lin}}$, modified by some suitable weight W. This corresponds to minimising $\|WN_0Q^{-1}\|_\infty$ subject to maintaining global stability; this is guaranteed in [MV96b] by ensuring that $\|I - M_0Q^{-1}\|_\infty < 1$:

  Proposition 5.4 (Miyamoto & Vinnicombe [MV96b])
  For stable plant P and any weight W such that $W, W^{-1} \in \mathcal{RH}_\infty$, there always exists $Q \in \mathcal{Q}$ such that
  $$\left\| \begin{bmatrix} WN_0Q^{-1} \\ M_0Q^{-1} - I \end{bmatrix} \right\|_\infty < 1$$
  and $M_0Q^{-1}(\infty) = I$; such a Q then solves Problem 5.1.

- Teel & Kapoor [TK97] propose to minimise the $\mathcal{L}_2$ gain from $\mathbf{Dzn}(\boldsymbol{u}_{\text{lin}})$ to the difference between a specified signal in the nonlinear system and its corresponding nominal signal, such as $\boldsymbol{u} - \boldsymbol{u}_{\text{lin}}$ or $\boldsymbol{y} - \boldsymbol{y}_{\text{lin}}$.

  A simple upper bound on the $\mathcal{L}_2$ gain from $\mathbf{Dzn}(\boldsymbol{u}_{\text{lin}})$ to $\boldsymbol{u} - \boldsymbol{u}_{\text{lin}}$, for interconnections satisfying the (multivariable) Circle Criterion, was recently given by Rantzer [Ran99].

  Note that no anti-windup scheme can do better than
  $$\|\boldsymbol{u} - \boldsymbol{u}_{\text{lin}}\|_2 \leq \|\mathbf{Dzn}(\boldsymbol{u}_{\text{lin}})\|_2 \quad \text{and}$$
  $$\|\boldsymbol{y} - \boldsymbol{y}_{\text{lin}}\|_2 \leq \|P\|_\infty \|\mathbf{Dzn}(\boldsymbol{u}_{\text{lin}})\|_2$$
  by Theorem 5.3. One scheme which achieves these bounds is the unmodified IMC scheme (see Zheng *et al* [ZKM94]), which sets $Q = M_0$; a choice which can be seen to cut the nonlinear loop in Figure 5.15. However, it has been pointed out by a number of authors (eg Weston & Postlethwaite [WP98]) that this choice may lead to poor performance if P has lightly damped or slow modes.

[3] Stoorvogel *et al* [SSS99] consider BIBO stabilisation of critically stable plants with saturation, but their work is not in the anti-windup framework, ie the linear controller is not assumed to be given *a priori*. The question of whether a $Q \in \mathcal{Q}$ achieving BIBO stability exists remains an open question.

We propose the following synthesis method, which uses the stability condition and performance bound of Corollary 3.10 (which is based on the multivariable circle criterion) in place of the small-gain condition of Proposition 5.4. In the light of Equations 5.2 to 5.5, we claim that this method is applicable to both of the performance criteria given above.

Theorem 5.5

For stable plant P, any weight W such that $W, W^{-1} \in \mathcal{RH}_\infty$, and any diagonal matrix $A = diag\{a_1, a_2, \cdots, a_n\}$ with $a_i \in (0,2)$ for each $i \in \{1, 2, \cdots, n\}$, there always exists $Q \in \mathcal{Q}$ such that

$$\left\| \begin{bmatrix} WN_0Q^{-1} \\ AM_0Q^{-1} - I \end{bmatrix} \right\|_\infty < 1$$

and $M_0Q^{-1}(\infty) = I$.

Furthermore, for any such Q, the interconnection in Figure 5.14 is stable, with

$$\begin{aligned} \|\boldsymbol{w}\|_2 &\leq \frac{\|A\|}{1 - \|AM_0Q^{-1} - I\|_\infty} \|\mathbf{Dzn}(\boldsymbol{u}_{lin})\|_2 \\ \|\boldsymbol{y} - \boldsymbol{y}_{lin}\|_2 &\leq \left\|N_0Q^{-1}\right\|_\infty \|\boldsymbol{w}\|_2 \\ &\leq \frac{\|A\| \, \|N_0Q^{-1}\|_\infty}{1 - \|AM_0Q^{-1} - I\|_\infty} \|\mathbf{Dzn}(\boldsymbol{u}_{lin})\|_2 \end{aligned}$$

PROOF OF THEOREM 5.5:

By a change of variable $\hat{Q} = AM_0Q^{-1}$, we consider the unconstrained problem

$$\inf_{\hat{Q} \in \mathcal{Q}} \left\| \begin{bmatrix} WPA^{-1}\hat{Q} \\ \hat{Q} - I \end{bmatrix} \right\|_\infty$$

which has infimum given by (Miyamoto & Vinnicombe [MV96b])

$$\frac{\|WPA^{-1}\|_\infty}{\sqrt{1 + \|WPA^{-1}\|_\infty^2}} < 1$$

We then conclude that the full problem has infimum

$$\max \left\{ \frac{\|WPA^{-1}\|_\infty}{\sqrt{1 + \|WPA^{-1}\|_\infty^2}}, \|A - I\| \right\} < 1$$

where the second term is due to the interpolation constraint $M_0Q^{-1}(\infty) = I$, which does not otherwise put up the achievable norm (see eg Vinnicombe [Vin00] Theorem 1.29)

Then by Corollary 3.10 the interconnection is stable, and moreover

$$\|\boldsymbol{w}\|_2 \leq \frac{\|A\|}{1 - \|AM_0Q^{-1} - I\|_\infty} \|\mathbf{Dzn}(\boldsymbol{u}_{\text{lin}})\|_2$$

from which $\boldsymbol{y} = \boldsymbol{y}_{\text{lin}}$ may be bounded as stated. ∎

Remark

1. The main application of this synthesis method is clearly to guarantee $\mathcal{L}_2$ performance from $\mathbf{Dzn}(\boldsymbol{u}_{\mathrm{lin}})$ to $\boldsymbol{y} - \boldsymbol{y}_{\mathrm{lin}}$ (or equivalently to $\boldsymbol{e} - \boldsymbol{e}_{\mathrm{lin}}$) However, since $\|M_0 Q^{-1}\|_\infty$ may be trivially bounded by $\|A^{-1}\| \left(\|AM_0Q^{-1} - I\|_\infty + 1 \right)$, we see that $\mathcal{L}_2$ performance from $\mathbf{Dzn}(\boldsymbol{u}_{\mathrm{lin}})$ to $\hat{\boldsymbol{u}} - \boldsymbol{u}_{\mathrm{lin}}$ and $\boldsymbol{u} - \boldsymbol{u}_{\mathrm{lin}}$ is also guaranteed, albeit less strongly.

2. A suitable solution to Theorem 5.5 (or Proposition 5.4) can be obtained by solving a standard $\mathcal{H}_\infty$ full-information problem with the weighted plant given by ($A = I$ corresponds to Proposition 5.4)

$$\begin{bmatrix} 0 & WPA^{-1} \\ -I & I \end{bmatrix}$$

If WPA^{-1} has a stabilisable and detectable state-space realisation

$$\left[\begin{array}{c|c} A_{WP} & B_{WP} \\ \hline C_{WP} & D_{WP} \end{array}\right]$$

then the weighted plant is given by

$$\left[\begin{array}{c|cc} A_{WP} & 0 & B_{WP} \\ \hline C_{WP} & 0 & D_{WP} \\ 0 & -I & I \end{array}\right]$$

and the "generalised plant" G_{FI} is given by

$$G_{\mathrm{FI}} = \left[\begin{array}{c|cc} A_{WP} & 0 & B_{WP} \\ \hline C_{WP} & 0 & D_{WP} \\ 0 & -I & I \\ \begin{bmatrix} I \\ 0 \end{bmatrix} & \begin{bmatrix} 0 \\ I \end{bmatrix} & \begin{bmatrix} 0 \\ 0 \end{bmatrix} \end{array}\right]$$

The $\mathcal{H}_\infty$ full information problem is then one of determining an internally stabilising K_{FI} such that

$$\|\mathcal{F}_l(G_{\mathrm{FI}}, K_{\mathrm{FI}})\|_\infty < 1$$

It is shown by Miyamoto & Vinnicombe [MV96a] that any solution to this full information problem satisfies $\hat{Q}, \hat{Q}^{-1} \in \mathcal{RH}_\infty$, and it will also be the case that the central solution satisfies $\hat{Q}(\infty) = I$. Hence $Q, Q^{-1} \in \mathcal{RH}_\infty$ and $M_0 Q(\infty) = A$, which unfortunately means that the central solution does not satisfy the interpolation condition $M_0 Q^{-1}(\infty) = I$ unless $A = I$; it is always possible, however, to choose such a Q given the parametrisation of all solutions.

The right-coprime factors of the plant ($M_0 Q^{-1}$ and $N_0 Q^{-1}$) are then trivially derived from the closed-loop transfer function; the compensator implementation is then given in terms of the left-coprime factors of the controller ($Q\tilde{V}_0$ and $Q\tilde{U}_0$), which may be computed easily.

Case II: unstable P

Proposition 5.2 and Theorem 5.3 indicate that for any unstable P, there are no solutions to Problem 5.1[4], and hence that we should consider instead Problem 5.2, ie synthesising Q to optimise local stability. As previously discussed, we consider only isolated disturbances occuring at *either* $\tilde{\boldsymbol{d}}_1$ or $\boldsymbol{d}_2$ or $\boldsymbol{y}_{\text{ref}}$, and for convenience we shall only discuss the case of $\tilde{\boldsymbol{d}}_1$ — the other two cases proceed in a similar manner.

There are two sensible types of disturbance which we could consider:

- Disturbances such that $\|\mathbf{Dzn}_K(\boldsymbol{u}_{\text{lin}})\|_2 < \varepsilon$, for some diagonal matrix $0 < K < I$ (eg Teel & Kapoor [TK97])
- Disturbances such that $\|\tilde{\boldsymbol{d}}_1\|_2 < \varepsilon$ (ie simple "balls" in $\mathcal{L}_2$)

We observe immediately that *both* of these possibilities have their drawbacks, since it is clear that there may exist a disturbance $\tilde{\boldsymbol{d}}_1$ such that

$$\boldsymbol{w} \equiv 0$$

and yet both $\mathbf{Dzn}_K(\boldsymbol{u}_{\text{lin}})$ (for any $K < I$) and $\tilde{\boldsymbol{d}}_1$ are not in $\mathcal{L}_2$ — for example, a persistent signal which makes $\lim_{t\to\infty} \boldsymbol{u}_{\text{lin}}(t) = 1$. We propose to use the latter type of set, to permit the use of the local stability analysis methods which we derived in Section 3.4.

Our basic framework is then the interconnection shown in Figure 5.15, which for disturbances only on $\tilde{\boldsymbol{d}}_1$ corresponds to the interconnection discussed in Section 3.4.1 with $\boldsymbol{z} = \tilde{\boldsymbol{d}}_1$ and

$$\begin{aligned} F &= CSP_{\text{lin}} \\ G &= M_0 Q^{-1} - I \end{aligned}$$

The only restriction on the application of the local stability analysis method presented in Section 3.4.1 is that $F = CSP_{\text{lin}}$ must be strictly proper, which simply requires that either C or P_{lin} be strictly proper — not an unreasonable assumption. Provided this assumption is satisfied, then we may use those methods to determine a number $Z^{\text{opt}}_{[F,G]} \geq 1$ such that the interconnection in Figure 5.15 is *locally stable* with respect to the set of disturbances

$$\left\{ z : \|z\|_2 < \tfrac{1}{\|F\|_2} Z^{\text{opt}}_{[F,G]} \right\}$$

Moreover, as mentioned at the end of Chapter 3, it is often possible to obtain significantly less conservative results from the local stability analysis procedure by considering a family of suitable "loop transformations", each of which gives rise to a new interconnection of the form discussed in Section 3.4.2 with different F, G and Δ.

[4] Recall that for "critically stable" plants it *may* be possible to achieve BIBO stability, but that finite gain stability is not possible.

One synthesis method would be to directly search over $Q \in \mathcal{Q}$ for the largest such set of permitted disturbances, however this is likely to be computationally inefficient.

An alternative to the direct search would be to recall that the results of Section 3.4.1 indicated the importance of two simple quantities

$$\mu := \|G\|_\infty \quad \text{and}$$
$$\rho := \frac{\|F\|_\infty \|G\|_2}{\|F\|_2}$$

Since F is fixed (by C, P_{lin} and P_{act}) we see that these two quantities are simply proportional to $\|M_0Q^{-1} - I\|_\infty$ and $\|M_0Q^{-1} - I\|_2$ respectively.

Specifically, we showed that $Z^{\text{opt}}_{[F,G]} \geq Z^{\text{opt}}_{[\text{upper}]}$ where

$$Z^{\text{opt}}_{[\text{upper}]} = \begin{cases} \left(\frac{\sqrt{\rho(\mu-1)}+\sqrt{\mu-\rho}}{\sqrt{\rho(\mu-\rho)}+\sqrt{\mu-1}}\right)^2 \in (1, \frac{1}{\rho}) & \text{if } \rho < 1 \\ 1 & \text{otherwise} \end{cases}$$

which suggests that keeping both $\|M_0Q^{-1} - I\|_\infty$ and $\|M_0Q^{-1} - I\|_2$ small is desirable.

In Theorem 2.4 we indicated the fundamental limitations on these quantities:

$$\inf_{Q \in \mathcal{Q}} \left\|M_0Q^{-1} - I\right\|_\infty = 1$$
$$\inf_{Q \in \mathcal{Q}} \left\|M_0Q^{-1} - I\right\|_2 = \sqrt{2\sum p_i}$$

where p_i are the right-half-plane poles of P. Furthermore, in Theorem 2.9 and Corollary 2.10 we indicated how to obtain a sub-optimal solution to

$$\min_{Q^{-1} \in \mathcal{RH}_\infty : \|M_0Q^{-1} - I\|_\infty < \gamma} \left\|M_0Q^{-1} - I\right\|_2$$

which, although it does not guarantee that $Q \in \mathcal{RH}_\infty$, nevertheless seems to be reasonable in use.

Appendix A illustrates the main points of the synthesis method for unstable plants with input saturation by means of a design example.

5.3.2 System with rate-limited actuator

The approach in this section will almost exactly parallel that in Section 5.3.1. To avoid unnecessary duplication, some of the implementational issues are not discussed fully here; the reader is referred to Section 5.3.1 for the details.

Implementation of nonlinear precompensator

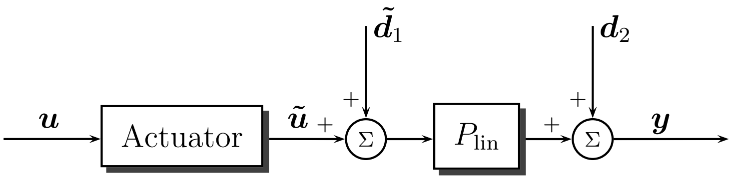

Figure 5.16: Model of rate-limited actuator and plant

Figure 5.16 shows our assumed model of a (possibly unstable) linear plant $P_{\text{lin}} \in \mathcal{R}_p^{n_y \times n_u}$ with rate-limited actuator. We make the same assumptions as in Sections 4.1.2 and 4.3.2, ie

$$\boldsymbol{y} = \begin{cases} P_{\text{lin}}(P_{\text{act}}\tilde{\boldsymbol{u}} + \tilde{\boldsymbol{d}}_1) + \boldsymbol{d}_2 & \text{if } P_{\text{act}}\boldsymbol{u} \in \mathfrak{R}_B \\ \text{undefined} & \text{otherwise} \end{cases}$$

for some (stable) nominal actuator dynamics $P_{\text{act}}(s) \in \mathcal{RH}_\infty^{n_u \times n_u}$ and diagonal matrix $B > 0$.

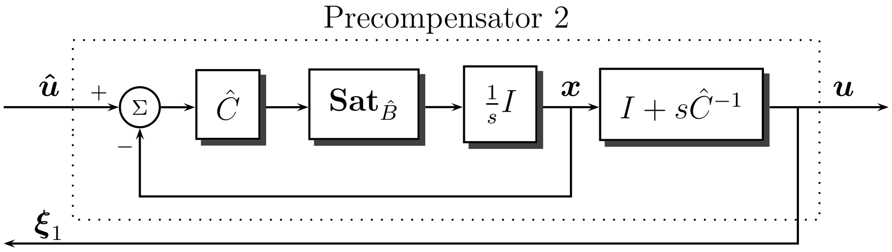

Figure 5.17: Precompensator 2

We saw in Section 4.3.2 that Precompensator 2 (with parameters $\hat{B} > 0$ and $\hat{C} > 0$) is a suitable precompensator for a rate-limited actuator with nominal dynamics $P_{\text{act}}(s)$ satisfying

$$\text{Diag}\{\tfrac{s+\hat{c}_i}{\hat{c}_i}\}P_{\text{act}}(s) = \text{Diag}\{q_1(s), q_2(s), \cdots, q_{n_u}(s)\}$$

with $\|q_i(s)\|_1 \leq 1$ for each $i \in \{1, 2, \cdots, n_u\}$, so long as the diagonal matrices $\hat{B}, \hat{C} > 0$ satisfy

$$B\hat{B}^{-1} \geq I \quad \text{and} \quad B\hat{B}^{-1} \geq 2C\hat{C}^{-1} - I$$

(In particular, this is true for first-order dynamics $P_{\text{act}}(s) = \text{Diag}\{\frac{c_1}{s+c_1}, \frac{c_2}{s+c_2}, \cdots, \frac{c_{n_u}}{s+c_{n_u}}\}$, which we conjecture is often the appropriate $P_{\text{act}}(s)$ for a rate-limited actuator.)

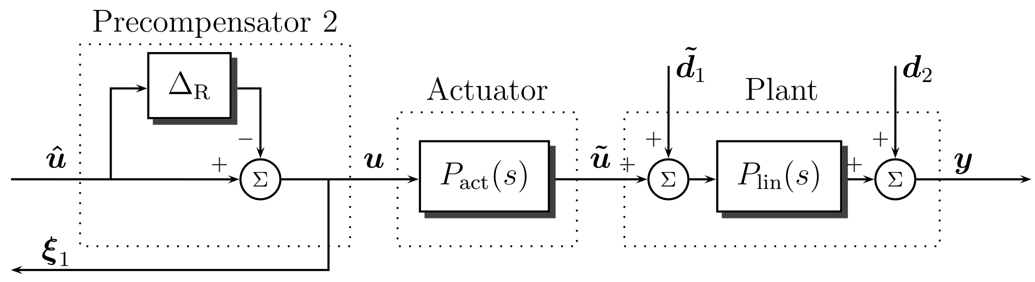

Figure 5.18: Precompensator 2, rate-limited actuator and linear plant

Since Precompensator 2 ensures that $P_\mathrm{act}\hat{\boldsymbol{u}} \in \mathfrak{R}_B$, we may represent the resulting interconnection of precompensator, actuator and plant as shown in Figure 5.18, where $\|\Delta_\mathrm{R}\| \le 1+\sqrt{2}$; note that this interconnection has only *one* nonlinear element, and that the signal $\boldsymbol{\xi}_1$ is exactly measurable.

Implementation of anti-windup compensator

As in Section 5.3.1 we define $P(s) := P_\mathrm{lin}(s)P_\mathrm{act}(s)$ and $\boldsymbol{d}_1 := P_\mathrm{act}^{-1}\tilde{\boldsymbol{d}}_1$, and consider $\boldsymbol{d}_1$ instead of $\tilde{\boldsymbol{d}}_1$, entering just *before* the actuator dynamics $P_\mathrm{act}(s)$. This gives a system of the form considered in Section 5.2.2 (cf. Figure 5.6)

For such a system we stated a coprime factor parametrisation of anti-windup controllers: given initial left- and right-coprime factorisations $C = \tilde{V}_0^{-1}\tilde{U}_0$ and $P = N_0 M_0^{-1}$ satisfying the Bezout identity (Equation 5.1) the anti-windup controller is given by

$$\hat{\boldsymbol{u}} = Q\tilde{U}_0\boldsymbol{e} + (I - Q\tilde{V}_0)\boldsymbol{\xi}_1$$

parametrised by $Q \in \mathcal{Q}$ (Equation 2.5) such that $Q(\infty) = M_0(\infty)$.

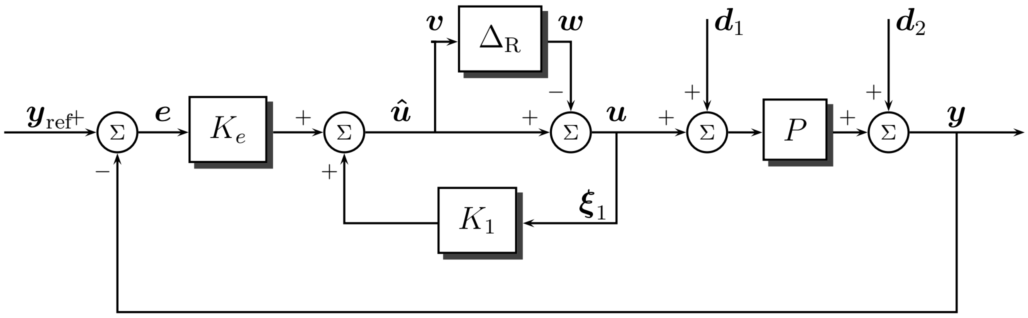

Figure 5.19: System with Precompensator 2 and coprime factor anti-windup controller

The resulting closed-loop interconnection, shown in Figure 5.19, can be described by the following LFT on $\boldsymbol{\Delta}_{\mathrm{R}}$:

$$\begin{bmatrix}\begin{bmatrix}\boldsymbol{e}\\ \boldsymbol{y}\\ \boldsymbol{u}\end{bmatrix}\\ \boldsymbol{v}\end{bmatrix} = \begin{bmatrix}\begin{bmatrix} S & -SP_{\mathrm{lin}} & -S\\ I-S & SP_{\mathrm{lin}} & S\\ CS & -CSP_{\mathrm{lin}} & -CS\end{bmatrix} & \begin{bmatrix} N_0Q^{-1}\\ -N_0Q^{-1}\\ -M_0Q^{-1}\end{bmatrix}\\ \begin{bmatrix} CS & -CSP_{\mathrm{lin}} & -CS\end{bmatrix} & I-M_0Q^{-1}\end{bmatrix}\begin{bmatrix}\begin{bmatrix}\boldsymbol{y}_{\mathrm{ref}}\\ \tilde{\boldsymbol{d}}_1\\ \boldsymbol{d}_2\end{bmatrix}\\ \boldsymbol{w}\end{bmatrix}$$

$$\boldsymbol{w} = \boldsymbol{\Delta}_{\mathrm{R}}(\boldsymbol{v})$$

where $S := (I+PC)^{-1}$. (Note that this relation is given in terms of the real disturbance $\tilde{\boldsymbol{d}}_1$)

It will be seen immediately that this is similar to the closed-loop system obtained in the case of a magnitude limitation (Figure 5.14), although the nonlinear perturbation is substantially different (and, importantly, has a possibly larger $\mathcal{L}_2$-$\mathcal{L}_2$ gain.)

Anti-windup compensator synthesis

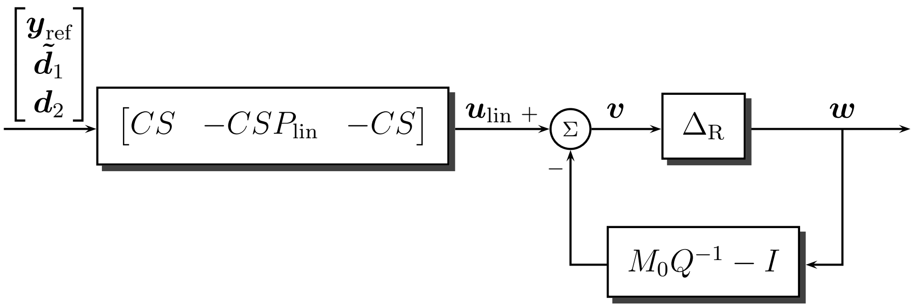

Figure 5.20: Representation of Figure 5.19 for stability analysis

For *stability* analysis we need consider only the simpler interconnection of Figure 5.20. The signals $\boldsymbol{e}, \hat{\boldsymbol{u}}, \boldsymbol{u}$ and $\boldsymbol{y}$ in Figure 5.19 are then simply given in terms of the nominal linear response of Figure 5.1 and $\boldsymbol{w}$, the output of the nonlinearity Δ_{R} in Figure 5.20:

$$\boldsymbol{e} - \boldsymbol{e}_{\mathrm{lin}} = N_0Q^{-1}\boldsymbol{w} \tag{5.6}$$

$$\hat{\boldsymbol{u}} - \boldsymbol{u}_{\mathrm{lin}} = (I - M_0Q^{-1})\boldsymbol{w} \tag{5.7}$$

$$\boldsymbol{u} - \boldsymbol{u}_{\mathrm{lin}} = -M_0Q^{-1}\boldsymbol{w} \tag{5.8}$$

$$\boldsymbol{y} - \boldsymbol{y}_{\mathrm{lin}} = -N_0Q^{-1}\boldsymbol{w} \tag{5.9}$$

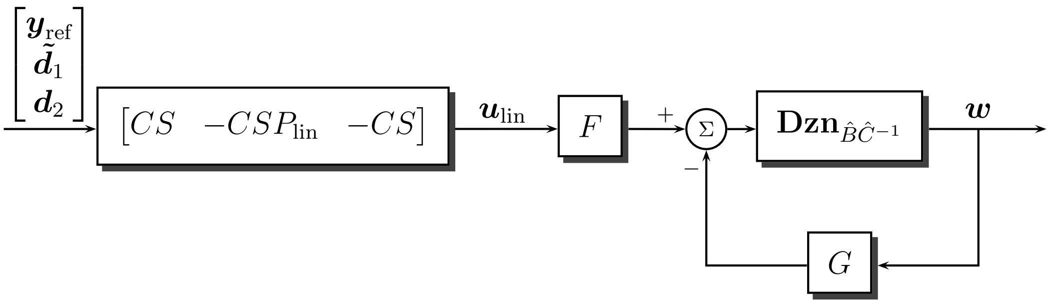

Figure 5.21: Alternative representation of Figure 5.20

Furthermore, if we use the representation of Δ_{R} from Figure 4.21, then Figure 5.20 is equivalent to Figure 5.21, where

$$F = \text{Diag}\{\tfrac{s}{s+c_i}\} \quad \text{and}$$
$$G = \text{Diag}\{\tfrac{s}{s+\hat{c}_i}\}M_0Q^{-1} - I$$

Note that the output of the nonlinearity is again $\boldsymbol{w}$.

By comparing Figures 5.21 and 5.15 it may be seen that applying the methods of Section 5.3.1 for the linear plant

$$P_1 = \left\{P\,\text{Diag}\{\tfrac{s+\hat{c}_i}{s}\}\right\} = \left\{N_0\right\}\left\{\,\text{Diag}\{\tfrac{s}{s+\hat{c}_i}\}M_0\right\}^{-1}$$

would result in Figure 5.15 having the same nonlinearity, and the same feedback element $\text{Diag}\{\frac{s}{s+\hat{c}_i}\}M_0Q^{-1} - I$, as Figure 5.21. Hence we conclude that Problem 5.1 for rate-limited systems is very closely related to the same problem for magnitude-limited systems.

Specifically, the problem of stabilising the rate-limited system with linear plant P must be equivalent to the problem of stabilising the magnitude-limited system with linear plant $P_1 = \left\{P\,\text{Diag}\{\frac{s+\hat{c}_i}{s}\}\right\}$. Note that P_1 is always unstable, and that if P has any open right half-plane poles, then P_1 has them too.

Theorem 5.6

Given $C = \tilde{V}_0^{-1}\tilde{U}_0$ and $P = N_0M_0^{-1}$ satisfying the Bezout identity (Equation 5.1), and with respect to the interconnection of Figure 5.19:

- *If **all** poles of P are in the open left half-plane then there exists at least one $Q \in \mathcal{Q}$ which solves Problem 5.1 and which satisfies $Q(\infty) = M_0(\infty)$*
- *If **any** poles of P are in the open right half-plane then there does not exist any $Q \in \mathcal{Q}$ which solves Problem 5.1 and which satisfies $Q(\infty) = M_0(\infty)$*

PROOF OF THEOREM 5.6:

If *all* poles of P are in the open left half-plane then it is clear, by Proposition 3.7, that the interconnection can be stabilised by choosing $Q = M_0$.

If *any* poles of P are in the open right half-plane then (by comparison with the problem of stabilising Figure 5.15 for the *unstable* linear plant $P_1 = P\,\mathrm{Diag}\{\frac{s+\hat{c}_i}{s}\}$) we conclude by Proposition 5.2 that Problem 5.1 cannot be solved. ∎

Case I: stable P

Theorem 5.6 indicates that for any stable P, there is at least one solution to Problem 5.1; we now consider synthesising Q to optimise a suitable performance measure while guaranteeing global stability of the interconnection. We consider the same performance criteria as in Section 5.3.1:

- By comparison with Miyamoto & Vinnicombe [MV96b], we propose to minimise the $\mathcal{L}_2$ gain from $\hat{\boldsymbol{u}}-\boldsymbol{u}$ $(=\boldsymbol{w})$ to the difference between the actual and nominal outputs $\boldsymbol{y}-\boldsymbol{y}_{\mathrm{lin}}$, modified by some suitable weight W. This corresponds to minimising $\|WN_0Q^{-1}\|_\infty$ subject to maintaining global stability, which can be guaranteed by ensuring that $\|I - M_0Q^{-1}\|_\infty < \frac{1}{1+\sqrt{2}}$:

  Theorem 5.7

  For stable plant P and any weight W such that $W, W^{-1} \in \mathcal{RH}_\infty$ and

  $$\|WP\|_\infty < \frac{1}{\left(2+\sqrt{8}\right)^{\frac{1}{2}}}$$

  there always exists $Q \in \mathcal{Q}$ such that

  $$\left\| \begin{bmatrix} WN_0Q^{-1} \\ M_0Q^{-1} - I \end{bmatrix} \right\|_\infty < \frac{1}{1+\sqrt{2}}$$

  and $M_0Q^{-1}(\infty) = I$; such a Q then solves Problem 5.1.

  Remark

  1. A suitable solution to Theorem 5.7 may be obtained in an identical manner to that discussed in the *remarks* following Theorem 5.5.

  PROOF OF THEOREM 5.7:

  It is shown by Miyamoto & Vinnicombe [MV96b] that

  $$\inf_{Q\in\mathcal{Q}} \left\| \begin{bmatrix} WN_0Q^{-1} \\ M_0Q^{-1} - I \end{bmatrix} \right\|_\infty = \frac{\|WP\|_\infty}{\sqrt{1+\|WP\|_\infty^2}}$$

  from which the maximum permitted size of $\|WP\|_\infty$ follows immediately. ∎

- The appropriate version of the performance criterion of Teel & Kapoor [TK97] would be to consider the $\mathcal{L}_2$ gain from $\Delta_{\mathrm{R}}(\boldsymbol{u}_{\mathrm{lin}})$ to $\boldsymbol{u} - \boldsymbol{u}_{\mathrm{lin}}$ or $\boldsymbol{y} - \boldsymbol{y}_{\mathrm{lin}}$. At the present time this is not a feasible problem, because there is no simple way to relate $\boldsymbol{w}$ to $\Delta_{\mathrm{R}}(\boldsymbol{u}_{\mathrm{lin}})$. However, we *can* state that the unmodified IMC scheme (see Zheng *et al* [ZKM94]), which sets $Q = M_0$, will achieve the following level of performance with respect to this criterion:

$$\begin{aligned} \|\boldsymbol{u} - \boldsymbol{u}_{\mathrm{lin}}\|_2 &\leq \|\Delta_{\mathrm{R}}(\boldsymbol{u}_{\mathrm{lin}})\|_2 \quad \text{and} \\ \|\boldsymbol{y} - \boldsymbol{y}_{\mathrm{lin}}\|_2 &\leq \|P\|_\infty \|\Delta_{\mathrm{R}}(\boldsymbol{u}_{\mathrm{lin}})\|_2 \end{aligned}$$

  which may be (by comparison to Theorem 5.3) the minimum achievable.

- An attractive alternative, although one which has no strong physical justification, would be to consider the $\mathcal{L}_2$ gain from $\mathbf{Dzn}_{\hat{B}\hat{C}^{-1}}(F\boldsymbol{u}_{\mathrm{lin}})$ to $\boldsymbol{u} - \boldsymbol{u}_{\mathrm{lin}}$ or $\boldsymbol{y} - \boldsymbol{y}_{\mathrm{lin}}$ (see Figure 5.21); unfortunately we cannot use the small-gain or circle criteria to show stability of the interconnection in Figure 5.21 since $G(0) = I$.

  Nevertheless, since we know that there exists at least one stabilising Q for this interconnection, it may be possible in future to formulate a tractable synthesis problem with respect to this performance criterion.

Case II: unstable P

In a similar manner to Case II in the case of a magnitude-limited actuator, we see that the local stability analysis methods of Section 3.4 may be applied to the interconnection in Figure 5.21 if (assuming a disturbance on $\tilde{\boldsymbol{d}}_1$ only) $\mathrm{Diag}\{\frac{s}{s+c_i}\}CSP_{\mathrm{lin}}$ is strictly proper.

Both of the proposed optimisation methods in that case may therefore be applied in this case also, ie direct search over $Q \in \mathcal{Q}$ for the largest set of admissable disturbances, or the mixed-norm minimisation of $\|G\|_\infty$ and $\|G\|_2$

5.3.3 System with rate- and magnitude-limited actuator

The approach in this section will almost exactly parallel that in Section 5.3.1. To avoid unnecessary duplication, some of the implementational issues are not discussed fully here; the reader is referred to Section 5.3.1 for the details.

Implementation of nonlinear precompensator

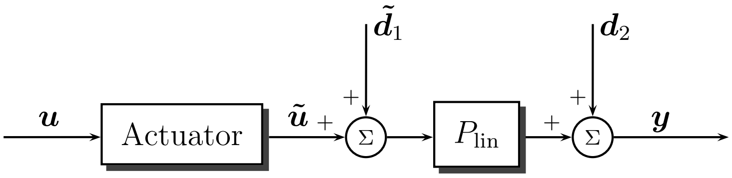

Figure 5.22: Model of rate- and magnitude-limited actuator and plant

Figure 5.22 shows our assumed model of a (possibly unstable) linear plant $P_{\text{lin}} \in \mathcal{R}_p^{n_y \times n_u}$ with rate- and magnitude-limited actuator. We make the same assumptions as in Sections 4.1.2 and 4.3.3, ie that

$$\boldsymbol{y} = \begin{cases} P_{\text{lin}}(P_{\text{act}}\tilde{\boldsymbol{u}} + \tilde{\boldsymbol{d}}_1) + \boldsymbol{d}_2 & \text{if } P_{\text{act}}\boldsymbol{u} \in \mathfrak{R}_B \cap \mathfrak{M}_A \\ \text{undefined} & \text{otherwise} \end{cases}$$

for some (stable) nominal actuator dynamics $P_{\text{act}}(s) \in \mathcal{RH}_\infty^{n_u \times n_u}$ and diagonal matrices $A, B > 0$.

We saw in Section 4.3.3 that a series composition of Precompensators 1 & 2 (with parameters $\hat{A} > 0$, $\hat{B} > 0$ and $\hat{C} > 0$) is a suitable precompensator for a rate- and magnitude-limited actuator with nominal dynamics $P_{\text{act}}(s)$ satisfying

$$\begin{aligned} P_{\text{act}}(s) &= \text{Diag}\{p_1(s), p_2(s), \cdots, p_{n_u}(s)\} \quad \text{and} \\ \text{Diag}\{\tfrac{s+\hat{c}_i}{\hat{c}_i}\}P_{\text{act}}(s) &= \text{Diag}\{q_1(s), q_2(s), \cdots, q_{n_u}(s)\} \end{aligned}$$

with $\|p_i(s)\|_1 \leq 1$ and $\|q_i(s)\|_1 \leq 1$ for each $i \in \{1, 2, \cdots, n_u\}$, so long as the diagonal matrices $\hat{A}, \hat{B}, \hat{C} > 0$ satisfy

$$A\hat{A}^{-1} \geq I \quad \text{and} \quad B\hat{B}^{-1} \geq I \quad \text{and} \quad B\hat{B}^{-1} \geq 2C\hat{C}^{-1} - I$$

(In particular, the assumption on $P_{\text{act}}(s)$ is true for first-order nominal dynamics $P_{\text{act}} = \text{Diag}\{\frac{c_1}{s+c_1}, \frac{c_2}{s+c_2}, \cdots, \frac{c_{n_u}}{s+c_{n_u}}\}$, which we conjecture is often the appropriate $P_{\text{act}}(s)$ for a rate- and magnitude-limited actuator.)

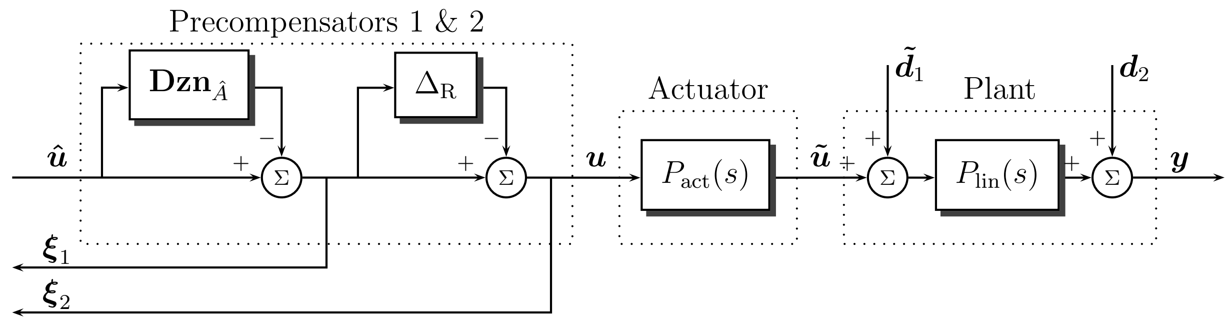

Figure 5.23: Precompensators 1 & 2 , rate- & magnitude-limited actuator and linear plant

Since Precompensators 1 & 2 ensure that $P_{\mathrm{act}}\hat{\boldsymbol{u}} \in \mathfrak{M}_A \cap \mathfrak{R}_B$, we may represent the resulting interconnection of precompensator, actuator and plant as shown in Figure 5.23, where $\|\Delta_{\mathrm{R}}\| \leq 1+\sqrt{2}$; note that this interconnection has only *two* nonlinear elements, and that the signals $\boldsymbol{\xi}_1$ and $\boldsymbol{\xi}_2$ are exactly measurable.

Implementation of anti-windup compensator

As in Section 5.3.1 we define $P(s) := P_{\mathrm{lin}}(s)P_{\mathrm{act}}(s)$ and $\boldsymbol{d}_1 := P_{\mathrm{act}}^{-1}\tilde{\boldsymbol{d}}_1$, and consider $\boldsymbol{d}_1$ instead of $\tilde{\boldsymbol{d}}_1$, entering just *before* the actuator dynamics $P_{\mathrm{act}}(s)$. This gives a system of the form considered in Section 5.2.3 (cf. Figure 5.8)

For such a system we stated a coprime factor parametrisation of anti-windup controllers: given initial left- and right-coprime factorisations $C = \tilde{V}_0^{-1}\tilde{U}_0$ and $P = N_0M_0^{-1}$ satisfying the Bezout identity (Equation 5.1) the anti-windup controller is given by

$$\hat{\boldsymbol{u}} = Q_1\tilde{U}_0\boldsymbol{e} + (I - Q_1Q_2^{-1})\boldsymbol{\xi}_1 + (I - Q_2\tilde{V}_0)\boldsymbol{\xi}_2$$

parametrised by $Q_1, Q_2 \in \mathcal{Q}$ (Equation 2.5) such that $Q_1(\infty) = Q_2(\infty) = M_0(\infty)$.

The resulting closed-loop interconnection, shown in Figure 5.24, can be described by the following LFT on $\begin{bmatrix}\mathbf{Dzn}_{\hat{A}} & 0\\ 0 & \Delta_{\mathrm{R}}\end{bmatrix}$:

$$\begin{bmatrix}\begin{bmatrix}\boldsymbol{e}\\ \boldsymbol{y}\\ \boldsymbol{u}\end{bmatrix}\\ \begin{bmatrix}\boldsymbol{v}_1\\ \boldsymbol{v}_2\end{bmatrix}\end{bmatrix} = \begin{bmatrix}\begin{bmatrix}S & -SP_{\mathrm{lin}} & -S\\ I-S & SP_{\mathrm{lin}} & S\\ CS & -CSP_{\mathrm{lin}} & -CS\end{bmatrix} & \begin{bmatrix}N_0Q_1^{-1} & N_0Q_1^{-1}\\ -N_0Q_2^{-1} & -N_0Q_2^{-1}\\ -M_0Q_1^{-1} & -M_0Q_2^{-1}\end{bmatrix}\\ \begin{bmatrix}CS & -CSP_{\mathrm{lin}} & -CS\\ CS & -CSP_{\mathrm{lin}} & -CS\end{bmatrix} & \begin{bmatrix}I-M_0Q_1^{-1} & I-M_0Q_2^{-1}\\ -M_0Q_1^{-1} & I-M_0Q_2^{-1}\end{bmatrix}\end{bmatrix}\begin{bmatrix}\begin{bmatrix}\boldsymbol{y}_{\mathrm{ref}}\\ \tilde{\boldsymbol{d}}_1\\ \boldsymbol{d}_2\end{bmatrix}\\ \begin{bmatrix}\boldsymbol{w}_1\\ \boldsymbol{w}_2\end{bmatrix}\end{bmatrix}$$

$$\begin{bmatrix}\boldsymbol{w}_2\\ \boldsymbol{w}_2\end{bmatrix} = \begin{bmatrix}\mathbf{Dzn}_{\hat{A}} & 0\\ 0 & \Delta_{\mathrm{R}}\end{bmatrix}\begin{bmatrix}\boldsymbol{v}_1\\ \boldsymbol{v}_2\end{bmatrix}$$

where $S := (I+PC)^{-1}$. (Note that this relation is given in terms of the real disturbance $\tilde{\boldsymbol{d}}_1$)

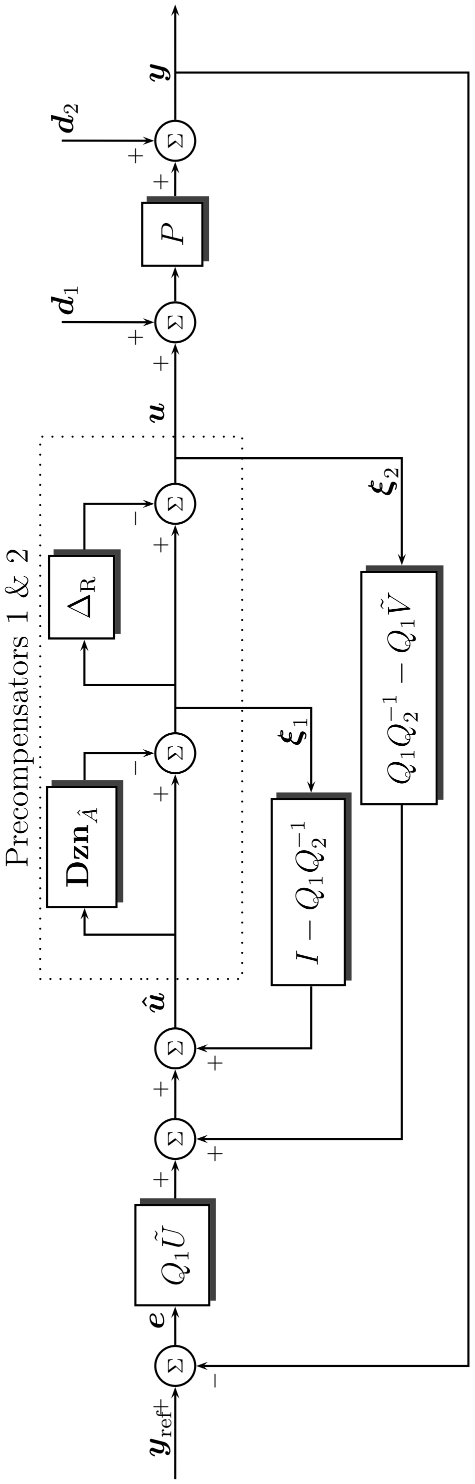

Figure 5.24: System with Precompensators 1 & 2 and coprime factor anti-windup controller

Anti-windup compensator synthesis

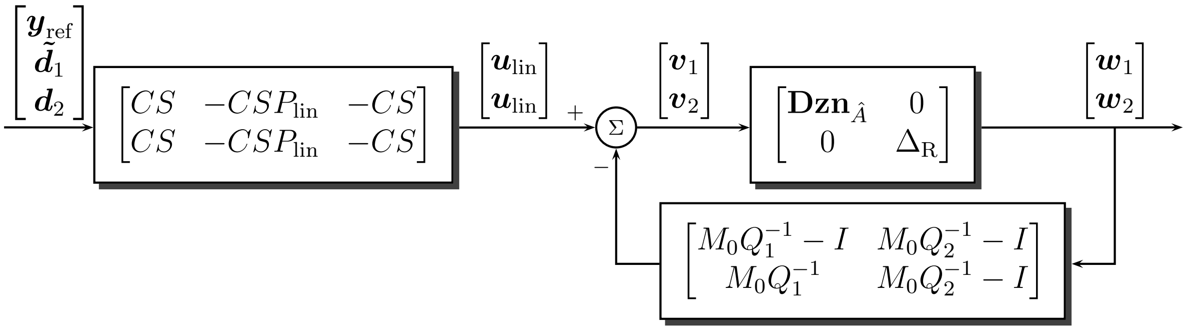

Figure 5.25: Representation of Figure 5.24 for stability analysis

For *stability* analysis we need consider only the simpler interconnection of Figure 5.25. The signals $\boldsymbol{e}, \hat{\boldsymbol{u}}, \boldsymbol{u}$ and $\boldsymbol{y}$ in Figure 5.24 are then simply given in terms of the nominal linear response of Figure 5.1 and $\boldsymbol{w}$, the output of the nonlinearity in Figure 5.25:

$$\boldsymbol{e} - \boldsymbol{e}_{\mathrm{lin}} = N_0Q_1^{-1}\boldsymbol{w}_1 + N_0Q_2^{-1}\boldsymbol{w}_2 \tag{5.10}$$

$$\hat{\boldsymbol{u}} - \boldsymbol{u}_{\mathrm{lin}} = (I - M_0Q_1^{-1})\boldsymbol{w}_1 + (I - M_0Q_2^{-1})\boldsymbol{w}_2 \tag{5.11}$$

$$\boldsymbol{u} - \boldsymbol{u}_{\mathrm{lin}} = -M_0Q_1^{-1}\boldsymbol{w}_1 - M_0Q_2^{-1}\boldsymbol{w}_2 \tag{5.12}$$

$$\boldsymbol{y} - \boldsymbol{y}_{\mathrm{lin}} = -N_0Q_1^{-1}\boldsymbol{w}_1 - N_0Q_2^{-1}\boldsymbol{w}_2 \tag{5.13}$$

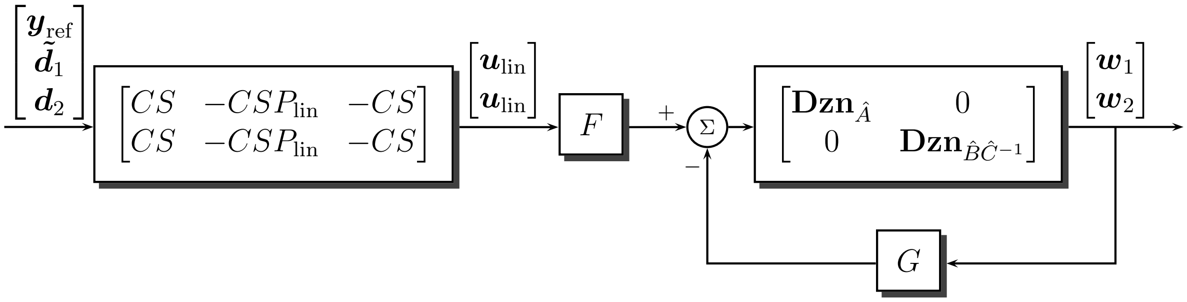

Figure 5.26: Equivalent representation of Figure 5.25

Furthermore, if we use the representation of Δ_{R} from Figure 4.21, then Figure 5.25 is equivalent to Figure 5.26, where

$$F = \begin{bmatrix} I & 0 \\ 0 & \mathrm{Diag}\{\frac{s}{s+\hat{c}_i}\} \end{bmatrix} \quad \text{and}$$

$$G = \begin{bmatrix} M_0Q_1^{-1} - I & M_0Q_2^{-1} - I \\ \mathrm{Diag}\{\frac{s}{s+\hat{c}_i}\}M_0Q_1^{-1} & \mathrm{Diag}\{\frac{s}{s+\hat{c}_i}\}M_0Q_2^{-1} - I \end{bmatrix}$$

Note that the output of the nonlinearity is again $\boldsymbol{w}$.

Theorem 5.8

Given $C = \tilde{V}_0^{-1}\tilde{U}_0$ and $P = N_0 M_0^{-1}$ satisfying the Bezout identity (Equation 5.1), and with respect to the interconnection of Figure 5.24:

- *If **all** poles of P are in the open left half-plane then there exists at least one pair $Q_1, Q_2 \in \mathcal{Q}$ which solve Problem 5.1 and which satisfy $Q_1(\infty) = Q_2(\infty) = M_0(\infty)$*
- *If **any** poles of P are in the open right half-plane then there does not exist a pair $Q_1, Q_2 \in \mathcal{Q}$ which solve Problem 5.1 and which satisfy $Q_1(\infty) = Q_2(\infty) = M_0(\infty)$*

PROOF OF THEOREM 5.8:

If *all* poles of P are in the open left half-plane then it is clear, by Proposition 3.8, that the interconnection can be stabilised by choosing $Q_1 = Q_2 = M_0$.

If *any* poles of P are in the open right half-plane then (by comparison with Proposition 5.2 and Theorem 5.6) we cannot stabilise the interconnection with either of the nonlinearities $\mathbf{Dzn}_{\hat{A}}$ or Δ_{R} individually. (Imagine relaxing one of the two limitations to a sufficiently large number so that the limitation is inactive.) Hence we deduce that it is impossible to stabilise both simultaneously. ∎

Case I: stable P

Theorem 5.8 indicates that for any stable P, there is at least one solution to Problem 5.1, so we may like to consider synthesising Q to optimise a similar performance measure to those of Miyamoto & Vinnicombe [MV96b] or Teel & Kapoor [TK97], as discussed in Sections 5.3.1 and 5.3.2.

Unfortunately, the nature of the interconnections in Figures 5.25 and 5.26 are such that guaranteeing stability by the small-gain or circle criteria is not trivial — in fact, something similar to Proposition 3.8 will be necessary. The following synthesis method may be expected to work well in practice:[5]

For stable plant P and weight $W = \begin{bmatrix} W_1 & W_2 \end{bmatrix}$ such that $W, W^{-1} \in \mathcal{RH}_\infty$, and scalars $h_1, h_2 > 0$, solve the $\mathcal{H}_\infty$ minimisation problem

$$\inf_{Q_1, Q_2 \in \mathcal{Q}} \left\| \begin{matrix} \begin{bmatrix} W_1 N_0 Q_1^{-1} & W_2 N_0 Q_2^{-1} \end{bmatrix} \\ \begin{bmatrix} h_1 & 0 \\ 0 & h_2 \end{bmatrix} \begin{bmatrix} M_0 Q_1^{-1} - I & M_0 Q_2^{-1} - I \\ M_0 Q_1^{-1} & M_0 Q_2^{-1} - I \end{bmatrix} \begin{bmatrix} \frac{1}{h_1} & 0 \\ 0 & \frac{1}{h_2} \end{bmatrix} \begin{bmatrix} 1 & 0 \\ 0 & 1+\sqrt{2} \end{bmatrix} \end{matrix} \right\|_\infty$$

If solutions $Q_1, Q_2 \in \mathcal{Q}$ exist such that this infimum is less than unity, then these Qs will solve Problem 5.1

(Proof that such Qs would then solve Problem 5.1 is immediate by Proposition 3.8.)

[5]For any particular set of parameters W_1, W_2, h_1 & h_2 there is *no* guarantee that the infimum will be less than unity, however there *does* exist at least one set W_1, W_2, h_1 & h_2 for which $Q_1 = Q_2 = M_0$ (a choice which is known to solve Problem 5.1) achieves a $\mathcal{H}_\infty$-norm less than unity.

Note that this mimimisation may be posed, for given W_1, W_2, h_1 & h_2, as a standard $\mathcal{H}_\infty$ problem; this formulation must, however, be as a search over $Q_1^{-1}, Q_2^{-1} \in \mathcal{RH}_\infty$, and hence cannot guarantee $Q_1, Q_2 \in \mathcal{RH}_\infty$. Nevertheless, it may be hoped that this method is often suitable, with appropriate choice of the scalars h_1 and h_2.

Case II: unstable P

We do not consider the unstable case in any detail, since G in Figure 5.26 is not strictly proper. It may often be possible to use "D-scaling" or a similar method to obtain an equivalent representation with a strictly proper "G", however it cannot be guaranteed that the resulting "$\boldsymbol{\Delta}$" will be appropriate for applying the methods of Section 3.4.

We might expect that the mixed-norm minimisation of $\|G\|_\infty$ and $\|G\|_2$ may be useful, but no results in this area have been obtained to date.

5.3.4 Systems with other nonlinear actuators

Provided an input nonlinearity may be represented with a cascaded, bounded perturbation of the form discussed in Section 5.2.3, it will always be possible to stabilise the interconnection for stable plants, by using

$$Q_1 = Q_2 = \cdots = Q_{n_\xi} = M_0$$

which is the unmodified IMC scheme (see Zheng *et al* [ZKM94])

Moreover, it should always be possible to formulate a synthesis algorithm similar to that proposed in the case of a stable plant with rate- and magnitude-limited actuator, provided that the $\mathcal{L}_2$-$\mathcal{L}_2$ gain of the nonlinear perturbations are known.

5.4 Summary and suggestions for further work

5.4.1 Summary

In this chapter we have

- Motivated anti-windup compensation, to maintain nominal behaviour when the nonlinearities are inactive.
- Derived a general coprime factor parametrisation of anti-windup compensators for systems with input-additive nonlinear perturbations.
- Demonstrated how to combine a precompensator and anti-windup compensated controller to control a system with nonlinear actuator.
- Discussed synthesis for stable or unstable plants with magnitude- and/or rate-limited actuators.
- Given a number of synthesis methods for stable plants with limited-authority actuators, which guarantee global stability and performance in some suitable sense

5.4.2 Suggestions for further work

Anti-windup synthesis for magnitude limitations

Although the methods outlined in Section 5.3.1 are quite powerful, there are some plant/controller combinations for which the resulting closed-loop performs badly. Indeed, we have already commented that the IMC scheme is "optimal" in a certain $\mathcal{L}_2$ sense, but that it may behave poorly if the plant has slow modes.

Anti-windup synthesis for rate limitations

We have rather skimmed over the synthesis problem for plants with rate-limited actuators (and, by implication, plants with rate- and magnitude-limited actuators.) Many avenues of research in this area remain open.

In particular, it may be possible to formulate other stability and performance criteria (using, for example, IQCs [MR97] or other LMI-based methods); whether these criteria are suitable for synthesis remains to be seen.

Chapter 6

Conclusions and suggestions for further work

We have discussed three aspects of systems with nonlinear actuators, namely *global and local stability analysis*, *modelling & precompensation* and *anti-windup compensator synthesis*:

Global and local stability analysis

With respect to a simple nonlinear feedback loop (Figure 3.5) we have presented a global stability criterion for $[0, 1]$ sector-bounded nonlinearities which is based on the well-known circle criterion but which is expressed in terms of an $\mathcal{H}_\infty$-norm (Theorem 3.9); furthermore, if the nonlinearity is an ideal deadzone, then this result is extended to give an $\mathcal{L}_2$ gain inequality (Corollary 3.10.)

We then considered the local stability properties of the same loop with an ideal unity deadzone nonlinearity. A novel method for relating the $\mathcal{L}_2$-norms of the (time-truncated) input and output was presented, which was shown to hold even for *unstable* interconnections (Theorem 3.11); some of the consequences of this result were then elaborated upon in more detail.

This method was then shown to apply to a large class of "deadzone-like" nonlinearities (Theorem 3.20), from which all of the results for the ideal deadzone case were generalised. Some simple illustrative examples were then given.

Extension of this local stability analysis could continue in a number of directions. Firstly, the assumption that the external signal passes through a low-pass filter should be investigated, to see how restrictive this is in practice. Secondly, the level of conservatism in these results is unknown, but expected to be quite poor in some cases. Some examples to show the best- and worst-case scenarios would be very useful.

Finally, it is clear that many interconnections may be "loop-shifted" in various ways; each new representation may be analysed separately, and by combining the results, a less conservative conclusion may be drawn. The practical use of this method, including useful "loop shifts" should be demonstrated by some case studies of both stable and unstable systems.

Modelling & precompensation of nonlinear actuators

A two-element model comprising a linear plant and nonlinear actuator was presented (Figure 4.1) for which we presented a number of physically-motivated assumptions regarding its behaviour.

In order to take account of the nonlinearity introduced by the actuator, and to avoid problems associated with direct measurement and/or modelling of the actuator, we proposed to implement a nonlinear precompensator *within* the controller (Figure 4.2) to ensure that the actuator remains within its nominal region of linear operation.

Suitable precompensators for actuators with magnitude, rate and both rate & magnitude limitations were proposed (Figures 4.6, 4.19 & 4.22 respectively) and shown to have a number of desirable properties (Theorems 4.6, 4.7 and 4.8 respectively.)

This method of precompensating for the nonlinear actuator is practically unknown in the literature, and this must therefore be considered a preliminary investigation. Many more types of actuator nonlinearity, including non-decentralised models and limitations on higher derivatives or other internal variables, should be considered; moreover, the behaviour of these devices has not yet been tried in practice (with the obvious caveat that all Digital-to-Analogue Convertors implicitly saturate their output.)

Anti-windup compensator synthesis

We have motivated the problem of compensating for input nonlinearities (Figures 5.1 and 5.2) and defined global and local stabilisation problems (Problems 5.1 and 5.2 respectively.) A parametrisation of anti-windup compensators based on coprime factors was then presented and shown to be suitable for a general class of cascaded input nonlinearities.

Using this parametrisation, we then discussed the synthesis problem for systems with magnitude-limited, rate-limited and both rate- & magnitude-limited actuators:

For magnitude-limited actuators, we have indicated the fundamental limits on achievable stability and performance (Proposition 5.2 and Theorem 5.3), and shown for *open-loop stable* systems that global stability and a certain guaranteed level of $\mathcal{L}_2$ performance can be achieved (Theorem 5.5.) This was followed by a brief discussion of the applicability of the local stability results of Chapter 3 to the open-loop unstable case.

For rate-limited actuators, the synthesis problem was shown to be closely related to the magnitude-limited case, with similar limitations (Theorem 5.6) and a synthesis procedure for *open-loop stable* systems was given (Theorem 5.7) which guarantees global stability. For open-loop unstable systems the local stability analysis method was again shown to be applicable in certain cases.

The case of the combined rate- & magnitude-limited actuator was discussed, and fundamental limitations were again deduced (Theorem 5.8.) A synthesis procedure for globally stabilising open-loop stable systems was proposed. This procedure depends on a number of scalar parameters, and for a given set of parameters is not guaranteed to have a solution; there does, however, exist at least one set of parameters for which there is a stabilising solution.

With the exception of the synthesis method for open-loop stable systems with magnitude-limiting, these synthesis procedures remain largely untested, either by simulation or practical implementation. Moreover, it is known that the $\mathcal{L}_2$ performance criterion is not always certain to produce acceptable results in practice; for example, the IMC scheme is "optimal" in one $\mathcal{L}_2$ sense, but has been observed to behave poorly for some plants. It is not clear whether good results can be achieved with simple weighting, nor indeed how one might choose the weights in general.

Bibliography

[AD96] F. Albertini and D. D'Alessandro. Asymptotic stability of continuous-time systems with saturation nonlinearities. *Systems & Control Letters*, 29:175–180, 1996.

[AR89] K. J. Astrom and L. Rundquist. Integrator windup and how to avoid it. In *Proceedings of the American Control Conference*, 1989.

[ASA93] J. Alvarez, R. Suarez, and J. Alvarez. Planar linear systems with single saturated feedback. *Systems & Control Letters*, 20:319–326, 1993.

[Bal95] V. Balakrishnan. Linear matrix inequalities in robustness analysis with multipliers. *Systems & Control Letters*, 25:265–272, 1995.

[BGFB94] S. Boyd, L. El Ghaoui, E. Feron, and V. Balakrishnan. *Linear Matrix Inequalities in System and Control Theory.* Society for Industrial and Applied Mathematics, 1994.

[BH89] D. S. Bernstein and W. M. Haddad. LQG control with an $\mathcal{H}_\infty$ performance bound: a Riccati euqation approach. *IEEE Transactions on Automatic Control*, 34:293–305, 1989.

[CM90] P. J. Campo and M. Morari. Robust control of processes subject to saturation nonlinearities. *Computers and chemical engineering*, 14(4-5):343–358, 1990.

[Cra99] S. Crawshaw. Local stability analysis of nonlinear systems. In *Proceedings of the 38th IEEE Conference on Decision & Control*, 1999.

[CV98] S. Crawshaw and G. Vinnicombe. Local stability properties of systems with saturation and deadzone nonlinearities. In *Proceedings of the 37th IEEE Conference on Decision & Control*, 1998.

[D'A96] R. D'Andrea. *Generalizations of H-infinity optimization / Control of rotating stall.* PhD thesis, California Institute of Technology, 1996.

[D'A99] R. D'Andrea. Generalised l_2 synthesis. *IEEE Transactions on Automatic Control*, 44(6):1145–1156, 1999.

[DFT92] J. C. Doyle, B. A. Francis, and A. R. Tannenbaum. *Feedback Control Theory.* Macmillan, 1992.

[EP97] C. Edwards and I. Postlethwaite. Anti-windup schemes with closed-loop stability considerations. In *Proceedings of the European Control Conference*, 1997.

[EP98] C. Edwards and I. Postlethwaite. Anti-windup and bumpless-tranfer schemes. *Automatica*, 34(2):199–210, 1998.

[EP99] C. Edwards and I. Postlethwaite. An anti-windup scheme with closed-loop stability considerations. *Automatica*, 35:761–765, 1999.

[Ful69] A. T. Fuller. In-the-large stability of relay and saturating control systems with linear controller. *International Journal of Control*, 10:457–480, 1969.

[GNLC95] P. Gahinet, A. Nemirovski, A. J. Laub, and M. Chilali. *LMI Control Toolbox User's Guide*. The MathWorks, Inc, 1995.

[HB98] H. Hindi and S. P. Boyd. Analysis of linear systems with saturation using convex optimization. In *Proceedings of the 37th IEEE Conference on Decision & Control*, 1998.

[HC99] K. Hui and C. W. Chan. Noise attenuation of compensators for rate and amplitude constrained systems. *Automatica*, 35:973–979, 1999.

[HHK97] B. Halder, B. Hassibi, and T. Kailath. Linearly combined suboptimal mixed $\mathcal{H}_2/\mathcal{H}_\infty$ controllers. In *Proceedings of the 36th IEEE Conference on Decision & Control*, 1997.

[HK98] B. Hassibi and T. Kailath. Upper bounds for mixed $\mathcal{H}_2/\mathcal{H}_\infty$ control. In *Proceedings of the 37th IEEE Conference on Decision & Control*, 1998.

[HKH87] R. Hanus, M. Kinnaert, and J.-L. Henrotte. Conditioning technique, a general anti-windup and bumpless transfer method. *Automatica*, 23:729–739, 1987.

[HL86] I. M. Horowitz and Y. K. Liao. Qualitative non-linear compensation design for saturating unstable uncertain plants. *International Journal of Control*, 44(4):1137–1146, 1986.

[HL99] T. Hu and Z. Lin. A complete stability analysis of planar linear systems under saturation. In *Proceedings of the 38th IEEE Conference on Decision & Control*, 1999.

[HQL97] T. Hu, L. Qiu, and Z. Lin. The controllability and stabilization of unstable LTI systems with input saturation. In *Proceedings of the 36th IEEE Conference on Decision & Control*, 1997.

[HQL98] T. Hu, L. Qiu, and Z. Lin. Stabilization of LTI systems with planar anti-stable dynamics using saturated linear feedback. In *Proceedings of the 37th IEEE Conference on Decision & Control*, 1998.

[KA90] P. Kapasouris and M. Athans. Control systems with rate and magnitude saturation for neutrally stable open loop systems. In *Proceedings of the 29th IEEE Conference on Decision & Control*, 1990.

[KCMN94] M. V. Kothare, P. J. Campo, M. Morari, and C. N. Nett. A unified framework for the study of anti-windup designs. *Automatica*, 30(12):1869–1883, 1994.

[KD97] N. Kapoor and P. Daoutidis. Stabilization of systems with input constraints. *International Journal of Control*, 66(5):653–675, 1997.

[KD99] N. Kapoor and P. Daoutidis. An observer-based anti-windup scheme for non-linear systems with input constraints. *International Journal of Control*, 72(1):18–29, 1999.

[KH98] V. Kapila and W. M. Haddad. Fixed-structure controller design for systems with actuator amplitude and rate nonlinearities. In *Proceedings of the 37th IEEE Conference on Decision & Control*, 1998.

[KM95] M. V. Kothare and M. Morari. Multiplier theory for stability analysis of anti-windup control systems. In *Proceedings of the 34th IEEE Conference on Decision & Control*, 1995.

[KM99] M. V. Kothare and M. Morari. Multiplier theory for stability analysis of anti-windup control systems. *Automatica*, 35:917–928, 1999.

[Kot97] M. V. Kothare. *Control of systems subject to constraints*. PhD thesis, California Institute of Technology, 1997.

[KPdQ99] V. Kapila, H. Pan, and M. S. de Queiroz. LMI-based control of linear systems with actuator amplitude and rate nonlinearities. In *Proceedings of the 38th IEEE Conference on Decision & Control*, 1999.

[KR91] P. P. Khargonekar and M. A. Rotea. Mixed $\mathcal{H}_2/\mathcal{H}_\infty$ control - a convex-optimisation approach. *IEEE Transactions on Automatic Control*, 36:824–837, 1991.

[KTD98] N. Kapoor, A. R. Teel, and P. Daoutidis. An anti-windup design for linear systems with input saturation. *Automatica*, 34(5):559–574, 1998.

[LB98] Z. Lin and J. M. Berg. Semi-global stabilization of linear systems with position and rate limited actuators in daisy chain. In *Proceedings of the 37th IEEE Conference on Decision & Control*, 1998.

[LH86] Y. K. Liao and I. M. Horowitz. Unstable uncertain plants with rate and amplitude saturations. *International Journal of Control*, 44(4):1147–1159, 1986.

[Lin97] Z. Lin. Semi-global stabilization of linear systems with position and rate-limited actuators. *Systems & Control Letters*, 30:1–11, 1997.

[Lin98] Z. Lin. Semi-global stabilization of discrete-time linear systems with position and rate-limited actuators. In *Proceedings of the 37th IEEE Conference on Decision & Control*, 1998.

[LS93] Z. Lin and A. Saberi. Semi-global exponential stabilization of linear systems subject to "input saturation" via linear feedbacks. *Systems & Control Letters*, 21:225–239, 1993.

[Meg94] A. Megretski. On the order of controllers in mixed $\mathcal{H}_2/\mathcal{H}_\infty$ control. In *Proceedings of the 33rd IEEE Conference on Decision & Control*, 1994.

[Meg99] A. Megretski. New IQC for quasi-concave nonlinearities. In *Proceedings of the American Control Conference*, 1999.

[Miy97] S. Miyamoto. *Robust control design - a coprime factorization and LMI approach.* PhD thesis, Cambridge University Engineering Dept, 1997.

[MR95] A. Megretski and A. Rantzer. System analysis via Integral Quadratic Constraints part I. Technical Report LUTFD2/TFRT-7531-SE, Lund Institute of Technology, 1995.

[MR97] A. Megretski and A. Rantzer. System analysis via integral quadratic constraints. *IEEE Transactions on Automatic Control*, 42(6):819–829, 1997.

[MV96a] S. Miyamoto and G. Vinnicombe. Robust control of plants with saturation nonlinearity based on coprime factor representations. Technical Report CUED/F-INFENG/TR 264, Cambridge University Engineering Dept, 1996.

[MV96b] S. Miyamoto and G. Vinnicombe. Robust control of plants with saturation nonlinearity based on coprime factor representations. In *Proceedings of the 35th IEEE Conference on Decision & Control*, 1996.

[PC95] J.-K. Park and C.-H. Choi. Dynamic compensation method for multivariable control systems with saturating actuators. *IEEE Transactions on Automatic Control*, 40(9):1635–1640, 1995.

[PHHB98] T. E. Pare, H. Hindi, J. P. How, and S. P. Boyd. Synthesizing stability regions for systems with saturation actuators. In *Proceedings of the 37th IEEE Conference on Decision & Control*, 1998.

[Pop62] V. M. Popov. Absolute stability of nonlinear systems of automatic control. *Automat. Remote Control (translation)*, pages 857–875, 1962.

[PTB97] C. Pittet, S. Tarbouriech, and C. Burgat. Stability regions for linear systems with saturating controls via circle and popov criteria. In *Proceedings of the 36th IEEE Conference on Decision & Control*, 1997.

[PVH96] Y. Peng, D. Vrancic, and R. Hanus. Anti-windup, bumpless, and conditioned transfer techniques for PID controllers. *IEEE Control Systems Magazine*, 16(4):48–57, 1996.

[PVHW98] Y. Peng, D. Vrancic, R. Hanus, and S. R. Weller. Anti-windup designs for multivariable controllers. *Automatica*, 34(12):1559–1565, 1998.

[Ran99] A. Rantzer. A simple performance criterion for anti-windup compensators. In *Proceedings of the European Control Conference*, 1999.

[RM96] A. Rantzer and A. Megretski. Stability criteria based on integral quadratic constraints. In *Proceedings of the 35th IEEE Conference on Decision & Control*, 1996.

[RM97] A. Rantzer and A. Megretski. System analysis via Integral Quadratic Constraints part II. Technical Report LUTFD2/TFRT-7559-SE, Lund Institute of Technology, 1997.

[RQC99] Z. Ren, L. Qiu, and J. Chen. Performance limitations in estimation. In *Proceedings of the 38th IEEE Conference on Decision & Control*, 1999.

[Sch95] C. W. Scherer. Multiobjective $\mathcal{H}_2$-$\mathcal{H}_\infty$ control. *IEEE Transactions on Automatic Control*, 40(6):1054–1062, 1995.

[SLT96] A. Saberi, Z. Lin, and A. R. Teel. Control of linear systems with saturating actuators. *IEEE Transactions on Automatic Control*, 41(3):368–378, 1996.

[SS90] E. D. Sontag and H. J. Sussmann. Nonlinear output feedback design for linear systems with saturating controls. In *Proceedings of the 29th IEEE Conference on Decision & Control*, 1990.

[SSS99] A. A. Stoorvogel, A. Saberi, and G. Shi. On achieving $\mathcal{L}_p$ (l_p) performance with global internal stability for linear plants with saturating actuators. In *Proceedings of the 38th IEEE Conference on Decision & Control*, 1999.

[SSY94] H. J. Sussmann, E. D. Sontag, and Y. Yang. A general result on the stabilization of linear systems using bounded controls. *IEEE Transactions on Automatic Control*, 39(12):2411–2425, 1994.

[SY91] H. J. Sussmann and Y. Yang. On the stabilizability of multiple integrators by means of bounded feedback controls. In *Proceedings of the 30th IEEE Conference on Decision & Control*, 1991.

[Szn94] M. Sznaier. An exact solution to general SISO mixed $\mathcal{H}_2/\mathcal{H}_\infty$ problems via convex optimization. *IEEE Transactions on Automatic Control*, 39:2511–2517, 1994.

[Tee92] A. R. Teel. Global stabilization and restricted tracking for multiple integrators with bounded controls. *Systems & Control Letters*, 18:165–171, 1992.

[TK97] A. R. Teel and N. Kapoor. The $\mathcal{L}_2$ anti-windup problem: its definition and solution. In *Proceedings of the European Control Conference*, 1997.

[Vid85] M. Vidyasagar. *Control System Synthesis: A Factorization Approach.* MIT Press, 1985.

[Vin93] G. Vinnicombe. *Measuring the robustness of feedback systems.* PhD thesis, Cambridge University Engineering Dept, 1993.

[Vin00] G. Vinnicombe. *Uncertainty and Feedback: $\mathcal{H}_\infty$ loop-shaping and the ν-gap metric*. Imperial College Press, 2000.

[Wei73] A. J. Weir. *Lebesgue Integration and Measure.* Cambridge University Press, 1973.

[Whi96] P. Whittle. *Optimal Control - basics and beyond.* John Wiley & sons, 1996.

[Wil71] J. C. Willems. *The Analysis of Feedback Systems.* M.I.T. Press, 1971.

[WP98] P. Weston and I. Postlethwaite. Linear conditioning schemes for systems containing saturating actuators. In *Proceedings of the IFAC Nonlinear Control System Design Symposium*, 1998.

[WS90] K. S. Walgama and J. Sternby. Inherent observer property in a class of anti-windup compensators. *International Journal of Control*, 52(3):705–724, 1990.

[YNF99] V. A. Yakubovich, S. Nakaura, and K. Furuta. Tracking domains for unstable plants with saturating-like actuators. In *Proceedings of the 38th IEEE Conference on Decision & Control*, 1999.

[You88] N. Young. *An Introduction to Hilbert Space.* Cambridge University Press, 1988.

[Zam66a] G. Zames. On the input-output stability of time-varying nonlinear feedback systems. Part I: conditions derived using concepts of loop gain, conicity, and positivity. *IEEE Transactions on Automatic Control*, AC-11(2):228–238, 1966.

[Zam66b] G. Zames. On the input-output stability of time-varying nonlinear feedback systems. Part II: conditions involving circles in the frequency plane and sector nonlinearities. *IEEE Transactions on Automatic Control*, AC-11(3):465–476, 1966.

[ZDG96] K. Zhou, J. Doyle, and K. Glover. *Robust and Optimal Control.* Prentice Hall, 1996.

[ZF68] G. Zames and P. L. Falb. Stability conditions for systems with monotone and slope-restricted nonlinearities. *SIAM Journal of Control*, 6(1):89–108, 1968.

[ZGBD94] K. Zhou, K. Glover, B. Bodenheimer, and J. Doyle. Mixed $\mathcal{H}_2$ and $\mathcal{H}_\infty$ performance objectives I: robust performance analysis. *IEEE Transactions on Automatic Control*, 39(8):1564–1574, 1994.

[ZKM94] A. Zheng, M. V. Kothare, and M. Morari. Anti-windup design for internal model control. *International Journal of Control*, 60(5):1015–1024, 1994.

Appendix A

Design example

Description of nonlinear system and nominal linear controller

For our design example we consider an unstable scalar LTI plant $\frac{s}{s-0.05}$ with an ideal unity saturation element at the plant input. This system satisfies the assumptions in Section 4.1.2 with

$$\begin{aligned} \boldsymbol{\mathcal{U}}_{\mathrm{act}} &= \mathfrak{M}_1 \qquad & P_{\mathrm{act}}(s) &= I \\ \boldsymbol{\mathcal{U}}_{\mathrm{nom}} &= \mathfrak{M}_1 \qquad & P_{\mathrm{lin}}(s) &= \tfrac{s}{s-0.05} \end{aligned}$$

and has nominal linear dynamics $P(s) = P_{\mathrm{lin}}(s)P_{\mathrm{act}}(s) = \frac{s}{s-0.05}$.

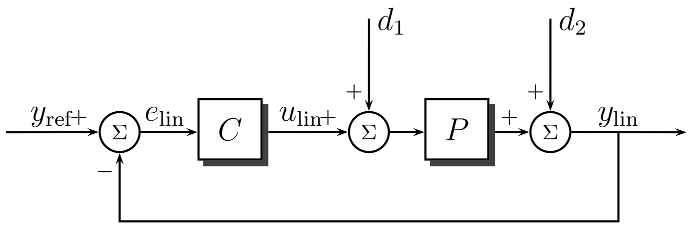

Figure A.1: Design example: nominal (linear) closed-loop interconnection

It may be easily verified that the linear controller[1]

$$C(s) = \tfrac{6.05}{s-5}$$

internally stabilises $P(s)$ in the absence of the nonlinearity (in a negative feedback interconnection, as in Figure A.1), placing both closed-loop poles at $-\frac{1}{2}$, and that normalised coprime factors $P = N_0 M_0^{-1}$ and $C = \tilde{V}_0^{-1}\tilde{U}_0$ satisfying the Bezout identity $\tilde{V}_0 M_0 + \tilde{U}_0 N_0 = I$ may be given by

$$\begin{bmatrix} M_0 \\ N_0 \end{bmatrix} = \begin{bmatrix} \frac{s-0.05}{s+0.05} \\ \frac{s}{s+0.05} \end{bmatrix} \qquad \begin{bmatrix} \tilde{V}_0 & \tilde{U}_0 \end{bmatrix} = \begin{bmatrix} \frac{(s-5)(s+0.05)}{(s+0.5)^2} & \frac{6.05(s+0.05)}{(s+0.5)^2} \end{bmatrix}$$

[1]Note that *any* strictly proper stabilising controller for this plant must itself be unstable.

The nominal linear behaviour (which, of course, will be observed if the system never enters saturation) may be described by the following relation:

$$\begin{bmatrix} e_{\text{lin}} \\ y_{\text{lin}} \\ u_{\text{lin}} \end{bmatrix} = \begin{bmatrix} (I+PC)^{-1} & -(I+PC)^{-1}P & -(I+PC)^{-1} \\ I-(I+PC)^{-1} & (I+PC)^{-1}P & (I+PC)^{-1} \\ C(I+PC)^{-1} & -C(I+PC)^{-1}P & -C(I+PC)^{-1} \end{bmatrix} \begin{bmatrix} y_{\text{ref}} \\ d_1 \\ d_2 \end{bmatrix}$$
$$= \begin{bmatrix} \frac{(s-0.05)(s-5)}{(s+0.5)^2} & \frac{-s(s-5)}{(s+0.5)^2} & \frac{-(s-0.05)(s-5)}{(s+0.5)^2} \\ \frac{6.05s}{(s+0.5)^2} & \frac{s(s-5)}{(s+0.5)^2} & \frac{(s-0.05)(s-5)}{(s+0.5)^2} \\ \frac{6.05(s-0.05)}{(s+0.5)^2} & \frac{-6.05s}{(s+0.5)^2} & \frac{-6.05(s-0.05)}{(s+0.5)^2} \end{bmatrix} \begin{bmatrix} y_{\text{ref}} \\ d_1 \\ d_2 \end{bmatrix}$$

Nonlinear precompensation

As discussed in Chapter 4, we propose to implement a nonlinear precompensator

1. to ensure that the actuator always operates within its nominal linear region, and
2. to provide a suitable feedback signal for anti-windup compensation.

An appropriate precompensator for input saturation is given by Precompensator 1 (see Figure 4.6 on page 107), which is itself a saturation element.

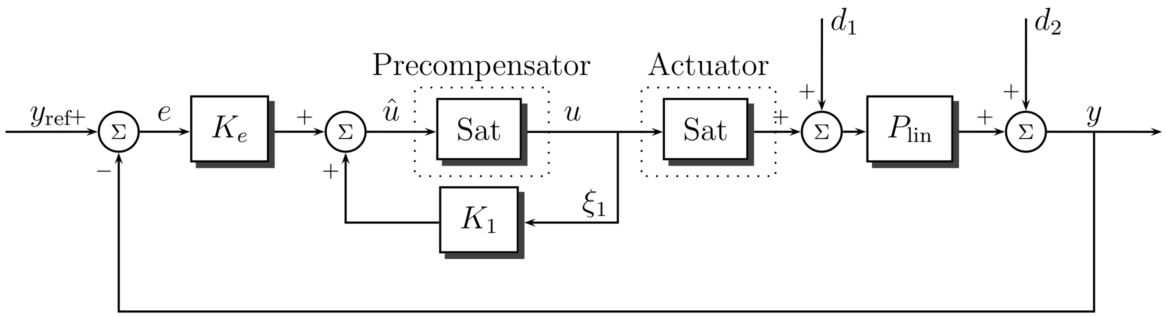

Figure A.2: Design example: nonlinear closed-loop interconnection

The overall nonlinear closed-loop interconnection is then as shown in Figure A.2 in which the nominal linear controller $C(s)$ has been replaced by $K_e(s)$ and $K_1(s)$.

The problem of designing an anti-windup compensator is now one of choosing K_e and K_1 appropriately.

Anti-windup compensation by choice of K_e and K_1

In Chapter 5 we listed some previously-studied compensation schemes; K_e and K_1 for two of these schemes[2] are given below:

- **no anti-windup:** $K_e = C$ and $K_1 = 0$
- **"conventional" scheme:** $K_e = \frac{6.05}{s+(6.05C_F-5)}$ and $K_1 = \frac{6.05C_F}{s+(6.05C_F-5)}$

where C_F is a tuning parameter (with $C_F > \frac{5}{6.05}$ if stability of K_e and K_1 is desired)

Our proposed scheme is based on a coprime factor parametrisation of anti-windup compensators (Kothare *et al* [KCMN94] and Miyamoto & Vinnicombe [MV96b])

- **coprime factor scheme:** $K_e = Q\tilde{U}_0$ and $K_1 = I - Q\tilde{V}_0$

where $Q \in \mathcal{Q}$ is a unit in $\mathcal{RH}_\infty$ (Equation 2.5) and should satisfy $Q(\infty) = M_0(\infty)$.

Note that, since the plant has a pole in the open right half-plane, it is impossible to globally stabilise the interconnection in Figure A.2. We will therefore consider local stability with respect to isolated disturbances, and for simplicity will assume disturbances at d_1 only.

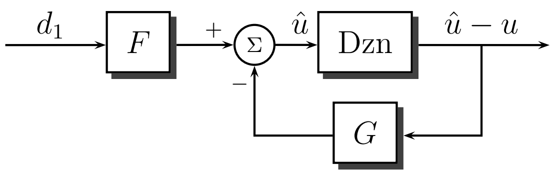

Figure A.3: Design example: simple interconnection for stability analysis

In Chapter 5 we saw that analysis of the interconnection in Figure A.2 is easier if we consider the (equivalent, in terms of local and global stability) simple interconnection of Figure A.3 where

$$F(s) = C(I + PC)^{-1}P = \tfrac{6.05s}{(s+0.5)^2}$$

$$G(s) = \begin{cases} \frac{-6.05s}{(s+0.5)^2} & \text{no anti-windup} \\ \frac{-6.05\{(1-C_F)s+C_F\}}{(s+0.5)^2} & \text{“conventional” scheme} \\ \frac{s-0.05}{s+0.05}Q^{-1} - I & \text{coprime factor scheme} \end{cases}$$

From this figure it is clear that the smallest signal (in $\mathcal{L}_2$-norm) which causes saturation, and which we will denote by d^{sat}, has $\|d^{\text{sat}}\|_2 = \frac{1}{\|F\|_2}$; this signal may be obtained by scaling the time-reversed impulse response of $F(s)$, and is clearly independent of the anti-windup scheme used.

[2]For this particular P and C neither Hanus' conditioning scheme nor the internal model (IMC) scheme are applicable.

Analysis of system behaviour without anti-windup compensation

Since the plant P and controller C require only one state each, we can investigate the behaviour of the system without anti-windup compensation by plotting the plant state x_P against the controller state x_C. The state-space representation of the open-loop transfer function $-CP$ is taken to be

$$-CP = \left[\begin{array}{cc|c} 0.05 & 0 & 0.05 \\ -1 & 5 & -1 \\ \hline 0 & 6.05 & 0 \end{array}\right] \quad \text{with state} \begin{bmatrix} x_P \\ x_C \end{bmatrix}$$

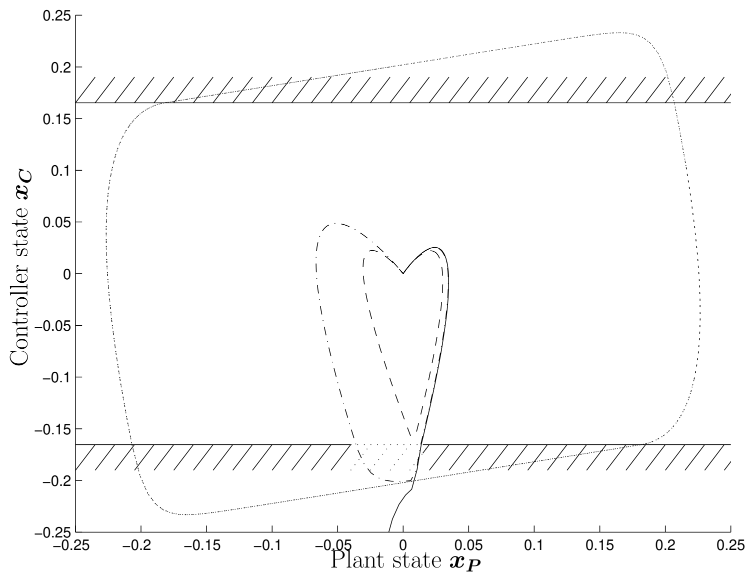

Figure A.4: Design example: state trajectories of uncompensated system

The following features of the system without anti-windup compensation are shown in Figure A.4:

- The region where the system is in saturation (shaded area)
- The boundary of the state-space region within which the unforced system returns to the origin[3] (shown as a dotted line)
- The evolution of the state when the input disturbance is given by
  1. $d_1 = d^{\text{sat}}$ (shown as a dashed line)
  2. $d_1 = 1.14d^{\text{sat}}$ (shown as a dash-dot line)
  3. $d_1 = 1.15d^{\text{sat}}$ (shown as a solid line)

  This last plot indicates that the system may be destabilised by a relatively small disturbance.

[3]Note that this boundary is a limit cycle, and may be obtained by simulating the time-reversed system.

Design of Q to maximise local stability properties

Recall that in Section 3.4 we showed that if $\|d_1\|_2 \le \frac{1}{\|F\|_2}$ then $\|\hat{u} - u\|_2 = 0$ (and hence that the system never enters saturation), which can be stated as

- The interconnection in Figure A.3 (equivalently, Figure A.2) is locally stable with respect to the set of disturbances
$$\left\{ z : \|z\|_2 < \tfrac{1}{\|F\|_2} \right\}$$

We also derived a method for determining a number $Z^{\text{opt}}_{[F,G]} \ge 1$ such that if $\|d_1\|_2 < \frac{1}{\|F\|_2} Z^{\text{opt}}_{[F,G]}$ then $(\hat{u} - u) \in \mathcal{L}_2$ (and hence that all signals in the loop are bounded), which can be stated as

- The interconnection in Figure A.3 (equivalently, Figure A.2) is locally stable with respect to the set of disturbances
$$\left\{ z : \|z\|_2 < \tfrac{1}{\|F\|_2} Z^{\text{opt}}_{[F,G]} \right\}$$

Our aim now is to choose $Q \in \mathcal{Q}$ to maximise $Z^{\text{opt}}_{[F,G]}$ (and, as a minimum requirement, to achieve $Z^{\text{opt}}_{[F,G]}$ strictly greater than unity.)

The method given in Section 3.4 for finding $Z^{\text{opt}}_{[F,G]}$ does not lend itself easily to direct synthesis of Q, but fortunately we also showed that $Z^{\text{opt}}_{[F,G]} \ge Z^{\text{opt}}_{[\text{upper}]}$ where

$$Z^{\text{opt}}_{[\text{upper}]} = \begin{cases} \left(\frac{\sqrt{\rho(\mu-1)} + \sqrt{\mu-\rho}}{\sqrt{\rho(\mu-\rho)} + \sqrt{\mu-1}} \right)^2 \in (1, \frac{1}{\rho}) & \text{if } \rho < 1 \\ 1 & \text{otherwise} \end{cases}$$

and where μ and ρ are given by

$$\mu := \|G\|_\infty \quad \text{and} \quad \rho := \tfrac{\|F\|_\infty}{\|F\|_2} \|G\|_2 = 1.4142 \, \|G\|_2$$

This relatively simple closed-form expression for $Z^{\text{opt}}_{[\text{upper}]}$ can be used to plot contours of constant $Z^{\text{opt}}_{[\text{upper}]}$ on axes of $\|G\|_\infty$ versus $\|G\|_2$; by plotting $\|M_0 Q^{-1} - I\|_\infty$ and $\|M_0 Q^{-1} - I\|_2$ on the same axes we may immediately determine a *guaranteed* level of local stability (since $Z^{\text{opt}}_{[F,G]}$ is no less than $Z^{\text{opt}}_{[\text{upper}]}$) for any given $Q \in \mathcal{Q}$.

Note that for both the system without anti-windup compensation

$$G = \tfrac{-6.05s}{(s+0.5)^2} \quad \|G\|_2 = 6.05\sqrt{\tfrac{1}{2}} \quad \|G\|_\infty = 6.05$$

and for the "conventional" anti-windup scheme (with *any* real value of C_F)

$$G = \tfrac{-6.05\{(1-C_F)s + C_F\}}{(s+0.5)^2} \quad \|G\|_2 = 6.05\sqrt{\tfrac{4+(5C_F-1)^2}{10}} \quad \|G\|_\infty = \begin{cases} 24.2\,|C_F| & \text{if } |C_F| \ge \sqrt{\frac{1}{8}} \\ \frac{6.05(1-C_F)^2}{\sqrt{1-2C_F-3C_F^2}} & \text{if } |C_F| < \sqrt{\frac{1}{8}} \end{cases}$$

we have that $Z^{\text{opt}}_{[\text{upper}]} = 1$.

We now recall that Corollary 2.10 on page 31 gave a computationally efficient method for minimising $\|M_0Q^{-1} - I\|_2$ subject to a constraint on $\|M_0Q^{-1} - I\|_\infty$, over a subset of $\mathcal{RH}_\infty$ comprising those elements $Q^{-1} \in \mathcal{RH}_\infty$ with a fixed denominator. For simplicity we choose denominators $(s+1)$, $(s+1)^3$ and $(s+1)^5$, and perform the optimisation for various $\mathcal{H}_\infty$-norm constraints between 1 and 2.

Figure A.5 shows the following:

- The results of the optimisations (solid lines) corresponding to $Q^{-1} \in \mathcal{RH}_\infty$ with denominators $(s+1)$ (top-right), $(s+1)^3$ (centre) and $(s+1)^5$ (bottom-left)
- Contours of constant $Z^{\text{opt}}_{\text{[upper]}}$ (dotted lines) ranging from $Z^{\text{opt}}_{\text{[upper]}} = 1.09$ (top-right) to $Z^{\text{opt}}_{\text{[upper]}} = 1.17$ (bottom-left) in increments of 0.01

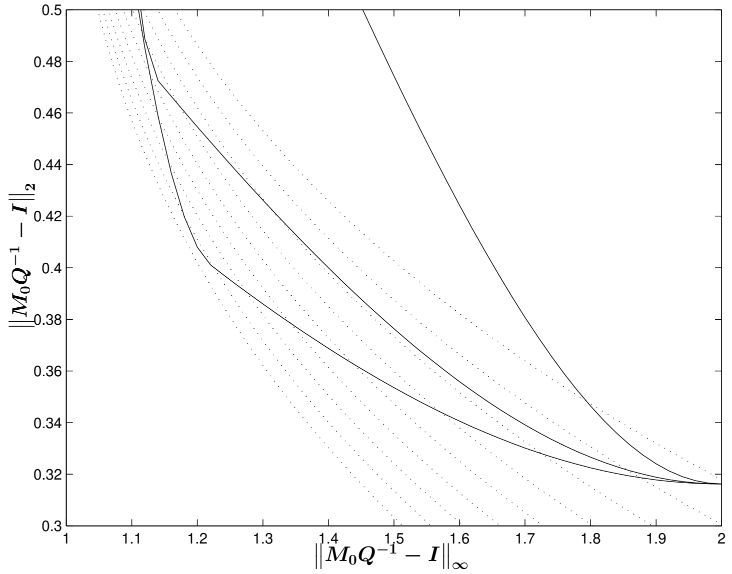

Figure A.5: Design example: results of mixed $\mathcal{H}_2$-$\mathcal{H}_\infty$ minimisation

We can make the following deductions from this plot:

1. The best $Z^{\text{opt}}_{\text{[upper]}}$ over all $Q^{-1} \in \mathcal{RH}_\infty$ with denominator $(s+1)$ is approximately 1.09, ie with the best such Q the system would be guaranteed to be locally stable with respect to disturbances with $\mathcal{L}_2$-norm up to 9% larger than $\|d^{\text{sat}}\|_2 = \frac{1}{\|F\|_2}$.

   Note that this is only slightly better than the "$\mathcal{H}_2$-optimal" solution, ie the Q for which $\|M_0Q^{-1} - I\|_2$ is minimised and $\|M_0Q^{-1} - I\|_\infty = 2$.

2. The best $Z^{\text{opt}}_{\text{[upper]}}$ over all $Q^{-1} \in \mathcal{RH}_\infty$ with denominator $(s+1)^3$ is approximately 1.12

3. The best $Z^{\text{opt}}_{\text{[upper]}}$ over all $Q^{-1} \in \mathcal{RH}_\infty$ with denominator $(s+1)^5$ is approximately 1.16 — large enough to guarantee stability if subjected to the disturbance $d_1 = 1.15d^{\text{sat}}$ which destabilised the uncompensated system (recall Figure A.4)

Based on Figure A.5 we choose two Qs for further investigation:

- The "$(s+1)^5$-optimal" solution, obtained by performing the mixed-norm minimisation with Q^{-1} having denominator $(s+1)^5$ and with the constraint $\|M_0 Q^{-1} - I\|_\infty < 1.2$. The best such Q is given by

$$Q = \frac{(s+1)^5}{s^5 + 4.841s^4 + 9.75s^3 + 8.405s^2 + 4.582s + 0.1983}$$

  and achieves

$$\mu = 1.200 \qquad \rho = 0.577 \quad \text{and} \quad Z^{\text{opt}}_{[\text{upper}]} = 1.163$$

  Figure A.6 (a) shows the "characteristic bounding curve" (as described in Section 3.4) as a solid line, and its conservative approximation as a dashed line, for this choice of Q. From this plot we can determine that $Z^{\text{opt}}_{[F,G]} = 1.66$, which is quite significantly larger than the guaranteed $Z^{\text{opt}}_{[\text{upper}]} = 1.16$ — and hence that the system will be much more resilient to disturbances than the lower bound $Z^{\text{opt}}_{[\text{upper}]}$ indicated.

- The "$\mathcal{H}_2$-optimal" solution, which corresponds to $Q = I$[4] and which is, in one sense, the simplest coprime-factor anti-windup scheme. This choice of Q achieves

$$\mu = 2.000 \qquad \rho = 0.447 \quad \text{and} \quad Z^{\text{opt}}_{[\text{upper}]} = 1.091$$

  Figure A.6 (b) shows the "characteristic bounding curve" and its conservative approximation for this choice of Q. From this plot we can determine that $Z^{\text{opt}}_{[F,G]} = 1.28$, which is again quite significantly larger than $Z^{\text{opt}}_{[\text{upper}]} = 1.09$, although not so spectacularly as in the previous case.

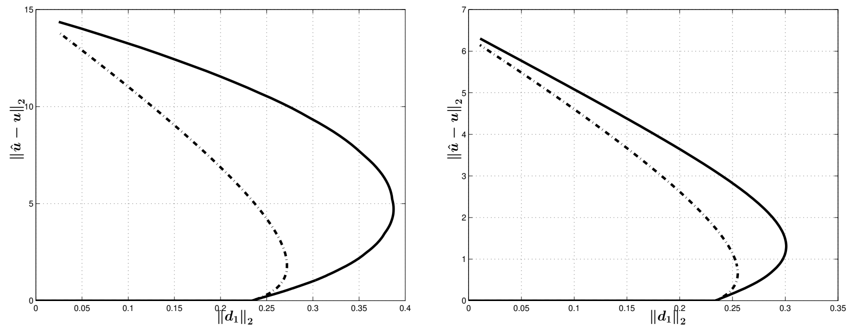

(a) "$(s+1)^5$-optimal" Q (b) "$\mathcal{H}_2$-optimal" Q

Figure A.6: Design example: characteristic bounding curves

[4]In general, the "$\mathcal{H}_2$-optimal" Q is not the identity, however in this case we have chosen M_0 to be all-pass (see Theorem 2.4 to see that $M_0 Q^{-1}$ all-pass minimises $\|M_0 Q^{-1} - I\|_2$ over $Q \in \mathcal{Q}$)

System responses

The final stage of the analysis is to simulate the closed-loop system response, with each of the anti-windup compensators, and with a number of different disturbances. For simplicity we consider only disturbances where d_1 is a simple scaling of d^{sat}, since this type of signal causes the maximum peak level of u_{lin} (in the nominal system) for given $\mathcal{L}_2$-norm.

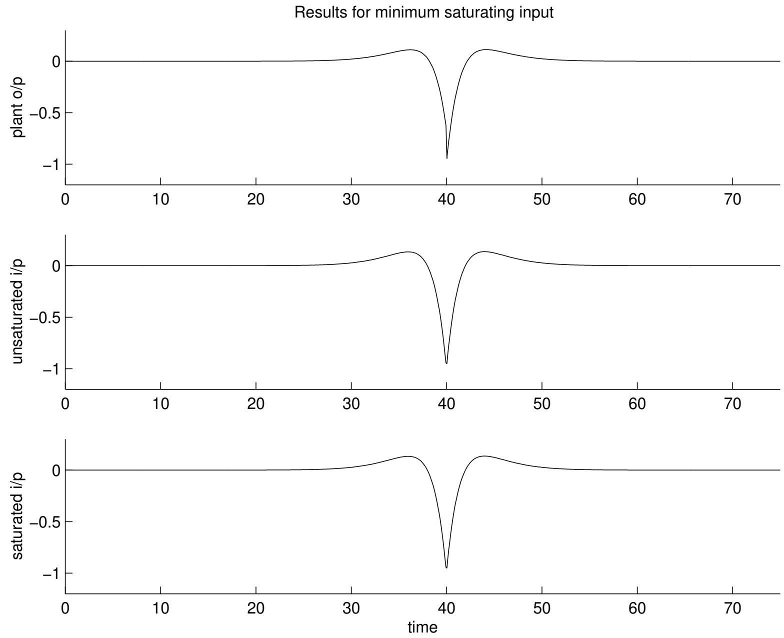

Figure A.7: Design example: responses to $d_1 = d^{\text{sat}}$

Figure A.7 shows the system response to a disturbance $d_1 = d^{\text{sat}}$; the response is the same for all anti-windup schemes, since this signal only just causes saturation.

Figures A.8 and A.9 show, respectively, the system response to disturbances $d_1 = 1.14d^{\text{sat}}$ and $d_1 = 1.15d^{\text{sat}}$; the responses for the uncompensated, "$\mathcal{H}_2$-optimal" and "$(s+1)^5$-optimal" anti-windup schemes are shown as solid, dash-dot and dashed lines respectively. We observe that the two coprime-factor compensators behave in a very similar manner to the nominal linear system, despite the significant level of saturation (approx 20%) — by contrast the system without anti-windup is noticeably nonlinear with $d_1 = 1.14d^{\text{sat}}$, and becomes divergent with $d_1 = 1.15d^{\text{sat}}$.

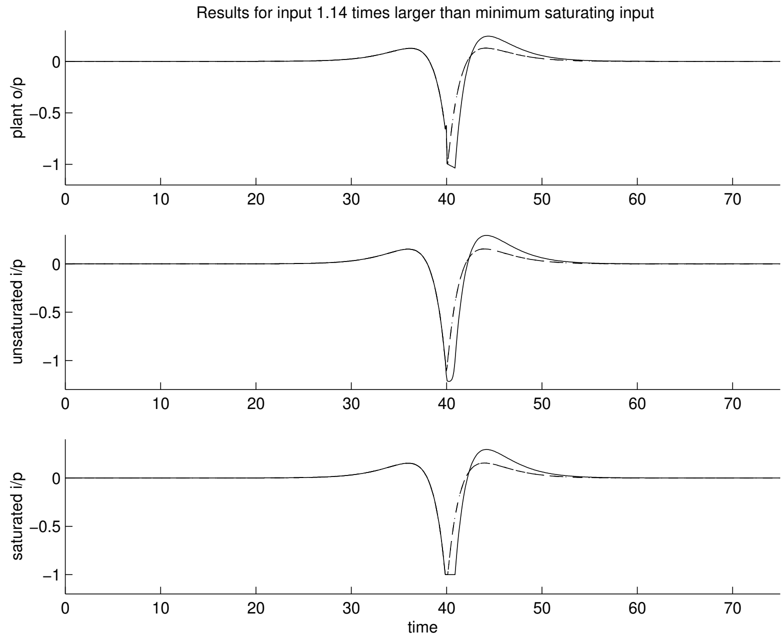

Figure A.8: Design example: responses to $d_1 = 1.14d^{\text{sat}}$

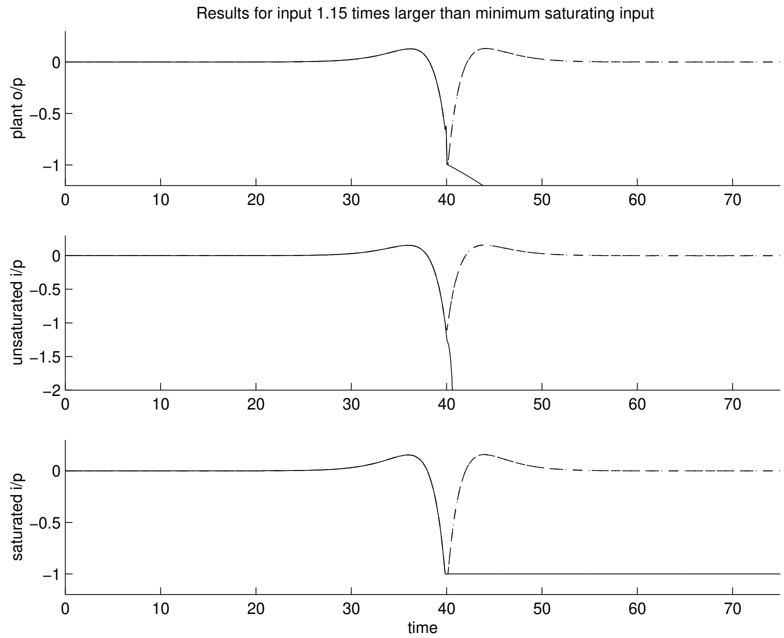

Figure A.9: Design example: responses to $d_1 = 1.15d^{\text{sat}}$

To illustrate the difference in behaviour between the "$\mathcal{H}_2$-optimal" and "$(s+1)^5$-optimal" anti-windup schemes, we need to increase the disturbance size considerably: Figure A.10 shows the system response to a disturbance $d_1 = 30d^{\mathrm{sat}}$, shown again as dash-dot and dotted lines. (The response for the uncompensated system is not shown - suffice to say that it becomes rapidly unstable!)

We observe that the "$\mathcal{H}_2$-optimal" compensator may be less satisfactory than the "$(s+1)^5$-optimal" compensator (it exhibits an extra "oscillation" from negative saturation to positive saturation and back), however it is obviously dangerous to make such an assumption based only on one simulation!

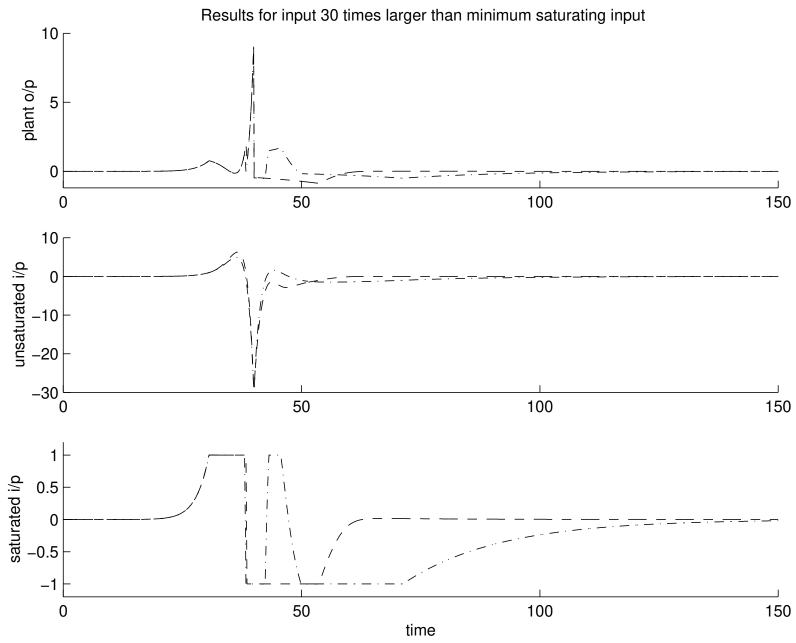

Figure A.10: Design example: responses to $d_1 = 30d^{\mathrm{sat}}$

Conclusions

We have shown how to apply the methods presented throughout this thesis to a simple unstable system with input saturation. The design methodology proposed in Chapter 5 has been used to synthesise an anti-windup compensation scheme which is able to tolerate disturbances of $\mathcal{L}_2$-norm approximately 65% larger than the minimum signal necessary to cause saturation — this is in contrast to the system without any anti-windup compensation, which could be destabilised by a disturbance of $\mathcal{L}_2$-norm only 15% larger than this minimum.

For comparison, we also analysed the local stability properties of a so-called "$\mathcal{H}_2$-optimal" coprime factor compensator; this compensator is generally of quite low order (which is desirable for implementation), although the local stability properties guaranteed are not as good as the best achievable.